NMDA receptors in cerebellar Purkinje cells:Development and synaptic plasticity in mice

Claire Piochon

THÈSE DE DOCTORAT DE
L'UNIVERSITÉ PIERRE ET MARIE CURIE (PARIS VI)

Spécialité
Neurosciences

Présentée par
Claire Piochon

Pour obtenir le grade de
DOCTEUR DE L'UNIVERSITÉ PIERRE ET MARIE CURIE

NMDA receptors in cerebellar Purkinje cells:
Development and synaptic plasticity in mice

Les récepteurs NMDA de la cellule de Purkinje du cervelet :
Développement et plasticité synaptique chez la souris

Soutenue le 4 septembre 2008

Devant le jury composé de :

Pr Jean Mariani	Directeur de Thèse
Dr Carole Lévénès	Directrice de Thèse
Dr Dominique Debanne	Rapporteur
Dr Christophe Mulle	Rapporteur
Dr Christian Hansel	Examinateur

« Développement et vieillissement du système nerveux central »
Laboratoire de Neurobiologie des Processus Adaptatifs
CNRS UMR7102 - Université Pierre et Marie Curie

A mes parents,

Remerciements

Je tiens tout d'abord à remercier Madame le Docteur Carole Lévénès de m'avoir encadrée tout au long de cette thèse qui restera pour moi une très belle aventure scientifique et humaine, certes lourde de travail et de sacrifices, mais ô combien exaltante et enrichissante. Merci Carole pour ta confiance, ainsi que pour ton soutien tant scientifique que moral, ta capacité à me remotiver dans les moments de découragement. Au-delà de ton précieux savoir et ton enthousiasme communicatif pour la Science, tu as su me transmettre ta passion, qui je l'espère, continuera de me porter longtemps. En grande épicurienne, tu sais concilier plaisir et travail, ce qui rend le quotidien au laboratoire toujours agréable, saupoudré d'humour et rempli de surprises ; merci donc pour tous ces bons moments, nos délires de fin de manip, nos discussions surréalistes à la terrasse d'un café, ou les soirées inattendues lors d'un congrès au bout du monde. J'espère que nous aurons dans l'avenir encore bien d'autres bons moments à partager.

Je remercie le Professeur Jean Mariani, directeur du laboratoire de Neurobiologie des Processus Adaptatifs (CNRS UMR 7102) de m'avoir accueillie dans son équipe et soutenue dans ce travail.

Je tiens à remercier les membres du jury, Messieurs les Docteurs Dominique Debanne, Christian Hansel et Christophe Mulle, de m'avoir fait l'honneur et le plaisir d'évaluer et de critiquer ce travail.

1000 mercis à Théano, la reine du confocal, et Abdel, pour la sympathie que vous m'avez témoignée dans nos collaborations, ainsi qu'à Daniel, qui a fait de notre set-up une formule 1 de l'électrophy. Merci de m'avoir appris tous ces milliers de petites choses extraordinaires, d'électronique ou de mécanique. Rosine, ce fut un grand plaisir de maniper avec toi ; j'emporte Ghadesh à Chicago ! Merci à Yannick pour son accueil à Strasbourg au début de cette thèse ; à Bertrand pour m'avoir appris les secrets de la single-cell RT-PCR.

A ceux qui sont déjà partis vers d'autres horizons post-doctoraux, mais que cette thèse m'a donné le plaisir de rencontrer : Julie, Ludo, Emeline, Emilie, Nathalie, Nizar. et puis un grand merci aux étudiants et post-doctorants de l'unité, Mathieu, Alexandra, Estelle, Emilie, Fanny, Sahra, Elodie, Hasan, J-B, Manu.

Je salue également le concours bienveillant des autres membres de l'équipe et de l'UMR 7102 dont je ne peux réaliser l'énumération sans risquer de faire d'impardonnables oublis mais qui se reconnaîtront…

Merci les filles, Aude, Anne-Laure et Jing…mes complices du labo ! Vous êtes pour moi un formidable coktail de bonne humeur, de réconfort et d'amitié. Une chose est sûre : vous allez beaucoup me manquer.

Merci à mes parents, pour leur indéfectible soutien. Dans mes échecs et mes moments de doutes, vous savez toujours me redonner confiance en moi-même. Merci à Mamie qui, petite, m'a mis sur de bons rails (en m'expliquant patiemment l'indispensable règle de 3, la preuve

par 9, et me faisant répéter tous les midis mes tables de multiplication…). Merci à toi Manu, mon grand-frère que j'admire, d'avoir montré l'exemple à tes petites sœurs, et transmis ton « fight power » !! Merci aussi à Marianne, ma petite sœur. « Je suis donc ben fière de toi » (avec l'accent québécois !). Merci à Laurent et Stéphane pour votre précieuse amitié.

A toi biensûr, Caro, ma super jumelle, merci d'être là depuis toujours, à me supporter (en tous les sens du terme). Tu es ma source de force et de courage. Merci pour tout ce que tu es, et aussi pour ton coup de patte artistique, sur quelques figures de ce manuscrit.

Mon Olivier…depuis les chemins du Mont-Blanc où tu m'as appris à marcher, à trouver mon souffle, tu es toujours là, pour le meilleur et pour le pire, à me soutenir et me donner des ailes. Que serais-je sans toi ?…qu'une Purkinje sans récepteurs NMDA ! ☺

Foreword

To accomplish this thesis, I received a Ph.D fellowship for 3 years from the French Ministry of Research and Education. For the last year of my Ph.D, I was funded by the French foundation for the medical research (*Fondation pour la Recherche Médicale - FRM*).

Parts of the work presented in this thesis have been published :

- **Article 1:** Neuroprotective effect of mifepristone involves neuron depolarization.
  Ghoumari AM., Piochon C., Tomkiewicz C., Eychenne B., Levenes C., Dusart I., Schumacher M., Baulieu EE.
  The FASEB Journal, 2006 Jul;20(9):1377-86.
- **Article 2:** NMDA receptor contribution to the climbing fiber response in the adult mouse Purkinje cell.
  Piochon C., Irinopoulou T, Brusciano D, Bailly Y, Mariani J, Levenes C.
  The Journal of Neuroscience, 2007 Oct 3;27(40):10797-809.

Some of these thesis results have also been presented in the poster sessions of different meetings:

- RU486 protects Purkinje cell from apoptosis: Role of Na+/K+ ATPase alpha3 and depolarization.
  Ghoumari AM., Piochon C., Tomkiewicz C., Eychenne B., Schumacher M.and E.E. Baulieu.
  BSN-SNE joint Meeting, St Anne College - University of Oxford, United-Kingdom, september 2005.
- Adult mouse Purkinje cells express functional NMDA receptors.
  Piochon C., Irinopoulou T., Brusciano D., Bailly Y, Mariani J. & Levenes C.
  FENS Forum, Vienna, Austria, July 2006.
- NMDA receptors appear in the late development at climbing fiber synapses in the mouse Purkinje cells
  Piochon C., Irinopoulou T., Brusciano D., Bailly Y., Mariani J.& Levenes C.
  Colloque de la société des Neurosciences, Montpellier, France, May 2007.
- NMDA receptors are expressed by adult Purkinje cells and contribute to the complex spike
  Piochon C., Irinopoulou T., Brusciano D., Bailly Y., Dusart I., Mariani J.& Levenes C.
  Neuroscience 2007 (SfN), San Diego (CA), USA, November 2007.
- NMDA receptors activation by the climbing fiber in Purkinje cell of adult mice
  Piochon C., Irinopoulou T., Brusciano D., Bailly Y., Dusart I., Mariani J.& Levenes C.
  First European Synapse Meeting, Bordeaux, France, March 2008.

I also presented these results during the 15th Doctoral School "3Cs" colloquium, Roscoff, France, Oct. 12, 2007. “NMDA receptors are expressed by adult Purkinje cells and contribute to the complex spike” (oral communication).

Table of contents

Table of illustrations

List of abbreviations

ADP	Afterdepolarization
AHP	Afterhyperpolarization
AMPA-R	Alpha-amino-3-hydroxy-5-methyl-4-propionic acid receptor
BBS	Bicarbonate buffered solution
BCM rule	Bienenstock-Cooper-Munroe rule
CaMKII	Calmodulin-dependent protein kinase II
CF	Climbing fiber
CRF	Corticotrophin-releasing factor
CS	Complex spike
DAG	Diacylglycerol
E_	Embryonic day
EAAT	Excitatory amino-acid transporter
EPSC	Excitatory postsynaptic current
EPSP	Excitatory post-synaptic potential
ER	Estrogen receptor
ERE	Estrogen Response Elements
GABA	Gamma-aminobutyric acid
GluRdelta2	Delta 2 glutamate receptor
Ho	Hotfoot
HP	Holding potential
iGluR	Ionotropic glutamate receptor
IP3	Inositol-trisphosphate
LJP	Liquid junction potential
LTD	Long-term depression
LTP	Long-term potentiation
mGluR1	Metabotropic glutamate receptor of the subtype 1
NMDA-R	N-methyl-D-aspartate receptor
NO	Nitric oxide
NOS	Nitric oxyde synthase
P_	Postnatal day
PBS	Phosphate-buffered saline
PC	Purkinje cell
PF	Parallel fiber
PKC	Protein kinase C
PLC	Phospholipase C
PPD	Paired pulse depression
PPF	Paired pulse facilitation
PSD	Postsynaptic density
RT	Room temperature
SEM	Standard error of the mean
SK or BK	Calcium-activated potassium channel with "small" or "big" conductance
SS	Simple spike
VGCC	Voltage-gated Ca2+ channel
VGluT2	Vesicular glutamate-transporter of the type 2
VOR	Vestibulo-ocular reflex
WT	Wild-type

1 Introduction

The cerebellum is traditionally regarded as a structure involved in motor control, but this view is now quite simplistic. Indeed, during the past decades, with the advent of functional neuroimaging methods, it has become increasingly clear that the cerebellum also plays an important role in higher level cognitive tasks. In the context of pathology, cerebellar dysfunctions are not only a cause of deficits in the coordinating motor activity or motor learning, but also induce various cognitive disorders. Thus, understanding how the cerebellum functions is a challenging question for biomedical research, in addition to any general principles applicable to the whole brain that we can gain from the study of this structure.

The beautifully regular and simple cellular organization of the cerebellar cortex is repeated in a crystalline manner across the entire cerebellum. The core of each fundamental cerebellar microcircuit is the Purkinje cell, one of the largest and most complex neurons in the brain, the most fascinating also. Because of its huge size (with a cell body of ∼20 μm in diameter in rat), this cell was the first neuron to be identified in 1837 (Figure 1.1), despite the low magnification and poor resolution of microscopes available at this time, by the famous Czech anatomist Johannes Evangelista Purkinje (1787-1869).

On their highly developed dendritic tree, Purkinje cells receive a tremendous amount of excitation originating from the spinal cord, cortex and other brain areas. After integration of this information, relayed by its two main glutamatergic afferences, climbing and parallel fibers, the Purkinje cell provides the sole output of the cerebellar cortex, by projecting its axon on the cerebellar deep nuclei. Any information exiting the cerebellum to the rest of the brain must go out from Purkinje cells. Knowledge of the connections between Purkinje cell and its afferences is thus particularly important when considering the role of these cells in processing different forms of information to ensure the overall function of the cerebellum.

During my thesis, I focused my attention on the way Purkinje cells receive and modulate their receptivity to excitatory inputs coming from glutamatergic afferences, throughout development and adulthood. Purkinje cells express a wide variety of glutamate receptors that mediate excitatory transmission. Among these diverse receptors, I was particularly interested by one type of ionotropic glutamate receptor, the N-methyl-D-aspartate receptor (NMDA-R).

Jan Evangelista Purkyně (1787-1869)
Physiologist and anatomist born in Libochovice, Bohemia (Czech Republic).

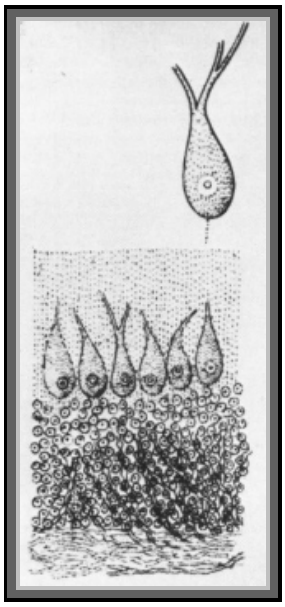

First description of the cerebellar Purkinje cell, drawn by J.E. Purkinje, and presented to the Congress of Physicians and Scientists in Prague, in 1837.

Figure 1.1: J.E.Purkinje and the famous cerebellar cell which bears his name

NMDA-Rs play a major role in many cerebral processes like development, neuroplasticity and neuronal death. They display unique features allowing them notably to act as “coincident detector”, of interest for instance in hebbian plasticity. They also mediate calcium signalling, which plays pivotal roles in many cellular processes. In Purkinje cells, a particular kind of NMDA-R is present during the first week of postnatal life in the mouse. However, their exact function in Purkinje cells is still a mystery. A study performed in collaboration during this thesis allowed us to propose their contribution in the neuroprotective depolarization that could

permit the survival of certain Purkinje cells during the time window of postnatal developmental cell death. Because no NMDA-Rs were detected after the first postnatal week, the Purkinje cells were widely considered as a rare example of an integrative neuron lacking NMDA-Rs. Actually, we demonstrated that, after a transient period of absence, between the second and the third postnatal week in mouse, a new type of NMDA-Rs appears at climbing fiber to Purkinje cell synapses, and is expressed throughout adulthood. We showed that these receptors take part in the climbing fiber excitatory transmission in a manner that suggests their role in many neuronal mechanisms, among them, synaptic plasticity. We also studied the possibility of a competition between this NMDA-R and another type of glutamate receptor that is specifically expressed in Purkinje cells, the delta2 glutamate receptor (GluRdelta2), which is essential for preventing extension and multiple innervation by climbing fibers. Our results do not support an interaction between these glutamate receptors. However, when innervation of Purkinje cell by multiple climbing fibers is maintained in adult mutant mouse lacking GluRdelta2, we observed that, NMDA-Rs participate only in the synaptic currents of the strongest climbing fiber. This suggests a role for NMDA-Rs in the choice and the stabilization of one climbing fiber, probably in a activity-dependent manner.

Before detailing and discussing these results, I will first present the cerebellum and its main connections, its cellular organization and development, and some of the main cerebellar functions. Then, I will focus on the excitatory network of cerebellar microcircuit, to cover the actors of the glutamatergic transmission at Purkinje cell synapses. Finally, NMDA-Rs and their patterned expression in Purkinje cells will be covered in the last part of this introductory literature review.

1.1 Cerebellum

1.1.1 Anatomical architecture and main connections

Located at the bottom of the brain, constituting the posterior part of the hindbrain, the cerebellum is divided into two large hemispheres connected by an intermediate region, the vermis. First comparative anatomical observations of the Dutch anatomist Lodewijk Bolk (published by Glickstein and Voogd, 1995), relating structure and function, identified three main cerebellar lobes: the anterior; posterior, and the flocculonodular lobes (Figure 1.2) According to the more recent phylogenic Larsell's subdivisions (Larsell, 1970), ten lobules can be distinguished in all mammalian species, and can be grouped in three main parts (overlapping partially the previous subdivisions):

- archicerebellum (composed of the flocculonodular lobe), the phylogenetically oldest part of cerebellum, implicated notably in balance and eye movements.
- paleocerebellum (comprising the anterior lobe, the vermis and its lateral borders, the paravermis), the first section of cerebellum to evolve, essentially concerned with regulating postural tone, and limb movements.
- neocerebellum (formed by the lateral hemispheres), last part to evolve, involved in planning movement and influencing neocortical activities.

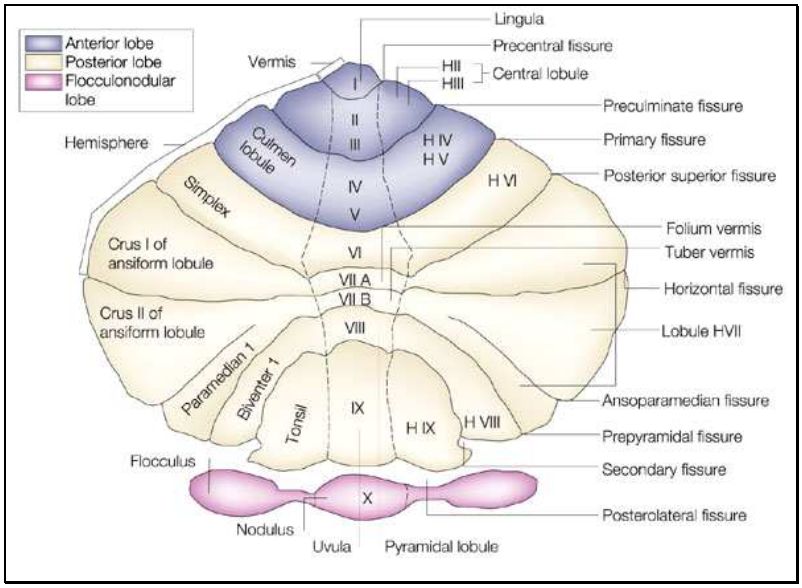

Figure 1.2: The cerebellum and its major anatomical subdivisions

Superior view of the unfolded cerebellum with schematic representation of its anatomical subdivisions. Colors represent Bolk's subdivisions, letters refer to Larsell's classification.
(from Manni & Petrosini, *Nature Reviews Neuroscience* 5, 241-249, 2004 doi:10.1038/nrn1347)

The cerebellum is connected to the pons and medulla by three major paired peduncles, composed of both afferent and efferent fibers (Palay and Chan-Palay, 1974, Figure 1.3):

- The superior peduncle mostly carries efferent fibers coming from deep cerebellar nuclei. It forms the major output pathway of the cerebellum projecting on various structures like the red nucleus, the thalamus (ventro-lateral and ventro-median), and the medulla.
- The middle peduncle. This one is the largest of the three peduncles. Entirely composed of afferent fibers originating from the pontine nuclei, it constitutes the cortico-ponto-cerebellar pathway, because fibers projecting on the pontine nuclei descend from the cerebral cortex.
- The inferior peduncle contains various types of afferent and efferent fibers. The spino-cerebellar tract comes from the medulla and conveys proprioceptive information to the archicerebellum. The inferior olive, that receives projections from the cerebral cortex as well as from the medulla, sends its own projections, the climbing fibers, through this peduncle on the whole cerebellum. It is also noteworthy that this peduncule carries to the vestibular nuclei the direct projections of Purkinje cells located in the flocculonodular lobe.

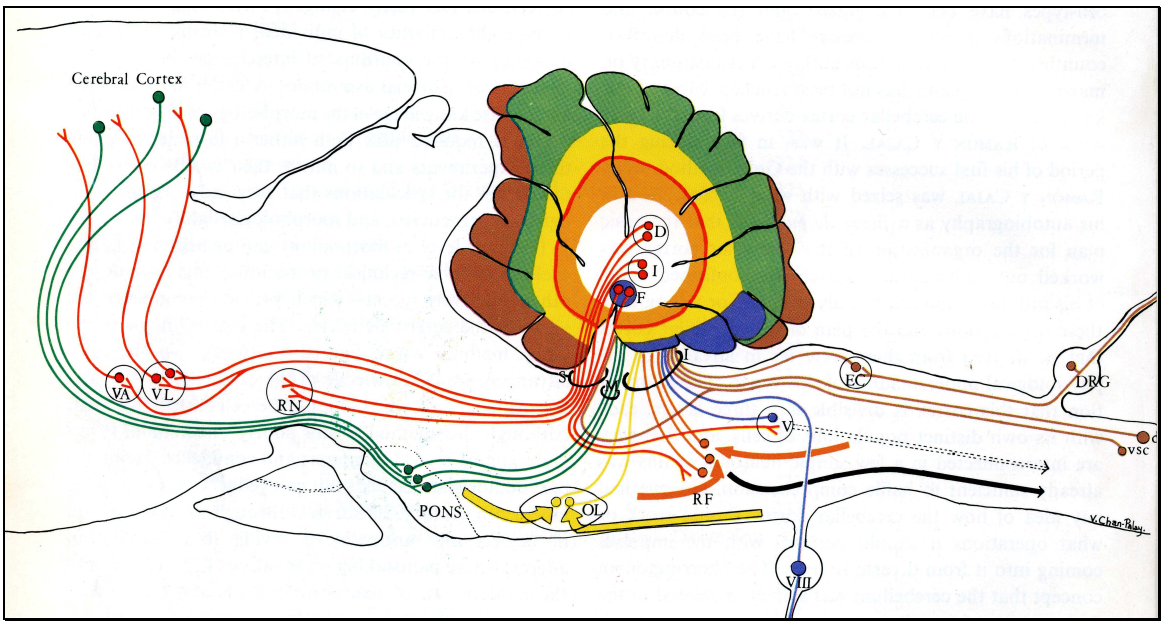

Figure 1.3: Afferents and efferents pathways of the cerebellum

The efferent pathways to the cerebellum and the distribution of these fibers in the cortex of the vermis are indicated by their respective colors. Afferents from the spinal cord (**brown**) reach the cortex mainly through the inferior cerebellar peduncle and distribute in the cerebellar anterior lobe and part of the posterior vermis (**brown**). Vestibular afferents (**blue**) distribute to the fastigial nucleus and the flocculonodular lobe (**blue**). Afferents from the reticular formation (RF) enter the cerebellum and distribute throughout the cortex (**orange**). The RF receives input from higher and lower centers (**orange arrows**). Fibers from the inferior olive (OL) (**yellow**) distribute to the entire cortex (**yellow**). Input to the OL comes from higher and lower brain centers

(**yellow arrows**). All of the above inputs enter through the inferior peduncle. Afferents from the pons (**green**) that receives inputs from the cerebral cortex (**green tracts**) enter through the middle peduncle to distribute to the entire cortex. The major efferents of the cerebellum (**red**) leave through the superior peduncle. The fibers from the dentate nucleus, interpositus nuclei, fastigial nuclei go to thalamus nuclei (ventrolateral and ventroanterior), red nucleus, RF and the vestibular nuclei.
(from Palay & Chan-Palay, 1974)

In the human brain, the cerebellum constitutes only 10% of the total brain volume but contains roughly half of the total number of brain neurons (Zagon et al., 1977). This impressive amount of neurons is extremely organized in this remarkable structure, described extensively since the first studies of Cajal (1911) and Eccles (1967) on the cerebellar anatomic and functional organisation.

1.1.2 Cellular organization of the cerebellum

The cerebellum has a relatively simple architecture: a three-layered cerebellar cortex (molecular, cellular and granular), a *corpus medullare* (white matter), where four deep nuclei are located (fastigial, *interpositus* [*globase* and emboliform], and dentate nuclei Figure 1.4a). Five major types of neurons have been identified in the cerebellar cortex, plus recently, Lugaro and unipolar brush cells. Five are inhibitory GABAergic neurons (Purkinje, Golgi, basket, stellate and Lugaro cells), and two are excitatory glutamatergic neurons (granule and unipolar brush cells). These different neurons take place in a highly uniform cytoarchitecture (Figure 1.4c and Figure 1.5). How are they interconnected?

One of the two major inputs to the cerebellum is provided by the mossy fibers which come from the brain stem (in particular from the pontine nuclei) and spinal cord. These glutamatergic fibers, that send collaterals to the deep nuclei, ascend to the granular layer to synapse on granule cells in specialized domains named glomeruli. Granule cell axons extend into the uppermost layer of the cortex (the molecular layer) where they bifurcate in “T”. The parallel fibers (PF) arising as axons from a single granule cell typically distribute information to over 2,000 Purkinje cells, via excitatory glutamatergic neurotransmission. Each Purkinje cell can receive converging input from over 200,000 granule cells via these PFs in rat cerebellum (Napper and Harvey, 1988).

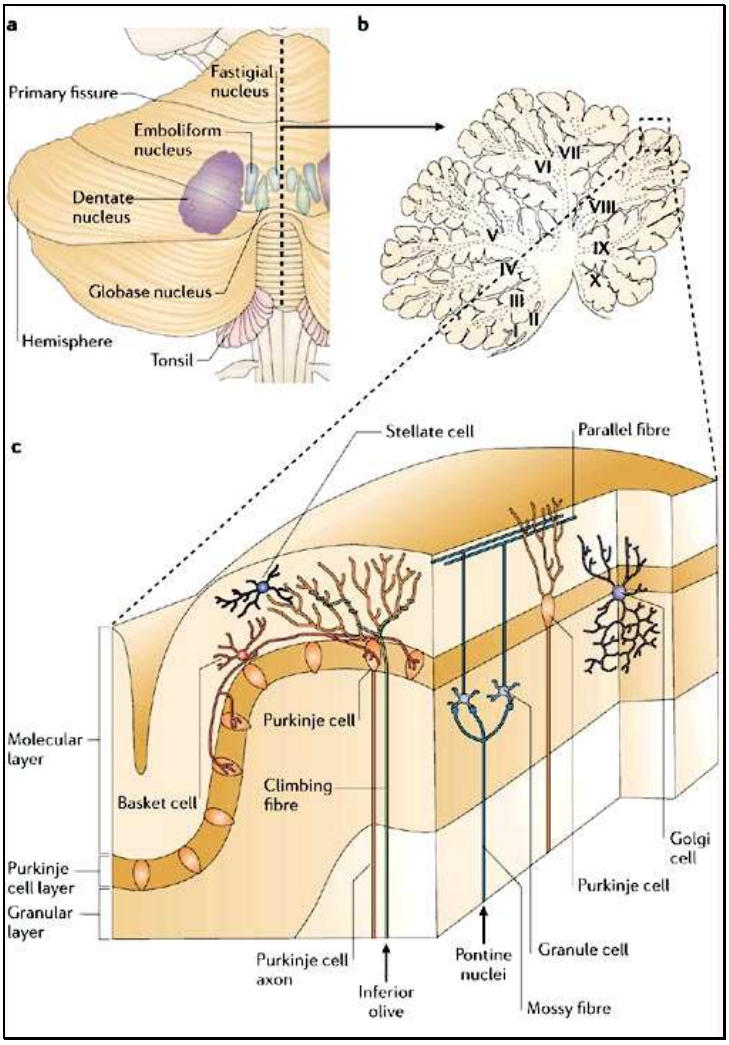

Figure 1.4: Organization of the cerebellar deep nuclei and cerebellar cortex.
(a) Posterior view of the human cerebellum, showing the cerebellar nuclei embedded below the cerebellar cortex. **(b)** Drawing of midsagittal cross-section through the cerebellum (dotted line indicates the plane of section), showing lobular organization. Each of the ten lobules is demarcated by a Roman numeral (I–X). **(c)** Cut-away illustration of an individual cerebellar cortical lobule, indicating the presence of three layers. The figure shows the relative positions of Purkinje cells and their main inputs (parallel and climbing fibres).
(from Ramnani *Nature Reviews Neuroscience* **7**, 511–522 (July 2006), doi:10.1038/nrn1953)

In addition, Purkinje cells receive glutamatergic input from climbing fibers (CF), which arise from the inferior olive. Unlike a PF, which makes a single synapse with Purkinje cells, CFs go one-on-one with Purkinje cells, wrap around the cell body and proximal dendrites, making around 1500 synaptic contacts. These CF terminals have high probability of glutamate release, which makes the CF-Purkinje cells connection remarkably strong (Dittman and Regehr, 1998; Foster et al., 2002). Purkinje cells perform a complex integration of the vast amount of excitatory inputs they receive from different regions of the brain, together with the control of the inhibitory network. From the integration of this vast amount of information, Purkinje cells generate an output (a “decision”) that inhibits neurons of the deep cerebellar nuclei.

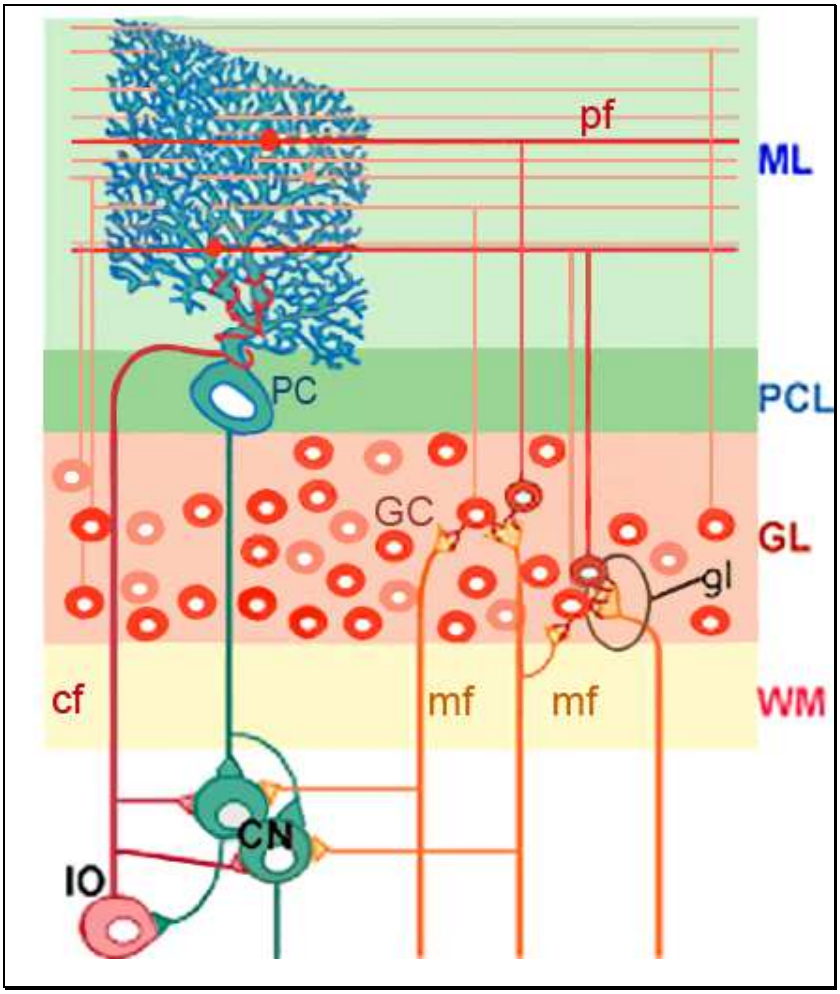

Figure 1.5: Schematic cellular organization of the cerebellar microcircuit.

Mossy fibers (**mf**) arising essentially from pontine nuclei send collaterals on neurons of the cerebellar nuclei (**CN**), deeply buried in the white matter (**WM),** and terminates their course by contacting granule cells (**GC**) in the granular layer (**GL**), in areas called glomeruli (**gl**). Each terminal of mossy fiber is contacted by dendrites from 50–60 distinct granule cells. In addition glomeruli contain the GABAergic synapses between Golgi cells and granule cells, and the glutamatergic contacts between mossy fibers and Golgi cells (unrepresented). Axons of granule cells bifurcate in the molecular layer (**ML**) and contact Purkinje cell (**PC**) arborisation by "en passant" synapses. The climbing fiber (**CF**) arises from a neuron of the inferior olivary (**IO**). It sends collaterals on neurons of the deep cerebellar nuclei and contacts intimately Purkinje cell proximal dendrites. After integration of its excitatory inputs, Purkinje cell can generate an inhibitory output on the cerebellar deep nuclei. **PCL**: Purkinje cell layer.
(adapted from http://www.cdtdb.brain.riken.jp/CDT/About.jsp

1.1.3 Postnatal development of the cerebellar cortex

In human, the cerebellum continues to develop through childhood and adolescence, reaching its full structural growth by the 15th to 20th years of life (Diamond, 2000). In rodents, the cerebellum is also remarkably immature at birth (Woodward et al., 1971), and undergoes an intense period of maturation that lasts for about 3 weeks (Figure 1.6), and that prolongs up to 7-8 weeks (McKay and Turner, 2005).

In early postnatal days, all Purkinje cells are innervated by multiple CFs (Crepel et al., 1976; Mariani and Changeux, 1981; Crepel, 1982). These multiple CFs initially form synapses on the perisomatic processes of Purkinje cell in newborn mice (Chedotal and Sotelo, 1993). Progressively, CFs forsake the soma to invade the Purkinje cell's proximal dendrites where they make strong synaptic contacts (Palay and Chan-Palay, 1974). Supernumerary CFs are eliminated eventually with the progress of postnatal development, and mono-innervation is attained by the end of the third postnatal week in mice (Kano et al., 1995). There have been several decades of investigations to understand the mechanisms of this selective activity-dependent regression. However, this question remains uncompletely resolved. The current view on the subject makes the developmental long term plasticities key players of these processes.

In the mouse, morphological data demonstrated that the synapses between PFs and Purkinje cell are established at around P7 (Zhao et al., 1998). Granule cells are generated by the vigorous proliferation of their progenitors in the external germinal layer during the first two postnatal weeks. This leads to a huge number of cells. Post-mitotic granule cells then bilaterally extend their axons, the PFs, and their cell bodies migrate downward in the developing molecular layer. By the third postnatal week, they finally settle in the internal granular layer underneath the Purkinje cell layer. During these first three weeks, cells in the pia mater play a role in granule cell proliferation and migration, whereas Bergman glia extends their processes into the molecular layer, guiding migrating granule cells (Altman, 1975). Internal granule cells further differentiate, forming synapse complexes in glomeruli that gather excitatory afferent mossy fibers and inhibitory Golgi cell axons. Some differentiating granule cells undergo an apoptotic cell death, which is thought to ensure the fine-tuning of the proper cell numbers and connectivity.

Simultaneously, Purkinje cells undergo a massive outgrowth of dendrites and form elaborate arborizations containing numerous synapses with extending PFs. Supernumerary CFs are pruned away by competing with PFs. In addition, the competition for Purkinje cell territories is mutually regulated between PFs and CFs by their respective activity.

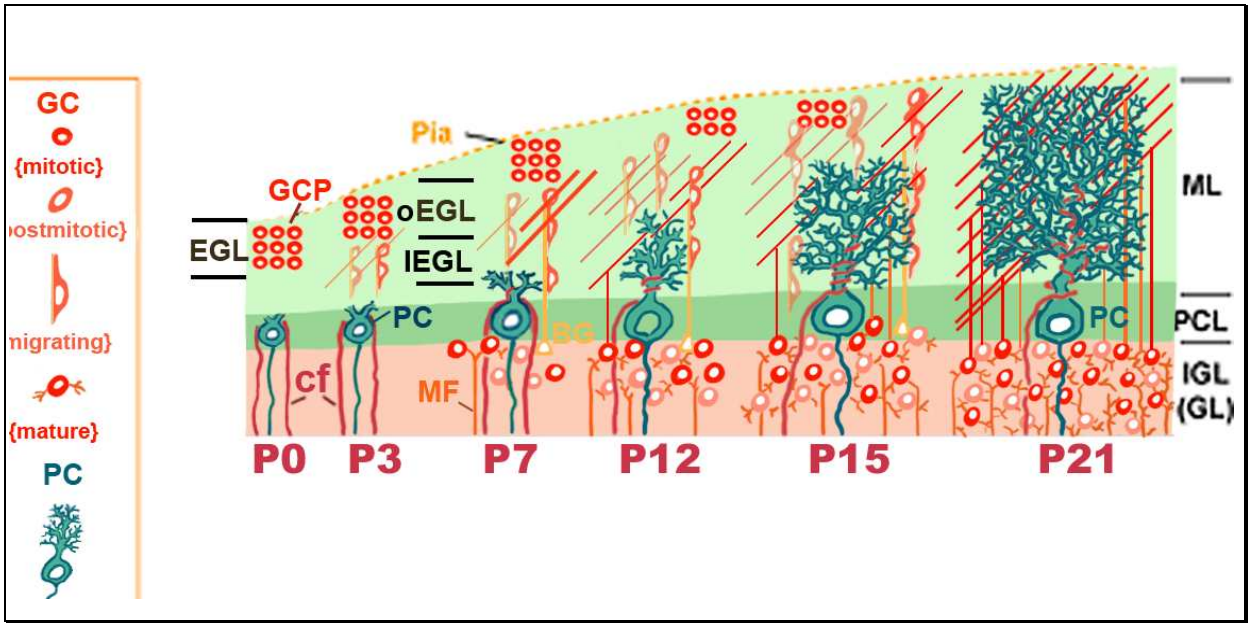

Figure 1.6: Postnatal development of the cerebellar cortex in mouse.

Schematic representation of the mouse cerebellar cortex at its main developmental stages during the three first postnatal weeks (P: postnatal day). EGL: external granular layer, GCP: granule cell progenitors, GL: granular layer, IGL: internal granular layer, ML: molecular layer, PCL: Purkinje cell layer; BG: Bergmann glia.

(adapted from http://www.cdtdb.brain.riken.jp/CDT/About.jsp)

1.2 Cerebellar functions

1.2.1.1 Cerebellum and motor control

How is information processed in the stereotyped cerebellar microcircuit? Independently of learning, the cerebellum plays a role in the adequate execution of movement. There are several trends of theories about cerebellar functions, sometimes controversial. Many of them are based on the notion that cerebellum contains “internal models” of the motor apparatus. These internal models encode the representation of dynamic properties of body part that enables the central nervous system to predict the consequences of motor commands and to determine those required to perform specific tasks. The internal model mimics the behaviour of the sensorimotor system in the external environment, and helps the brain, by prediction, to perform the movement precisely, without the need to refer to feedback from the moving body part. These internal models allow to predict the more adequate set of actions in a given context but the changes in the context, or the learning of new movements, requires them to be plastic. For this reason, in addition to this classical view of its acute correction of motor programs, the cerebellum has long been proposed to be the place of motor learning.

1.2.1.2 Cerebellum and motor learning

It is thought that the cerebellum might store motor memory in the form of internal models (Imamizu et al., 2000; Kawato et al., 2003).The unusual architecture of the cerebellar cortex first inspired theoretical models of its function, later confirmed by experimentation. Brindley (1969) proposed that we initially generate movements "consciously," under higher cerebral control. As the movement is practiced, the cerebellum learns to link this movement to the context in which it is executed. Marr and Albus (in 1969-1971), soon followed by Ito (1972), proposed that the linkage between the contextual input and the appropriate motor output is established and stored in the cerebellar neuronal microcircuit, through the PF-Purkinje cell synapses. This is the so called Marr-Albus-Ito model of learning in the cerebellum (Figure 1.7). The PF-Purkinje cell connection is modified during the period of learning by the activity of the CF which conveys error signals and induces a long term change in synaptic strength. This change is input specific and is named the long-term depression (LTD) of PF–Purkinje-cell synapses (for reviews, see Ito, 2001, 2006). When the linkage is complete, the occurrence of the context (represented by a certain input to the cerebellum) will trigger through the cerebellar microcircuit the appropriate motor response (output). This explains how we become able to move skillfully after repeated practice. The "learned" movement is

distinguished from the "unlearned" conscious movement by being automatic, rapid, and stereotyped. It is worth mentioning here that the first experimental evidence of LTD in the early 1980s came from the observation of changes in the rate of discharge of rabbit Purkinje cells *in vivo* (Ito et al., 1982; Ekerot and Kano, 1985). These changes were attributed to synaptic plasticity. Even though this LTD was confirmed by the study of synaptic currents later on, one can not exclude that a part of this plasticity could rely on intrinsic plasticity.

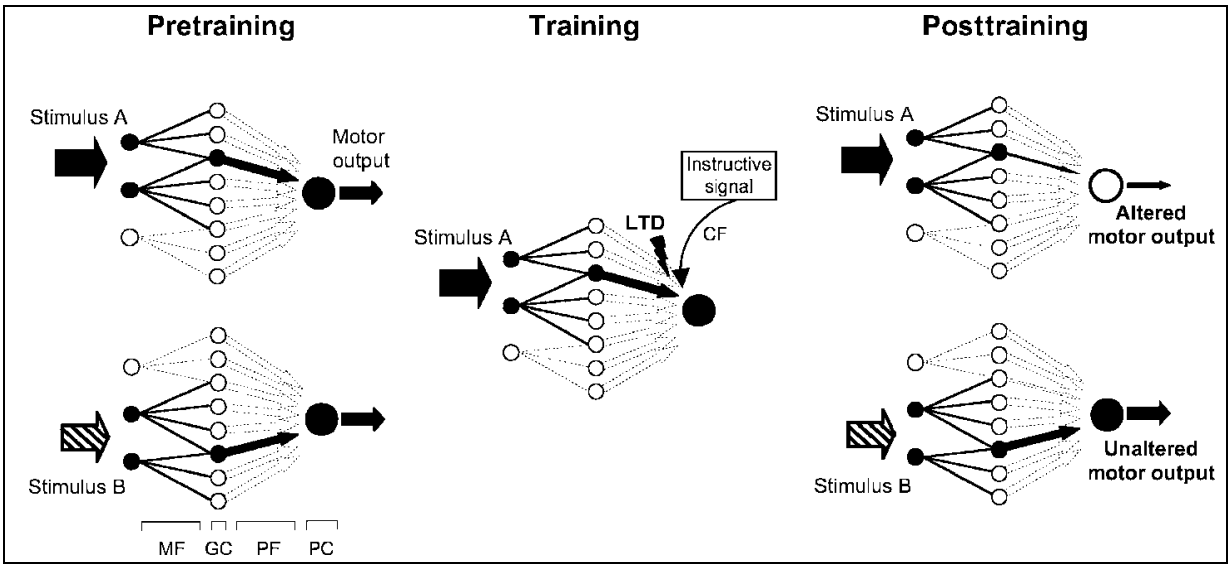

Figure 1.7: The Marr-Albus model of motor learning.

In this model, sparse reencoding in the cerebellum enables learning to create very precise stimulus-response mappings. Granule cells (GC) spike only when sufficient mossy fiber (MF) input is present, causing overlapping mossy fiber input patterns to be reencoded in nonoverlapping populations of granule cells. Plasticity controlled by climbing fibers (CF) weakens the strength of parallel fiber (PF)–Purkinje cell (PC) synapses (via LTD, indicated by the lightning bolt). LTD alters the efficacy of stimulus A firing the Purkinje cell and thus produces altered motor output. Because stimulus B activates different PFs than stimulus A activates, the motor response to stimulus B is unaltered by training. Open circles and dotted lines indicate inactive neurons and synapses. Filled circles and solid lines indicate active neurons and synapses. The thin PF arrow indicates a synapse weakened by LTD.
(Figure extracted from Boyden et al, Annual Review of Neuroscience Vol. 27: 581-609, July 2004)

Since the Marr-Albus-Ito model, cerebellar functions of sensorimotor integration and control motor have been substantiated by an impressive body of evidence. Experimental studies of simple behavioural models of motor learning, like the adaptation of the vestibulo-ocular reflex (VOR), or the associative eyeblink conditioning, have strengthened this theory (Bracha, 2004; Manzoni, 2007). In addition, LTD can be studied in cerebellar slices *in vitro* which provide means to dissect the underlying cellular mechanisms (Ito, 2001). As a consequence, the PF-Purkinje cell LTD has been extensively studied and appear to be important in the cerebellar motor learning, but many other sites and types of plasticity, synaptic and non-synaptic, also

exist in the cerebellar circuit, for reviews, see (for reviews, see Hansel et al., 2001; Boyden et al., 2004; De Zeeuw and Yeo, 2005). These additional plasticities probably also contribute to the cerebellum-dependent learning. Here are some of different forms and sites of plasticity, other than the classical PF-Purkinje cell synaptic LTD, identified in the cerebellar circuit:

- presynaptic long-term potentiation (LTP) PF-Purkinje cell synapses (Salin et al., 1996; Linden and Ahn, 1999; Qiu and Knopfel, 2007),
- postsynaptic LTP of PF-Purkinje cell synapse(Lev-Ram et al., 2002; Lev-Ram et al., 2003),
- postsynaptic CF-Purkinje cell LTD (Hansel and Linden, 2000)
- LTP and LTD of inhibitory interneuron - Purkinje cell synapse (Jorntell and Ekerot, 2002),
- LTP and LTD of PF- interneuron synapse (Rancillac and Crepel, 2004),
- LTP and LTD of mossy fiber-granule cell synapse (D'Angelo et al., 1999; Gall et al., 2005),
- LTP and LTD of synapses received by deep nuclear cells (Racine et al., 1986; Aizenman et al., 1998)
- non-synaptic changes (intrinsic plasticity) in cerebellar neurons (Schreurs et al., 1998).

This variety of cellular mechanisms provide the cerebellum with a wide flexibility to refine the code and dynamics of learned responses, enable storage of motor memories over different timescales, and allow bidirectional alteration of movement amplitude. However, going from the cell to the behaviour still remains a big step to pass over.

Finally, if internal models theory explains the control motor capacity of the cerebellum, this concept is also instrumental in understanding the involvement of the cerebellum in “cognitive” higher functions (Ito, 2005, 2008). In this case, the internal models reproduce the properties of mental representations in the cerebral cortex.

1.2.1.3 Cerebellum and cognition

The most important function of the cerebellum may be to coordinate motor function so that movements can be performed smoothly, but new evidence has emerged during recent years, indicating that the cerebellum may also play a key role in cognitive process in the central nervous system. First evidence for the involvement of the cerebellum in cognition arose from the demonstrations of its anatomical connections with multiple cortical regions including frontal and parietal cortex, through the pons and thalamus (Middleton and Strick, 1994;

Schmahmann, 1996; Middleton and Strick, 2001; Allen et al., 2005). These pathways facilitate cerebellar incorporation into the distributed neural circuits governing intellect, emotion and autonomic function in addition to sensorimotor control.

Using *in vivo* neuroimaging, extensive studies have also demonstrated during the past decade that the cerebellum is co-activated with prefrontal and temporo-parietal cortices during a variety of mental activities (even when motor activity is well-controlled), for instance in emotion attribution, language tasks, facial recognition, directed attention, theory of mind attributions, mental calculations, various types of memory (Parsons and Fox, 1997; Cabeza and Nyberg, 2000; Ioannides and Fenwick, 2005). However, in many cases, activation of the human cerebellum in imaging studies may also be related to actual or planned movement of the eyes, vocal apparatus or fingers (Glickstein, 2007). In addition, the extreme folding and the long latency of the bold signal detected in fMRI make the cerebellum a structure that is hard to study with this technique. Therefore, these imaging studies must be carefully interpreted.

Lesion studies have been a classic method for studying regional functions. Many studies have suggested that the primary effect of lesions in the cerebellum is impairment in motor coordination or motor learning, supporting the prevailing view of the primary cerebellar functions (Bastian et al., 1998). However other more subtle functions can also be affected by cerebellar lesions. Cognitive and affective deficits have been reported in case of lesions of posterior cerebellar regions in adult patients (Exner et al., 2004). Time perception and production are impaired in subjects with cerebellar injuries, suggesting that the cerebellum might facilitate time estimation (Keele and Ivry, 1990; Mathiak et al., 2004). Other studies have demonstrated that cerebellar lesions might produce symptoms that are similar to those of psychiatric disorders, such as mutism (Ersahin et al., 1997). However, lesions studies hold limits, since cerebellar lesions do not systematically produce psychotic symptoms, as they do not always manifest ataxic motor syndromes.

An important domain of evidence involving the cerebellum in cognition has also emerged from observations of cerebellar impairments in various mental disorders such as dyslexia, autism or schizophrenia (for review, see Gordon, 2007). Decreased Purkinje cell size and decreased excitatory input to them from the granule cells have been reported in schizophrenia (Tran et al., 1998). In patients diagnosed with autism, a disorder that has many features in

common with schizophrenia, such as impairments in cognition and social awareness, the most consistently reported abnormalities are the selective loss of Purkinje cells and the cerebellar atrophy (Courchesne et al., 2004). Because the cerebellum seems to participate in many different cortical activities, cerebellar dysfunctions and particularly during the development of the brain could lead to many different types of cortical malfunction. In turn, this could lead to the wide diversity of symptoms and cognitive dysfunctions that can be observed in the clinical forms of schizophrenia, or autism. Interestingly, these pathologies are disorders of brain development, and as previously mentioned, the cerebellum is poorly developed at birth and display a slow postnatal development. Current working hypotheses suggest that faults of cerebellar development at microstructural level could result in altered interconnectivity between cerebellum and frontal cortex resulting in the impairment of diverse functional systems (emotional, sensory, autonomic, memory, etc.) (Courchesne et al., 2005; Andreasen and Pierson, 2008).

Investigating the development and the function of the cerebellum could help to better understand these pathologies. The central neuron of cerebellar function, the Purkinje cell, thus deserves particular interest. During my thesis, I endeavoured to understand more particularly how the excitatory glutamatergic transmission is mediated in this cell.

1.3 Actors of the glutamatergic transmission in Purkinje cells

Parallel and climbing fibers bring the two main excitatory inputs to the Purkinje cell. At both types of synapses, these fibers liberate glutamate as neurotransmitter. Who are the actors of this glutamatergic transmission? What are the resulting excitatory responses?

1.3.1 Glutamate receptors of Purkinje cells

1.3.1.1 AMPA-Receptors

Purkinje cells express different types of glutamate receptors. Alpha-amino-3-hydroxy-5-methyl-4-propionic acid receptors (AMPA-R) represent the major class and are expressed at both CF and PF synapses (Zhang et al., 1990; Petralia et al., 1998). In developing and mature Purkinje cells, AMPA-Rs mainly mediate fast excitatory transmission. They are heterotetramers, principally composed of Glu-R2, -R3 and -R1 subunits, with GluR2 being the most abundant (Lambolez et al., 1992; Ripellino et al., 1998). The GluR2 subunit determines the Ca^{2+} permeability of the receptor channel. In the absence of GluR2, the AMPA-R is Ca^{2+} permeable, whereas the presence of GluR2 reduces considerably its Ca^{2+} permeability. Thus, the contribution of Ca^{2+} influx through AMPA-Rs seems to be functionally negligible (Kuruma et al., 2003). AMPA-Rs activation in Purkinje neurons can however provide the depolarization necessary for the opening of voltage-gated Ca^{2+} channels (VGCCs), which contribute to synaptic Ca^{2+} signaling.

1.3.1.2 Kainate receptors

In contrast to AMPA-Rs, Kainate receptor expression is low in Purkinje cells, especially in mature animals (Hausser and Roth, 1997; Ripellino et al., 1998). However, both GluR5 and KA1 kainate receptor subunits are expressed by Purkinje cells (Wisden and Seeburg, 1993). It has been shown more recently that GluR5-containing kainate receptors could be responsible for ~5% of the CF-excitatory postsynaptic current (EPSC) (Huang et al., 2004). However, it should be noticed that the animals used in this study were not adult (mice aged from P15 to P19). Thus the situation might be still different in the adult.

1.3.1.3 Metabotropic glutamate receptors

The metabotropic glutamate receptor of the subtype 1 (mGluR1), is strongly expressed in Purkinje cells at parallel fiber synapses, where it gives rise to a slow excitatory postsynaptic

current (Batchelor et al., 1994) in response to tetanic parallel fiber stimulation. mGluR1 is coupled to phospholipase C β (PLCβ) through Gq proteins, and leads to the production of diacylglycerol (DAG) and inositol-trisphosphate (IP3) that activates Ca^{2+} release from intracellular stores (Finch and Augustine, 1998). This Ca^{2+} combines with DAG to elevate protein kinase C (PKC) activity. mGluR1 has also been reported at CF-Purkinje cell synapses (Dzubay and Otis, 2002). At these synapses however, mGluR1 currents have been observed after CF stimulation: 1) when glutamate uptake is blocked, 2) when a train of stimulation is given to CF, indicating their peri- or extrasynaptic location (Dzubay and Otis, 2002) or 3) with the coincident presence of an mGluR1 agonist (Yuan et al., 2007). High levels of mGluR7 are also found in Purkinje cells terminals (Phillips et al., 1998; for review about mGluR7 in Purkinje cells, see Knopfel and Grandes, 2002). mGluRs are implicated in LTD and generate synaptic-induced retrograde signaling (Hartell, 1994; Levenes et al., 2001).

1.3.1.4 Delta2 glutamate receptors (GluRdelta2)

Remarkably, Purkinje cells also express delta2 glutamate receptors (GluRdelta2), which are orphan receptors expressed almost exclusively by these cells. GluRdelta2 are located specifically at PF–Purkinje cell synapses, except during a short period of the early development in which they are also found at CF synapses (Araki et al., 1993; Takayama et al., 1996; Zhao et al., 1998). GluRdelta2 have been cloned by sequence homology with AMPA-Rs and NMDA-Rs (Yamazaki et al., 1992a; Araki et al., 1993; Lomeli et al., 1993). Interestingly, the structural comparison with other ionotropic glutamate receptors has recently demonstrated that the amino acid composition of the ligand-binding cavity of GluRdelta2 is most similar to that of the NR1 subunit of the NMDA-R (Naur et al., 2007). Like NR1 subunit, GluRdelta2 can bind Glycine or D-serine. However, neither its agonist (if one), nor its physiological role, has been clearly identified.

Last but not least, NMDA receptors, which are the focus of this thesis, are also expressed in postnatal and adult Purkinje cells. They will be extensively treated in the last part of this review.

1.3.2 Glutamate Transporters

Often viewed as secondary actors of the glutamatergic transmission, glutamate transporters however deeply influence and shape synaptic transmission (for review, see Tzingounis and Wadiche, 2007). Excitatory amino-acid transporters (EAATs) rapidly bind released glutamate

to remove it from the extracellular space into glial or neuronal cells. This glutamate uptake is coupled to the transport of ions and its stoechiometry is responsible for keeping the tonic extracellular glutamate concentration at 25 nM, below the level which activates receptors (Herman and Jahr, 2007). In the cerebellum, Bergmann glial cells are closely apposed to Purkinje cells synapses (Palay and Chan-Palay, 1974); see Figure 1.8. At PF and CF synapses with Purkinje cells, Bergmann glial cells express predominantly EAAT1, with a small contribution by EAAT2 transporters (Furuta et al., 1997). Purkinje cells express not only the ubiquitous EAAT3 neuronal transporter but also the high-affinity EAAT4, which is expressed at a high density, in particular at CF synapses (Tanaka et al., 1997; Dehnes et al., 1998) and mediates a synaptic transporter current (Otis et al., 1997; Auger and Attwell, 2000).

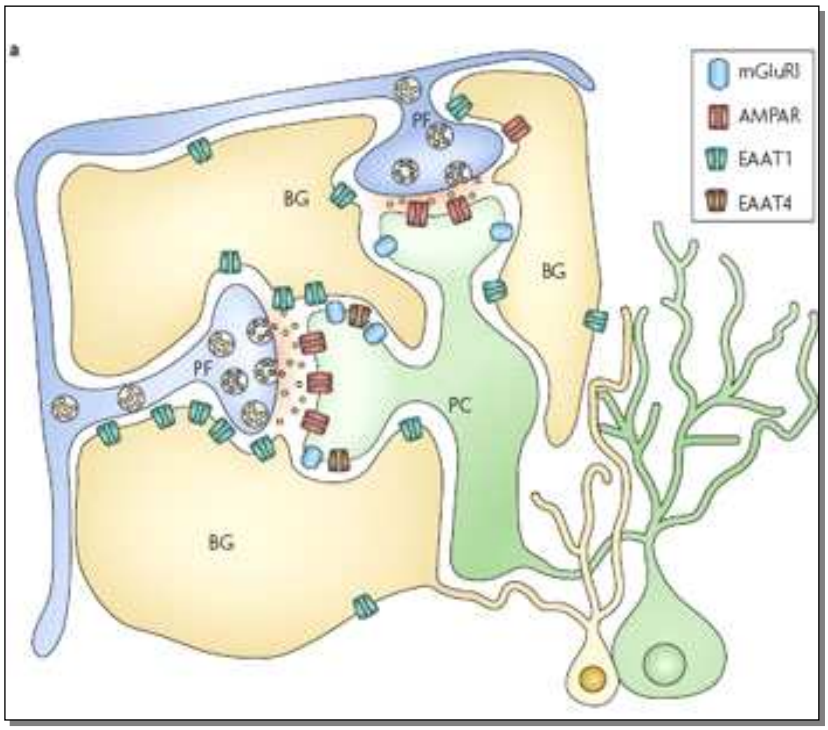

Figure 1.8: Organization of glutamate transporters at parallel fiber to Purkinje cell synapses.

Parallel fibres (PFs) originating from granule cells make en passant synapses on PCs. Each synaptic contact is nearly fully ensheathed by Bergmann glial (BG) membranes. Purkinje cell glutamate transporters (EAAT4) are located perisynaptically, whereas glial transporters face the synapse. Note that the scale of the various cellular components is distorted to more clearly emphasize the key points (figure extracted from Tzingounis and Wadiche, 2007).

One of the most important roles of glutamate transporters is to limit the activation of extrasynaptic receptors, for example, NMDA-Rs of Purkinje cells (see in Results chapter, 2nd part), or mGluRs that are pivotal for cerebellar synaptic plasticity (Hartell, 1994). Interestingly, in juvenile rats, stimulation protocols that induce a LTD at the CF-Purkinje cell synapse (Hansel and Linden, 2000; Shen et al., 2002), concomitantly induce a LTP of glutamate transporter currents through PKC activation (Shen and Linden, 2005). It could well be that CF-LTD relies, at least partly, on this LTP of glutamate transporters.

In conclusion, the patterned expression, the number and the activity of both glutamate receptors and transporters mediate and shape the excitatory input to Purkinje cells, as well as control the induction of their plasticity.

1.3.3 Excitatory responses evoked in Purkinje cells by its glutamatergic afferents

1.3.3.1 Parallel fiber response

In response to PF activation, Purkinje cell discharge in "simple spikes" (SSs) at frequencies that can attain rates of >200 Hz during motor performance (Thach, 1967). It has been estimated that ~50 PFs are enough to evoke a spike (Barbour, 1993). A single suprathreshold activation of PFs produces a Na^+ spike and a local dendritic Ca^{2+} signal that relies on Ca^{2+} entry through VGCCs (Eilers et al., 1995), whereas tetanic stimulation produces a biphasic response: the first component depends on AMPA-R activation, the second requires mGluR1 receptors.

1.3.3.2 Climbing fiber response

In contrast to PFs, CF discharge occurs at very low rate, ~1 Hz in quiescent animals (Armstrong and Rawson, 1979). Climbing fiber activation evokes a massive all-or-none spike of complex waveform and origin, the "complex spike" (CS). CS results from widespread activation of AMPA-Rs in the dendrite, associated to the activation of mGluR1 receptors. In addition, as we demonstrated in this thesis, there is also a NMDA-component in the CS in the adult. The Na^+ influx through AMPA-Rs depolarizes the Purkinje cell causing dendritic Ca^{2+} spikes that are carried mainly by P/Q- and T-types VGCCs. The elevation of internal concentrations of Ca^{2+} also activates calcium-activated potassium conductances (K_{Ca2+}) that are of two different types in Purkinje cells: the "small" and "big" K_{Ca2+}, named respectively BK and SK channels.

In acute cerebellar slices, during whole-cell current clamp recording from singe Purkinje cell activated by the CF, the depolarization spreads towards the soma and evokes a regular Na^+ spike that is recorded as the first active component in the CS (Figure 1.9). It has been suggested that both resurgent-Na^+ and Ca^{2+} currents contribute to the following slow complex spike components, and to the afterdepolarization (ADP), while a last slow afterhyperpolarization (AHP) is due to K^+ efflux (Schmolesky et al., 2002; Schmolesky et al.,

2005); Figure 1.9B. By evoking widespread dendritic Ca^{2+} transients (Miyakawa et al., 1992), the CF discharge is known to be a key signal for synaptic plasticity, in particular the LTD of PF-Purkinje cell synapses (see for review Ito, 2001).

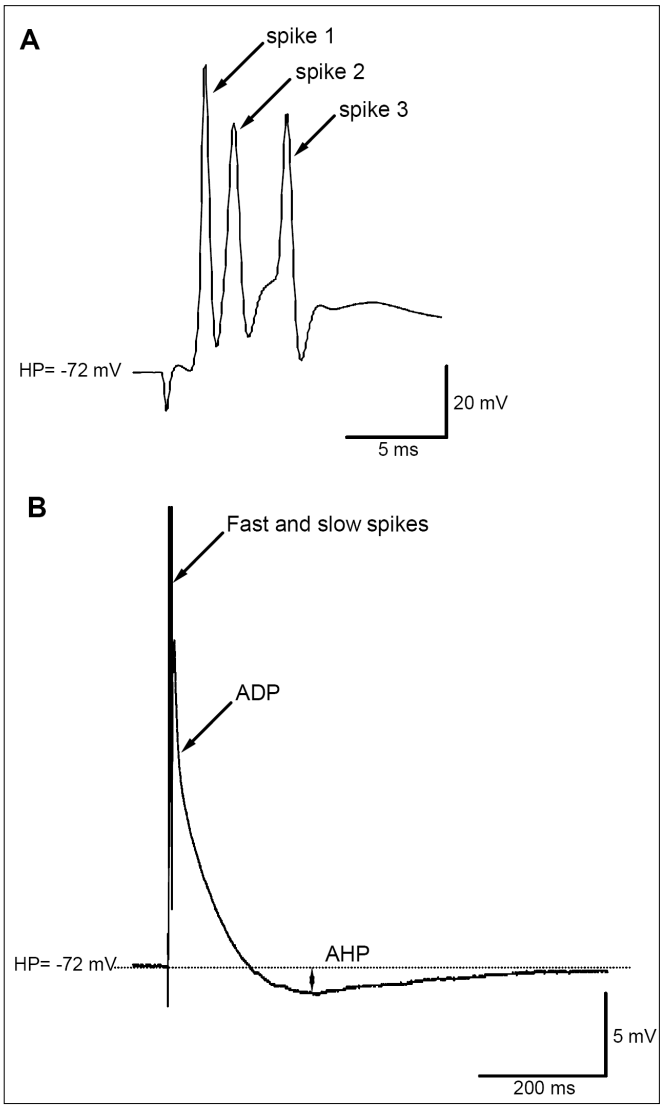

Figure 1.9: The climbing fiber excitation evokes a complex spike in the Purkinje cell.

(A) A complex spike recorded from the Purkinje cell soma demonstrates one fast Na^+ spike (spike 1) and one or four slower spikes at the top of a depolarization plateau. (B) Subsequent to the fast and slow spikes, a complex spike is composed of a slow afterdepolarization (ADP) and afterhyperpolarization (AHP).

1.3.3.3 Spontaneous activity

Purkinje cells are spontaneously active. This spontaneous activity has previously been attributed to the continuous glutamate release from PFs synapses (Eccles et al., 1967). However, in isolation from the rest of the cerebellar circuitry, or by blocking fast synaptic transmission, Purkinje cells tonically fire (Llinas and Sugimori, 1980b; Llinas and Sugimori, 1980a; Hausser and Clark, 1997). Because of their intrinsic membrane properties, relying in particular on non-inactivating Na^+ currents (Raman and Bean, 1997), Purkinje cells display high firing rate of Na^+ spikes, i.e. spontaneous simple spikes (Womack and Khodakhah, 2002; 2004). From P21 in mouse, as the cerebellum achieves its anatomical and functional maturation, Purkinje cells show a complex trimodal pattern of spontaneous activity in which

they continuously cycle among tonically firing, bursting, and silent modes (Womack and Khodakhah, 2002; McKay and Turner, 2005). The rate and pattern of the intrinsic activity of Purkinje cells is modified by synaptic inputs from CF and PFs. In particular, the CF input to Purkinje cell exerts an inhibitory action on the spike-generating system to maintain SS activity at a low level (Cerminara and Rawson, 2004). Similarly, the CS is followed *in vivo* by a pause in ongoing simple spike activity (Simpson et al., 1996). It has been suggested that the AHP component of the CS could cause this pause (Schmolesky et al., 2005). Thus, modulations of the CS components can have deep effects on the regulation of Purkinje cell spontaneous activity.

1.4 NMDA-receptors in Purkinje cells

The present review about NMDA-Rs in Purkinje cell was written in order to be submitted for publication.

1.4.1 NMDA-R: general properties

NMDA-Rs are ionotropic glutamate receptors that play a major role in many cerebral processes like development, neuroplasticity and neuronal death. They display unique features among ligand-gated ionotropic receptors. To be activated, they not only must bind both glutamate and the co-agonist glycine -or D-serine- (Johnson and Ascher, 1987), but they also require a coincident membrane depolarization, in order to relieve a Mg^{2+} block of the receptor ion channel (Mayer et al., 1984). This remarkable property of both voltage-dependent and ligand-gated channel confers on the NMDA-R the capacity to act as a molecular coincidence detector of simultaneous pre- and postsynaptic excitation. Since NMDA-Rs display a high permeability to Ca^{2+} ions, their activation causes a large influx of Ca^{2+} into cells (MacDermott et al., 1986) that initiates signal transduction cascades, triggering for instance LTD or LTP of synaptic currents.

NMDA-Rs are heteromeric complexes of different subunits classified, to date, in three families: NR1 (eight splice variants), NR2 (NR2A, -2B, -2C, and -2D), and the recently characterized NR3 subunits family (NR3A and NR3B). In the mouse, some NMDA-R subunits are differently denominated: NR-Zeta, NR-epsilon1, -epsilon2, -epsilon3, -epsilon4, NR-chi1, -chi2 which correspond to NR1, NR2A, -2B, -2C, -2D, NR3-A and -3B respectively. To simplify the understanding of the present thesis report, I have chosen the first denomination, whatever the species.

NMDA-Rs are tetramers of two mandatory glycine-binding NR1 subunits and two glutamate-binding NR2 subunits that can be identical or different. The type of NR2 subunit is critical in determining some of the key biophysical and pharmacological properties of the receptor, like agonist affinity, magnesium sensitivity, deactivation kinetics, modulation by polyamines and channel conductance (for review, see Dingledine et al., 1999). The Glycine-binding NR3 subunit could act as a dominant-negative subunit in the NMDA-R complex, notably by reducing calcium permeability (Nishi et al., 2001; Perez-Otano et al., 2001), but the role of this subunit remains to be clearly determined.

Each type of NMDA-receptor subunit and isoform exhibit a different developmental and regional pattern of expression in the brain, resulting in an important source of functional diversity among NMDA-Rs. In Purkinje cells, let us see what kinds of NR1 isoforms and/or NR2 subunits are successively expressed throughout postnatal life and adulthood.

1.4.2 Purkinje cells express NR1 subunits throughout the postnatal and adult life

While NR2 subunit expression has long been controversial, there was early compelling evidence for the NR1 expression by Purkinje cells, in young as well as in mature animals. Indeed, most of *in situ* hybridization (Moriyoshi et al., 1991; Monyer et al., 1992; Akazawa et al., 1994; Laurie and Seeburg, 1994; Monyer et al., 1994; Watanabe et al., 1994; Nakagawa et al., 1996) and immunohistochemical studies (Petralia et al., 1994a; Garyfallou et al., 1996; Hafidi and Hillman, 1997; Thompson et al., 2000) showed that the NR1 subunit is expressed by Purkinje cell as early as E13 in the mouse (Watanabe et al., 1994) and throughout adulthood.

NR1 occurs as eight distinct splice variants that influence NMDA-Rs properties and that are regionally and developmentally regulated (Sugihara et al., 1992; Laurie and Seeburg, 1994) for review see (Zukin and Bennett, 1995). NR1 isoforms result from the alternative splicing of exon 5 (the N1 amino-terminal cassette), exon 21 (the C1 carboxy-terminal cassette), and 22 (when this C2 carboxy-terminal cassette is deleted, the C2' cassette replaces it); see Figure 1.10. In the terminology of Hollmann et al. (1993), the eight NR1 splice variants are denominated NR1-1a, -1b, -2a, -2b, -3a, -3b, -4a and -4b. The number indicates the variant at the carboxy-terminal end (1 = no deletion; 2, 3, and 4 = deletions of C1, C2, C1+C2 respectively). In the a-subtype, N1 is absent, whereas the b-subtype displays N1 (Hollmann et al., 1993).

The N1 cassette directly controls proton inhibition (Figure 1.10A) and voltage-independent inhibition by Zn^{2+} ions of NMDA-Rs. Alternative splicing of the NR1 C-terminal affects the trafficking, cell surface expression, and synaptic targeting of NMDA-Rs in an activity-dependent manner (Ehlers et al., 1995; Okabe et al., 1999; Mu et al., 2003).

- All NR1 isoforms also contain a C0 cassette which, together with C1, mediates protein–protein interactions for instance with calmodulin (Ehlers et al., 1996), (Baude et al.)-actinin (Wyszynski et al., 1997), neurofilaments (Ehlers et al., 1998), and a

protein YOTIAO (Lin et al., 1998) as well as signalling to the nucleus (Bradley et al., 2006) and export from the endoplasmic reticulum (ER) (Wenthold et al., 2003).

- The C1 cassette has been shown to contain an endoplasmic reticulum retention signal (Scott et al., 2001) that can be masked by the C2' cassette (Standley et al., 2000), and/or by the association with NR2 subunit (Hawkins et al., 2004; Yang et al., 2007). Thus, NR1-1 subunits (C1/C2) alone are likely to be retained in the ER (see further).
- The C2 cassette is necessary for maintenance of dendritic spines in hippocampal pyramidal neurons (Alvarez et al., 2007). Indeed, either NR1-1 -containing (C0/C1/C2) or NR1–2 -containing (C0/C2) receptors are able to preserve some levels of spine density.
- The C2' cassette contains a terminal PDZ-binding motif that mediates interactions with PSD-95, PSD-93, synapse-associated protein-102 (SAP-102), and SAP-97 (for review, see O'Brien et al., 1998). mRNA splicing that regulates C2/C2' expression is activity-regulated such that activity blockade leads to enhanced expression of C2'-containing NR1 subunits and promotes surface expression of NMDA-Rs (Mu et al., 2003). In contrast, NR1–3 -containing receptors (C0/C1/C2') are insufficient to maintain spine density and do not enhance the spine recovery by C2-containing receptors. Thus, although the C2' domain is required for interactions with PSD-95 and may be important for anchoring to the PSD, it seems not to be necessary for spine maintenance.

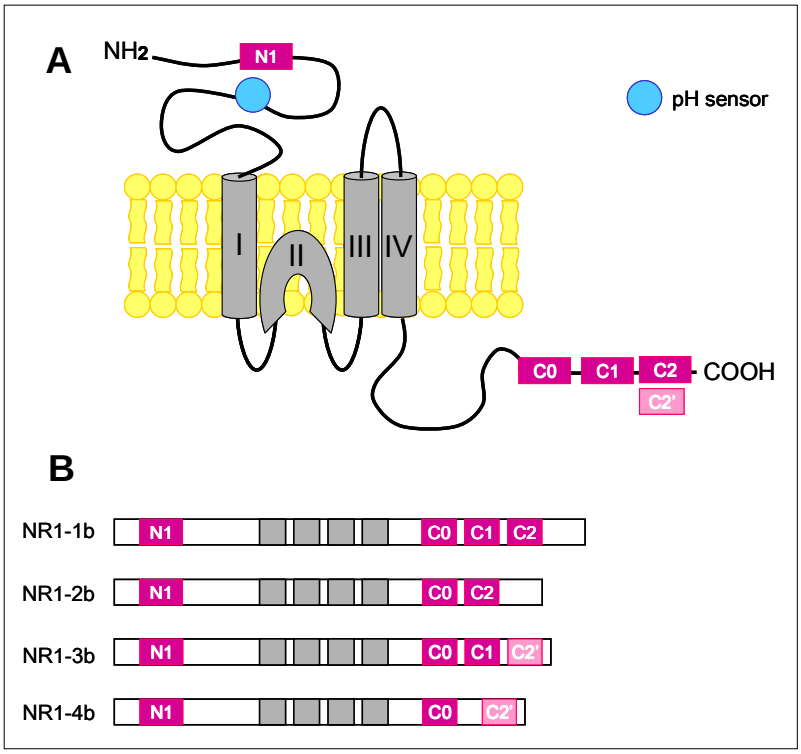

Figure 1.10: Schematic structure of the NR1 subunit and representation of some NR1 isoforms

(**A**) Like other ionotropic glutamate receptor subunits, NR1 possess four hydrophobic regions within the central portion of the sequence (gray). The second transmembrane domain forms a re-entrant loop giving an extracellular N-terminus and intracellular C-terminus. A "pH sensor" is present in the N-terminus domain. A surface loop encoded by the N1 cassette can limit proton access to this site. Polyamines, Zn2+, and ifenprodil also act, at least in part by modulating the proton sensitivity. (**B**) Schematic representation of the different splicing combinations in NR1 isoforms of the b-subtype.

In the rat cerebellum, *in situ* hybridization (Laurie and Seeburg, 1994; Laurie et al., 1995) showed that Purkinje cells express different NR1 splice variants, depending on the development stage. Because the alternative splicing of the NR1 mRNA has been shown to be activity-dependent, it could be of interest to understand the signals regulating this mechanism in Purkinje cells. Similarly, the actual influence of the NR1 isoforms on NMDA-Rs properties remains rather unexplored in these cells, maybe because these receptors were presumed to be absent in the adult. However, the type of NR1 subunit could be relevant to understand the diverse functions of NMDA-Rs expressed in Purkinje cells at different ages.

In addition to the influence of NR1 isoforms, the identity of NR2 subunits within the NMDA-R complex also strongly affects NMDA-R properties. NR2 subunits are differentially regulated during development and the different NR1/NR2 subunit combinations expressed in neonatal versus adult Purkinje cells make functional NMDA-Rs with remarkably different, and even opposite, properties.

1.4.3 NMDA-Rs of Purkinje cells in neonatal rodents (first postnatal week)

From P0 to P8, Purkinje cells mainly express NR1 lacking the C1 cassette (NR1-2, -4). NR1 splice variants of neonatal Purkinje cells are thus well suited to favour the expression of NMDA-Rs at the external membrane. Accordingly, NMDA-Rs currents are clearly detected in postnatal Purkinje cells (Rosenmund et al., 1992; Momiyama et al., 1996; Misra et al., 2000).

NR2 subunits of the neonate Purkinje cells are of the NR2D subtype. Both recombinant and native NR1-NR2D receptors that are expressed by immature Purkinje cells have unique properties (Momiyama et al., 1996; Misra et al., 2000). These are low single-channel conductance displaying two levels, a main one of 38pS and a sub-conductance of 18 pS. Typically of these receptors, transitions between the two levels are asymmetrical, transitions from the main to the sub-conductance being more frequent than in the other direction (Momiyama et al., 1996). These low-conductance channels are distinct in their properties from the ‘conventional’ 50 pS NMDA-Rs containing NR2A or –B subunits. They have low sensitivity to Mg^{2+} block and a low EC50 for glutamate (concentration producing half-maximal response) compared to NR1-NR2A or –B. Their high affinity for glutamate results in extremely slow deactivation kinetics in response to brief application of glutamate (Monyer et al., 1994). Channel openings have been shown to occur as late as 30 s after brief glutamate

applications (Misra et al., 2000). They also display no apparent desensitization in the continued presence of agonist while NR2A or –B containing NMDA-Rs rapidly and strongly desensitize (Wyllie et al., 1998; for review see Dingledine et al., 1999).

These properties have remarkable consequences: from a functional point of view, the NR1/NR2D receptors are easily activatable at low threshold of neuronal activity. From an experimental point of view, NR2D-containing NMDA-Rs can be easily detected with exogenous glutamate application compared to NR2A/B, especially if the method of agonist application is slow, as it is generally the case in slice preparations. This probably explains why they were the first NMDA-Rs to be detected in Purkinje cells (Dupont et al., 1987; Garthwaite et al., 1987; Krupa and Crepel, 1990; Yuzaki et al., 1990; Rosenmund et al., 1992). On the other hand, these specific properties, in particular high affinity for glutamate, make them poorly suitable for classical fast synaptic transmission. Accordingly, they have not been detected in CF excitatory postsynaptic currents of immature Purkinje cells (CF-EPSCs) (Llano et al., 1991; Lachamp et al., 2005). What can be their function?

During the three postnatal weeks, the cerebellum undergoes major anatomical changes (see Figure 1.6 and Figure 1.11). The developmental profile of NMDA-Rs subunits remarkably matches some key steps of the Purkinje cell excitatory synaptogenesis, suggesting that these receptors could play a role in this phenomenon. Among the different possibilities:
1) they could contribute to CF synaptogenesis and/or could participate to the regression of supernumerary CF synapses,
2) they could be involved in the neuroprotection of neonatal Purkinje cells,
3) and/or they could finally participate to the PF synaptogenesis.

1.4.3.1 NMDA receptors and climbing fibers synaptogenesis

By CF “synaptogenesis”, one has to understand here both the formation of synapses and the selection of the future only one contact.

NMDA-R blockade *in utero* (E17 to E20) does not impair AMPA-R expression and clustering in the early developing cerebellum (Lachamp et al., 2005). This suggests that NMDA-Rs are not necessary for CFs synaptogenesis, which starts as early as at E19 in rats (Morara et al., 2001). In addition, no obvious histological defects have been explicitly reported in the cerebellum of mice defective in the NR2D subunit (Ikeda et al., 1995), although it is worth mentioning that, in this latter study, the cerebellum may not have been carefully examined.

During the first postnatal week in rats and mice, the major, if not only, glutamatergic inputs of Purkinje cells are multiple CFs with similar strength. In rats, the multiple innervation by CFs has been reported to reach a peak at P5 (Crepel and Mariani, 1976; Crepel et al., 1976; Mariani and Changeux, 1981). The exact mechanism of the regression of supernumerary CFs is not yet fully known, but it has been shown that an early stage of the process of CF maturation consists in the differentiation of initially equally strong synapses into one large and several small synaptic inputs. In mice, differences in the strengths of multiple CFs become larger from P3 to P6 (Hashimoto and Kano, 2003). From the end of the first postnatal week, a massive elimination of supernumemary CFs occurs, leading to a final stage, at about P21 in mouse, in which all the Purkinje cells are innervated by a single CF. This regression of multiple innervation is impaired *in vivo* by chronic infusion of the NMDA-Rs antagonist, D-APV, between P4 and P5 (Rabacchi et al., 1992). On the other hand, this *in vivo* infusion of D-APV blocks all the NMDA-Rs of the zone. Thus, it is not clear if this effect results from NMDA-Rs of the Purkinje cells or of the other cells around.

Bosman et al. (2008) have shown that in rats, a new form of LTP is expressed uniquely and just for a restricted period of early development (from P4 to P10) in the large CF input. This LTP could allow the activity-dependent selection of the future unique climbing fiber. As major actors of some LTP processes, NMDA-Rs could participate to this activity-dependent selection of the future unique climbing fiber. However, this LTP is not blocked by antagonists of NMDA-Rs (Bosman et al., 2008). Thus, NMDA-Rs of immature Purkinje cells are unlikely to be involved in the regression of multiple innervation. This is in accordance with the fact that a big part of this phenomenon occurs when immature NMDA-Rs have largely disappeared (from P7 to P21 in mice).

1.4.3.2 NMDA receptors and the neuroprotective depolarization

Because NMDA-Rs of neonatal Purkinje cells have a high affinity for glutamate, display no apparent desensitization, slowly deactivate and are poorly inhibited by protons or Zn^{2+}, they can be easily and robustly activated by small transients of glutamate. Thus, neonate Purkinje cells would be more sensitive to excitotoxicity than their adult counterparts because of these NMDA-Rs. However, in primary cultures made from wild-type (WT) mice at E18 or P0, in which most of the Purkinje cells die within the first 4 days *in vitro* (div), NMDA-Rs in Purkinje cells were shown to directly enhance the survival of immature Purkinje cells *in vitro* (Yuzaki et al., 1996). In addition, Purkinje cells death was greater in cultures made from NR1 knockout mice. Conversely, adding exogenous NMDA or [(NR1-/-) granule cells] to the

cultures increased Purkinje cell survival (Yuzaki et al., 1996). Thus, immature NMDA-Rs of Purkinje cells *themselves* support their survival in culture.

This suggests that juvenile NMDA-Rs could protect Purkinje cells from developmental cell death *in vivo*. By the way of a collaborative study, we have provided evidence that depolarization protects immature Purkinje cells from apoptotic death, at least in organotypic cultures. We also showed that at this critical age, coculturing cerebellar slices with glutamatergic inferior olivary neuron preparation protected Purkinje cells (Ghoumari et al., 2006, see in Results, 1st part). These results support a pivotal role of excitatory inputs, provided by CF innervation, in the survival of neonatal Purkinje neurons. Although NMDA-Rs of immature Purkinje cells do not seem to play a direct role in the CF synaptogenesis, it can be proposed that they act as sensors of ambient glutamate released by CFs to promote the survival of Purkinje cells targeted by growing CF.

1.4.3.3 NMDA receptors and parallel fibers synaptogenesis

Do immature NMDA-Rs contribute to parallel fibers synaptogenesis? In fact, the temporal concordance between the increasing parallel fiber synaptogenesis and the disappearance of NR2D (Figure 1.11), rather suggests that parallel fiber activity could trigger the regression of NR2D subunits. Some experimental data support this hypothesis. Staggerer mice hold a mutation leading to a selective absence of synapse formation between parallel fibers and Purkinje cells, which leads to a secondary loss of most granule cells and to multiple innervation of Purkinje cells by climbing fibers. Staggerer Purkinje cells show a much greater sensitivity to NMDA than the cells of control mice (Dupont et al., 1984), suggesting that they retain the expression of the neonatal NR2D-containing NMDA-Rs. Actually, *in situ* hybridization as well as immunohistochemical data show that Staggerer Purkinje cells express both NR2D and NR2A (Nakagawa et al., 1996). It is thus rather tempting to hypothesize that neonatal NMDA-Rs are down-regulated by the parallel fiber/Purkinje cell synaptogenesis. However it remains difficult to distinguish between a causal versus concomitant relationship. Thus, the role of these juvenile receptors in synaptogenesis of Purkinje cells, if any, remains to be elucidated.

1.4.4 Second postnatal week: a gap in the expression of NMDA-Rs

1.4.4.1 Estrogen responsive element in the gene encoding NR2D

The GRIN2D gene that encodes for NR2D subunits contains four half-palindromic Estrogen Response Elements (EREs) in its 3' untranslated region (Watanabe et al., 1999). This characteristic repeat of ERE is not observed in the other genes coding NMDA-R subunits. More than one isoform of the estrogen receptor (ER) exists in mammals, and estrogen regulation via the ER-α and ER-β isoforms on the NR2D-ERE are not equivalent. It has been indeed shown that ER-α up regulates the NR2D mRNA whereas ER-β induces its down regulation (Vasudevan et al., 2002). In the cerebellum, the expression of estrogen receptors varied with age and cell-type, but not gender. In the developing rat cerebellum, ER-α is expressed in P3 Purkinje cells (Perez et al., 2003), whereas ER-β is first detected on postnatal day 6 (P6), with peak intensities of immunostaining coinciding with the initiation of axonal and dendritic growth that occurs between P7 and P8 (Jakab et al., 2001). Expression of ER-β remains high during maturation of Purkinje cell dendrites, and then decreases to a lower level maintained in the adult (Price and Handa, 2000; Jakab et al., 2001).

Active estrogen formation in the gonads does not occur during neonatal life but exposure to maternal estrogens can still persist for the few days after birth, and Purkinje cells may themselves synthesize estrogen during the postnatal period (Sakamoto et al., 2003). It is thus likely that estrogen acts directly on Purkinje cells through intranuclear ER-α to up regulate the NR2D mRNA expression in Purkinje cells during the first postnatal week. Then, from P6, estrogens probably down regulate the expression of NR2D subunit by acting on ER-β. This is in accordance with the expression profile observed for NR2D subunit during the Purkinje cell postnatal development, see Figure 1.11 (Momiyama et al., 1996).

At P6 in mouse, estrogens were shown to promote dendritic growth, spinogenesis, and synaptogenesis of Purkinje cells (Sasahara et al., 2007). In adult mouse, estrogens enhance induction of LTP at the PF to Purkinje cell synapse, whereas it does not affect LTD (Andreescu et al., 2007). Moreover, it increases the density of PF to Purkinje cell synapses, whereas it does not affect the density of CF synapses (Andreescu et al., 2007). At this age, NR2D expression may be down regulated by estrogens. This needs to be further studied and could give clues on the function of juvenile NMDA receptors.

1.4.4.2 NR1 homomeric NMDA receptors are not functional

Between the second and the third postnatal week, Purkinje cells do not seem to express significant amount of NR2 subunits anymore but express NR1 alone. As stated before, it is rather unlikely that NR1-homomers reach external membranes. Accordingly, NMDA currents detected in P5 young rat or mouse markedly declined with age (Crepel and Krupa, 1990; Krupa and Crepel, 1990). However, because some small currents remained detectable after the first postnatal week (Crepel and Krupa, 1990), NR1 homomers have been suspected to mediate these small currents in Purkinje cells, like those recorded in *Xenopus* oocytes expressing NR1 homomers (Moriyoshi et al., 1991). However, a recent study showed that these small homomeric currents observed in *Xenopus* oocytes are, in fact, caused by an endogenous NR2-like protein. This confirmed that NMDA-Rs are not functional as homomers (Schmidt and Hollmann, 2008).

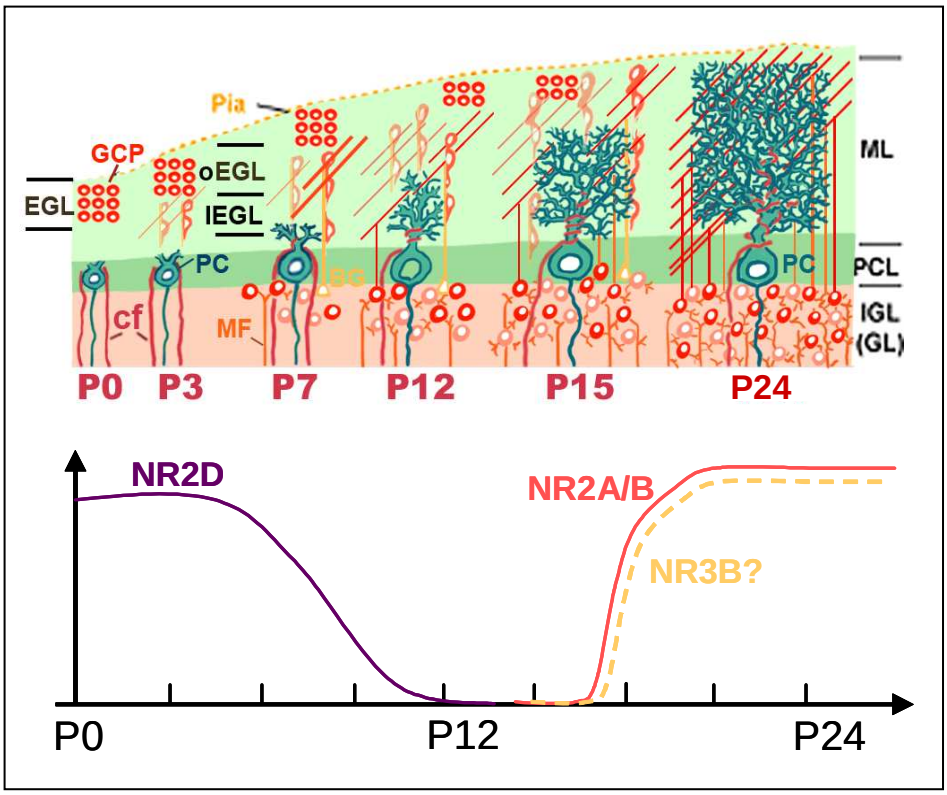

Figure 1.11: Schematic representations of the developmental patterned expression of NR2 subunits in Purkinje cells in respect of the main steps of Purkinje cell maturation

For detailed legend of the top figure, see figure 1.6.
Bottom figure is schematic. Left axis is not scaled because amounts of different NR2 subunits relative to each other are not known. The temporal profiles of NR2D and NR2A/B are however based on Momiyama et al. *J. Physiol. Lond (1996), 494.2, pp.479-492*, and Piochon et al. *J. Neurosc. (2007), 27(40):10797-108*, respectively. Although NR3B subunits have been recently evidenced in adult Purkinje cells, their temporal profile is still not known during postnatal development. Dotted line is thus speculative.

1.4.5 NMDA-Rs of the adult Purkinje cells: a controversy

1.4.5.1 Features of the NR1 isoforms expressed in the adult Purkinje cells

After P21 in rats as well as in adult humans, NR1 splice variants of Purkinje cell lack the N1 cassette (Laurie and Seeburg, 1994; Laurie et al., 1995 in rats; for human, see Scherzer et al., 1997). At physiological pH, NMDA-Rs that lack N1 are tonically inhibited (by ~50%), whereas those that include N1 are fully active. A surface loop encoded by the N1 cassette may act as a tethered pH-sensitive modulator of NMDA-R (Figure 1.10A). Polyamines could shield the proton sensor of NR1 and this may explain the ability of polyamines to potentiate NMDA-Rs containing NR1 subunit lacking N1 (Traynelis et al., 1995). Voltage-independent Zn^{2+} inhibition acts similarly on NR1 lacking the N1 cassette (Traynelis et al., 1998). The coassembly with NR2 subunits also influences the effects of N1 on Zn^{2+} inhibition (Chen et al., 1997; Traynelis et al., 1998; Rumbaugh et al., 2000). For instance, inhibition by proton or Zn2+ is stronger when the NR1 isoform lacking N1 is assembled with NR2A or NR2B (Traynelis et al., 1998). This is actually the case of adult Purkinje cells whose NR1 lack N1 and co-assemble with NR2A and to a lesser extent NR2B (Piochon et al., 2007; Renzi et al., 2007). The NR2A subunit (see below) is highly sensitive to Zn^{2+} inhibition (Chen et al., 1997) Therefore, the NMDA-Rs of mature Purkinje cells are expected to be tonically blocked at physiological pH by protons and Zn^{2+}. This could thus help to protect mature Purkinje cells from NMDA-R-mediated glutamate toxicity.

After the third week (P21), rats Purkinje cells express the NR1-1, -2 and -4 types (containing C1+C2, C2, C2' respectively; (Laurie and Seeburg, 1994; Laurie et al., 1995). Alvarez et al. (2007) recently showed that the physical interactions of the C-tail of NMDA-Rs with some proteins can mediate the long-term stabilization of synapses and spines. This maintenance of normal spine density and synapse stability requires the coexpression of the two specific splice isoforms of the NR1 subunit that contain the C-terminal C2 cassette (Alvarez et al., 2007). In adult Purkinje cells, the NMDA-Rs composed of C2-containing NR1 splice variants and NR2 subunits could thus favor the stability of some synapses and spines (in particular climbing fiber synapses, see below).

1.4.5.2 In search of NR2 subunits in mature Purkinje cells

Until recently, the expression of NR2 subunits in adult Purkinje cells remained unclear. Although differencies among various species used in the diverse previous studies can still

exist, it now appears in the light of more recent studies that, in mature animals, Purkinje cells express NMDA-Rs actually activated by the climbing fiber stimulation.

First electrophysiological studies with intracellular recordings already suggested the presence of NMDA-Rs in the proximal dendrites of Purkinje cells (Kimura et al., 1985; Quinlan and Davies, 1985; Sekiguchi et al., 1987) in adult rat and guinea pig. Similarly, other authors showed that 25 to 30% of adult Purkinje cells still respond to iontophoretic applications of NMDA (Dupont et al., 1987; Krupa and Crepel, 1990). Interestingly, an *in vivo* study in the adult rat revealed that NMDA currents induced in most Purkinje cells of control animals were no longer present after climbing fiber deprivation (Billard and Pumain, 1989).

In contrast with these studies performed with intracellular or extracellular recordings, patch-clamp studies focused on Purkinje cells from animals for the most younger than 3 weeks, this technique preferring cells with a less developped arborization for proper space clamp (Llano et al., 1991). Between P12 and P21, most of patch-clamp studies failed to detect any functional NMDA-Rs (Konnerth et al., 1990; Farrant and Cull-Candy, 1991; Llano et al., 1991). From these results, adult Purkinje cells have since been widely considered as neurons lacking NMDA-Rs. Purkinje cells indeed lack NMDA-R currents between the second and the third postnatal week.They nevertheless can not be considered as mature: in rat Purkinje cells, ~P12 to ~P18 corresponds to a period of rapid maturation, consisting of a marked expansion of the dendritic tree, that coincides with important changes in electrophysiological properties, for instance a rapid maturation of the Ca^{2+} spike-mediated discharge patterns (McKay and Turner, 2005). Howerver, after P21, there is still a maturation that prolongs up to P90. Thus, Purkinje cells maturation is not completed in animals younger than 3 weeks.

Besides electrophysiological studies, immunohistochemistry or *in situ* hybridization studies drew discrepant conclusions about the expression of NR2 subunits in adult Purkinje cells. NR2A mRNA was evidenced in rats as well as in humans (Akazawa et al., 1994; Rigby et al., 1996; Scherzer et al., 1997), whereas some other studies did not detect any NR2 mRNA in adult rodent Purkinje cells (Monyer et al., 1994; Watanabe et al., 1994). Similarly, low immunoreactivity for NR2A/B subunits was detected in adult mice (Yamada et al., 2001), while Thompson et al. (2000) found clear NR2-B labeling in Purkinje cells from adult rats and mice, as well as NR2-A labelling in mice only (Thompson et al., 2000, this study also points out the importance of species specificity in this debate). Finally, in addition to

differences among experimental procedures, discrepancies in different studies can be attributable to the different temporal limits to "adulthood" given by different authors (some authors considering rats or mice as "adults" at ~P21).

The question of the expression of functional NMDA-Rs in mature Purkinje cells thus deserved some re-examinations. Using adult mice aged more than 8 weeks, we not only demonstrated that mature Purkinje cells effectively express functional NMDA-Rs, but also that these receptors participate to climbing fiber synaptic transmission. Moreover, synaptic NMDA currents become detectable from the third week after birth (Figure 1.11). Our results of the present report that will be detailed in the second part of the results chapter, have been partly confirmed by the independent group of Stuart Cull-Candy in London (Renzi et al., 2007).

1.4.5.3 NR3B, an additional subunit in the game of Purkinje cell NMDA-R

The recent discovery of two novel types of NMDA receptor subunits - NR3A and NR3B (Ciabarra et al., 1995; Sucher et al., 1995; Nishi et al., 2001; Chatterton et al., 2002; Matsuda et al., 2002) - has further expanded the diversity of the NMDA receptors. Intensive research are now conducted on these "non-conventional" NMDA-Rs, but the actual knowledge on the subject still largely comes from studies using various heterologous expression system.

- In *Xenopus* oocytes and HEK296 cells, NR3A/B subunits have been shown to co-assemble with NR1 subunits to form excitatory glycine receptors, as they require glycine alone for activation, in the absence of glutamate (Chatterton et al., 2002; Smothers and Woodward, 2007). Whether these glycine-sensitive excitatory channels are functionally present in neurons is not entirely clear.
- In contrast to NR1, NR3A/B subunits bind glycine with very high affinity (Yao and Mayer, 2006). However, in the absence of NR1, NR3 can not substitute for NR1 to form functional channels as no glutamate/glycine-activated currents were induced when the NR3 was paired with any NR2 subunit (Chatterton et al., 2002; Smothers and Woodward, 2007).
- When coexpressed with NR1 and NR2, NR3 subunits strongly decreases NMDA-R currents, acting in a dominant negative manner (Nishi et al., 2001; Chatterton et al., 2002), and particularly reduces Mg^{2+} sensitivity of NMDA-induced currents and Ca^{2+} permeability (Matsuda et al., 2002). These tri-heteromeric NMDA receptors require both glutamate and glycine to be activated (Smothers and Woodward, 2007). Thus, in

the presence of NR2 subunits, excitatory glycine- NR1-NR2-NR3 heteromers may not exist in great abundance. Finally, NR3 subunits could also control membrane trafficking of NMDA-Rs (Matsuda et al., 2003).

By modulating the properties of NMDA-Rs, NR3 subunits may therefore contribute to the regulation of physiological and pathological processes, such as neurodevelopment, synaptic plasticity or excitotoxicity. Nevertheless, studies of native NR3-containing NMDA receptors are complicated by their pronounced desensitization by free glycine (Chatterton et al., 2002; Madry et al., 2007), the small amplitude of their currents, in addition to an atypical pharmacology (Smothers and Woodward, 2007). Transgenic mice lacking or over expressing NR3A subunits have thus been recently generated to study physiological roles of NR3 subunit (Tong et al., 2008). Analysis of hippocampal and cerebro-cortical neurons of these mice suggested that NR3A subunits are incorporated into endogenous NMDA-Rs and modulate their properties, in the same manner as previously observed in heterologous expression system. However, native glycine-excitatory NMDA currents have not been reported and could be specific of the NR3 expression in heterologous system (Tong et al., 2008).

Like NR1 and NR2 subunits, NR3A and NR3B are developmentally and spatially regulated. In the rat central nervous system, NR3A protein was found to peak at P8, and to decrease gradually from P12 to adulthood. In adult, only weak NR3A protein was expressed in the cerebellar cortex, more highly in granule cells than in Purkinje cells (Wong et al., 2002). In the whole brain, while NR3A mRNA decreases after the second postnatal week, NR3B mRNA is constant through development and in adult (Matsuda et al., 2002). Very recently, it has been shown that in 8-weeks old rats, Purkinje cells display a strong NR3B immunostaining; see Figure 1.12 (Wee et al., 2008). The NR3B labeling extended from the soma to the branched dendritic tree in the molecular layer, colocolazing with NR1 immunolabeling (Figure 1.13). In adult mice, the eventual presence of NR3B subunit in Purkinje cells will be discussed in the following results section. Because, NR3 subunits decrease the calcium permeability of NMDA receptors, their presence in mature Purkinje cells could have functional implications on the long term synaptic plasticity or other mechanisms such as neuroprotection from glutamate-mediated excitotoxicity.

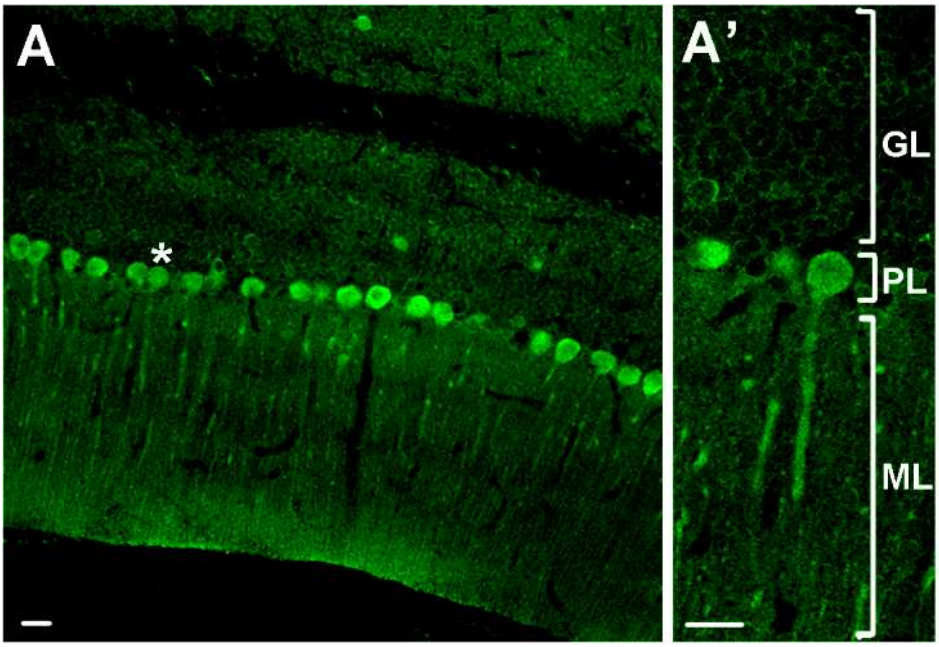

Figure 1.12: Fluorescent photomicrographs showing NR3B immunoreactivity in rat cerebellum.

(A) Distribution patterns of NR3B immunoreactivity (green) in the granule cells and Purkinje cells. NR3B staining in the molecular layer is mostly in the neuropil, although occasional staining of cell bodies was also observed. (A') is the high-magnification image of the area around the asterisk in A. ML, molecular layer; GL, granular layer; PL, Purkinje layer; 20 μm.

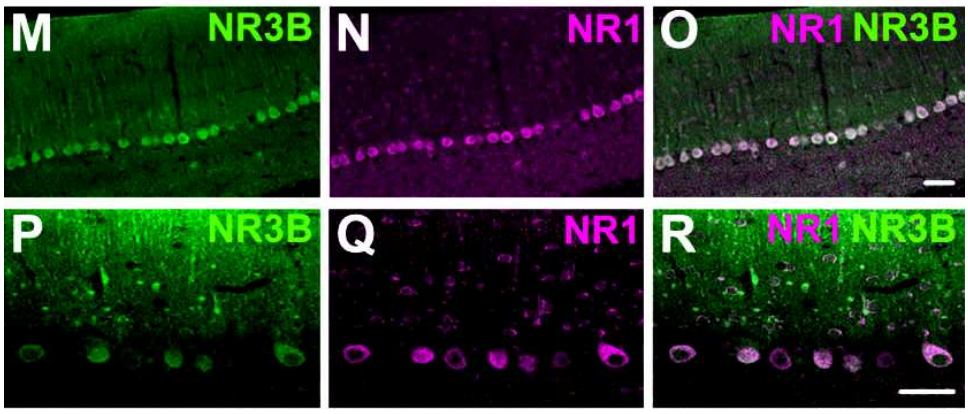

Figure 1.13:NR3B is coexpressed with NR1 in Purkinje cells.

Photomicrographs of cells showing immunoreactivity for both NR3B (green) and NR1 (magenta) in cerebellum (M–R). Colocalization of NR1 and NR3B is shown at low magnification in the substructures of the cerebellum (M–O). Colocalization of NR1 and NR3B is also shown at high magnification in (P–R). Scales bars 40 μm.
(Figures from Wee et al., 2008, *J Comp Neurol* 509(1): 118-35.)
functional implications on the long term synaptic plasticity or others mechanisms such as neuroprotection from glutamate-mediated excitotoxicity.

1.5 Problem and work hypothesis

While NMDA-Rs expressed in neonatal Purkinje cells have still unknown functions, those expressed in adult mouse Purkinje cells were so far ignored. The goal of this thesis was thus to clarify the function of the neonatal NMDA-Rs and to investigate the expression and the functions of the NMDA-Rs in adult mouse Purkinje cells.

Consequently, we started our study with the following work hypotheses:

1) Juvenile NMDA-Rs can induce prolonged depolarization of postnatal Purkinje cells. It was thus necessary to better understand the effect of depolarization in these cells, in particular during the time window of developmental cell death that occurs between P3 and P5.
2) The assumption that Purkinje cells do not express NMDA-Rs was mainly based on patch-clamp studies of rodents younger than 2 to 3 weeks. A careful examination of excitatory responses of Purkinje cells from “true” adult mouse (older than 8 weeks) was thus needed.

Using whole-cell patch-clamp recordings, completed by immunohistochemical studies (see in the following section, Material and Methods), here are the main results that we obtained:

1) By means of a collaboration, we demonstrated that depolarizing agents, including NMDA, or the presence of CFs, have a neuroprotective effect on postnatal Purkinje cells in organotypic cultures. This will be presented in the first part of the results chapter. This study provides some clues to understand the role of developmental NMDA-Rs in juvenile Purkinje cells.
2) We evidenced the presence of NMDA-Rs in adult mouse Purkinje cells, and their participation to CF responses. These results and their possible implications in adult mouse Purkinje cell physiology will be more extensively detailed and discussed in the second part of the Results chapter.
3) In a third part will be presented our study of NMDA-Rs expression in Purkinje cells lacking the GluRdelta2 receptors. In Purkinje cells remaining innervated by multiple CFs, we observed that NMDA-Rs mediate the responses of the strongest CF uniquely, suggesting their role in the selection and/or the stabilization of one afferent CF during development.
4) Finally, I will present our results in progress on the involvement of NMDA-Rs in PF-LTD induction in adult mouse Purkinje cell.

2 Materials and methods

2.1 Animals

Animals breeding and all the experiments were performed in conformity with animal care protocols approved by the French Ministry of Agriculture and the guidelines of the European Community Council. In accordance with the French Law, I received a specific formation authorizing to perform experiments on animals. A minimal number of animals was used and handled with maximum care to minimize their stress and suffering.

Except in the first study presented here (Ghoumari et al., 2006), in which we used Sprague-Dawley rats (*Rattus norvegicus*), we used C57Bl/6J mice (*Mus musculus*) provided by the "Elevages Janvier" (Le Genest-St-Isles, France). Ho-Nancy mice used in the third study presented in this thesis are on the C57Bl/6J background, and express the Nancy allele, in which the deletion in the GRID2 gene spans three of the four transmembrane domains of the GluR-delta2 protein. This mutant mouse has been previously described in (Guastavino et al., 1990) and (Lalouette et al., 2001).

2.2 Slice preparation

Equipment setup

Extractor hood. The use of the volatile anaesthetic 2-bromo-2-chloro-1,1,1-trifluoroethane (halothane) requires particular caution; animal anesthesia must be performed under an extractor hood equipped with the appropriate filter.

Instruments: standard fine tools and adequate dissection kit. For Pasteur pipette: the thin part of a Pasteur pipette is cut off. A pipette ball is attached to the cut end of the pipette, and the blunt end is used to gently move slices from one place to the other.

Dissection microscope: with a magnification factor of 5–10.

Vibratome: Vibratome Leica VT1000S, equipped with a cold light source, a magnifier glass, knife holder, a specimen disc. The inner buffer-chamber is filled with ice-cold BBS (bicarbonate buffered solution, see composition further) and the outer chamber with ice. The frequency is set at 6, the speed at 2.5 and cutting thickness at 180 µm.

Incubation chamber: a submerged chamber optimized to ensure sufficient oxygenation of the tissue is filled with BBS, and bubbled continuously with carbogen (95% oxygen, 5% carbon dioxide) at room temperature.

Dissection and slice procedure:

Animals are first anesthetized by halothane inhalation and then rapidly decapited. The skin is removed from the posterior part of the cranium. The skull is cut laterally and along the line separating the cerebellum from the forebrain, with micro-dissection scissors. The cerebellar vermis is removed from the brain, and rapidly transferred to ice-cold, carbogen saturated slicing solution in a Petri dish. Under microscope visual control, the meninges are gently removed, in order to facilitating the subsequent slicing. The vermis is slid laterally onto a thin film of cyanoacrylate glue on the cooled specimen disc that is next fixed in the vibratome chamber, then filled with ice-cold carbogen-saturated BBS. Parasagittal 180 µm-thick slices are cut and placed in the incubation chamber (containing carbogen-saturated BBS) for at least 60 min at room temperature, until use. Slices are generally usable for 5–6 hours after incubation.

2.3 Electrophysiology

Erwin Neher and Bert Sakmann developed the patch clamp in the late 1970s and early 1980s. This technique (Hamill et al., 1981) relies on the particular capacity of cellular membranes to form a tight contact with a glass pipette apposed to the cell surface. The recording of picoampere-sized currents with a good resolution and a relatively low background noise is allowed by the high resistance seal that can be obtained between the glass and the cell membrane (a "gigaseal", since the electrical resistance of the seal is in excess of a gigaohm). Patch-clamp technique has been adapted by (Edwards et al., 1989) for *in situ* cell recording, in acute brain slices.

Equipment setup

Vibration isolation table: in our case, a pneumatic system is used, with a compressed air supply. This isolates the experimental setup from vibrations.

Shielding and grounding: The setup is enclosed in a Faraday cage connected to the ground that shields from interference and electric fields. Furthermore, electrical apparatus (microscope, manipulators…) and any conductive material in the setup are grounded in the same single-point.

Upright microscope: our Zeiss Axioskop-FS microscope is equipped with the followings:

- Nomarski differential interference contrast optics,
- a water-immersion objective: 40 times, which enables long working distance (>2 mm electrodes are inserted at a steep angle of >25°),
- a magnifier, placed between the objective and a video camera CCD, offers 2.25 times magnification (Nikon). A black and white video monitor allows the visualization, without requiring the microscope oculars.

Patch-clamp amplifier: Axopatch-200A amplifier (Molecular Devices) which allows voltage- as well as current- clamp recordings.

Recording equipment: a standard oscilloscope allows to directly access to the amplifier output, and the computer acquires and stores crude data with the ACQUIS1 software (Bio-Logic, France).

Motorized micromanipulators: They allow continuous sub-micron movements by piezoelectric actuators systems, and are oriented so that each pipette can be changed independently. One is from Burleigh Instrument (PCS-5000) and the two others are from Luigs&Neuman (LN unit 4MRE).

Pipettes: are made of thick-walled, borosilicate glass capillary, filamented to ease filling with internal solution (see below for composition). Pipettes are pulled on a horizontal 2-stage puller (Sutter Instrument) and fire polished (MF-830; Narishige) to a final resistance of 2-5 MΩ depending on the internal solution used. Patch-pipette solutions are filtered with 0.2 µm pore filters and disposable fillers (Microloader, Eppendorf) are used to fill pipettes. Electrodes are made of a silver wire coated with silver chloride. Pipettes are stably kept by pipette holders. The patch-pipette holder is connected by a catheter to a disposable syringe which enables positive pressure as well as pulses of suction applications. A manometer monitors pressure and suction changes.

Experimental slice chamber and perfusion system: A glass-bottomed chamber is used and continuously perfused at a fairly high rate (typically 1–2 ml/min), with carbogen-saturated (and heated, if relevant) BBS to ensure adequate oxygenation. The BBS is removed from the chamber via outflow tubing connected to a peristaltic pump (Gilson). The pump rate of aspiration is monitored via a pressure transducer immersed in the recording chamber. When solutions are heated prior to entry (to 32-35°C, by a heating jacket around the inflow), a small temperature probe close to the slice is used to accurately monitor recording temperature. A “harp”, a U-shaped piece of flattened platinum with nylon threads (pulled from nylon tights) glued across it, is used to hold down the cerebellar slice in the recording chamber. A reference

electrode, consisting in a silver wire coated with silver chloride, is also immersed in the recording chamber and connected to the ground of the amplifier headstage.

Patch-clamp procedure

The cerebellar slice is gently transferred in the perfused recording chamber. Purkinje cells are visually identified from their position, size and shape. Candidate cells are chosen on their "healthy looking" somata and in function of their accessibility to patch-pipette (Edwards et al., 1989).

The patch-pipette is filled with internal solution (~15 µl) and inserted in the pipette holder. A positive pressure is applied before entering the bath solution. The pipette is lowered into the bath, and moved into position, just above the cell. In voltage clamp, a 'test pulse' (-10 mV, 10 ms square pulse of voltage, applied at >3 Hz) is applied and the current required for this voltage pulse is monitored on an oscilloscope. At this time, the resistance of the pipette tip can be calculated using Ohm's law (Resistance = Voltage/Current). On the patch-clamp amplifier, any voltage offset between the electrode and the bath ("pipette potential") is zeroed.

Bath and "intra-pipette" solutions are composed of different anions and cations concentrations with different mobility, generating a liquid junction potential (LJP). This LJP is thus also compensated at this time, when any voltage offset is zeroed. After achieving the whole-cell voltage clamp, the pipette solution is no longer in direct contact with the bath solution, thus, its LJP disappears, but its compensating amplifier offset remains. Internal solutions KCl or CsCl based induce small LJP, and this error can be neglected in these cases. For other internal medium, in which the error can not be neglected, the LJP can be calculated and the correction on the imposed potential can be applied on-line or *a posteriori*.

Then, the pipette is approached to the cell surface with a continuous focus on the tip of the electrode. When a dimple starts to appear, the pressure on the pipette is immediately released, light negative pressure is then applied to the pipette via gentle suction and finally the holding voltage potential (- 70 mV) is applied. Once a stable giga-seal has formed, pipette capacitance compensations (slow and fast) can be done. Then, the cell membrane beneath the pipette tip is broken by brief suction to enter the whole-cell recording mode. Series resistance (access + pipette resistances) and membrane capacitance are estimated and compensated (70-75%). Signals are filtered at 2 or 5 kHz (low-pass) and usually sampled at 25-37 µs.

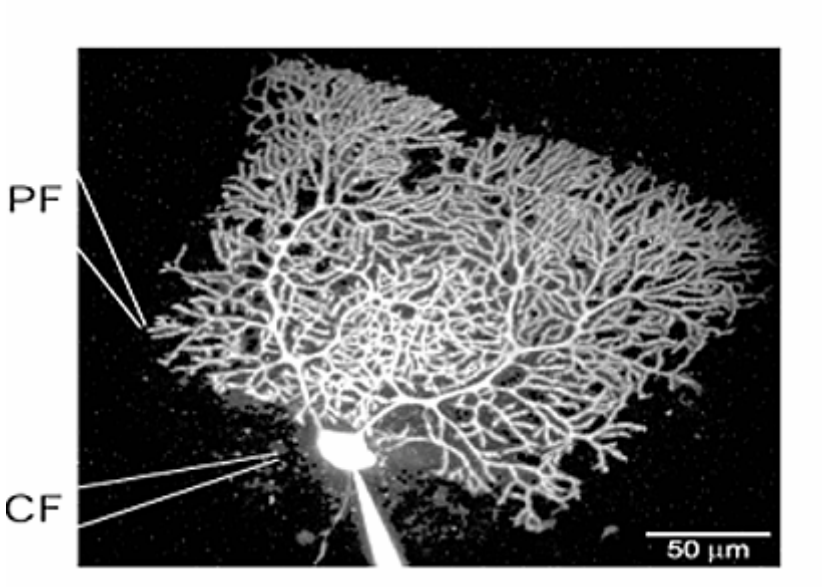

Figure 2.1 : Purkinje cell filled with Magnesium Green through a patch pipette (bottom), with glass pipettes for PF and CF activation (straight white outlines). (from Wang et al, 2000)

Electrical stimulations of Purkinje cell afferences

Extracellular stimulations of CFs or PFs were performed with constant voltage isolated units (0.1 ms square voltage pulses; 1-90 V) through pipettes filled with external solution. This pipette was moved around in the granular layer or molecular layer in the vicinity of the recorded Purkinje cell until the search response was obtained: for climbing fiber, an all-or-nothing strong response, displaying paired-pulse depression (40 ms interval); for parallel fiber, a gradual response depending on the stimulation intensity and displaying paired-pulse facilitation.

PF-LTD induction

For plasticity experiments, except when otherwise specified, the recording pipette was filled with a K-Gluconate based internal solution containing 1 mM EGTA (see further). Stimulation pipettes were set in a similar manner as shown on Figure 2.1. CF was rapidly searched after the entry in the whole-cell patch-clamp mode. If the CF response was not found in the following 10 minutes, the cell was not used for plasticity experiment, because of the intracellular content dialyse that occurs in this patch-clamp configuration. PF responses were recorded during a 10 minutes control period, in which PFs were stimulated at a frequency of 0.2 Hz. Next, in current clamp mode, we used a protocol of LTD-induction adapted from Wang et al. (2000), consisting of a train of 5 to 8 PF stimuli evoked at 100 Hz, followed by

the CF stimulation 50 to 150 ms later. This pairing was delivered at 1 Hz during 5 minutes. Then, in voltage-clamp mode, PF responses were still stimulated at 0.2 Hz.

PF-LTP induction

The protocol was the same as the PF-LTD protocol previously described, but CF was not stimulated.

Ionophoresis experiments

Ionophoretic pipettes have a final resistance of 40-50 MΩ when filled with 10mM NMDA in BBS (pH was set at 7.5). NMDA was ejected using negative square pulses ranging from 100 to 250 nA. To limit diffusion of NMDA in the BBS, a small positive retention current (usually 10-15 nA) was continuously applied to the ionophoresis pipette between ejections.

2.4 Solutions and pharmacology

Extracellular solutions

	BBS	**BBS "Mg free"**
Component (in mM)		
NaCl	130	130
KCl	2.5	2.5
$CaCl_2$	2.0	2.0
$MgCl_2$	1.0	0
$NaHCO_3$	26.0	26.0
NaH_2PO_4	1.3	1.3
Glucose	10.0	10.0

The bicarbonate buffered solution (BBS) is used for slicing, for incubating slices and for electrophysiological recordings. This solution was modified for experiments in which the absence of magnesium was required (BBS "Mg free"). The BBS solution is prepared daily from a 10 times concentrated stock. Its pH is 7.4 at room temperature after carbogen (95% CO_2, 5% O_2) saturation. Its osmolarity is ∼300 mOsm.

Intracellular solutions

	KCl-1EGTA	**KGluconate/ 6 KCl 10 EGTA**	**KGluconate/ 6 KCl 1 EGTA**	**CsGluconate 10 EGTA**
Component (in mM)				
KCl	150	6.0	6.0	0
K-Gluconate	0	144	144	0
Cs-Gluconate	0	0	0	150
$MgCl_2$	4.6	4.6	4.6	4.6
HEPES acid	10.0	10.0	10.0	10.0
EGTA	1.0	10.0	1.0	10.0
$CaCl_2$	0.1	1.0	0.1	1.0
ATP-Na	4.0	4.0	4.0	4.0
GTP-Na	0.4	0.4	0.4	0.4
pH adjustment	With KOH	With KOH	With KOH	With CsOH

Intracellular solutions based on K^+ ions were preferred because they are considered as more physiologic. Gluconate was used instead of Cl in order to prevent Cl currents in Purkinje cells. In some experiments, including current-voltage (I-V) curve protocols, the solutions contained Cs to replace K^+ ions in order to block K^+ conductances, which can decrease background noise during recordings. All internal solutions had an osmolarity of ∼300 mOsm and the pH was adjusted to 7.3. They were aliquoted, then frozen and stored at -18°C until utilization.

In some specified experiments, we added 1 or 3 mM of (5R,10S)-(+)-5-methyl-10,11-dihydro-5H-dibenzo[a,d]cyclohepten-5, 10-imine hydrogen maleate (MK8001) to the internal solution to block postsynaptic NMDA-Rs; no differences were detectable between the two concentrations.

List of the drugs used

Bicuculline methiodide (20 µM, Sigma, France) was systematically added to the BBS during electrophysiological recordings, in order to block $GABA_A$-mediated currents. Similarly, 25 µM Glycine was also systematically added in BBS.

Commercial name	Complete chemical name	Provider	Effect	Generally used concentration
Glycine	Glycine	Sigma	NMDA-R coagonist	25 µM (bath)
MK801	(5R,10S)-(+)-5-methyl-10,11-dihydro-5H-dibenzo[a,d]cyclohepten-5,10-imine hydrogen maleate (MK8001)	Sigma	NMDA-R channel blocker	1 to 3 mM ("internal" use)
NBQX	1,2,3,4-tetrahydro-6-nitro-2,3-[f]-quinoxaline-7-sulfonamide	Sigma	Selective AMPA-R antagonist	10 µM (bath)
D-APV	D-(-)-2-amino-5-phosphonopentanoic acid	Tocris	Selective NMDA-R antagonist	50 µM (bath)
NMDA	N-Methyl-D-Aspartate	Tocris	Selective NMDA-R agonist	20 to 100 µM (bath) 10 mM (iontophoresis)
CNQX	6-cyano-7 nitroquinoxaline-2,3-dione	Tocris	AMPA-R antagonist	10 to 50 µM (bath)
TTX	tetrodotoxine	Tocris	Na+ voltage-dependent channels blocker	1 µM (bath)
AIDA	(RS)-1-aminoindan-1,5-dicarboxylic acid	Tocris	selective Group 1 mGluR antagonist	100 µM (bath)
DL-TBOA	DL-threo-β-benzyloxyaspartic acid	Tocris	Specific and non transported glutamate transporter blocker	100 µM (bath)
RU486 (mifepristone)	17β-hydroxy-11β-(4-methylamino-phenyl)-17α)-(1-propynyl)estra-4,9-	Sigma	See publication 1	1 -50 µM (bath and cultures)

	dien-3one			
Bicuculline	Bicuculline methiodide	Sigma	$GABA_A$ receptor inhibitor	10 or 20 µM (bath)
RO25-6981	R-(R,S)-{alpha}-(4-hydroxyphenyl)-{beta}-methyl-4-(phenylmethyl)-1-piperidine propranol	Tocris	Selective antagonist of NR2B-containing NMDA-Rs	3 to 30 µM (bath)

2.5 Data analysis and inclusion criteria

In the current-clamp mode, cells that were spontaneously more depolarized than -50 mV and that needed large current injection to maintain their membrane potential at -70 mV were considered to be damaged and were discarded.

To estimate whether a cell displays a detectable D-APV-sensitive and NBQX-resistant EPSC, the amplitude of the NBQX-resistant EPSCs in control and during bath application of D-APV were compared using a Mann-Whitney one-tailed statistical test. If the two populations of amplitudes (control and D-APV) were statistically different ($p<0.05$, where p is the null hypothesis probability), D-APV was considered as having an effect, and the percentage of blockade induced by D-APV was calculated.

For analysis of complex spikes, spikes and spikelets were first identified with a threshold detection protocol (usually 20 mV). Spike or spikelet latencies were estimated by calculating the time between the stimulation and the occurrence of the spike or spikelets.

Averages are given as mean +/- SEM. For statistical comparisons, unless specified, Mann-whitney or Wilcoxon procedures were used, and p is given as the probability of the null hypothesis.

2.6 Immunohistochemistry

Parasagittal 60 µm slices were prepared as previously described except that a slicing sucrose BBS was used. This solution (containing in mM: 1 CaCl2, 5 MgCl2, 10 Glucose, 4 KCl, 26 NaHCO3, 248 Sucrose, 1.3 NaH2PO4, pH 7.35) was cooled to 4°C and bubbled with 95% O2 and 5% CO2. Immediately after slicing, slices were fixed with 4% paraformaldehyde in phosphate-buffered saline (PBS) for 2 hours. They were then rinsed 3 times with PBS.

Permeabilization and saturation were performed during 1 h on free-floating sections with PBS containing 0.25% Triton X-100 and 0.25% fish gelatine (PBS-G-T).

For NR2-C and NR2-D immunodetection, two types of anti-NR2 antibodies were used: a rabbit anti-NR2-D raised against amino acids 268-386 of human NR2D, and a goat anti-NR2C/D raised against a peptide mapping at the C terminus of NR2D of mouse. The latter also recognizes NR2C (sc-1471; Santa Cruz Biotechnology, distributed by Tebu, Le Perray en Yvelines, France). For NR2A/B immunodetection, rabbit anti-NR2-A/B raised against the C-terminus tail of the rat NR2A subunit was used. It recognizes both NR2A and NR2B mouse proteins equally (AB1548; Chemicon, Temecula, CA, distributed by Euromedex, Mundolsheim, France). Slices were divided into three batches and incubated overnight at room temperature in the following combinations:
(1) with only the rabbit anti-NR2-A/B antibody (1 µg/ml),
(2) with NR2-A/B, mouse anti-Calbindin-D28k (1/10000; Swant, Bellizona, Switzerland) and guinea pig anti-Vesicular Glutamate Transporter 2 (VGLUT2) (1/3000; Chemicon) - antibodies,
(3) with PBS-G-T only (control).

Slices were then incubated 2 hours with the fluorescent secondary antibodies (10 µg/ml; Invitrogen): Alexa Fluor 546 goat anti-rabbit (combinations 1-3), Alexa Fluor 633 goat anti-mouse and Alexa Fluor 488 goat anti-guinea pig (combinations 2 and 3). The labeled slices were mounted in Vectashield medium (Vector Laboratories) and viewed with a confocal laser-scanning microscope (SP2; Leica) using a 63x objective. In multiple labeling experiments, acquisition of the signal was systematically performed in sequential mode. Alexa Fluor 488 was excited at 488 nm (argon laser), Alexa Fluor 546 at 543 nm (helium-neon laser), and Alexa Fluor 633 at 633 nm (helium-neon laser). Fluorescence signals were corrected for background fluorescence by measuring slices from control combination 3.

Three dimensional reconstructions were performed using the Imaris-4software (Bitplane).

3 Results

3.1 Publication 1:

Neuroprotective effect of mifepristone involves neuron depolarization

« En général, la mort fait que l'on devient plus attentif à la vie. »

Paulo Coelho, *L'Alchimiste*

3.1.1 Introduction

It is generally accepted that the process of programmed cell death is common of the physiological neuronal development. In the developing cerebellum *in vivo*, there are two major periods of programmed cell death for Purkinje cells: (i) an early embryonic period around E15 (Ashwell, 1990), and (ii) a postnatal period between P1 and P5 with a peak at P3 (Ghoumari et al., 2000). Similarly, survival of mouse Purkinje cells in organotypic cultures is age-dependent. In particular, a vast majority of Purkinje cells die by apoptosis when cerebellar slices are taken from P1 to P5 mouse and rat pups, but before and after this period, Purkinje cells survive in cultures (Dusart et al., 1997). This period of Purkinje cell vulnerability corresponds to a time window when Purkinje cells *in vivo* are engaged in intense synaptogenesis, dendritic remodelling and cell death.

The role of NMDA-Rs in neonate Purkinje cells *in vivo* remains to be elucidated. *S*ome clues have been however brought by an *in vitro* study of Yuzaki et al. (1996) who showed that NMDA-Rs of Purkinje cells themselves support their survival in culture. Indeed, in primary cultures made from WT mice at E18 or P0, in which most of the Purkinje cells die within the first 4 days *in vitro*, NMDA-Rs were shown to enhance the survival of immature Purkinje cells. NMDA-Rs antagonists inhibit this effect in cultures in a dose-dependent manner. In

cultures made from NR1 knockout mice, Purkinje cells death was more important. Conversely, adding exogenous NMDA or (NR1-/-) granule cells to the cultures increased Purkinje cells survival (Yuzaki et al., 1996). This study thus suggests that juvenile NMDA-Rs could protect postnatal Purkinje cells *in vivo*, in particular during the critical periods of developmental cell death. In the following study, we did not directly test the mechanism by which NMDA-Rs enhance the survival of postnatal Purkinje cells, but we propose that it involves depolarization, as we show that mifepristone, as other depolarizing agents, has strong neuroprotective effects at P3.

Mifepristone is an antagonist of the glucocorticosteroid and progesterone receptors that is better known as RU486, its designation at the Roussel Uclaf company, which designed the drug in 1980. Although mifepristone is mainly used as an abortifacient, as an emergency contraceptive or as a treatment for obstetric bleeding, it has also been shown to protect rat hippocampal neurons from apoptosis after oxidative stress *in vitro* (Behl et al., 1997), or traumatic brain injury *in vivo* (McCullers et al., 2002). These observations suggested that mifepristone could be of biomedical interest for neuroprotective strategies in brain after stroke, injury or under pathological conditions. Mifepristone also protects Purkinje cells from apoptosis in organotypic slice cultures of postnatal rodent cerebellum and this neuroprotective effect is independent of the activation of glucocorticoid or progesterone receptors (Ghoumari et al., 2003).

The first aim of the following collaborative study was to understand the neuroprotective mechanism of mifepristone. It revealed that mifepristone induces a down regulation of the Na^+/K^+-ATPase expression that causes a neuroprotective depolarization of the postnatal Purkinje cell. This study also showed that, more generally, depolarizing agents and interestingly, excitatory inputs provided at least by climbing fibers, protect postnatal Purkinje cells in cultures.

3.1.2 Summary of the results

- DNA microarrays and immunoblotting assays showed that mifepristone prominently inhibits the increase of the expression of the Na^+/K^+-ATPase alpha3 subunit in organotypic cultures of P3 cerebella. In mifepristone-treated slices, the enzymatic activity of the Na^+/K^+-ATPase pump is returned to a level comparable to that observed *in vivo*. Ouabain, a blocker of the

Na^+/K^+-ATPase pump, prevents Purkinje cells death in cultured P3 cerebellar slices, mimicking the effect of mifepristone.

- We brought our expertise of patch-clamp recordings to compare the electrophysiological behaviour of Purkinje cells in P3 cerebellar slices treated with mifepristone *versus* in control conditions. We demonstrated that the resting potential of Purkinje cells treated with mifepristone was significantly more depolarized than control cells. Moreover, mifepristone-treated Purkinje cells do not fire action potentials, either spontaneously (in absence of current injection), or in response to square current pulses, whatever their holding potential. Thus mifepristone induces Purkinje cells depolarization and prevents action potential firing.

- P3 cerebellar slices were treated with different depolarizing agents such as high K^+, the K^+ channel blocker TEA and the Na^+ channel activator veratridine, that all prevented the apoptosis of Purkinje cells in cultures. Similarly, the depolarization of Purkinje cells with veratridine supports their survival, and is probably mediated by T-type calcium channels, since this effect was blocked only by flunarizine.

- Although the mifepristone-associated depolarization of Purkinje cells is accompanied by an increase of cytoplasmic Ca^{2+}, voltage-gated Ca^{2+} channels are probably not involved in the neuroprotective effect of mifepristone, as shown by the absence of effect of Ca^{2+} chelator EGTA, or of T- and L-types voltage-gated Ca^{2+} channels blockers on mifepristone-associated survival.

- Organotypic cultures of cerebellum made from P1 to P7 are deprived from their main glutamatergic inputs: the climbing fibers. Conversely, olivo-cerebellar cocultures allowed the restoration of climbing fibers connections on P3 Purkinje cells, and this was associated with an increase of the Purkinje cells survival.

For figures and details, see accompanying paper.

Neuroprotective effect of mifepristone involves neuron depolarization

A. M. Ghoumari,*[,1] C. Piochon,[†] C. Tomkiewicz,[‡] B. Eychenne,[1] C. Levenes,[†] I. Dusart,[†] M. Schumacher,* and E. E. Baulieu*

*INSERM UMR788 and University Paris XI, Bicêtre, France; [†]UMR7102 CNRS-Université Pierre et Marie Curie, Paris, France; and [‡]INSERM U490, Paris, France

ABSTRACT **In several regions of the developing nervous system, neurons undergo programmed cell death. In the rat cerebellum, Purkinje cell apoptosis is exacerbated when cerebellar slices are cultured during the first postnatal week. To understand the mechanism of this developmental apoptosis, we took advantage of its inhibition by the steroid analog mifepristone. This effect did not involve the classical steroid nuclear receptors. Microarray analysis revealed that mifepristone down-regulated mRNA levels of the Na^+/K^+-ATPase α3 subunit more than three times. Consistent with the down-regulation of the Na^+/K^+-ATPase, mifepristone caused Purkinje cell membrane depolarization. Depolarizing agents like ouabain (1 μM), tetraethylammonium (2 mM), and veratridine (2 μM) protected Purkinje cells from apoptosis. These results suggest a role of excitatory inputs in Purkinje cell survival during early postnatal development. Indeed, coculturing cerebellar slices with glutamatergic inferior olivary neuron preparations allowed rescue of Purkinje cells. These findings reveal a new neuroprotective mechanism of mifepristone and support a pivotal role for excitatory inputs in the survival of Purkinje neurons. Mifepristone may be a useful lead compound in the development of novel therapeutic approaches for maintaining the resting potential of neurons at values favorable for their survival under neuropathological conditions.—Ghoumari, A. M., Piochon, C., Tomkiewicz, C., Eychenne, B., Levenes, C., Dusart, I., Schumacher, M., Baulieu, E. E. Neuroprotective effect of mifepristone involves neuron depolarization. *FASEB J.* 20, 1377–1386 (2006)**

Key Words: Purkinje cells · Na^+/K^+-ATPase · rat cerebella

Purkinje cells die by apoptosis in organotypic culture when cerebellar slices are taken between P1 and P7 (1, 2). Although protein kinase C (PKC), the mitochondrial pathway of apoptosis, and microglial cells are involved in this developmental Purkinje cell death, the underlying cellular and molecular signaling mechanisms remain unknown (2–4). As Purkinje cells in organotypic cultures die precisely at a time when increased neuronal apoptosis is observed *in vivo* and when intense dendrite remodeling and synaptogenesis take place (4–6), the event is likely to reflect a physiologically relevant developmental process.

We previously demonstrated that mifepristone, well known as an antagonist of the glucocorticosteroid and progesterone receptors (7), protects Purkinje cells from apoptotic death in organotypic slice cultures of postnatal rat and mouse cerebella by a novel mechanism that involves neither classical intracellular steroid receptors nor the antioxidant properties of the steroid analog (8). Mifepristone had already been shown to protect hippocampal neurons from apoptosis after traumatic brain injury or during oxidative stress (9, 10).

The strong neuroprotective effect of mifepristone was expected to give clues to the age-dependent Purkinje cell death and to reveal important developmental features of this neuron. We show that mifepristone prevents the increase in Na^+/K^+-ATPase α3 subunit expression and activity that normally follows the culture process, thus maintaining the Purkinje cells in a depolarized status resulting in their survival. Indeed, various depolarizing procedures such as high external K^+, blockade of K^+ channels and of the Na^+/K^+-ATPase, and activation of Na^+ channels were able to mimic the protective effects of mifepristone on Purkinje cells. The catalytic α3 subunit isoform of the Na^+/K^+-ATPase is expressed in the nervous system, particularly in rat Purkinje cells (11–12), and blocking the pump leads to a rapid depolarization of Purkinje cells (13).

Most important, the restoration of excitatory synaptic afferents from inferior olivary neurons allowed partial rescue of Purkinje cells. The present findings reveal a novel mechanism involved in the neuroprotective effects of mifepristone, and provide further support for a pivotal role of excitatory inputs, provided at least in part by climbing fiber innervation, in the survival of postnatal Purkinje neurons.

[1] Correspondence: INSERM U488, 80 rue du Général Leclerc, Kremlin-Bicêtre 94276, France. E-mail: ghoumari@kb.inserm.fr

doi: 10.1096/fj.05–5832com

MATERIALS AND METHODS

Slice cultures and cocultures

Cerebellar slices were prepared from postnatal day 3 (P3) Sprague-Dawley rats (Janvier, Le Genest St. Isle, France). For each experiment, at least 3 animals and 18 slices were used. After decapitation, brains were dissected out into cold Gey's balanced salt solution containing 5 mg/ml glucose (Glc) (GBSS-Glu) and meninges were removed. Cerebellar parasagittal slices (350 μm thick) were cut on a Macllwain tissue chopper and transferred onto membranes of 30 mM Millipore culture inserts with 0.4 μm pore size (Millicell, Millipore, Bedford, MA, USA).

Transverse slices (350 μm thick) of the ventral medial portion of the anterior medulla containing the inferior olivary neurons (14) were obtained from the same P3 Sprague-Dawley rat and cut on a Macllwain tissue chopper. Cerebellar slices and the slices containing inferior olivary neurons were cocultured on membranes of 30 mM Millipore culture inserts. Even if the ventral medial portion of the anterior medulla contains neurons other than inferior olivary neurons, in this study we use the terminology of inferior olivo-cerbellar coculture as used in a study by Audinat et al. (14).

Slices were maintained in culture in 6-well plates containing 1 ml of medium at 35°C in an atmosphere of humidified 5% CO_2. The medium was composed of 50% basal medium with Earle's salts (Invitrogen, Gaithersburg, MD, USA), 25% Hanks' balanced salts solution (Life Technologies, San Diego, CA, USA), 25% horse serum (Life Technologies), L-glutamine (1 mM), and 5 mg/ml Glc.

Chemicals

The principal steroids and chemical compounds used were RU486 (mifepristone: 17β-hydroxy-11β-(4-methylamino-phenyl)-17α)-(1-propynyl)estra-4,9-dien-3 one), ouabain, tetraethylammonium (TEA), veratridine, tetrodotoxin (TTX), nifedipine, flunarizine (Sigma, St. Louis, MO, USA), and KCl (Merck, Rahway, NJ, USA). Doses with maximal efficiency retained were 1–50 μM for all compounds except for TEA (1–5 mM) and KCl (30 mM). Cerebellar slices were treated with these compounds the day of culture and maintained for 5 days *in vitro* (5DIV). Medium with the respective steroids or drugs was replaced once after 2 or 3 days.

RNA isolation and cDNA probe synthesis

Cerebellar slices from rat P3 were cultured in the presence or not of 20 μM RU486. After 1 h incubation, total RNA isolation, poly(A)$^+$ RNA enrichment, and cDNA probe synthesis were carried out for treated or untreated cells with the Atlas Pure Total RNA labeling system (Clontech, Palo Alto, CA, USA), as specified by the manufacturer. Prior to purification of poly(A)$^+$ RNA, total RNA was treated with DNase I. Poly(A)$^+$ RNA enrichment was done on 50 μg of total RNA.

Hybridization of labeled cDNA to Atlas plastic microarrays

Plastic microarrays (Atlas Plastic Mouse 5K microarray-S2838, Clontech, Palo Alto, CA, USA) were prehybridized for 30 min at 60°C with prewarmed hybridization solution. Equal counts of labeled probe from treated or untreated cells were added independently, after denaturation in a boiling water bath (95–100°C) for 5 min, onto two plastics microarrays. The reaction was allowed to proceed overnight at 60°C in roller bottles. The next day the plastic microarrays were washed twice with a high-salt wash solution at 58°C for 5 min. Two additional washes with a low salt solution were done at 58°C for 5 min. The plastic microarrays were then exposed to a PhosphorImaging screen for 24 h and scanned at a resolution of 50 μm on a PhosphorImager (Storm 840, Molecular Dynamics, Sunnyvale, CA, USA). Analysis of differential gene expression was performed with the Atlasimage 2.0.1 software (BD Biosciences, San Jose, CA, USA). This experiment was repeated twice and the genes regulated by RU486 in both experiments were selected.

Immunoblot assay

Cerebellar slice cultures were cultured in the absence (controls) or presence of 20 μM RU486 for 30 min, 1 h, 3 h, or 9 h. Slices were then washed with PBS and dissolved in Laemmli buffer. Identical amounts of proteins from each sample (25 μg) were separated by electrophoresis using 10% polyacrylamide gel, then transferred onto PVDF membranes by semi-dry transfer. After blocking with 5% dry milk, the membranes were incubated overnight at 4°C with a primary monoclonal anti-Na^+/K^+-ATPase alpha3 antibody (Ab) (1/1000 dilution; Ozyme, St. Quentin En Yvelines, France). After washing with Tween20-PBS buffer, membranes were incubated for 1 h with peroxidase-conjugated AffiniPure goat anti-mouse (1/20000 dilution; Jackson Immunoresesearch Laboratories, Inc., West Grove, PA, USA). The blots were developed with an enhanced chemiluminescence+plus detection kit (Amersham, Little Chalfont, UK).

Na^+/K^+-ATPase activity

Purified rat Na^+/K^+-ATPase was prepared from the organotypic slice cultures of P3 rat cerebella by an optimized method of the method of Jørgensen (15) and the one of Muszbek (16). The slices were untreated (Ctr) or treated separately with 20 μM RU486 or 1 μM ouabain for 3 h. Enzyme preparations were stored in ice-cold 0.25M sucrose, 30 mM histidine (pH 7.2). Homogenates were centrifuged twice with renewing buffer for 45 min at 60,000 rpm. Protein concentration was determined by the Lowry method using BSA as a standard. Fifty micrograms of each sample were transferred to tubes for enzyme assays with ATP (1 mM), $MgCl_2$ (3 mM), NaCl (130 mM), KCl (20 mM), and histidine (30 mM). After 30 min at room temperature, the reaction was stopped with 250 μl TCA; the inorganic phosphate (Pi) complex with phosphomolybdate was measured using spectrophotometer at 623 nM. Enzyme activity is expressed in μmoles P_i/min per milligram protein and mean values ± SE are calculated for groups of at least 3 animals.

Antibodies and staining procedures

Rabbit polyclonal and mouse monoclonal antibodies against calbindin D-28K (diluted 1/10,000, Swant, Bellinzona, Switzerland) were used to visualize Purkinje cells, and Ab against guinea pig VGluT2 (1/350, Chemicon, Temecula, CA, USA) was used to label climbing fibers but also mossy and parallel fibers (1, 17, 18). These first antibodies were revealed, respectively, with secondary antibodies against goat anti-rabbit CY3 Ab (1/200 dilution; Jackson ImmunoResearch Laboratories, Inc.), goat antimouse Alexa Fluor488 (1/1000 dilution, Molecular Probes, Leiden, Netherlands), and donkey anti-guinea pig CY3 (1/200 dilution, ImmunoResearch Laboratories). Staining procedures were performed as described previously (1, 2).

Quantification of Purkinje cell survival

To determine the Purkinje cell survival in the cultures, neurons were immunostained with the anticalbindin Ab and counted under a fluorescence microscope (axiovert 135M; Zeiss, Oberkochen, Germany) as described previously (8). Under these conditions, we counted the total number of surviving Purkinje cells per slice and calculated the means. Images of the immunostained Purkinje cells in organotypic slice cultures of rat and mice cerebella were acquired using an image analyzing system, confocal Zeiss LSM 410 (Zeiss). Images were acquired with a nonconfocal configuration (488 nM excitation).

Electrophysiology

Cerebellar slices were prepared from Sprague-Dawley rats (P3-P4). The cerebellum was rapidly removed and submerged in ice-cold bicarbonate-buffered solution (BBS) bubbled with 95% O_2, 5% CO_2. Sagittal slices 180 μm thick were cut with a vibroslicer (LEICA VT-1000S) and incubated at room temperature (20–22°C) for at least 1 h prior to electrophysiological recordings either in standard BBS supplemented with 0.5 ‰ alcohol (as the vehicle) for controls or in standard BBS + 25 μM RU486 for test experiments. Slices were then transferred in a recording chamber superfused at a rate of 1.5 ml/min with oxygenated BBS containing, in mM: NaCl, 130; KCl, 2.5; $MgCl_2$, 1; $CaCl_2$, 2; $NaHCO_3$, 26; NaH_2PO_4, 1.3; Glc, 10; final pH 7.35 at 20°C.

Purkinje neurons were visually identified from their position, size, and shape using Nomarski differential interference optics [40× water immersion objective (Zeiss) plus a 2.25 × zoom (Nikon)] mounted on an upright Axioskop fibrous sheath microscope (Zeiss). Patch-pipettes were pulled with a 2-stage puller (Sutter Instrument, Movato, CA, USA) from borosilicate capillary glass tubing. Pipettes were fire polished to a final resistance of 3–5 MΩ when filled with the following internal solution (in mM): KCl, 150; HEPES, 10; EGTA, 1; $MgCl_2$, 4.6; $CaCl_2$, 0.1; ATP-Na, 4; GTP-Na, 0.4; pH was adjusted to 7.3 with KOH. In some experiments 150 mM KCl was replaced by 150 mM K-gluconate to prevent chloride currents. As no difference was observed between cells patched with K-gluconate compared to those patched with KCl-based internal solution, results were pooled. Purkinje cells were recorded by patch-clamp in whole-cell configuration using an AXOPATCH 200A amplifier (Axon Instruments, Union City, CA, USA). Patch and estimation of capacitance and series resistance were made in voltage-clamp mode and series resistances were partially compensated (60–70%). Recordings were then made in the current-clamp mode. Acquisition and storage were made on a PC running the ACQUIS1 software (Biological). The Mann-Whitney procedure was used for statistical comparison of means; P is given as the probability of the null hypothesis. Statistical values are given as mean ± SE.

Measurement of intracellular Ca^{2+} levels

Cytoplasmic free calcium levels were analyzed in different regions of the P3 slices using calcium Fluo-4 (Molecular Probes, Inc., Eugene, OR, USA). P3 cerebellar slices were made in culture in the absence (Ctr) or presence of 20 μM RU486. At the same time, 10 μM calcium Fluo-4 was added to cultures for 1 h at 37°C, then washed with serum-free Glc-supplemented Eagle basal medium medium to remove Fluo-4 in excess. The fluorescent signal (excitation at 480 nM; emission, 510 nM) was visualized using an image analyzing system, confocal Zeiss LSM 410 and measured using the NIH image software. The calcium Fluo-4 staining density was quantified on a continuous scale of 0–255 (darkest). To minimize differences among the respective measurements, we set as control an arbitrary concentration of staining 100. The Fluo-4 staining density was evaluated as a percentage of (light pixels/light+dark pixels)

Statistical analysis

Data were expressed as mean for at least 18 cerebellar slices (n=18) from three animals (n=3) and in three independent experiments ± SE. The significance of differences between means was evaluated by Newman-Keuls tests after 1-way ANOVA and by the Mann-Whitney procedure.

RESULTS

Mifepristone inhibits the increase in Na^+/K^+-ATPase mRNA, protein, and activity in cerebellar slices

To study the neuroprotective mechanisms of mifepristone, P3 rat cerebella were cut into slices and immediately cultured in the presence or absence of 20 μM of the steroid analog. After 1 h in culture, RNA extracted from control and mifepristone-treated slices was hybridized on plastic microarrays. Analysis of changes in gene expression revealed that mifepristone down- or up-regulated the expression of several genes. The most prominent change observed was the > 3-fold decrease in the expression of the gene encoding the Na^+/K^+-ATPase α3 subunit when compared to control (ratio of mifepristone/control=0.31).

Immunoblotting assays showed a corresponding decrease in Na^+/K^+-ATPase α3 subunit protein levels in the cerebellar slices after 1 h of treatment with mifepristone when compared to untreated slices (**Fig. 1*A***). The reduction in the Na^+/K^+-ATPase α3 subunit protein could still be observed after 3 h and slightly increased after 9 h of culture (Fig. 1*A*). The enzymatic activity of the Na^+/K^+-ATPase was also decreased ~3-fold after treating the cerebellar slices for 3 h with mifepristone (control: 126±41; mifepristone: 43.5±12 nmol Pi/min/mg of protein) (Fig. 1*B*). Most important, Na^+/K^+-ATPase activity in cerebellar slices treated with mifepristone was comparable to that observed *in vivo* (46.9±4.7 nmol Pi/min/mg of protein). These results suggested that mifepristone may prevent an increase in Na^+/K^+-ATPase expression and activity resulting from the culture process and that this effect may be related to its neuroprotective action.

Inhibiting the increase of Na^+/K^+-ATPase activity in cerebellar slices prevents Purkinje cell death

We then examined whether a direct down-regulation of the Na^+/K^+-ATPase activity by ouabain in cultured P3 cerebellar slices in which nearly all Purkinje cells die also allowed rescue of these neurons. We first verified that addition of a low concentration of ouabain (1 μM) to the medium at the beginning of the culture for 3 h

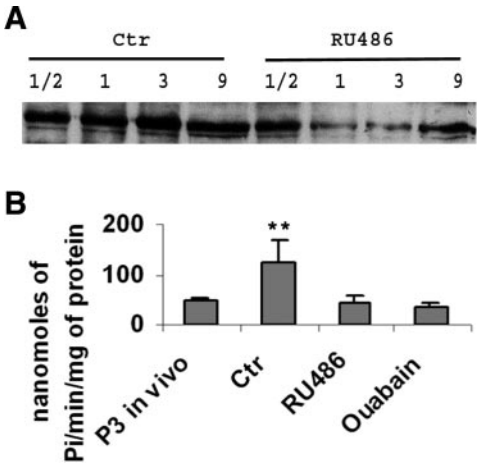

Figure 1. RU486 down-regulates the Na^+/K^+-ATPase alpha3 expression and activity. *A)* Immunoblotting assay was performed on the Na^+/K^+-ATPase alpha 3 isoform. Time courses of Na^+/K^+-ATPase alpha3 protein expression were determined in cerebellar slices treated or not by 20 μM RU486 for 1/2, 1, 3, and 9 h. *B)* Enzymatic activity of the pump was measured in RU486- and ouabain-treated P3 cerebellar slices and in untreated P3 cerebellar slices. This Na^+/K^+-ATPase alpha3 activity was determined by measuring inorganic phosphate (Pi) complexes with phosphomolybdate at 623 nM. Enzyme activity is expressed in nanomoles P_i/min per milligram protein and mean values ± SE were calculated for groups of at least 3 animals. RU486 maintains the Na^+/K^+-ATPase activity at the *in vivo* concentration. Thus, RU486 inhibits the increase rather than strongly inhibits Na^+/K^+-ATPase activity. $^{**}P \leq 0.01$ as indicated by Newman-Keuls tests after 1-way ANOVA.

partially reduced the activity of the pump to 34.3 ± 11 nmol Pi/min/mg of protein, comparable to the normalization observed after mifepristone treatment (Fig. 1*B*). Cerebellar slices from P3 rats were then cultured for 5 days *in vitro* (5DIV) in the absence or presence of 20 μM mifepristone or 1 μM ouabain (**Fig. 2**). Purkinje cell survival was assessed by counting the total number of calbindin D-28K immunostained cells in the slices. Results confirmed the strong protective effect of mifepristone on Purkinje cells in P3 cerebellar slices (Fig. 2*B, D*). The neuroprotective effect mifepristone could be mimicked by reducing the Na^+/K^+-ATPase activity with ouabain (Fig. 2*C, D*). As expected, very few Purkinje cells survived in untreated slices (~10 Purkinje cells/slice, Fig. 2*A*). However, the mean number of surviving Purkinje cells was 2087 ± 105 and 1300 ± 80 in slices treated respectively with mifepristone or ouabain (Fig. 2*D*). Thus, inhibiting the culture-dependent increase of Na^+/K^+-ATPase activity by either mifepristone or a low concentration of ouabain protects Purkinje cells from the apoptotic process described in cultures of young rat cerebellar slices (2). We also noted that adding mifepristone or ouabain to the culture medium for periods as short as 3 h was sufficient to prevent some Purkinje cells from death (data not shown).

Mifepristone induces Purkinje cell depolarization

It has been reported that inhibition of the Na^+/K^+-ATPase activity in neurons leads to their depolarization (13, 19). We therefore compared the membrane potentials between Purkinje cells of P3 cerebellar slices cultured in the absence or presence of mifepristone. In control slices, the resting membrane potential (RP) of Purkinje cells fluctuated over time between −60/−70 mV and more depolarized values, i.e., −49.4 mV on average (see below). Such a typical "two-state" behavior (−70/−50 mV) was never observed in Purkinje cells treated with mifepristone (n=18). Therefore, to allow reliable comparison between untreated and mifepristone-treated cells, mean resting potential of control cells was calculated from the more depolarized state. Mean resting potential value of mifepristone treated cells was –30.9 ± 2.8 mV (n=18), being significantly above the mean resting potential in control cells (–49.4±2.8 mV; n=14; P<0.001, **Fig. 3*C***). Therefore, treatment with mifepristone caused a persistent depolarization of Purkinje cells.

The action potential firing properties of Purkinje cells treated with mifepristone were then compared to untreated cells. In the absence of mifepristone, 9 of 14 Purkinje cells (64%) displayed spontaneous action potentials when no current was injected, as described (20–21). In contrast, only 1 of the 18 mifepristone-treated Purkinje cells (5%) fired spontaneously at resting potential.

To test the spiking properties of Purkinje cells in

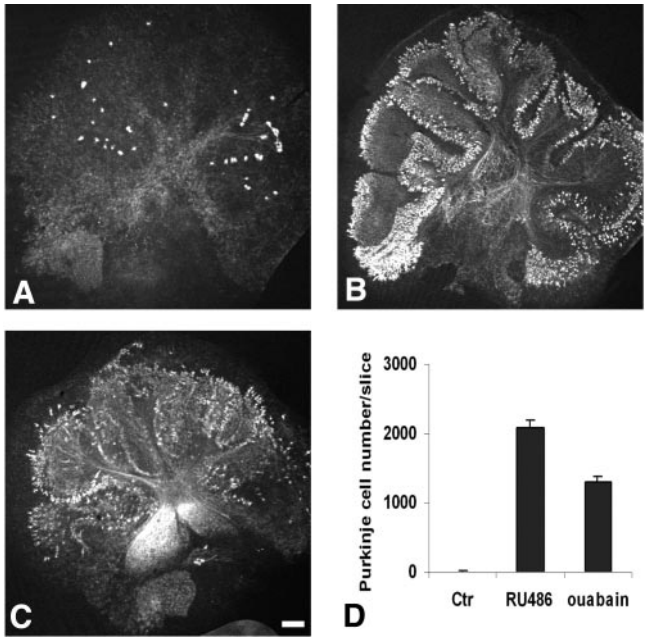

Figure 2. Inhibiting the increase of Na^+/K^+-ATPase alpha3 either by RU486 or by ouabain prevents Purkinje cell death in organotypic slice cultures of rat cerebellum. Slices of 3-day-old (P3) rats were cultured for 5 days *in vitro* (5DIV). Slice cultures were immunostained with anticalbindin D28-K Ab to label Purkinje cells. *A)* Untreated control slices (Ctr): very few Purkinje cells were present. *B)* Slices treated with 20 μM RU486. *C)* Slices treated with 1 μM ouabain, the specific Na^+/K^+-ATPase inhibitor. *D)* Quantitative analysis of Purkinje cell survival after treatment with RU486 or with ouabain. In the treated slices with either RU486 or with ouabain, high Purkinje cell survival was observed. Scale bars: 200 μm.

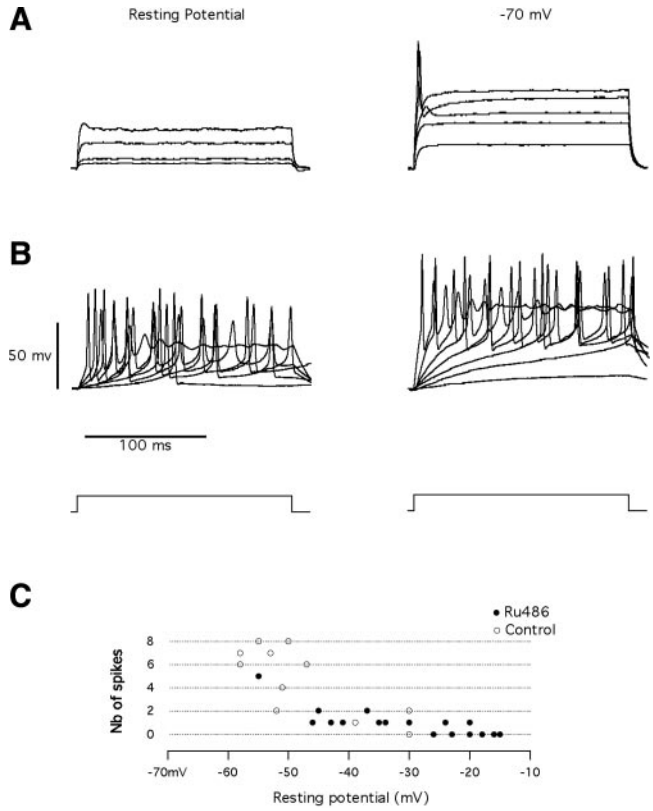

Figure 3. Depolarized resting potential and lack of firing behavior in RU486-treated cells. Purkinje cell membrane potential was recorded in current clamp mode. *A)* Typical recordings of a RU486-treated cell. *B)* Control cells. Figures illustrate the lack of repetitive firing in the RU486 treated cells when square current pulses of increasing amplitude (180 ms in duration) are injected. This behavior is observed either at resting potential (left) or at –70 mV (right). *C)* Relationship between resting potential and the number of spikes generated by depolarizing pulses. RU486 cells (black spots) were more depolarized and fireless than control cells (open spots).

response to depolarization, square current pulses 180 ms in duration of increasing amplitude (+10 up to +500 pA) were injected across the Purkinje cell membrane through the patch pipette. Cells were first left at their resting potential (Fig. 3*A–C*, left panels). In control cells a threshold current stimulus produced repetitive firing in 9 of 12 cells (Fig. 3*B*). In cells treated with mifepristone, similar depolarizing current pulses induced no spike in 5 cells, one spike in 9 and more than one spike in 3 of the 17 cells tested (Fig. 3*A–C*, left panel). Thus, when left at their resting potential, Purkinje cells treated with mifepristone display either no or very few spikes in response to depolarization. As expected and as illustrated in Fig. 3*C*, there was a strong correlation between the membrane potential and the number of action potentials induced by the depolarizing pulses. Indeed, when Purkinje cells are depolarized, they fire fewer action potentials.

We next tested whether maintaining mifepristone-treated Purkinje cells at –70 mV by a continuous injection of current could restore their discharge capabilities by allowing voltage-dependent channels to recover from inactivation. In this condition, Purkinje cells treated with mifepristone still displayed no or low spiking activity, similar to Purkinje cells left at their resting potential (Fig. 3*A*, right panel). Indeed, the depolarizing current pulses induced no spike in six cells or a maximum of one spike in eight cells. Only 3 of the 17 cells tested displayed more than one spike on depolarizing pulses. Thus, mifepristone significantly depolarizes Purkinje cells from P3 slices and prevents action potential firing.

Depolarizing agents promote Purkinje cell survival

To further test the role of depolarization in preventing the apoptosis of Purkinje cells, we treated P3 cerebellar slices with different depolarizing agents, including high K^+, the K^+ channel blocker TEA and the Na^+ channel activator veratridine. Treatment of the slices during 5 DIV with high K^+ (30 mM) significantly increased the number of surviving Purkinje cells: ~70-fold more Purkinje cells survived than in slices cultured in the presence of standard concentrations of K^+ (5 mM) (**Fig. 4*C***). Thus, high K^+ allows the rescue of some of Purkinje neurons in cerebellar slice cultures of P3 rat cerebellum. Purkinje cell survival could also be increased by treating slices during 5 DIV with TEA (2 mM, Fig. 4*B, C*) (~300-fold increase in Purkinje cell survival when compared to untreated slices, Fig. 4*A*). This neuroprotective effect of TEA was dose dependent. Even at a concentration as low as 0.5 mM, TEA resulted in an ~100-fold increase in Purkinje cell survival compared with control (data not shown).

Treatment of P3 cerebellar slices with 0.5–5 μM of veratridine, another depolarizing agent, also increased Purkinje cell survival in a dose-dependent manner (a significant increase in Purkinje cell survival could already be observed at 2 μM) (Fig. 4*D–F*). To confirm that veratridine increases Purkinje cell survival through its effect on voltage-sensitive Na^+ channels, slices were simultaneously treated with veratridine and with tetrodotoxin (TTX), a noncompetitive antagonist of Na^+ channels. The neuroprotective effect of veratridine was indeed abolished by 2.5 μM TTX (Fig. 4*E, F*). This observation suggests that Purkinje neurons may be dependent on sodium ion influx for their survival. However, TTX only partially blocked the neuroprotective effects of mifepristone or TEA (data not shown), suggesting different direct targets.

Mifepristone-induced Purkinje cell survival and Ca^{2+} influx

Neuronal membrane depolarization can drive Ca^{2+} influx, for instance, through voltage-dependent Ca^{2+} channels, and Ca^{2+} has been widely implicated in cell death and survival. In P3 cerebellar slices, Purkinje cell survival supported by veratridine could be completely blocked by the coapplication of the low voltage-activated T-type calcium channel inhibitor flunarizine (5

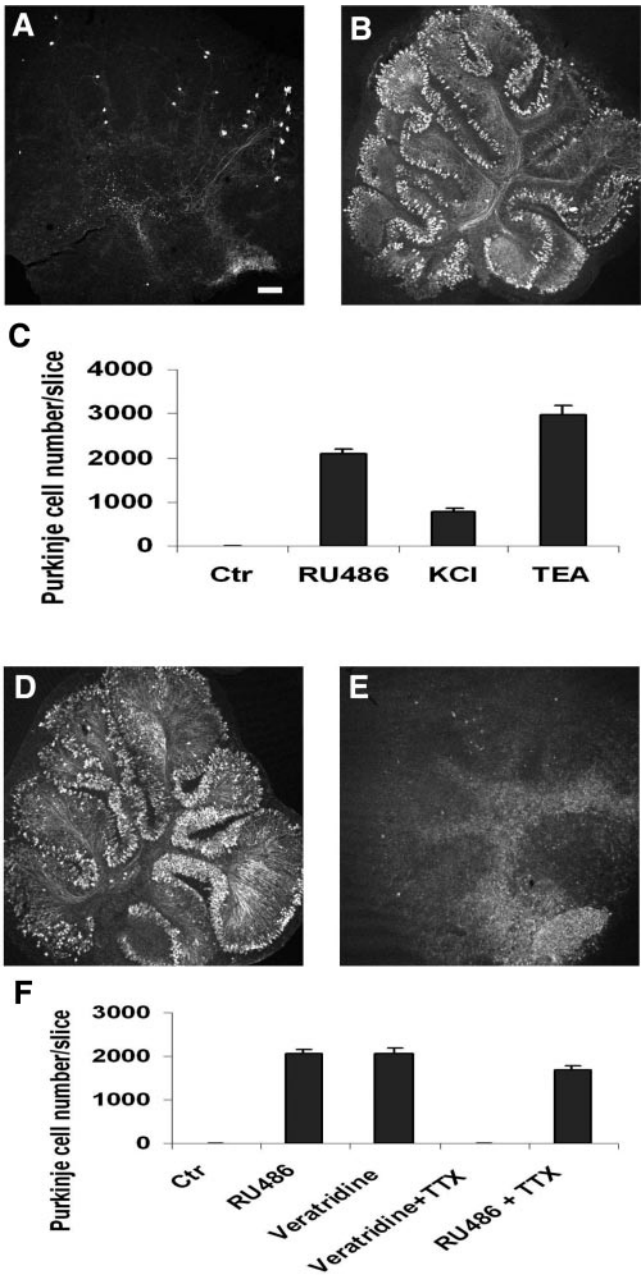

Figure 4. Purkinje cell death in organotypic slice cultures of postnatal rat cerebellum is mainly rescued by depolarizing stimulus. To confirm the effect of depolarization on Purkinje cell survival, depolarizing agents such as high K^+ (30 mM), TEA, and veratridine were used in this study. *A)* Untreated P3 control slices (Ctr). *B)* Slices treated with 2 mM TEA. *C)* Quantitative analysis of Purkinje cell survival after treatment with 20 μM RU486 or with depolarizing agents KCl (30 mM) or with TEA (2 mM). *D)* Slices treated with 2 μM veratridine. *E)* The veratridine effect was abolished when cultures were simultaneously treated by veratridine (2 μM) and by 2.5 μM tetrodotoxin (TTX), a noncompetitive antagonist of voltage-gated sodium channels. *F)* Quantitative analysis of Purkinje cell survival after treatment with 20 μM RU486 or with depolarizing agent veratridine (2 μM). Note that TTX abolished the effect of veratridine but not that of RU486, suggesting that RU486 does not act via the voltage-gated sodium channels. Scale bar is 200 μm.

μM). In contrast, the L-type calcium channel antagonist nifedipine (10 μM) did not affect the survival effect of veratridine (**Fig. 5*C***). These results demonstrate that the depolarization of Purkinje cells with veratridine

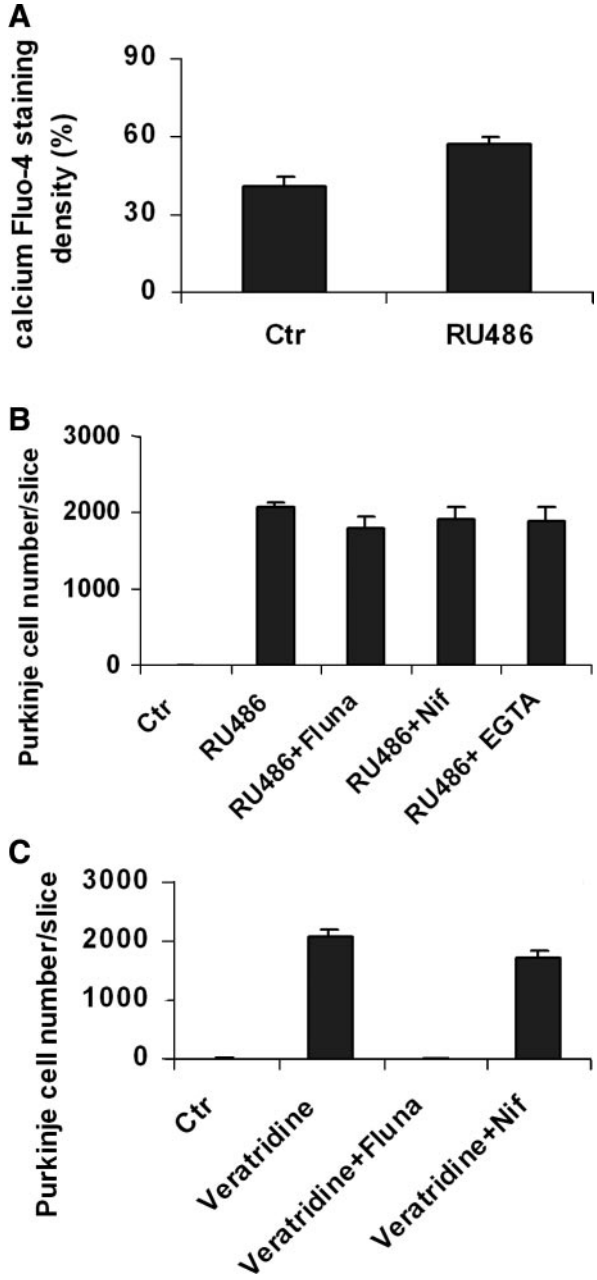

Figure 5. Treatment by RU486 is followed by a moderate increase in Ca^{2+} influx. *A)* Representative whole slice fluorescence of Ca^{2+} release in response to application of 20 μM RU486, as determined by quantifying the calcium Fluo-4 staining density. *B)* Neither T-type nor L-type voltage-gated Ca^{2+} channels [blocked respectively by flunarizine (Fluna, 5 μM) and nifedipine (Nif, 10 μM)] was necessary for the effect of RU486 on Purkinje cell survival. In addition, the extracellular Ca^{2+} chelator EGTA (1 mM) did not block the effect of RU486. *C)* The depolarizing agent, veratridine, induced Purkinje cell survival in cerebellar slice cultures by Ca^{2+} influx through T-type voltage-gated Ca^{2+} channels, as it was blocked only by flunarizine.

promotes their survival by increasing the influx of Ca^{2+} through T-type calcium channels.

We then examined whether treatment by mifepristone also causes an increase in Ca^{2+} influx. Our electrophysiological results showed that after 1 h in culture, mifepristone depolarized Purkinje cells in cerebellar slices. This depolarization was accompanied by a 1.4-fold increase in the cytoplasmic concentrations of Ca^{2+} as determined by quantifying calcium Fluo-4 staining density (Fig. 5*A*). However, as shown in Fig. 4, neither flunarizine nor nifedipine significantly reduced the effects of mifepristone on Purkinje cell survival. In agreement with this observation, the extracellular Ca^{2+} chelator EGTA (1 mM) was also ineffective (Fig. 5*B*). Thus, voltage-gated Ca^{2+} channels seem not to be involved in the neuroprotective effects of mifepristone, but the release of Ca^{2+} from internal stores (ER) may play a role.

Purkinje cells survive in inferior olivo-cerebellar cocultures

Inferior olivary neurons, through their olivo-cerebellar projections, dynamically regulate the maturation and functions of Purkinje neurons. However, in organotypic cerebellar slice cultures, Purkinje cells are deprived of these glutamatergic excitatory synapses, which mainly derive from climbing fibers (22–23). To test the hypothesis that the lack of excitatory inputs from inferior olivary neurons may contribute to the death of Purkinje cells in cerebellar slice cultures at P3, we performed an olivo-cerebellar organotypic slice coculture.

After 5 DIV, we counted 2.3-fold more surviving Purkinje cells in olivo-cerebellar slice cultures than in cerebellar slices cultured alone (**Fig. 6*B***). In many of these olivo-cerebellar slices, the surviving Purkinje cells were localized at the boundary in proximity of the olivary slices (Fig. 6*A*). Moreover, VGluT2 (vesicular glutamate transporter) immunoreactive fibers were observed to enter the cerebellar slices and in close apposition with the Purkinje cell soma and dendrites (Figure 6*C, D*). At that age, three types of VGluT2 immunoreactive fibers have been described in the rodent cerebellum: climbing, mossy, and parallel fibers (17–18). However, in cerebellar slices, cultured alone, an extremely low labeling with VGluT2 was detected (Fig. 6*E–J*), indicating that in the coculture experiments, the VGluT2 positive fibers originate from the olivary slices. Furthermore, the fact that these fibers terminate on Purkinje cell soma and dendrites suggests that they are more likely climbing fibers than mossy fibers. Indeed, mossy fibers normally do not contact Purkinje cells directly. These results strongly suggest that olivo-cerebellar connections may play a role in Purkinje cell survival during postnatal development.

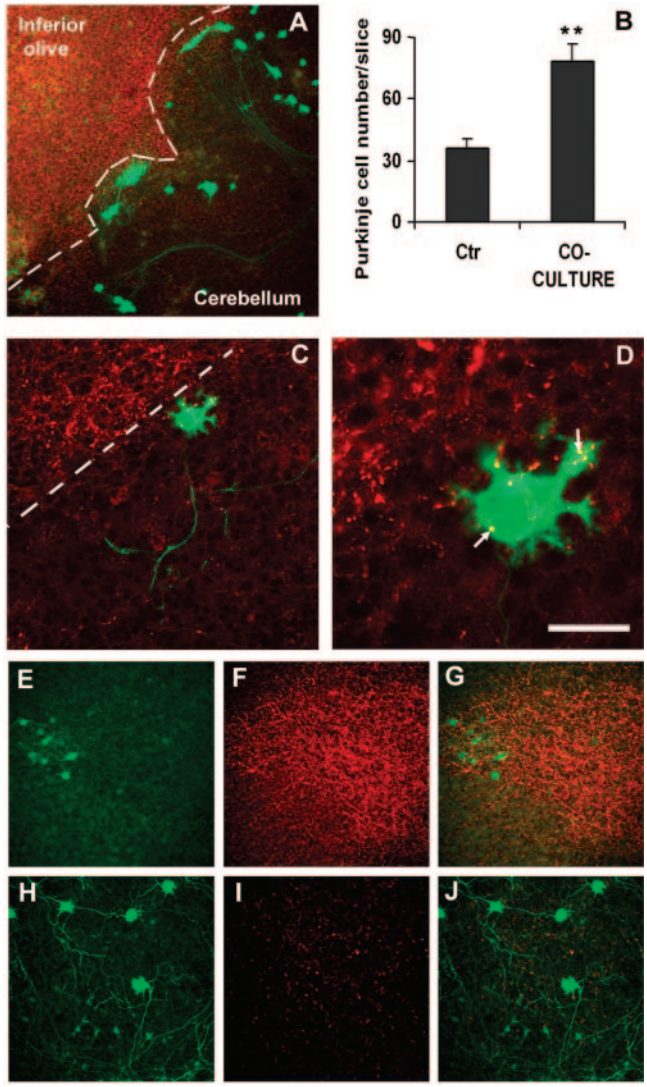

Figure 6. Purkinje cell survival in inferior olivo-cerebellar cocultures. *A)* P3 cerebellar slices were cocultured with the inferior olivary slices for 5DIV and double immunolabeling with VGluT2 (red) and CaBP (green) to visualize respectively glutamatergic fibers and Purkinje cells. The dashed lines represent the borderlines between inferior olivary and cerebellum slices in the cocultures. *B)* Quantification of surviving Purkinje cells in the olivo-cerebellar coculture. *C)* Apposition between glutamatergic fibers and Purkinje neurons. *D)* Higher magnification of panel *C*. Double immunostaining for VGluT2 and CaBP are pointed in Purkinje cell somata and dendritic shafts by the arrows. Scale bar: 250 μm (*A*), 60 μm (*C*), 20 μm (*D*). *E, F)* Slices of P3 inferior olivary neurons were separately cultured and respectively immunostained with CaBP and with VGluT2. *G)* A merger of panels *E* and *F*. *H, I)* Slice cultures of P3 cerebellum were respectively immunostained with CaBP and with VGluT2. *J)* A merger of panels *H* and *I*. Note that VGluT2 immunostaining was high in inferior olivary slices but extremely low in cerebellum. In inferior olivary slice cultures, some neurons were CaBP-positive (green). Scale bar: 200 μm in panels *E–I*.

DISCUSSION

We previously demonstrated that mifepristone, well known as an antagonist of the glucocorticosteroid and progesterone receptors (7), exerts a powerful neuro-

protective action on postnatal Purkinje cells in organotypic slice cultures of postnatal rat and mouse cerebellum. This mifepristone effect involves a novel mechanism, since neither classical intracellular steroid receptors nor the antioxidant properties of the steroid analog were found to be involved (8). Here, we demonstrate that mifepristone promotes survival of these Purkinje cells by causing their persistent depolarization. Further, results strongly suggest that this could result from inhibiting the increase in Na^+/K^+-ATPase α3 subunit expression and activity. Thus, a certain degree of excitation may be necessary for Purkinje cells to survive during the early postnatal period, corresponding to a developmental stage when intense cerebellar remodeling and synaptogenesis take place (4–6). Depolarizing agents such as high K^+, TEA, and veratridine also promoted Purkinje cell survival in organotypic culture. However, the neuroprotective effect of mifepristone involved the Na^+/K^+ pump and bypassed the voltage-gated ion channels, as it could be mimicked by low concentrations of the Na^+/K^+-ATPase inhibitor ouabain and was not inhibited by the sodium channel blocker TTX, by Ca^{2+} channel blockers flunarizine and nifedipine, or by the extracellular Ca^{2+} chelator EGTA. The current data reveal another interesting feature of the developing Purkinje neurons: after being placed in culture, they respond with an increase in Na^+/K^+-ATPase expression and activity, which is restored to levels comparable to those observed *in vivo* by mifepristone or ouabain treatment of the slices. This contrasts with the generally observed decrease in neuronal Na^+/K^+-ATPase activity and α3 subunit expression in response to injury (24–26). The Na^+/K^+-ATPase increase, most likely resulting in Purkinje cell hyperpolarization (12), turns out to be fatal for the immature neurons relying on excitatory innervation for their survival, provided by climbing fibers. Indeed, coculturing cerebellar slices with slices containing glutamatergic excitatory inferior olivary neurons allowed rescue of part of the Purkinje cells.

Regulation of the Na^+/K^+-ATPase and Purkinje cell survival

Down-regulation of the Na^+/K^+-ATPase α3 subunit in the presence of mifepristone revealed by microarray analysis was confirmed by measuring protein levels and pump activity. The inhibition of increased Na^+/K^+-ATPase expression could already be observed after 1 h of treatment, started immediately at the beginning of the culture, and protein levels then slightly increased after 9 h. These results indicate that a transient action of mifepristone may be sufficient for its neuroprotective effects. Indeed, treating cerebellar slices with mifepristone for only 12 h was sufficient to rescue a large number of Purkinje cells, which normally die at P3 by apoptosis. We have shown that the caspase-3 pathway is already activated in Purkinje cells 3 h after being placed in culture (2).

Decreasing Na^+/K^+-ATPase activity by a low concentration of ouabain also strongly enhanced Purkinje cell survival, suggesting that down-regulation of the pump may account for the neuroprotective effects of mifepristone. A reduction in Na^+/K^+-ATPase activity is generally associated with neuron death (26), but it has also been proposed to be involved in adaptative responses of brain cells to hypoxia or ischemia (27). Furthermore, down-regulation of the Na^+/K^+-ATPase has been shown to protect neurons in culture against hypoxia, glutamate, or low extracellular K^+ (28–30). Down-regulation of the Na^+/K^+-ATPase could also provide a pro-survival signal for neurons and stimulate DNA and protein synthesis (31–34). Thus, depending on the pathophysiological context, a transient decrease in Na^+/K^+-ATPase activity may exacerbate or protect against neuronal death. Here, we show that decreasing the Na^+/K^+-ATPase by mifepristone prevents the age-dependent Purkinje cell death in organotypic cultures. The classical steroid receptors seem not to be involved in the effect of mifepristone on $Na+/K^+$ATPase, as neither progesterone nor corticosterone inhibited this effect (data not shown) This is consistent with our previous finding that mifepristone protects Purkinje cells in slices of progesterone and glucocorticoid receptor knockout mice. It would be of interest to elucidate the novel mechanism by which mifepristone could regulate Na/K-ATPase expression.

Neuroprotective effects of mifepristone and depolarization of Purkinje cells

Each cycle of the Na^+/K^+ pump extrudes three Na^+ ions from the cell and moves 2 K^+ ions into the cell. Thus, blocking its activity has two consequences for Purkinje cells: their rapid depolarization due to the removal of the associated hyperpolarizing current and, at longer time scales, a modification of the Na^+ and K^+ membrane gradients (13). As a consequence, transmembrane electrochemical gradients of these ions are changed and Purkinje cells are expected to display reduced spiking capabilities even when maintained at –70 mV. This is indeed what we observed here. Thus, the inhibition of spike discharge in Purkinje cells treated with mifepristone is not simply a consequence of their persistent depolarization, but most likely also reflects a shift in Na^+ and K^+ concentrations, expected to disrupt the driving force of these ions and to block action potential discharge. Indeed, Purkinje cells treated with mifepristone were continuously depolarized, displayed either little or no action potential firings, and, as could be expected, neither TTX nor flunarizine blocked the neuroprotective effects of mifepristone. This would favor the possibility that there are at least additional mechanisms of mifepristone action.

The activity of the Na^+/K^+ pump was increased in P3 Purkinje cells following the culture process and their deprivation of main afferents. Thus, under these conditions the response of the neurons at P3 appears to be inappropriate, as it rapidly leads to their death. As we demonstrate here, preventing induction of the

Na^+/K^+ pump with mifepristone protects P3 Purkinje cells from apoptosis in culture and depolarizing procedures promotes their survival. McKay and Turner recently reported that Purkinje cells at P0 are depolarized at rest (–34±3 mV) and cannot fire sodium spikes even when hyperpolarized (35). This electrophysiological status of P0 Purkinje cells closely resembles that of P3 Purkinje cells treated by RU486. This could be one reason why P0 Purkinje neurons survive well in culture. In this view, one could consider that mifepristone treatment at P3 brings the cells back to a less mature status, thereby protecting them from death in culture.

The age-dependent death of Purkinje cells in organotypic cultures

In organotypic cultures of rat cerebellum, Purkinje cell apoptosis is age dependent (1). Most of these cells degenerate when cerebellar slices are taken between P1 and P5, but they survive before or after this period. This critical period of Purkinje cell vulnerability corresponds to a time window when Purkinje cells are engaged in intense synaptogenesis, dendritic remodeling, and cell death (4–6). We previously showed that neurotrophic factors, known to play a crucial role in the development and survival of nerve cells namely, brain-derived neurotrophic factor, neurotrophin 3, and insulin-like growth factor I have only marginal effects on the survival of P3 Purkinje cells (3). Membrane depolarization by the Na^+/K^+-ATPase blocker (ouabain), high potassium chloride (KCl), or other depolarizing agents such as TEA and verataridine treatment has been shown to prevent the death of many neuronal cell types (29, 30, 36–39). Our present results suggest for the first time that depolarization could be one of the mechanisms by which the steroid mifepristone allows neuron survival. Indeed, we show here that all the compounds that maintain or induce a depolarization (either down-regulation of Na^+/K^+-ATPase by mifepristone or the use of depolarizing agents such as high K^+, TEA, or veratridine) induce Purkinje cell survival.

At the first postnatal week of rat cerebellum development, glutamatergic excitatory synapses on Purkinje neurons are mainly derived from climbing fibers originating in the inferior olive nucleus, whereas the excitatory actions of parallel fibers only appear by the end of the first postnatal week (40–43). Postnatal Purkinje cells receive multiple innervation by climbing fibers, which is maximal between P3 and P7, in contrast to the one-to-one relationship characteristic of the adult stage (44, 45). Our present data suggest that the strong excitation arising from the transient multiple innervation by climbing fibers may play an important role in the survival of immature Purkinje cells. Indeed, removal of this excitatory innervation by the culturing process may explain the age-dependent death of Purkinje cells between P3 and P7 in cerebellar slice preparations. This conclusion is supported by the observations that *1)* coculturing cerebellar slices with inferior olivary slices promotes Purkinje cell survival; and *2)* climbing fibers originating from the olivary neurons, as documented by our results and as reported by Audinat *et al.* (18), form contacts with the surviving Purkinje cells.

Thus, neuron depolarization is necessary for Purkinje cell survival in cerebellar slice culture and it represents a novel function of the steroid receptor antagonist mifepristone. Treatment of the cerebellar slices by mifepristone may allow restoration of the physiological environment and maintenance of the resting potential at a value permitting neuron survival. These observations will be of interest for neuroprotective strategies in other brain regions after injury or under pathological conditions. FJ

We thank Philippe Leclerc for image analysis. This work was supported in part by an Artemis-Fondation Nationale de Gerontologie grant to E.E.B. and by the EXELGYN company.

REFERENCES

1. Dusart I., Airaksinen, M. S., and Sotelo, C. (1997) Purkinje cell survival and axonal regeneration are age dependent: an in vitro study. *J. Neurosci.* **17,** 3710–3726
2. Ghoumari A. M., Wehrle R., Bernard O., Sotelo, C., and Dusart, I. (2000) Implication of Bcl-2 and Caspase-3 in age-related Purkinje cell death in murine organotypic culture: an in vitro model to study apoptosis. *Eur. J. Neurosci.* **12,** 2935–2949
3. Ghoumari A. M., Wehrle R., De Zeeuw C. I., Sotelo C., and Dusart I. (2002) Inhibition of protein kinase C prevents Purkinje cell death but does not affect axonal regeneration. *J. Neurosci.* **22,** 3531–3542
4. Marin-Teva J. L., Dusart I., Colin C., Gervais A., van Rooijen, N., and Mallat, M. (2004) Microglia promote the death of developing Purkinje cells. *Neuron* **41,** 535–547
5. Gardette R., Debono M., Dupont, J. L., and Crepel, F. (1985) Electrophysiological studies on the postnatal development of intracerebellar nuclei neurons in rat cerebellar slices maintained in vitro. II. Membrane conductances. *Brain Res.* **352,** 97–106
6. Armengol, J. A., and Sotelo, C. (1991) Early dendritic development of Purkinje cells in the rat cerebellum. A light and electron microscopic study using axonal tracing in 'in vitro' slices. *Brain Res. Dev.* **64,** 95–114
7. Baulieu, E. (1989) Contragestion and other clinical applications of RU 486, an antiprogesterone at the receptor. *Science* **245,** 1351–1357
8. Ghoumari, A. M., Dusart, I., El-Etr, M., Tronche, F., Sotelo, C., Schumacher, M., and Baulieu, E. E. (2003) Mifepristone (RU486) protects Purkinje cells from cell death in organotypic slice cultures of postnatal rat and mouse cerebellum. *Proc. Natl. Acad. Sci. U. S. A.* **100,** 7953–7958
9. Behl, C., Trapp, T., Skutella, T., and Holsboer, F. (1997) Protection against oxidative stress-induced neuronal cell death-a novel role for RU486. *Eur. J. Neurosci.* **9,** 912–920
10. McCullers, D. L., Sullivan, P.G., Scheff, S. W., and Herman, J. P. (2002) Mifepristone protects CA1 hippocampal neurons following traumatic brain injury in rat. *Neuroscience* **109,** 219–230
11. Peng, L., Martin-Vasallo, P., and Sweadner, K. J. (1997) Isoforms of Na,K-ATPase alpha and beta subunits in the rat cerebellum and in granule cell cultures. *J. Neurosci.* **17,** 3488–3502
12. Biser, P. S., Thayne, K. A, Kong, J. Q., Fleming, W. W., and Taylor, D. A. (2000) Quantification of the alpha(3) subunit of the Na(+)/K(+)-ATPase in developing rat cerebellum. *Brain Res. Dev.* **123,** 165–172
13. Genet, S., and Kado, R. T. (1997) Hyperpolarizing current of the Na/K ATPase contributes to the membrane polarization of the Purkinje cell in rat cerebellum. *Pfluegers Arch.* **434,** 559–567
14. Audinat, E., Gahwiler, B. H., and Knopfel, T. (1992) Excitatory synaptic potentials in neurons of the deep nuclei in olivocerebellar slice cultures. *Neuroscience* **49,** 903–911

15. Jørgensen, P. L. (1974) Isolation of (Na+ plus K+)-ATPase. *Methods Enzymol.* **36,** 434–438
16. Muszbek, L., Szabo, T., and Fesus, L. (1977) A high sensitive method for the measurement of ATPase activity. *Anal. Biochem.* **77,** 286–288
17. Hioki, H., Fujiyama, F., Taki, K., Tomioka, R., Furuta, T., Tamamaki, N., and Kaneko, T. (2003) Differential distribution of vesicular glutamate transporters in the rat cerebellar cortex. *Neuroscience* **117,** 1–6
18. Miyazaki, T., Fukaya, M., Shimizu, H., and Watanabe, M. (2003) Subtype switching of vesicular glutamate transporters at parale fibre-Purkinje cell synapses in developing mouse cerebellum. *Eur. J. Neurosci.* **17,** 2563–2572
19. Cousin, M. A., Nicholls, D. G., and Pocock, J. M. (1995) Modulation of ion gradients and glutamate release in cultured cerebellar granule cells by ouabain. *J. Neurochem.* **64,** 2097–2104
20. Crepel, F., and Delhaye-Bouchaud, N. (1978) Intracellular analyses of synaptic potentials in cerebellar Purkinje cells of the rat. *Brain Res.* **155,** 176–181
21. Llinàs, R., and Sugimori, M. (1980) Electrophysiological properties of in vitro Purkinje cell dendrites in mammalian cerebellar slices. *J. Physiol.* **305,** 171–195; 197–213
22. Ito, M. (1984) The modifiable neuronal network of the cerebellum. *Jpn. J. Physiol.* **34,** 781–792
23. Kaneko, T., Itoh, K., Shigemoto, R., and Mizuno, N. (1989) Glutaminase-like immunoreactivity in the lower brainstem and cerebellum of the adult rat. *Neuroscience* **32,** 79–98
24. Gonzalez, S., Grillo, C., Gonzalez, Deniselle, M. C., Lima, A., McEwen, B. S., and De Nicola, A. F. (1996) Dexamethasone up-regulates mRNA for Na+,K(+)-ATPase in some spinal cord neurones after cord transection. *NeuroReport* **7,** 1041–1044
25. Labombarda, F., Gonzalez, S. L., Gonzalez, D. M., Guennoun, R., Schumacher, M., and De Nicola, A. F. (2002) Cellular basis for progesterone neuroprotection in the injured spinal cord. *J. Neurotrauma* **19,** 343–355
26. Yu, S. P. (2003) Na(+), K(+)-ATPase: the new face of an old player in pathogenesis and apoptotic/hybrid cell death. *Biochem. Pharmacol.* **66,** 1601–1609
27. De Angelis, C., and Haupert, G. T., Jr. (1998) Hypoxia triggers release of an endogenous inhibitor of Na(+)-K(+)-ATPase from midbrain and adrenal. *Am. J. Physiol.* **274,** F182–F188
28. Murphy, T. H., Schnaar, R. L., Coyle, J. T., and Sastre, A. (1988) Glutamate cytotoxicity in a neuronal cell line is blocked by membrane depolarization. *Brain Res.* **460,** 155–160
29. Isaev, N. K., Stelmashook, E. V., Halle, A., Harms C., Lautenschlager, M., Weih, M., Dirnagl, U., Victorov, I. V., and Zorov, D. B. (2000) Inhibition of Na(+),K(+)-ATPase activity in cultured rat cerebellar granule cells prevents the onset of apoptosis induced by low potassium. *Neurosci. Lett.* **283,** 41–44
30. Salthun-Lassalle, B., Hirsch, E. C., Wolfart, J., Ruberg, M., and Michel, P. P. (2004) Rescue of mesencephalic dopaminergic neurons in culture by low-level stimulation of voltage-gated sodium channels. *J. Neurosci.* **24,** 5922–5930
31. Zhou, X., Jiang, G., Zhao, A., Bondeva, T., Hirszel, P., and Balla, T. (2001) Inhibition of Na,K-ATPase activates PI3 kinase and inhibits apoptosis in LLC-PK1 cells. *Biochem. Biophys. Res. Commun.* **285,** 46–51
32. Orlov, S. N., Thorin-Trescases, N., Pchejetski, D., Taurin, S., Farhat, N., Tremblay, J., Thorin, E., and Hamet, P. (2004) Na+/K+ pump and endothelial cell survival: [Na+]i/[K+]i-independent necrosis triggered by ouabain, and protection against apoptosis mediated by elevation of [Na+]i. *Pfluegers Arch.* **448,** 335–345
33. Orlov, S. N., Taurin, S., Tremblay, J., and Hamet, P. (2001) Inhibition of Na+,K+ pump affects nucleic acid synthesis and smooth muscle cell proliferation via elevation of the $[Na^+]_i/[K^+]_i$ ratio: possible implication in vascular remodelling. *J. Hypertension* **19,** 1559–1565
34. Orlov, S. N., Thorin-Trescases, N., Kotelevtsev, S. V., Tremblay, J., and Hamet, P. (1999) Inversion of the intracellular Na+/K+ ratio blocks apoptosis in vascular smooth muscle at a site upstream of caspase-3. *J. Biol. Chem.* **274,** 16545–16552
35. McKay, B. E., and Turner, R. W. (2005) Physiological and morphological development of the rat cerebellar Purkinje cell. *J. Physiol.* **567,** 829–850
36. Gallo, V., Kingsbury, A., Balazs, R., and Jorgensen, O. S. (1987) The role of depolarization in the survival and differentiation of cerebellar granule cells in culture. *J. Neurosci.* **7,** 2203–2213
37. D'Mello, S. R., Galli, C., Ciotti, T., and Calissano, P. (1993) Induction of apoptosis in cerebellar granule neurons by low potassium: inhibition of death by insulin-like growth factor I and cAMP. *Proc. Natl. Acad. Sci. U. S. A.* **90,** 10989–10993
38. Scott, B. S., and Fisher, K. C. (1970) Potassium concentration and number of neurons in cultures of dissociated ganglia. *Exp. Neurol.* **27,** 16–22
39. Tanaka, S., and Koike, T. (1995) Up-regulation of L-type Ca^{2+} channel associated with the development of elevated K(+)-mediated survival of superior cervical ganglion cells in vitro. *Dev. Biol.* **168,** 166–178
40. Crepel, F., Mariani, J., and Delhaye-Bouchaud, N. (1976) Evidence for a multiple innervation of Purkinje cells by climbing fibers in the immature rat cerebellum. *Neurobiology* **7,** 567–578
41. Shimono, T., Nosaka, S., and Sasaki, K. (1976) Electrophysiological study on the postnatal development of neuronal mechanisms in the rat cerebellar cortex. *Brain Res.* **108,** 279–294
42. Mason, C. A., Christakos, S., and Catalano, S. M. (1990) Early climbing fiber interactions with Purkinje cells in the postnatal mouse cerebellum. *J. Comp. Neurol.* **297,** 77–90
43. Scelfo, B., and Strata, P. (2005) Correlation between multiple climbing fibre regression and parallel fibre response development in the postnatal mouse cerebellum. *Eur. J. Neurosci.* **21,** 971–978
44. Crepel, F. (1971) Maturation of climbing fiber responses in the rat. *Brain Res.* **35,** 272–276
45. Mariani, J., and Changeux, J. P. (1981) Ontogenesis of olivocerebellar relationships. I. Studies by intracellular recordings of the multiple innervation of Purkinje cells by climbing fibers in the developing rat cerebellum. *J. Neurosci.* **1,** 696–702

Received for publication February 6, 2006.
Accepted for publication February 27, 2006.

Supplemental data

- In primary cultures, Yuzaki et al. (1996) have shown that NMDA-Rs of Purkinje cells are directly involved in the survival of Purkinje cells. In our model of organotypic cultures, NMDA-Rs could also promote the survival of Purkinje cells. To test this hypothesis, P3 cerebellar slices cultures were treated for 2 days *in vitro* in the absence or presence of NMDA (20 μM, Figure 3.1, A and B). Purkinje cell survival was assessed by counting the averaged number of calbindin positive cells per lobules (Figure 3.1D). The data clearly confirmed the protective effect of NMDA on Purkinje cells in P3 cerebellar slices. Moreover, this effect was abolished when slices were simultaneously treated with (20 μM) NMDA and (100 μM) of the NMDA-channel blocker MK801 (Figure 3.1C).

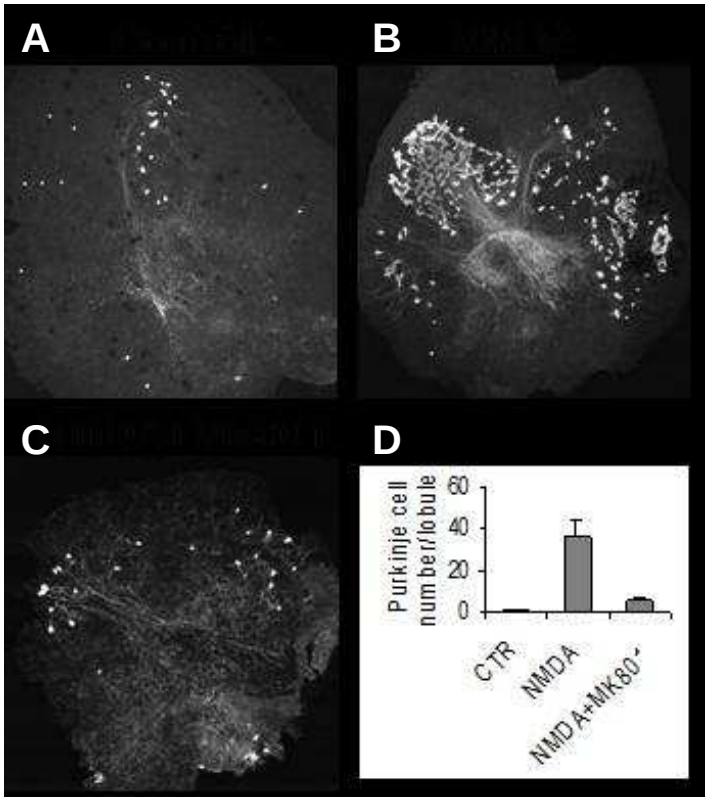

(Unpublished data, by courtesy of Abdel Ghoumari)

Figure 3.1: Purkinje cell death in organotypic slice cultures of postnatal rat cerebellum is rescued by NMDA treatment.

(A) Untreated P3 control slices. (B) P3 slices treated with 20 μM NMDA. (C) The effect of NMDA (20 μM) was abolished when cultures were simultaneously blocked by the NMDA-channel blocker MK801 (100μM). (D) Quantitative analysis of Purkinje cells survival in control, after treatment with 20 μM NMDA, and after simultaneous treatment with NMDA (20 μM) and MK801 (100 μM).

3.1.3 Discussion

3.1.3.1 Mifepristone induces Purkinje cells depolarization

The powerful protective effect of mifepristone on postnatal Purkinje cells in organotypic slices cultures remained to be explained since neither the classical intracellular steroid receptors, nor the antioxidant properties of mifepristone were found to be involved (Ghoumari et al., 2003). This study demonstrates that mifepristone increases the survival of P3 Purkinje cells in cultures most probably by inducing their persistent depolarization, *via* the down-regulation of the Na^+/K^+-ATPase pump expression. Blocking the activity of this pump by a low concentration of ouabain also strongly enhances Purkinje cells survival. We demonstrated that mifepristone, by down-regulating the Na^+/K^+-ATPase, not only continuously depolarizes Purkinje cells, but also inhibits their spike discharge. This inhibition of the firing is not a simple consequence of the voltage-gated channels inactivation by depolarization, but most likely reflects a profound modification of the Na^+ and K^+ membrane gradients, probably resulting from the down-regulation of the Na^+/K^+-ATPase.

3.1.3.2 Purkinje cells depolarization is neuroprotective

The present results reveal that the transduction as well as the activity of the Na^+/K^+-ATPase alpha3 subunit increases in developing Purkinje cells after being placed in culture. The alpha3 subunit is considered as an “auxillary” isoform that is recruited during increased cellular activity (Blanco and Mercer, 1998). Indeed, with depolarization and the repeated firing of action potentials, the Na^+ and K^+ gradients are dissipated. Under these conditions, while the alpha 1- and alpha 2-isoforms are working at saturation, the alpha 3-isoform is activated. In this manner, alpha 3 functions as a spare pump to help restoring the resting membrane potential. In addition, its high affinity for ATP endows alpha 3 with the ability to use ATP even in conditions of low concentrations occurring after intense neuronal activity. The recruitment of this “emergency” subunit is thus likely to result from the injury made to the cells when Purkinje cells are placed in culture at P3.

The Na^+/K^+-ATPase increase results in the Purkinje cell hyperpolarization (Genet and Kado, 1997; Biser et al., 2000) that turns out to be fatal for immature neurons in P3 cerebellar slices cultures. Accordingly, this study showed that different depolarizing agents promoted the Purkinje cells survival. Thus, Purkinje cells may need a minimal degree of continuous

excitation to survive during the early phase of development, this excitation relying particularly on excitatory innervation. Indeed, this work presents data in favour of an important role played by climbing fibers in neuroprotection of immature Purkinje cells, since coculturing cerebellar slices with inferior olivary slices promotes Purkinje cells survival. Nevertheless, the effect of TTX, which blocks the action potential-mediated release of neurotransmitters, has not been tested in olivo-cerebellar organotypic cultures. This experiment would help to clarify the role of excitatory inputs from climbing fibers on the Purkinje cell survival in this preparation.

3.1.3.3 The role of neurotrophic factors in neuroprotection

Independently of the possible neuroprotective role of climbing fibers excitatory inputs, the Purkinje cell survival observed in olivo-cerebellar cocultures could be due to the contribution of neurotrophic factors, known to play a crucial role in the development and survival of nerve cells. While brain-derived neurotrophic factor, neurotrophin 3, and insulin-like growth factor I have been shown to play only marginal roles on the survival of P3 Purkinje cells (Ghoumari et al., 2003), other factors could however exert neuroprotective effects on Purkinje cells in olivo-cerebellar cocultures. Interestingly, depolarizing stimuli appear to enhance the response of certain neuronal populations to neurotrophic stimulation (Ghosh, 1996). Consequently, the depolarization induced by glutamate released by climbing fibers could also act in synergy with neurotrophic factors, to protect postnatal Purkinje cells from cell death. Which glutamate receptor could mediate the neuroprotective depolarization?

3.1.3.4 Juvenile NMDA-Rs and Purkinje cell neuroprotection

In a complementary set of experiments to the present study, we focused our attention on a candidate target of glutamate: the NMDA-R of postnatal Purkinje cells. P1 to P7 corresponds to the period when immature NMDA-Rs are present in Purkinje cells, while at P10 they are almost completely absent from these cells (Momiyama et al., 1996). These juvenile NMDA-Rs do not participate to the climbing fiber synaptic currents in postnatal Purkinje cells (Lachamp et al., 2005), and their functional role remains to be elucidated. As we showed in this study, NMDA, like other depolarizing agents, protects Purkinje cells in organotypic cultures. This result echoes with results of Yuzaki et al. (1996) who demonstrated in a model of primary cultures that NMDA-Rs expressed by neonate Purkinje cells directly promote their survival. From these observations, it can be proposed that ambient glutamate released from climbing fibers acts through NMDA-Rs of immature Purkinje cells. Because juvenile NMDA-

Rs are composed of the NR2D subunit (which confers high affinity for glutamate, no desensitization and slow deactivation), their relatively long lasting activation is able to induce prolonged depolarization of Purkinje cells. This could protect them from developmental cell death. Oppositely, Purkinje cells devoid of functional contacts with climbing fibers would then be eliminated following a physiological process. Thus, instead of promoting excitotoxicity, juvenile NMDA-Rs could represent an advantage for Purkinje cells at P3, when depolarization displays a neuroprotective effect on these cells.

A first step to test this hypothesis would be to perform inferior olivo-cerebellar cocultures in presence of D-APV, a selective antagonist of NMDA-R, or of MK801, a NMDA-channel blocker. If the glutamate released by climbing fibers induces a neuroprotective depolarization by activating NMDA-Rs expressed by postnatal Purkinje cells, then the inhibition of NMDA-Rs should block the Purkinje cell survival. Similarly, small interfering RNA could be used to specifically disrupt the expression of NR2D subunits that are expressed in postnatal Purkinje cells, in order to test their involvement in the survival of Purkinje cells in P3 olivo-cerebellar cocultures.

Although NMDA significantly promotes Purkinje cells survival in P3 cerebellar slices cultures, its effect is relatively modest compared with the effect of mifepristone or of other depolarizing agents. Actually, to be fully activated, NMDA-Rs require a simultaneous membrane depolarization to relieve the magnesium block. In our organotypic cultures, part of the effect of NMDA is possible because juvenile NMDA-Rs composed of the NR2D subunit have a low sensitivity for magnesium block. Nevertheless, it is likely that the NMDA neuroprotective effect on Purkinje cells would be enhanced in a magnesium free culture medium. In a more physiological context, AMPA/Kainate receptors that are highly expressed in P3 Purkinje cells at synapses with climbing fiber (Zhao et al., 1998; Momiyama et al., 2003; Douyard et al., 2007) could contribute to the Purkinje cell depolarization, allowing relieving the magnesium block of juvenile NMDA-Rs. It is worth mentioning here that during the first week after birth, GABAergic inputs that are present on immature Purkinje cell are depolarising through $GABA_A$ receptors (Eilers et al., 2001). Moreover, it has been recently shown in newborn cortical neurons that GABA depolarization cooperates with NMDA-R activation to regulate excitatory synapses formation (Wang and Kriegstein, 2008). The study of such interactions between GABA-A and NMDA receptors will be important next steps in understanding the physiology of excitatory systems in the immature cerebellum.

Finally, after the critical time window between P3 and P5, Purkinje cells survive in cerebellar organotypic cultures. One can propose that the establishment of functional synapses with parallel fibers, that starts from ~P5-P7 (Zhao et al., 1998), could compensate for the lack of climbing fiber inputs by providing to Purkinje cells a neuroprotective depolarization (if this neuroprotection process is still needed at this age).

3.2 Publication 2:

NMDA receptor contribution to the climbing fiber response in the adult mouse Purkinje cell

"What gets us into trouble is not what we don't know.
It's what we know for sure that just ain't so."
Mark Twain

3.2.1 Introduction

There has been decades of conflicting results about the expression of functional NMDA-Rs by Purkinje cells (depending for instance on species, age and/or techniques). With the advent of the patch-clamp technique used in cerebellar slices, almost 20 years ago, the possibility arose to directly study whole-cell currents. To ensure a better space clamp, Purkinje cells with a less developped dendritic tree are usually preferred for patch-clamp recordings (Roth and Hausser, 2001), thus animals younger than three weeks were mainly used in previous investigations. Because these studies did not detect NMDA currents in Purkinje cells of this age, with it came the abusive conclusion that Purkinje cells do not express functional NMDA-Rs after the first week of the postnatal development.

Despite the fact that the quality of space-clamp during somatic recording of synaptic currents is imperfect in patch-clamp recordings of mature Purkinje cells, the study of synaptic currents remains qualitatively valid in these cells, keeping in mind that recorded currents are substantially distorted in both their kinetics and amplitudes (Roth and Hausser, 2001). Thus, all other things being equal, we could perform an attentive examination of the excitatory currents generated in Purkinje cells of animals older than 3 weeks. In the following study, we showed that, in adult mice, mature Purkinje cells actually express NMDA-Rs that become detectable from the third postnatal week and participate to the CF synaptic transmission.

3.2.2 Summary of experimental results

- Mice older than 8 weeks were used to test the effect of bath or iontophoretic applications of NMDA on Purkinje cells recorded in whole cell patch-clamp in acute cerebellar slices. In both cases, in presence of NBQX, bicuculline, and TTX in the Mg^{2+}-free external solution, applications of NMDA induced currents, accompanied by an increase of current noise that is typical of NMDA currents.

- The contribution of NMDA-mediated currents to synaptic currents evoked by the PF or the CF stimulation was tested, in the presence of bicuculline in the Mg^{2+}-free external solution. Whereas PF-EPSCs do not display an NMDA component, CF-EPSCs surprisingly showed a NBQX-resistant component, which could be reversibly inhibited by D-APV as well as by Mg^{2+}.

- The contribution of GABA-A-mediated currents to the NBQX-resistant CF-EPSC was unlikely because of the continuous presence of bicuculline in the bath, and the use of low chloride concentration-based internal solutions. Blocking AMPA/Kainate receptors with higher concentrations of NBQX (50 μM), or blocking group 1 mGluRs with AIDA had no further effect on the NBQX-resistant CF-EPSCs. These results suggested that the NMDA-mediated CF-EPSC did not result from the indirect activation of GABA-A receptors, AMPA/Kainate receptors, or group1 mGlu receptors.

- To test the contribution of glutamate transporters to the NBQX-resistant CF-EPSCs, we used the specific and non-transported glutamate transporter blocker DL-TBOA. Instead of blocking the NBQX-resistant CF-EPSCs, DL-TBOA potentiated the responses, suggesting that glutamate transporters limit the amplitude of these currents. This suggested that NMDA mediated CF-EPSC would be smaller, or absent at more physiological temperatures (which favor the activity of glutamate transporters). However, at 32-35°C, although the NBQX-resistant CF-EPSC was potentiated, the relative NMDA-dependent component of this current remained the same. In conclusion, glutamate transporters do not prevent the activation of NMDA-Rs, even at more physiological temperatures.

- The addition of MK801 to the internal solution contained in the recording pipette specifically blocked the NMDA-mediated CF-EPSC. This experiment showed that this

current is mediated by NMDA-Rs post-synaptically expressed. This conclusion was further confirmed by analyzing the I-V relationship of the NMDA-mediated CF-EPSCs. As expected, the I-V relationship was linear in absence of Mg^{2+} in the external solution, whereas it displays the typical j-shape in presence of Mg^{2+}.

- To investigate the NR2 subunits composing the functional NMDA-Rs detected in Purkinje cells, immunolabelings of NR2 subunits, along with that of calbindin as markers of Purkinje cells, and VGluT2 as signals of climbing fibers terminals, were observed in confocal imaging. A strong labeling of Purkinje cells somas and proximal dendrites was observed with NR2-A/B antibodies, whereas no labelings were observed for NR2C and NR2D antibodies. In the proximal dendrites of Purkinje cells observed at higher magnification, the labeling for NR2-A/B often coincided with VGluT2 labeling, while it was less intense in the distal Purkinje cells dendrites. This distribution of NR2-A/B immunolabelings in Purkinje cells thus confirmed the presence of functional NMDA-Rs evidenced in patch-clamp experiments.

- To establish the developmental profile of this NMDA-mediated currents, we analyzed the Purkinje cells CF-EPSCs of mice aged of 12 days to 12 weeks. The proportion of cells displaying a detectable NMDA component in the CF-EPSCs became significant from P21 and the amplitudes of this current increased dramatically from P18 to P21.

- We noticed that in previous studies which investigated the nature of Purkinje cells synaptic currents, CNQX was widely used as a specific blocker of AMPA receptors. However, as we showed here, CNQX partly blocked the NMDA-mediated CF-EPSCs.

- We next investigated the contribution of NMDA-Rs in the complex spike in mature animals. In absence of Mg^{2+} in the bath, we first demonstrated that NMDA-Rs underlie a non-negligible part of the complex spike. This NMDA - excitatory post-synaptic potential (EPSP) was all or none with a mean amplitude of 14 mV. In presence of Mg^{2+}, blocking NMDA-Rs by D-APV reduced the fast depolarization plateau and the slow afterdepolarization of the complex spike. It also reversibly increased the spikes and spikelets latencies, and sometimes even reduced their number.

For figures and details, see accompanying paper.

Cellular/Molecular

NMDA Receptor Contribution to the Climbing Fiber Response in the Adult Mouse Purkinje Cell

Claire Piochon,[1] Theano Irinopoulou,[2] Daniel Brusciano,[1] Yannick Bailly,[3] Jean Mariani,[1,4] and Carole Levenes[1]

[1]Université Pierre et Marie Curie-Paris 6, Unité Mixte de Recherche (UMR) 7102, Centre National de la Recherche Scientifique (CNRS), Laboratoire Neurobiologie des Processus Adaptifs, Équipe Développement et Vieillissement du Système Nerveux, 75005 Paris, France, [2]Unité 536/Unité 706, Inserm, Institut du Fer à Moulin, F-75005 Paris, France, [3]Neurotransmission et Sécrétion Neuroendocrine, Institut des Neurosciences Cellulaires et Intégratives UMR 7168, CNRS, Université Louis Pasteur, 67084 Strasbourg, France, and [4]Hôpital Charles Foix, Assistance Publique–Hôpitaux de Paris, 94 Ivry sur Seine, France

Among integrative neurons displaying long-term synaptic plasticity, adult Purkinje cells seemed to be an exception by lacking functional NMDA receptors (NMDA-Rs). Although numerous anatomical studies have shown both NR1 and NR2 NMDA-R subunits in adult Purkinje cells, patch-clamp studies failed to detect any NMDA currents. Using more recent pharmacological and immunodetection tools, we demonstrate here that Purkinje cells from adult mice respond to exogenous NMDA application and that postsynaptic NMDA-Rs carry part of the climbing fiber-mediated EPSC (CF-EPSC), with undetectable contribution from presynaptic or polysynaptic NMDA currents. We also detect NR2-A/B subunits in adult Purkinje cells by immunohistochemistry. The NMDA-mediated CF-EPSC is barely detectable before 3 weeks postnatal. From the end of the third week, the number of cells displaying the NMDA-mediated CF-EPSC rapidly increases. Soon, this EPSC becomes detectable in all the Purkinje cells but is still very small. Its amplitude continues to increase until 12 weeks after birth. In mature Purkinje cells, we show that the NMDA-Rs contribute to the depolarizing plateau of complex spikes and increase their number of spikelets. Together, these observations demonstrate that mature Purkinje cells express functional NMDA receptors that become detectable in CF-EPSCs at ~21 d after birth and control the complex spike waveform.

Key words: **Purkinje cell; cerebellum; development; climbing fiber; complex spike; NMDA**

Introduction

The NMDA receptor (NMDA-R) has unique properties that underlie its roles in developmental, physiological, and pathological processes in the brain (for review, see Dingledine et al., 1999; Cull-Candy et al., 2001; Mori and Mishina, 2003). NMDA-Rs are expressed in almost all principal neurons, but, so far, they seemed to be absent from adult Purkinje cells. Thus, these cells are often used as experimental model neurons lacking NMDA-Rs. Although immature rodent Purkinje cells express NR1/NR2-D-containing NMDA-Rs (Dupont et al., 1987; Rosenmund et al., 1992; Cull-Candy et al., 1998), there are numerous contradictory findings regarding the actual expression of functional NMDA-Rs by adult Purkinje cells. Using patch clamp, electrophysiologists concluded that Purkinje cells no longer express functional NMDA-Rs after the first postnatal (PN) week (Konnerth et al., 1990; Farrant and Cull-Candy, 1991; Llano et al., 1991). Discrepancies remained, however, with previous studies using intracellular or extracellular current-clamp techniques and showing that adult rat or mouse Purkinje cells respond to ionophoretic applications of NMDA (Quinlan and Davies, 1985; Dupont et al., 1987; Billard and Pumain, 1989; Krupa and Crepel, 1990) or providing evidence for functional NMDA-Rs in adult guinea pig Purkinje cells (Kimura et al., 1985; Sekiguchi et al., 1987). Immunohistochemistry or *in situ* hybridization studies display contradictions as well. Although the NR1 subunit is abundantly expressed by Purkinje cells throughout adulthood (Moriyoshi et al., 1991; Monyer et al., 1992, 1994; Akazawa et al., 1994; Laurie and Seeburg, 1994; Petralia et al., 1994a; Watanabe et al., 1994; Nakagawa et al., 1996; Hafidi and Hillman, 1997), the expression of NR2 in the adult remains unclear: some authors found signal for NR2-A mRNA in rat and human Purkinje cells (Akazawa et al., 1994; Scherzer et al., 1997), whereas others detected no messengers for NR2 (Monyer et al., 1994; Watanabe et al., 1994). Similarly, low immunoreactivity for NR2-A/B proteins was detected in young rats (Petralia et al., 1994b) and adult mice (Yamada et al., 2001), whereas Thompson et al. (2000) found clear NR2-B labeling in Purkinje cells from adult rats and mice, as well as NR2-A labeling in mice only. Beyond differences in the species and techniques, the important remaining question is the age of the animals, i.e., the temporal definition given to adulthood. In the present study, we used mice older than 8 weeks to demonstrate the expression of functional NMDA-Rs in mature Purkinje cells and their contribution to the waveform of the complex spike induced by the stimulation of the climbing fiber (CF). These NMDA-Rs contain NR2-A and/or NR2-B subunits and partici-

Received July 4, 2006; revised Aug. 9, 2007; accepted Aug. 21, 2007.

This work was supported by National Institutes of Health Grant NS34309 and by a 1 year salary provided by the Fondation pour la Recherche Medicale. We thank Dr. Carmen Cifuentes-Diaz for her kind and efficient advice on the immunolabeling study; Drs. Bertrand Lambolez, Jean-Luc Dupont, Ann Lohof, and Fabien Tell for their valuable comments on this study; and Laure and Thibaut for their enthusiastic contribution.

Correspondence should be addressed to Dr. Carole Levenes, Université Pierre et Marie Curie, Équipe Développement et Vieillissement du Système Nerveux, Case Courrier 14, 9 quai St. Bernard, 75005 Paris, France. E-mail: carole.levenes@snv.jussieu.fr.

DOI:10.1523/JNEUROSCI.2422-07.2007

 0270-6474/07/2710797-13$15.00/0

pate in the synaptic currents mediated by the CF in Purkinje cells (CF-EPSCs). We show that the NMDA-mediated CF-EPSC develops with maturation of Purkinje cells, being hardly detectable before postnatal day 21 (P21). In addition, we show that the NMDA-mediated CF-EPSC is half blocked by 10 μM 6-cyano-7-nitroquinoxaline-2,3-dione (CNQX). These observations explain the apparent lack of NMDA-Rs in Purkinje cell of pre-adult rodents, as observed by some authors, and indicate that NMDA-Rs are important to control the mature CF to Purkinje cell connection.

Materials and Methods

Care and use of animals. Animal housing and all procedures were performed in accordance with the guidelines of the French Ministry of Agriculture and the European Community. A minimal number of animals was used and handled with maximum care to minimize their suffering

Slice preparation. C57BL/6 mice (*Mus musculus*; Elevage Janvier, Le Genest-St-Isle, France), aged between 12 d and 6 months, were used in these experiments. Animals were first anesthetized with halothane and then rapidly decapitated. The cerebellar vermis was immediately removed and cooled to 4°C in oxygenated bicarbonate buffered solution (BBS) (see below). Parasagittal 180-μm-thick slices were cut with a vibratome (VT-1000S; Leica, Wetzlar, Germany). Slices were then incubated for at least 1 h at room temperature (RT) in the following BBS (in mM): 130 NaCl, 2.5 KCl, 2.0 $CaCl_2$, 1.0 $MgCl_2$, 26.0 NaHCO3, 1.3 NaH_2PO_4, and 10.0 glucose, pH 7.4 (when bubbled with 95% O_2 and 5% CO_2).

Whole-cell recording procedure. The recording chamber was continuously superfused with oxygenated BBS at a rate of 1–2 ml/min, at room temperature. In some experiments indicated in the text, the perfusion solution was warmed to near physiological temperatures (32–35°C) in the recording chamber. Purkinje cells were visually identified from their position, size, and shape using Nomarski differential interference contrast optics [40× water-immersion lens (Zeiss, Oberkochen, Germany) plus a 2.25× Nikon (Tokyo, Japan) zoom mounted on an upright Zeiss Axioskop-FS microscope]. Whole-cell voltage- and current-clamp recordings were made with an Axopatch-200A amplifier (Molecular Devices, Union City, CA). Signals were filtered at 2 or 5 kHz (low-pass) and usually sampled at 25–37 μs. Data acquisition and storage were performed on a personal computer running the ACQUIS1 software (Bio-Logic, Orsay, France). Patch pipettes were made of borosilicate glass capillary tubing pulled on a horizontal puller (Sutter Instruments, Novato, CA) and fire polished (MF-830; Narishige, Tokyo, Japan) to a final resistance of 2–5 MΩ depending on the internal solution used. The internal solutions used were as follows (in mM): 144.0 K gluconate, 6.0 KCl, 4.6 $MgCl_2$, 10.0 HEPES acid, 10.0 EGTA (or 1.0 for complex spike recordings), 1.0 (or 0.1 in 1 mM EGTA solutions) $CaCl_2$, 4.0 ATP-Na, and 0.4 GTP-Na, pH 7.3 adjusted with KOH. In some experiments, including current–voltage (*I–V*) curve protocols, the solutions contained the following (in mM): 150 Cs-gluconate, 4.6 $MgCl_2$, 10.0 HEPES acid, 10.0 EGTA, 1.0 $CaCl_2$, 4.0 ATP-Na, and 0.4 GTP-Na, pH 7.35 adjusted with CsOH. In some experiments, we added 1 or 3 mM of (5*R*,10*S*)-(+)-5-methyl-10,11-dihydro-5H-dibenzo[a,d]cyclohepten-5, 10-imine hydrogen maleate (MK801) to this internal solution to block postsynaptic NMDA-Rs; no differences were detectable between the two concentrations. Series resistances were partially compensated (70–75%). Holding potential was set at −70 mV, and liquid junction potential was not corrected (except when otherwise specified). When used, Mg^{2+}-free BBS external solutions were supplemented with 25 μM glycine. Bicuculline methiodide (10 or 20 μM; Sigma, St. Quentin Fallavier, France) was always added to block $GABA_A$-mediated currents. In the current-clamp mode, a few cells that were spontaneously more depolarized than −50 mV and that needed large current injection to maintain their membrane potential at −70 mV were considered to be damaged and were discarded. For ionophoresis experiments, when filled with 10 mM NMDA, ionophoretic pipettes had a final resistance of 40–50 MΩ. NMDA was ejected using negative square current pulses ranging from 100 to 250 nA. To limit diffusion of NMDA in the BBS, a small positive retention current (usually 10–15 nA) was continuously applied to the ionophoresis pipette between ejections. Extracellular stimulation of CFs or parallel fibers (PFs) was performed with a constant voltage isolated unit (0.1 ms square voltage pulses; 1–90 V) through a glass pipette filled with external solution. This pipette was moved around in the granular layer or white matter in the vicinity of the recorded Purkinje cell until the climbing fiber all-or-nothing response was obtained.

Glycine, MK801, 1,2,3,4-tetrahydro-6-nitro-2,3-[*f*]-quinoxaline-7-sulfonamide (NBQX) were from Sigma. NMDA, tetrodotoxin (TTX), CNQX, (*RS*)-1-aminoindan-1,5-dicarboxylic acid (AIDA), D-(−)-2-amino-5-phosphonopentanoic acid (D-APV), and DL-threo-β-benzyloxyaspartic acid (DL-TBOA) were from Tocris Bioscience (distributed by Fisher Bioblock Scientific, Illkirch, France).

To estimate whether a cell displays a detectable D-APV-sensitive NBQX-resistant EPSC, the amplitudes of the NBQX-resistant EPSCs in control and their amplitudes during bath application of D-APV were compared using a Mann–Whitney one-tailed statistical test. If the two populations of amplitudes (control and D-APV) were statistically different ($p > 0.05$), D-APV was considered as having an effect, and the percentage of blockade induced by D-APV was calculated.

For analysis of complex spikes, spikes and spikelets were first identified with a threshold detection protocol (usually 20 mV). Spike or spikelet latencies were estimated by calculating the time between the stimulation and the occurrence of the spike or spikelets.

Immunohistochemistry. Parasagittal 60 μm slices were prepared as described previously in a slicing sucrose BBS (in mM: 1 $CaCl_2$, 5 $MgCl_2$, 10 glucose, 4 KCl, 26 $NaHCo_3$, 248 sucrose, and 1.3 NaH_2PO_4, pH 7.35) cooled to 4°C and bubbled with 95% O_2 and 5% CO_2. Immediately after slicing, the slices were fixed with 4% paraformaldehyde in PBS for 2 h. They were then rinsed three times with PBS. Permeabilization and saturation were performed during 1 h on free-floating sections with PBS containing 0.25% Triton X-100 and 0.25% fish gelatin (PBS-G-T). Three types of anti-NR2 antibodies were used: (1) rabbit anti-NR2-D raised against amino acids 268–386 of human NR2-D; (2) goat anti-NR2-C/D raised against a peptide mapping at the C terminus of NR2-D of mouse; it also recognizes NR2-C (sc-1471; Santa Cruz Biotechnology, distributed by Tebu, Le Perray en Yvelines, France); and (3) rabbit anti-NR2-A/B raised against the C terminus of the rat NR2-A subunit. It recognizes both NR2-A and NR2-B mouse proteins equally (AB1548; Chemicon, Temecula, CA, distributed by Euromedex, Mundolsheim, France). The anti-NR2-C/D or anti-NR2-D antibodies were used only in single-labeling experiments and were revealed with Alexa Fluor 546 rabbit anti-goat or goat anti-rabbit antibodies (10 μg/ml; Invitrogen, Carlsbad, CA), following the procedure detailed hereafter. For NR2-A/B immunodetection, slices were divided into three batches and incubated overnight at room temperature in the following combinations: batch 1 with only the rabbit anti-NR2-A/B antibody (1 μg/ml); batch 2 incubated with NR2-A/B, mouse anti-calbindin-D28k (1:10000; Swant, Bellizona, Switzerland), and guinea pig anti-vesicular glutamate transporter 2 (VGluT2) (1:3000; Chemicon) antibodies; and batch 3 incubated with PBS-G-T only (control). Slices were then incubated 2 h with the fluorescent secondary antibodies (at 10 μg/ml; Invitrogen): Alexa Fluor 546 goat anti-rabbit (batches 1–3), Alexa Fluor 633 goat anti-mouse and Alexa Fluor 488 goat anti-guinea pig (batches 2 and 3). In some experiments, sheep anti-rabbit IgG cyanine 3-coupled (Cy3) (Sigma) was also used as a secondary antibody to reveal NR2-A/B. The labeled slices were mounted in Vectashield medium (Vector Laboratories, Burlingame, CA) and viewed with a confocal laser-scanning microscope (SP2; Leica, Manheim, Germany) using a 63× objective. In multiple-labeling experiments, acquisition of the signal was systematically performed in sequential mode. Alexa Fluor 488 was excited at 488 nm (argon laser), Alexa Fluor 546 and Cy3 dye at 543 nm (helium–neon laser), and Alexa Fluor 633 at 633 nm (helium–neon laser).

Three-dimensional reconstructions were performed using the Imaris-4 software (Bitplane, Zurich, Switzerland).

Statistics. Averages are given as mean ± SEM. Mann–Whitney or Wil-

coxon's tests were used for statistical comparisons, and p is given as the probability of the null hypothesis.

Results

Bath or ionophoretic applications of NMDA induce currents in Purkinje cells

Purkinje cells from animals older than 8 weeks were voltage clamped at −70 mV in the whole-cell patch-clamp configuration (see Materials and Methods). NMDA was applied in the bath for 1 min in the presence of NBQX (10 μM), TTX (1 μM), and bicuculline (20 μM). In these conditions, NMDA elicited inward currents in all the Purkinje cells tested ($n = 16$), with a mean amplitude of 38 ± 6.4, 110 ± 20.8, and 115 ± 56.1 pA for 20, 50, and 100 μM NMDA, respectively (Fig. 1*A*). NMDA was also applied locally using the ionophoresis technique, always in the presence of NBQX, TTX, and bicuculline at the same concentration as above. Applications at the level of the upper third part of the dendrites generally elicited no response unless using long-lasting ejections (for instance 1 s). Applications at the level of the lower two-thirds of the Purkinje cell dendrites generated large inward currents of 349.9 ± 54.9 pA ($n = 8$) that were completely abolished by D-APV ($n = 4$) (Fig. 1*B*) or by external Mg^{2+} ($n = 4$). These currents could reach >800 pA by increasing the ejection time. We preferred, however, working on smaller responses to limit diffusion of the NMDA. Thus, all tested Purkinje cells of adult mice respond to exogenous application of NMDA.

With slow methods of agonist application, like bath application, if the receptors involved are rapidly desensitizing, the resulting currents are very small. The fact that the NMDA current is very small during our bath application experiments compared with that induced by ionophoresis indicates strong desensitization of the response. Thus, the NMDA-Rs demonstrated here are unlikely to contain the neonatal NR2-D subunits that are known to display particularly low desensitization (Misra et al., 2000). Because of their biophysical features, NR2-D subunits are not compatible with synaptic currents (Misra et al., 2000), whereas other NR2 subunits are involved in NMDA-mediated synaptic transmission. It was therefore of interest to test the participation of the NMDA-Rs demonstrated here in the synaptic transmission of adult Purkinje cells.

PF-EPSCs display no NMDA component

The participation of some NMDA-Rs in EPSCs of Purkinje cells was examined in nominal Mg^{2+}-free solution to prevent NMDA-R blockade by external Mg^{2+} ions. PF-EPSCs, elicited by extracellular stimulation at 3 or 5 s intervals in the molecular layer, were identified by their graded amplitude increasing with stimulus intensity and by their characteristic paired-pulse facilitation in response to 30 ms interval paired stimulations (Konnerth et al., 1990). PF-EPSCs were inhibited by 10 μM NBQX in the bath ($n = 7$) (Fig. 1*C*). In a few cells ($n = 4$), a small EPSC (~30 pA) persisted in the presence of NBQX but was not further blocked by D-APV. Thus, low-frequency-evoked single PF-EPSCs display no detectable NMDA component.

CF-EPSCs display an NMDA component

CF-EPSCs were elicited by 30 s interval extracellular stimulation in the granular layer and could be identified by their all-or-none nature, very large amplitude, and paired-pulse depression (PPD) (40 ms interval) (Konnerth et al., 1990). CF-EPSCs during control periods were acquired at −70 mV (liquid junction uncorrected), in nominal Mg^{2+}-free solution and in the presence of 100 or 500 nM NBQX to reduce voltage-clamp escape attributable to the very large amplitude of CF-EPSCs (Fig. 1*D*). In contrast to PF-EPSCs, adding 10 μM NBQX to the bath did not completely abolish CF-EPSCs. A residual CF-EPSC of 228.9 ± 25 pA persisted in 46 of 47 adult Purkinje cells tested (Figs. 1*D*, 2). This NBQX-resistant CF-EPSC was all or none and displayed PPD. D-APV (50 μM) and Mg^{2+} (1 mM), respectively, blocked 87 ± 5.5% ($n = 9$) (Fig. 2*A*) and 72.6 ± 4% ($n = 10$) (Fig. 2*B*) of this NBQX-resistant EPSC. The washout of D-APV allowed this NBQX-resistant CF-EPSC to fully recover (Fig. 2*A*).

The NMDA-mediated CF-EPSC does not result from the indirect activation of AMPA/kainate receptors, metabotropic glutamate receptors type 1, $GABA_A$ receptors, or glutamate transporters

Purkinje cells respond to exogenous application of NMDA in the presence of NBQX, bicuculline, and TTX in the bath, i.e., when the contribution of polysynaptic NMDA currents is strongly reduced. This suggests that, surprisingly enough, these cells express NMDA-Rs. This is further supported by the existence of an NMDA-mediated component in the CF-EPSC. However, considerable previous evidence indicated that NMDA-Rs are not, or very weakly, expressed by adult Purkinje cells (Crepel et al., 1982; Garthwaite et al., 1987; Konnerth et al., 1990; Krupa and Crepel, 1990; Farrant and Cull-Candy, 1991; Llano et al., 1991). If this is true, the NMDA-mediated CF-EPSC evidenced here has to be of presynaptic origin. How could presynaptic NMDA-Rs carry part of the CF-EPSC? One possibility lies in the indirect activation of presynaptic NMDA currents, located at both inhibitory and excitatory terminals. The stimulation of a single climbing fiber causes the simultaneous release of multiple glutamate vesicles at numerous release sites (Wadiche and Jahr, 2001). The resulting spillover of glutamate could activate some presynaptic NMDA-Rs, located on parallel fibers (Petralia et al., 1994a,b) (but see Diez-Garcia et al., 2005; Shin and Linden, 2005) or inhibitory interneurons (Glitsch and Marty, 1999; Clark and Cull-Candy, 2002). These presynaptic NMDA-Rs would then drive the release of glutamate from parallel fibers or GABA from interneurons. GABA mediates currents in Purkinje cells during bath applications of NMDA (Llano et al., 1991; Glitsch and Marty, 1999). In the present study, however, all applications of NMDA were made in the continuous presence of TTX, bicuculline, and NBQX, and thus, Na^+ action potentials, $GABA_A$, and AMPA/kainate receptor-mediated currents were blocked. In these conditions, the contribution of polysynaptic NMDA-associated currents is strongly reduced, if not completely eliminated. In addition, during the application of exogenous NMDA, we never observed any miniature inward currents, which, in summation, could have accounted for the NMDA current (Llano et al., 1991). Finally, the existence of $GABA_A$-mediated currents in Purkinje cells is very unlikely here, because, in addition to bicuculline in the bath, recordings were made with low chloride concentration-based internal solutions. The total estimated chloride concentrations were 5.6 and 15.4 mM, respectively, for Cs- and K-based solutions. In these conditions, at approximately −70 mV, chloride currents are either outward or their driving force is low. Thus, in the Purkinje cell recorded here, the contribution of GABA-mediated currents to the NMDA inward current is either absent or strongly reduced.

Another possibility involves the contribution of NMDA-Rs located at parallel fibers (see above). In this hypothesis, some

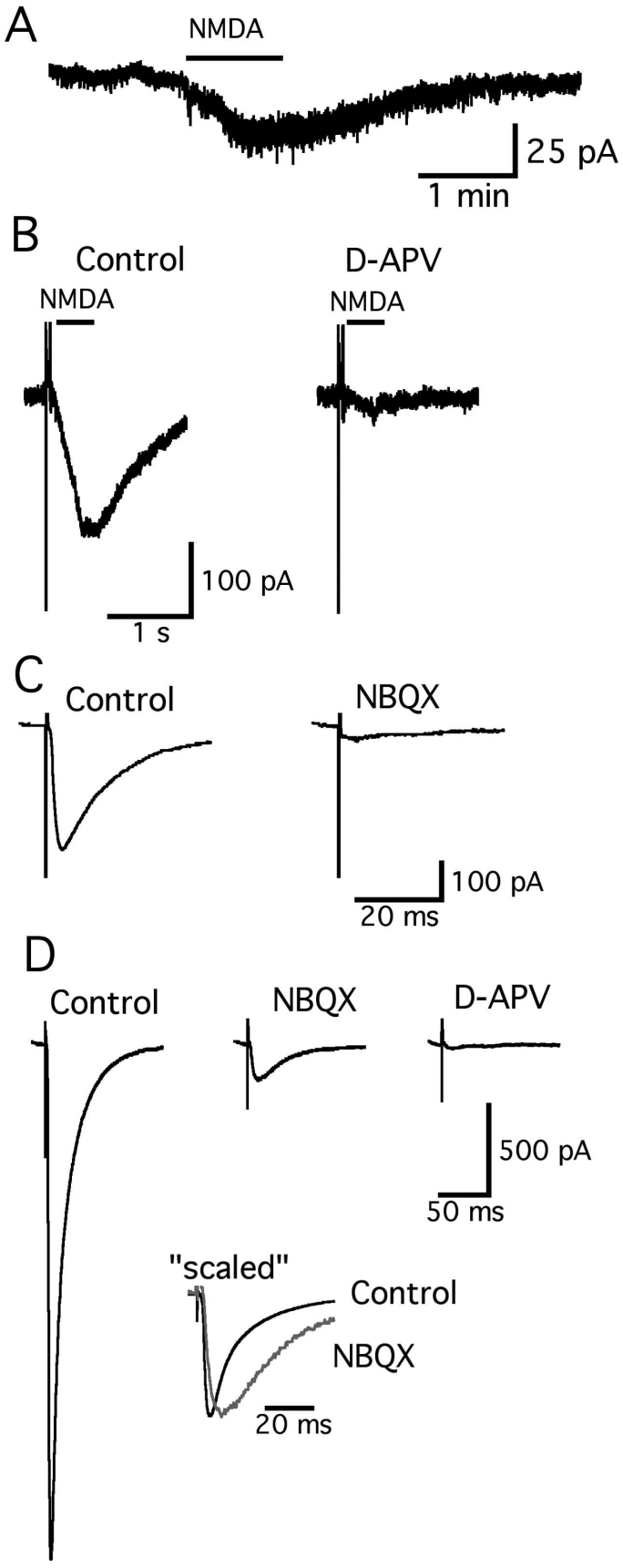

Figure 1. NMDA currents recorded in adult (>8 weeks) mouse Purkinje cells and their contribution to the climbing fiber EPSC. ***A***, Bath application of 50 μM NMDA performed in the presence of NBQX (10 μM), bicuculline (20 μM), and TTX (1 μM). ***B***, Inward currents induced by ionophoretic applications of NMDA (left) are completely blocked by 50 μM D-APV (right). Recordings made in the presence of NBQX, bicuculline, and TTX in the bath (same concentrations as in ***A***). ***C***, PF-EPSCs are blocked by NBQX. Averaged PF-EPSCs from one cell in control conditions (left) and in the presence of 10 μM NBQX (right). ***D***, CF-EPSCs display an NMDA-mediated component. Averaged CF-EPSCs recorded in control conditions (bicuculline only, left), after addition of 10 μM NBQX (middle), and in the presence of NBQX plus 50 mM D-APV (right). Inset, Superimposed scaled control-mediated (black) and NMDA-mediated (gray) CF-EPSCs.

presynaptic NMDA-Rs located at parallel fibers could drive the release of glutamate that could, in turn, activate different targets on Purkinje cells, such as AMPA/kainate receptors, metabotropic glutamate receptors type 1 (mGluR1), and glutamate transporters. Concerning the two first candidates, 50 μM NBQX ($n = 4$) or the group I mGluR antagonist AIDA (100 μM; $n = 3$) (Fig. 2*D*) have no effect on the NBQX-resistant CF-EPSC. Glutamate transporters deserve specific attention because they have been shown to mediate an NBQX-resistant CF-EPSC (Otis et al., 1997; Auger and Attwell, 2000). Therefore, we blocked glutamate transporters with DL-TBOA, a specific and nontransported glutamate transporter blocker that does not induce glutamate release by heteroexchange (Shimamoto et al., 1998). When applied to Purkinje cells, DL-TBOA (100 μM in the bath) did not block but, in fact, increased the amplitude of the NMDA-mediated CF-EPSCs from 238.1 ± 24.5 pA in the control period to 402.6 ± 75 pA ($n = 5$, Wilcoxon's test, $p < 0.05$) (Fig. 2*C*). These potentiated responses were blocked by D-APV (50 μM), showing that they were carried by NMDA-Rs (Fig. 2*C*). Thus, the NMDA-mediated CF-EPSC does not result from the indirect activation of AMPA/kainate receptors, mGluR1, or glutamate transporters in Purkinje cells.

The large potentiation of the NMDA-mediated CF-EPSCs observed in the presence of DL-TBOA shows that glutamate transporters limit the amplitude of these currents, raising the possibility that the NMDA-mediated CF-EPSC would be strongly reduced or even absent at physiological temperatures (because of enhanced glutamate uptake). To test this, we raised the temperature of the bath to 32–35°C and estimated the relative contribution of the NMDA-mediated current to the total NBQX-resistant CF-EPSC by adding D-APV at the end of the recordings. To calculate the true NMDA-mediated CF-EPSC, the amplitude of the CF-EPSC recorded in NBQX plus D-APV was subtracted from the CF-EPSC in NBQX alone. As illustrated in supplemental Figure 1*A* (available at www.jneurosci.org as supplemental material), the mean NBQX-resistant CF-EPSC was increased in amplitude (397.6 ± 58.8 pA; $n = 5$) when compared with RT (usually 25°C) experiments (261.6 ± 45.3; $n = 8$ pA). However, the relative NMDA-dependent component remained the same at both temperatures (supplemental Fig. 1*B*, available at www.jneurosci.org as supplemental material) (196.6 ± 80.1, $n = 5$ at 32–35°C vs 212.5 ± 44.3 pA, $n = 8$ at RT). The remaining NBQX-resistant CF-EPSC that is potentiated at 32–35°C and that is not mediated by NMDA-Rs probably corresponds to the CF-EPSC carried by glutamate transporters (Otis et al., 1997; Auger and Attwell, 2000; Huang et al., 2004). Thus, even at more physiological temperature, CF-EPSCs display a clear and constant NMDA-mediated current, which indicates that glutamate transporters do not prevent the activation of NMDA-Rs located at climbing fiber to Purkinje cell connections.

These observations indicate that some NMDA-Rs of Purkinje cells are located relatively close to climbing fiber terminals. In addition, because of the potentiating effect of DL-TBOA, there might also be additional NMDA-Rs at some distance from the

←

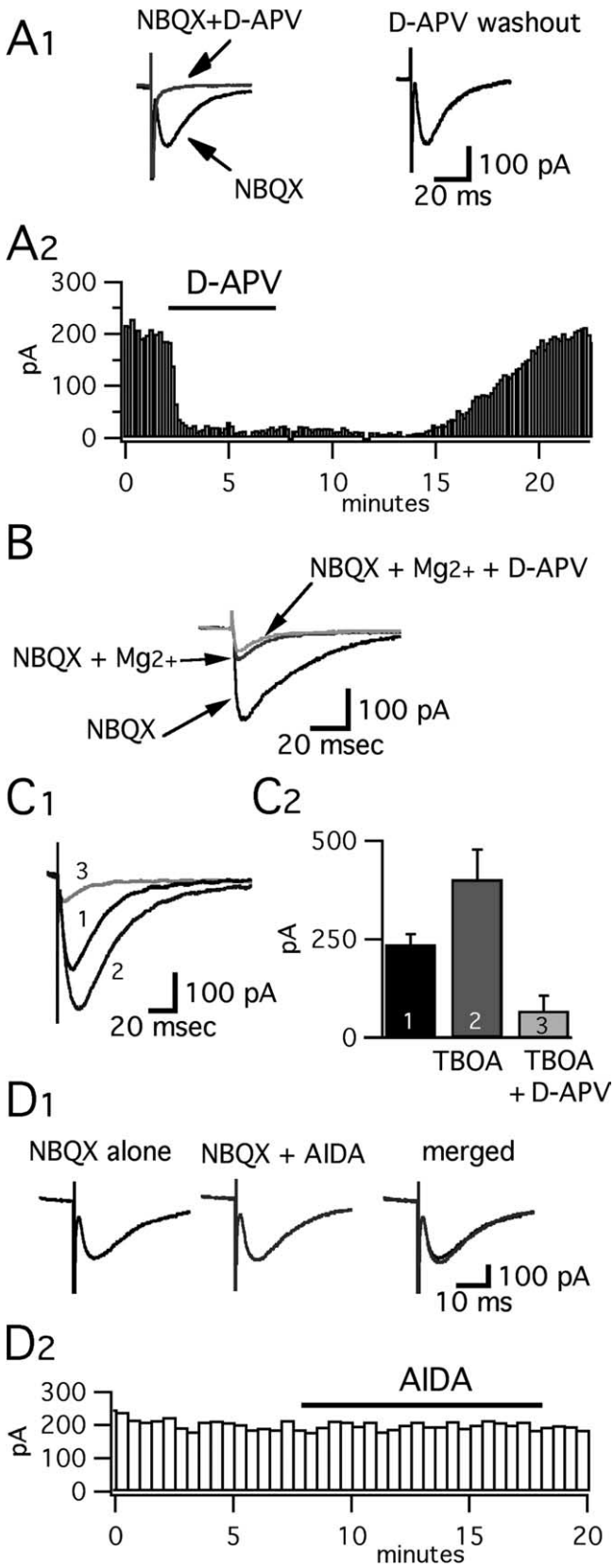

Figure 2. Most of the NBQX-resistant CF-EPSC is carried by NMDA-Rs in the absence of Mg^{2+}. ***A***, D-APV (50 μM) reversibly blocks the NBQX-resistant CF-EPSC. ***A1***, Averaged CF-EPSCs recorded in one cell before, during, and after the application of D-APV (as indicated on the traces). ***A2***, Same cell as ***A1***. Amplitude of the CF-EPSCs plotted over time; note the washout of D-APV. ***B***, Effect of Mg^{2+} on the NBQX-resistant CF-EPSC. Superimposed averaged NBQX-resistant CF-EPSCs recorded before and after addition of 1 mM external Mg^{2+} (as indicated on the traces) are shown. Additional application of 50 μM D-APV does not further block the response. ***C***, Blocking glutamate transporters with 100 μM of DL-TBOA potentiates the NMDA-mediated CF-EPSC. ***C1***, Averaged NBQX-resistant CF-EPSCs (trace 1, black) are potentiated by TBOA (trace 2, dark gray). These potentiated responses are blocked by the final addition of 50 μM D-APV (trace 3, light gray) showing that they are carried by NMDA-Rs. ***C2***, Mean ± SEM amplitude ($n = 5$ cells) of the NMDA-mediated CF-EPSCs in control (NBQX at 10 μM), after addition of TBOA (100 μM), and after further addition of D-APV (50 μM). Numbers correspond to ***C1***. ***D***, Blocking group 1 mGluRs with AIDA (100 μM) has no effect on the NBQX-resistant CF-EPSC. ***D1***, Averaged NBQX-resistant CF-EPSCs in control (NBQX alone) and during bath application of AIDA (NBQX + AIDA). Sweeps are merged for comparison (right). ***D2***, Amplitude of the NBQX-resistant CF-EPSC plotted over time before and during the application of AIDA (as indicated).

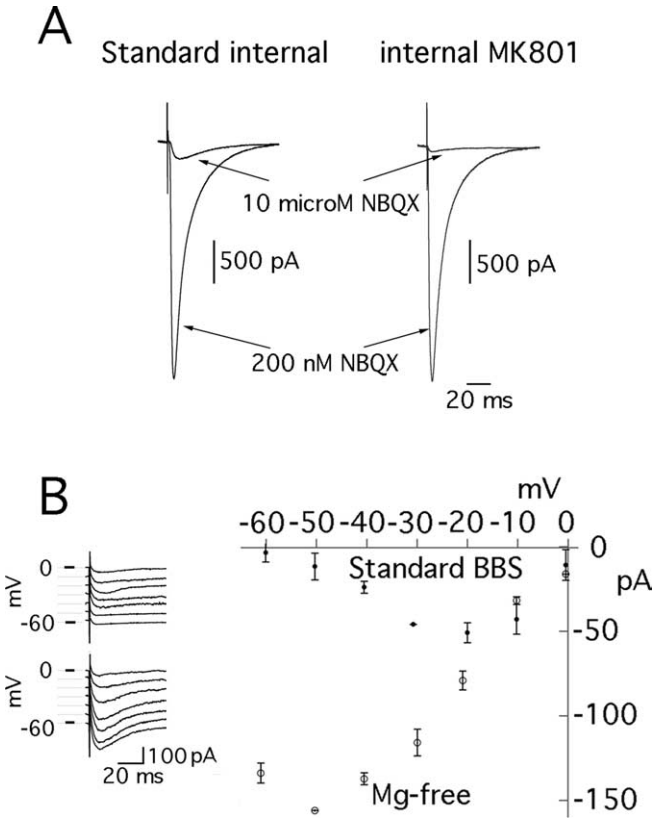

Figure 3. NMDA-mediated CF-EPSCs are postsynaptic. ***A***, Internal MK801 blocks the NBQX-resistant CF-EPSC. Left, Averaged total CF-EPSCs recorded in one cell with standard K-based internal solution in the presence of 200 nM NBQX to reduce voltage-clamp escape and after addition of 10 μM NBQX. Right, Another cell recorded in the same conditions but with 3 mM MK801 added to the intracellular medium. Note that the infusion of MK801 in the Purkinje cell illustrated in the right blocks the NBQX-resistant CF-EPSC. ***B***, Left, NBQX-resistant CF-EPSCs recorded from one cell at different holding potentials (indicated on the left) to establish their *I–V* curve. Top traces, In the presence of external Mg^{2+}; bottom traces, in nominally Mg^{2+}-free BBS. Right, Corresponding *I–V* curve established with the mean ± SEM peak amplitude of three successive EPSCs recorded at a given potential, in the presence (filled circles; standard BBS) or in the absence of external Mg^{2+} (open circles; Mg-free).

releasing sites. This raises the possibility that, under conditions of saturation of glutamate transporters (i.e., sustained or repetitive glutamatergic synaptic transmission), NMDA receptors near CF terminals could be massively recruited.

In conclusion, there is no detectable contribution of indirect/polysynaptic NMDA currents to the NMDA-mediated CF-EPSC in our conditions. However, other neurotransmitters and/or mechanisms cannot be ruled out from a complex model of possible indirect NMDA currents. For this reason, it

was important to clarify the presynaptic or postsynaptic origin of the NMDA-mediated CF-EPSC with more direct approaches.

Blocking postsynaptic NMDA-Rs inhibits the NMDA-mediated CF-EPSC

Postsynaptic NMDA-Rs were blocked specifically in the recorded Purkinje cell by adding MK801 to the internal solution. MK801 is a pore blocker of NMDA-Rs that has been used successfully in the internal medium to block postsynaptic NMDA responses in single cells (Berretta and Jones, 1996; Humeau et al., 2003; Massey et al., 2004; Samson and Pare, 2005). MK801 was added to the internal medium (1 or 3 mM with no detectable differences), the climbing fiber was stimulated, and 10 μM NBQX was added to the bath. The mean amplitude of the NBQX-resistant CF-EPSC was then estimated. With MK801 in the pipette, it was of 50.6 ± 7.5 pA ($n = 9$) on average, whereas it was of 228.9 ± 25 pA in controls (Fig. 3*A*) ($p < 0.001$). This remaining MK801-resistant current of 50.6 ± 7.5 pA was not further blocked by D-APV (50 μM). Thus, postsynaptic MK801 has blocked all the NMDA component of the CF-EPSC.

These experiments show that the NMDA-mediated CF-EPSC is postsynaptic with no detectable presynaptic component. This conclusion, based on pharmacology, was further confirmed by analyzing the *I–V* relationship of the NMDA-mediated CF-EPSCs.

The *I–V* relationship of the NMDA-mediated CF-EPSCs displays the typical j-shape of postsynaptic NMDA-Rs

If the NMDA-mediated CF-EPSC is actually postsynaptic, its *I–V* relationship is expected to display a negative slope between −70 and −20 mV in the presence of external Mg^{2+} (the *I–V* curve is "j-shaped"). Changing the holding potential of Purkinje cells will relieve the Mg^{2+} block of postsynaptic but not of presynaptic NMDA-Rs. To address this issue, *I–V* curves of the NMDA-mediated CF-EPSCs were recorded in the presence or absence of external Mg^{2+}.

Because of their very large and fully developed dendrites, it is not possible to accurately voltage clamp adult Purkinje cells (Llano et al., 1991). The situation is even worse at depolarized potentials, at which voltage-dependant ionic channels open, increasing voltage-clamp escape. Thus, one expects that the EPSCs recorded at positive potentials would be rather small and that their reversal potential would be above the theoretical value of 0 mV. In these experiments, it was not possible to reduce this problem by pharmacologically blocking voltage-dependent Na^+ or Ca^{2+} channels: (1) the diffusion of internal channel blockers in the distal dendrites was not sufficient to prevent voltage-clamp escape, and (2) we could not use external blockers because they also inhibit neurotransmitter release. We therefore started the *I–V* curve protocols at 0 mV, letting the voltage-dependent currents inactivate, and then progressively repolarized the cell to −60 mV (liquid junction estimated at −12 mV and corrected), focusing on the effect of external Mg^{2+} ions on the shape of the *I–V* curve at these potentials. In standard 1 mM external Mg^{2+}, for all cells tested, the *I–V* curves displayed the typical j-shape of NMDA-mediated currents at negative potentials (Fig. 3*B*). In contrast, in nominally Mg^{2+}-free external solution, for all but one of the Purkinje cells recorded ($n = 15$), the NMDA-mediated CF-EPSCs displayed a linear *I–V* relationship, with a positive slope between −50 and 0 mV (Fig. 3*B*). A slight blockade of the NMDA-mediated EPSC was often still apparent at potentials below −60 mV in the Mg^{2+}-free solution (Fig. 3*B*). This is probably attributable to the presence of contaminating Mg^{2+} ions that persist in slices.

These results confirm that the NMDA-mediated CF-EPSC is carried by postsynaptic NMDA-Rs.

Immunolabeling reveals the presence of NR2-A/B subunits on Purkinje cells

Our results imply the existence of functional NMDA-Rs on Purkinje cell membranes, i.e., of NMDA-Rs composed of heteromeric NR1/NR2 subunits, particularly in the vicinity of climbing fibers terminals. Although the expression of NR1 by adult Purkinje cells is well documented, that of NR2 subunits is less clear (for instance, see Yamada et al., 2001, as opposed to Thompson et al., 2000). We thus performed immunolabeling of the NR2 subunits, along with that of calbindin and VGluT2 as markers of Purkinje cells and climbing fibers terminals, respectively. Acquisition of the fluorescent signal with a confocal microscope revealed no labeling for NR2-C or NR2-D subunits in adult Purkinje cells, with any of the antibodies used (see Materials and Methods and data not illustrated). However, a clear and constant labeling of NR2-A/B subunits was found in Purkinje cell soma and proximal dendrites throughout the cerebellar vermis (Fig. 4). In the molecular layer, cells and dendrites labeled by NR2-A/B antibodies were almost exclusively calbindin positive (Fig. 4*B*,*C*). In the first two-thirds of the molecular layer, corresponding to the zone of climbing fiber terminals, the NR2-A/B subunits were clearly concentrated in the Purkinje cell dendrites (Fig. 4). This NR2-A/B staining was homogenous throughout the lobules. It was present in either NR2-A/B single- or multiple-labeling experiments (Fig. 4), thereby excluding any interference from cross-reactions attributable to multiple-staining procedures. Because of the rather diffuse labeling of NR2-A/B in the overall Purkinje cells dendrites, nonconfocal images of the 60 μm slices show a constant and diffuse staining of the molecular layer in which only soma and large dendrites of Purkinje cells were distinguishable. Confocal images observed in 1-μm-spaced stacks revealed clear NR2-labeled dendrites (Fig. 4*B*). Three-dimensional (3D) reconstructions of confocal stacks show strong labeling by NR2-A/B antibodies throughout the proximal dendrites (Fig. 4*C*). In the proximal dendrites of Purkinje cells observed at higher magnification, the labeling for NR2-A/B often coincided with VGluT2 labeling (Fig. 4*D*).

A lighter and more diffuse labeling of NR2-A/B was also observed in the distal dendrites of Purkinje cells, including in the upper third of the molecular layer, a zone of contacts exclusively between parallel fibers and Purkinje cells, as assessed by the absence of VGluT2 labeling in this zone (Fig. 4*B*,*C*). Although the labeling was less intense in this zone, this observation opens the possibility of the existence of some extrasynaptic NMDA-Rs on Purkinje cells near parallel fiber synapses. Alternatively, it could also correspond to some presynaptic NR2-A/B subunits. In the granular layer, NR2-A/B and VGluT2 labeling also coincide. This most probably corresponds to glomeruli, in which mossy fiber terminals express VGluT2 (Hioki et al., 2003) and granule cell dendrites NR2-A (as well as NR2-C that are not labeled by the present antibody) in mature animals (Akaike et al., 1981; Cathala et al., 2000). In agreement with the observation that mRNA for NR2-A and NR2-B subunits is absent from stellate and basket cells (Akazawa et al., 1994), no labeling was detected in these neurons.

Adult Purkinje cells express high levels of NR1 subunits (Petralia et al., 1994a; Hafidi and Hillman, 1997; Thompson et al., 2000). Thus, the description of some NR2 subunits in these cells

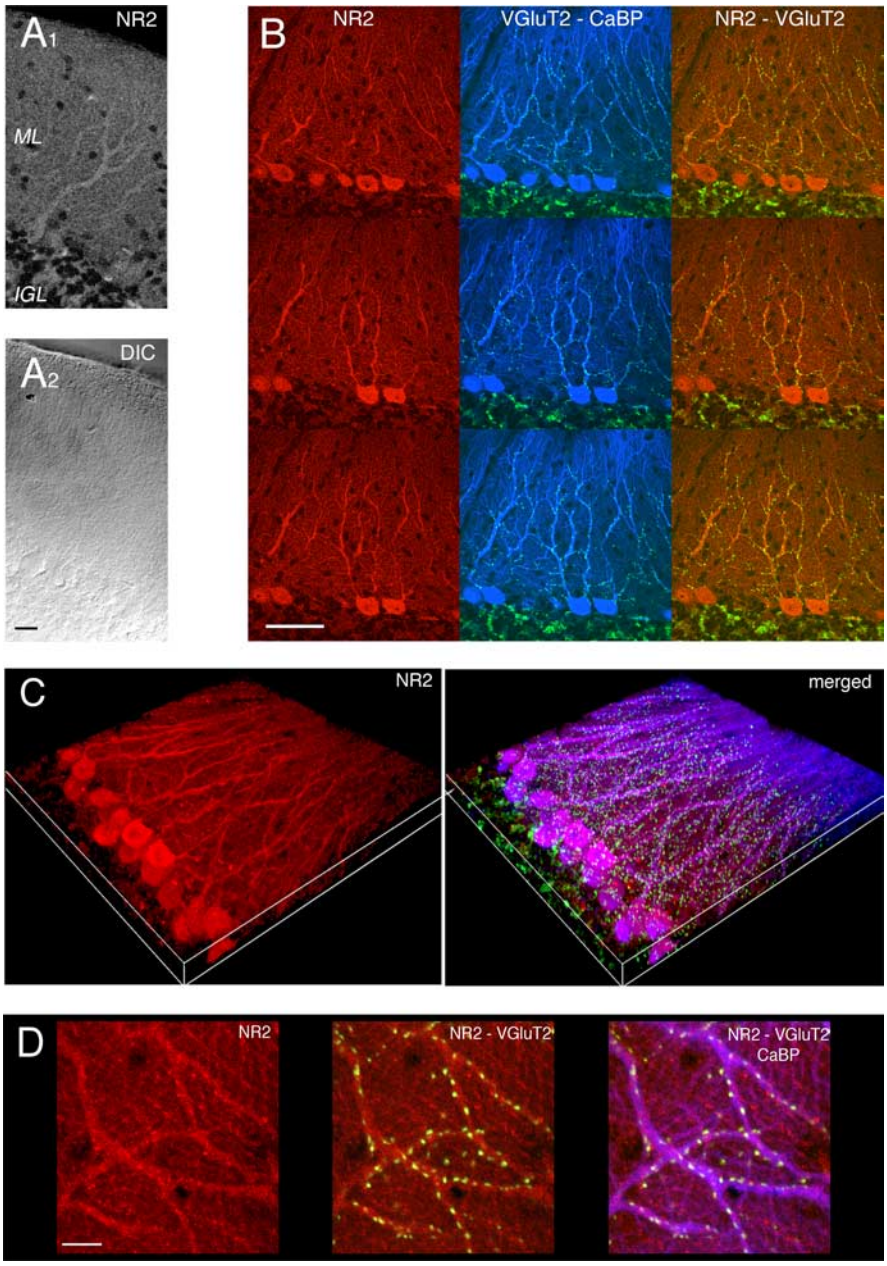

Figure 4. Distribution of NR2-A/B immunofluorescence on sagittal slices observed with confocal imaging. ***A1***, Single NR2-A/B immunolabeling showing the soma and primary dendrites of a Purkinje cell. ***A2***, Same area observed in differential interference contrast microscopy (DIC). Scale bar, 20 μm. ML, Molecular layer; IGL, internal granular layer. Note the presence of presumably NR2-A at the level of glomeruli in the IGL. ***B***, Successive 1-μm-spaced confocal sections showing NR2-A/B (red), calbindin (CaBP, blue), as well as VGluT2 (green) labeling. Scale bar, 40 μm. ***C***, Three-dimensional reconstruction of a stack of 30 successive 1-μm-spaced confocal sections displaying the NR2-A/B immunolabeling alone (left) and NR2-A/B (red) plus CaBP (blue) plus VGluT2 (green) merged (right). Same zone as in ***B***. Note that the merged 3D stack reveals that distal dendrites of Purkinje cell in the upper third of the molecular layer displays less intense immunoreactivity for NR2-A/B. ***D***, High-power image (4×) of CaBP-positive (blue) dendrites showing NR2-A/B (red) and VGluT2 (green). Scale bar, 10 μm.

is not surprising and confirms the presence functional NMDA-Rs. In addition, supporting our data, the distribution of NR2-A/B labeling described here exactly matches that of NR1 subunits in Purkinje cells (Petralia et al., 1994a).

The NMDA component of the CF-EPSC appears at the end of 3 weeks PN and progressively increases with Purkinje cell maturation

Our data converge toward the presence of NMDA-Rs in mature Purkinje cells from animals older than 8 weeks. Most of the authors that did not detect NMDA-Rs in fact worked with much younger animals. The developmental profile of the NMDA-mediated CF-EPSC was therefore investigated by quantifying the effect of D-APV on the amplitude of the CF-EPSC recorded in 10 μM NBQX from P12 to 12 weeks PN (see Materials and Methods). As illustrated in Figure 5*B*, the NMDA-mediated component of CF-EPSCs can hardly be detected before P21. Both the number of cells displaying NMDA-mediated CF-EPSC (Fig. 5*B*) and the mean amplitude of these NMDA currents increase from P18 to P21 (Fig. 5*C*), at least in the vermis, in which our recordings were performed. From P22, all the cells tested displayed significant NMDA-mediated CF-EPSCs, but their amplitudes were still rather modest and continued to increase, reaching 69.5 ± 4.8% ($n = 7$) 8 weeks after birth (Fig. 5*C*). Taking into account cells from animals ranging in age from 12 weeks to 6 months, the mean blockade induced by D-APV was 87 ± 5.5% (Fig. 5*C*). Thus, there is still a slight increase in the amplitude of the NMDA-mediated CF-EPSC after 8 weeks PN. These data show that the NMDA-mediated component of the CF-EPSC appears by P21 but is still very small at this age, probably explaining the difficulty to detect these receptors in previous studies.

CNQX partly blocks the NMDA-mediated CF-EPSC

The presence of functional NMDA-Rs in Purkinje cells and the existence of NMDA-mediated currents in CF-EPSCs were investigated previously mostly in immature animals (Perkel et al., 1990; Farrant and Cull-Candy, 1991; Llano et al., 1991); thus, the absence of detectable NMDA currents is not surprising considering our results. However, a study from Perkel et al. (1990) did not show any NMDA component in the CF-EPSCs of 4- to 6-week-old rats. Although species differences cannot be completely excluded, examination of this study shows that it was done using CNQX as a specific blocker of AMPA receptors. CNQX has been widely described as being also an antagonist at NMDA-Rs, in part by competing with glycine at its modulatory site (Birch et al., 1988; Harris and Miller, 1989; Kessler et al., 1989; Pellegrini-Giampietro et al., 1989; Lester and Jahr, 1990; Mead and Stephens, 1999) and also with glutamate at its binding site (Lester and Jahr, 1990). In contrast, NBQX has no effect on NMDA currents (Sheardown et al., 1990). We therefore studied the effect of CNQX on the NMDA-mediated CF-EPSC in mice older than 8 weeks at concentrations commonly used in cerebral tissue slices (Fig. 5*D*). At 10, 20, and 50 μM, the residual NMDA-mediated CF-EPSC

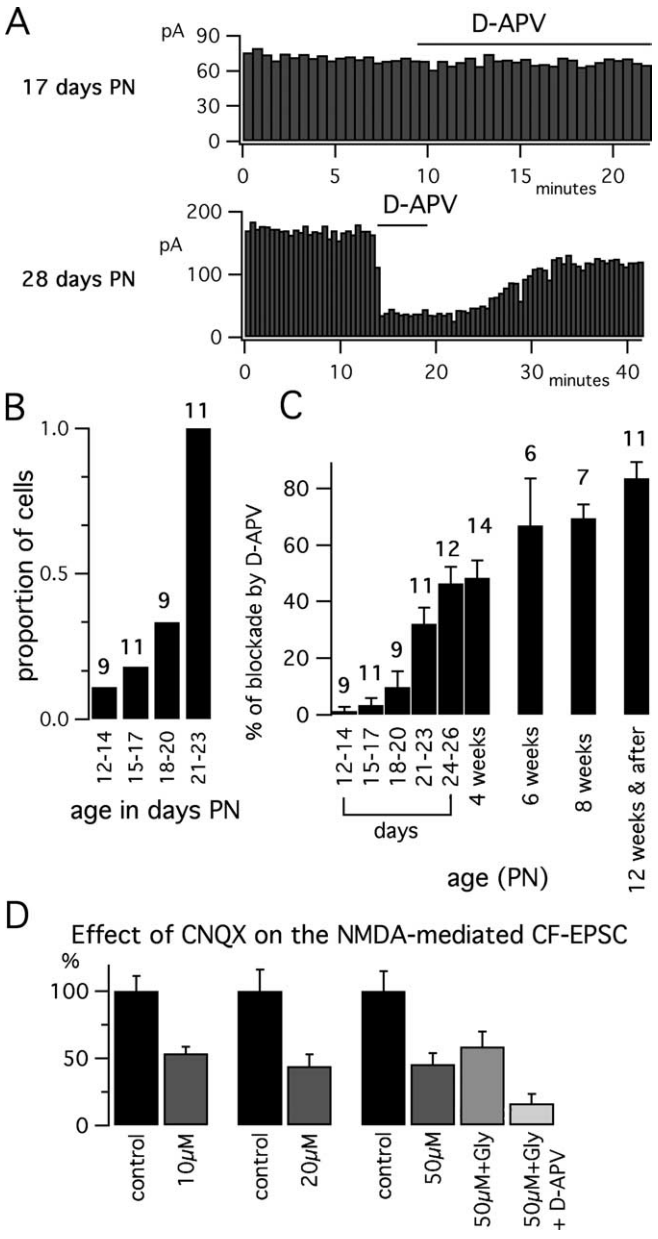

Figure 5. Development of the NMDA-mediated CF-EPSCs and their blockade by CNQX. ***A***, Amplitude of the NBQX-resistant CF-EPSC over time, in Mg^{2+}-free external medium, in two different Purkinje cells from P17 and P26 mice. Addition of 50 μM D-APV in the bath reversibly blocks the NBQX-resistant CF-EPSC at P26, whereas it has no effect at P17. ***B***, Proportion of Purkinje cells displaying a detectable NMDA component, observed at different postnatal ages. The total number of cells (*n*) recorded at each age is indicated above the bars. ***C***, Percentage of blockade of the NBQX-resistant CF-EPSCs induced by D-APV (50 μM) over the development. Ages are indicated at the bottom of the graph. The total number of cells recorded at each age is indicated above the bars. ***D***, Mean ± SEM peak amplitude of the NBQX-resistant CF-EPSCs in control (10 μM NBQX alone) and after addition of three different concentrations of CNQX (10, 20, or 50 μM as indicated). On the right, further application of 200 μM glycine tends to reverse the blockade by CNQX. Final addition of D-APV blocks the response reduced by CNQX and partially reversed by glycine, showing that it is carried by NMDA-Rs.

was 105 ± 10.4, 107.4 ± 21.3, and 123.5 ± 15.6 pA, respectively, compared with 194.8 ± 20.1 ($n = 6$), 256.4 ± 40 ($n = 5$), and 270.5 ± 16 pA ($n = 4$) in control periods. The residual responses in 50 μM CNQX were partially reversed by 200 μM glycine, as expected from the previously described competition between CNQX and glycine (Lester and Jahr, 1990). This response was further blocked by D-APV (50 μM), showing that it was indeed mediated by NMDA-Rs (Fig. 5*D*). In conclusion, CNQX, a widely used AMPA/kainate antagonist, at usual doses, blocks approximately half of the NMDA-mediated CF-EPSC, probably by competing with glycine and possibly with glutamate at their binding sites. Taking into account this inhibitory effect of CNQX on the NMDA current, together with the still small amplitude of this EPSC in young animals, our data predict that, in the presence of 10 μM CNQX and at 4 weeks PN, the CF-EPSC should have an amplitude of ~60 pA. This explains rather well why some authors, such as Perkel et al. (1990), did not detect these NMDA-Rs. The study from Krupa and Crepel (1990) is also interesting because they detected NMDA-Rs in adult rat Purkinje cells (8 weeks PN). The fact that only 25% of the Purkinje cells responded to NMDA in adults whereas 100% responded during the first week PN under the same experimental conditions is probably attributable to the differences in subunit composition of the NMDA-Rs at these two ages. The NR1/NR2-D NMDA-Rs is particularly easy to detect with exogenous glutamate compared with NR1/NR2-A/B of the adults. In 1990, these different subunits and their properties were still unknown, and, compared with juvenile currents, the NMDA currents of the adults apparently decline with age. Interestingly, the authors themselves already proposed this hypothesis in their discussion (Krupa and Crepel, 1990, their second to last paragraph). In addition, this study was performed with intracellular voltage-clamp recordings, a technique that is less appropriate than patch clamp for the recording of currents.

NMDA-Rs contribute to the complex spike in mature animals

The NMDA-mediated CF-EPSC is rather small compared with the AMPA-mediated CF-EPSC, which raises the question of the functional role of these receptors in Purkinje cell physiology. First, in adults, it is important to note that dendritic currents recorded at the soma are highly filtered and that voltage is improperly controlled in dendrites, resulting in an underestimation of the amplitude of the NMDA-mediated CF-EPSC. Second, the physiological effect of an ionic conductance does not entirely depend on its amplitude; the location of the channels may also be at least as important. To better estimate the potential physiological relevance of the NMDA-Rs of the adult Purkinje cell, we next switched to recordings in the current-clamp mode and stimulated the climbing fiber to record the characteristic response, the complex spike. In this mode, we found two categories of Purkinje cells: (1) silent cells (no spontaneous spiking activity) with a resting potential at approximately −65/−70 mV; and (2) cells with a resting potential at approximately −55 mV with intermittent periods of spontaneous spiking activity. Spontaneous activity complicated the estimation of the resting potential of cells and of the shape of complex spikes over time. Therefore, in spontaneously active cells, we injected a small negative current through the recording pipette to maintain the Purkinje cell membrane at approximately −70 mV and to prevent activity.

As expected, the stimulation of the climbing fiber induced an all-or-none complex spike that consisted of one large spike followed by two to five shorter spikelets at the top of a fast depolarization plateau (Eccles et al., 1966) (for review, see Schmolesky et al., 2002) (see Fig. 7). This fast plateau was followed by a slow afterdepolarization (ADP) (Schmolesky et al., 2005) (see Fig. 7*A*). The duration of the plateau and the number of spikelets were rather variable among cells, but, for each individual Purkinje cell,

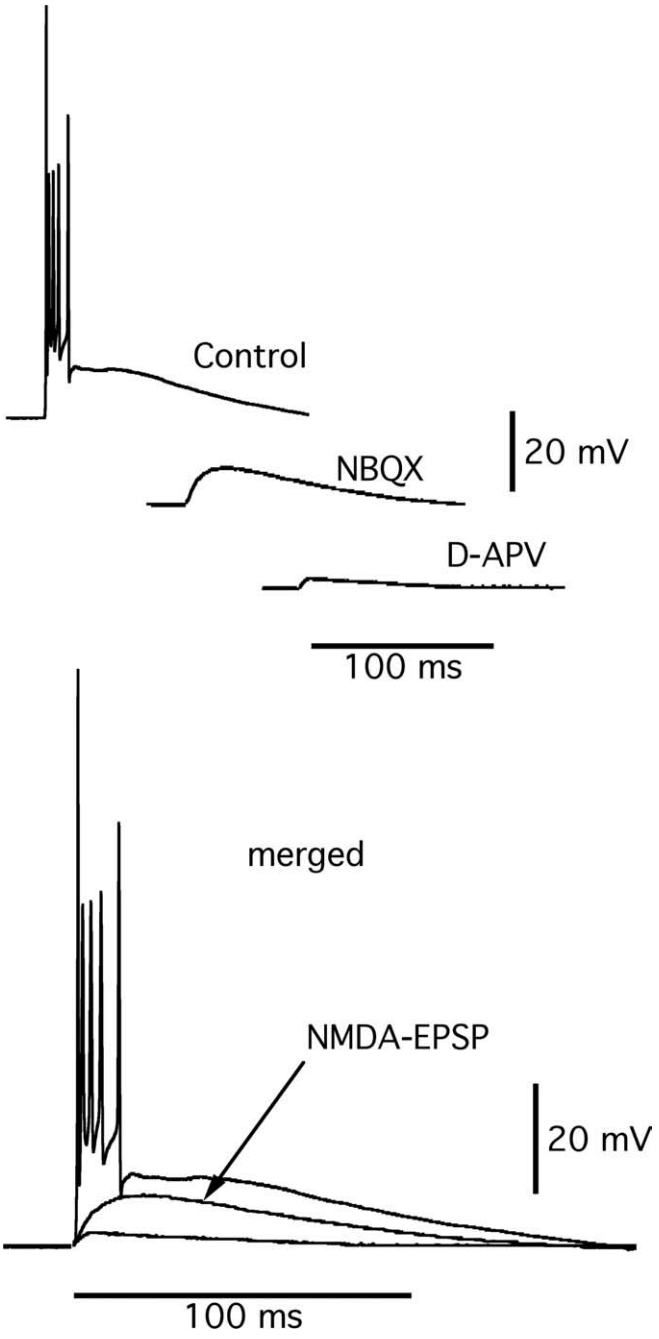

Figure 6. Blocking the complex spike with NBQX reveals an NMDA-EPSP. Whole-cell current-clamp recording of a Purkinje cell from a mature animal (6 months old) in the absence of external Mg^{2+}. Complex spike illustrated before (control) and after addition of NBQX (10 μM). NBQX suppresses spikes and spikelets of the complex spike and reveals an NBQX-resistant CF-EPSP (top middle trace) that is completely inhibited by 50 μM D-APV (top right trace). Note the kinetics of the complex spike and of NMDA-EPSP superimposed below.

at room temperature, the waveform of the complex spike was remarkably stable over time, even for long recordings (up to 1 h). In some cases, an antidromic spike preceded the complex spike itself. The climbing fiber was stimulated at 0.1 Hz, and the existence of an NMDA-mediated CF-EPSP was first investigated in magnesium-free BBS (Fig. 6). In this configuration, adding 10 μM NBQX to the bath while recording the complex spike suppressed spikes and spikelets, leaving a large NBQX-resistant CF-EPSP (Fig. 6). This EPSP was completely abolished by D-APV (50 μM) or Mg^{2+} (1 mM) in all the Purkinje cells tested ($n = 7$) (Fig. 6, right), showing that it is an NMDA-mediated CF-EPSP (NMDA-EPSP). This NMDA-EPSP was all or none, with a mean amplitude of 14 ± 1.9 mV ($n = 7$) (Fig. 6, middle).

The contribution of this NMDA-EPSP to the complex spike was then investigated in more physiological conditions, i.e., in the presence of 1 mM Mg^{2+} in the bath (Fig. 7). We measured five different parameters in the complex spike: the amplitude of the fast depolarization plateau (plateau), the amplitude of the ADP, the number of spikes and spikelets, their delays, and the membrane potential over time (Fig. 7) (table in supplemental Fig. 1, available at www.jneurosci.org as supplemental material). Eight cells were recorded at room temperature (24–26°C), and three cells were recorded at 34°C. In all these 11 cells, D-APV (50 μM added to the bath) had a significant effect on these parameters (table in supplemental Fig. 1, available at www.jneurosci.org as supplemental material). However, when present, the delay of the initial antidromic spike was not affected by D-APV, except for one cell in which it disappeared in D-APV and reappeared during washout. In all but one cell ($n = 11$), D-APV increased delays of spikes and spikelets (Fig. 7) (table in supplemental Fig. 1, available at www.jneurosci.org as supplemental material). At room temperature, the resting potential slightly but not significantly increased during D-APV application (Fig. 7*A2*). At 34°C, this effect was more prominent. Because modest changes in membrane potential can significantly modify the complex spike waveform, we maintained the membrane potential at −70 mV during the entire recording to reliably compare the complex spikes during D-APV together with controls. In 7 of 11 cells, the increase in spike and spikelet delay ultimately led to a reduction in their number, thereby significantly changing the spike waveform (Fig. 7*B*). In five of these cells, this change of waveform was too important to estimate the effect of D-APV on the plateau and ADP (table in supplemental Fig. 1, available at www.jneurosci.org as supplemental material). For the remaining six cells, D-APV reduced the amplitude of the depolarization plateau and of the ADP (Fig. 7*A*) (table in supplemental Fig. 1, available at www.jneurosci.org as supplemental material). All these effects of D-APV were fully reversible on washout, showing that they did not result from rundown over time (Fig. 7*B*). In 5 of 11 cells, this washout was accompanied by a rebound increase of the amplitude of the fast plateau and of the number of spikelets in the complex spike (as in example of Fig. 7*B*). The smaller the effects of D-APV were, the larger this rebound was. This indicates that, from the beginning of the experiment, some of the NMDA-Rs were already desensitized/inactivated, suggesting that there might be a tonic activation of the NMDA component, at least in our conditions.

In conclusion, blocking NMDA-Rs reduces the amplitude of the plateau and ADP, increases spike and spikelet latency, and, in some cases, reduces their number. What might cause these effects? In the complex spike, the latency of spikes depends, among other parameters, on the amplitude of the underlying potential: increasing the potential amplitude reduces latency because the threshold of discharge is reached faster. Thus, the magnitude of the latency shift induced by D-APV likely depends on the amplitude of the underlying NMDA potential. Furthermore, if the NMDA potential is large, the latency shift in D-APV will also be accompanied by the disappearance of some spikes or spikelets because their threshold will no longer be reached during the complex spike.

These results show that NMDA-Rs increase the depolarization induced by the complex spike and prolong its duration. These effects are likely to favor calcium entry in the dendrites

as well as their propagation, and, because they occur in the presence of physiological concentrations of Mg^{2+} and near physiological temperature, NMDA-Rs are potent actors in the physiology of adult Purkinje cells.

Discussion

We demonstrate that Purkinje cells from adult mice respond to exogenous NMDA applications in the presence of TTX, bicuculline, and NBQX. In agreement with Sekiguchi et al. (1987), we show that Purkinje cells respond to ionophoresis of NMDA at their proximal but not their distal dendrites. Accordingly, we detect NMDA-Rs by immunohistochemistry in the lower two-thirds of the Purkinje cell dendrites, i.e., near climbing fiber synapses. Confirming these observations, NMDA receptors carry part of the CF-EPSC. In Mg^{2+}-free solution, the major part of the NBQX-resistant CF-EPSC is typical of NMDA currents, i.e., potentiation by glycine and blockade by D-APV, MK801, and external Mg^{2+} ions. Three direct lines of evidence demonstrate that the NMDA-mediated CF-EPSCs is postsynaptic: (1) the immunolabelings of NR2-A/B; (2) the blockade of NMDA-mediated CF-EPSCs by internal MK801; and (3) their voltage-dependent block at hyperpolarized potentials in the presence, but not in the absence, of external Mg^{2+}.

The NMDA-mediated CF-EPSC was present in all but one of the mature Purkinje cells tested in the study, showing that, in adult mice, it is a consistent component of climbing fiber to Purkinje cell synapses. How can discrepancies between our results and previous studies be explained? Differences among various species used cannot be completely excluded. However, NMDA-Rs have also been previously detected in guinea pig, rats, and humans (Quinlan and Davies, 1985; Billard and Pumain, 1989; Krupa and Crepel, 1990; Scherzer et al., 1997; Thompson et al., 2000). In light of our data, the difficulty in finding NMDA currents mainly results from (1) differences in the age of the animals, (2) the use of CNQX, and (3) the lack of information about properties of the different NMDA subunits at the time of these studies. In fact, most of the groups that looked for NMDA currents in adult Purkinje cells worked in animals younger than 3 weeks. However, we now show that the adult-type NMDA current is barely detectable before 3 weeks PN and remains small until 6 weeks. In addition, as observed previously in other cell types, CNQX blocks half of the NMDA-mediated CF-EPSC. Consequently, as long as the NMDA current remains relatively small, CNQX leaves a hardly detectable NMDA-mediated CF-EPSC. This probably explains why Perkel et al. (1990), for instance, did not detect the NMDA responses in their study performed using 4- to 6-week-old animals.

Many of the studies performed before 1990 in the "true adult" support our present data by indicating NMDA responses in Purkinje cells, although these studies provided only indirect evidence attributable to technical and pharmacological problems. Interestingly, some of them even provided evidence for the location of NMDA-Rs at climbing fibers synapses (Kimura et al., 1985; Quinlan and Davies, 1985; Sekiguchi et al., 1987; Billard and Pumain, 1989). Examination of these studies shows that they were not done with patch-clamp but with extracellular or intracellular microelectrode recordings. The two latter techniques are compatible with the use of adult animals, whereas patch-clamp studies prefer immature cells to ensure proper voltage clamp. Thus, the advent of patch-clamp technique in slices, by constraining authors to work in immature ("subadult") animals,

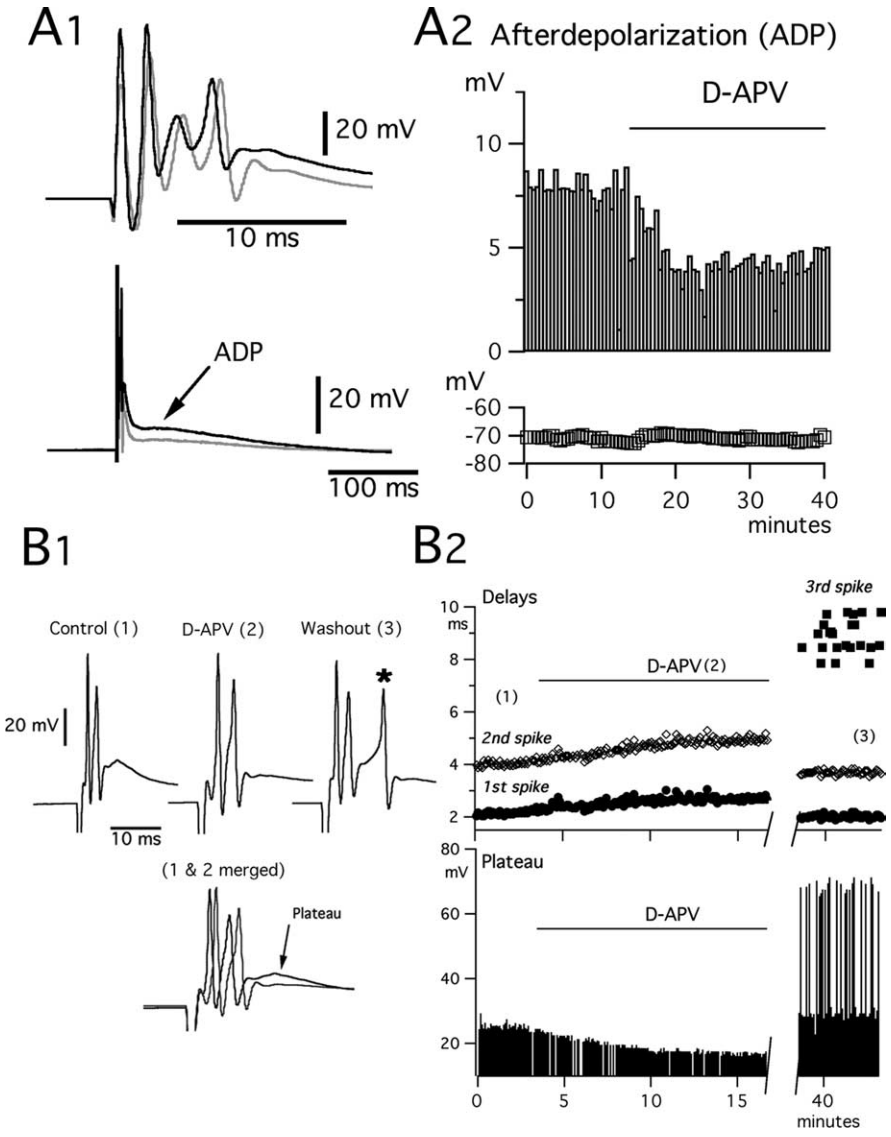

Figure 7. NMDA-R contribution to the complex spike in standard (1 mM Mg^{2+}) BBS. Whole-cell recordings from mature Purkinje cells in the presence of external Mg^{2+} (1 mM) at room temperature. ***A1***, Complex spikes recorded in bicuculline only (black trace) and in bicuculline plus D-APV (50 μM, gray trace). In this example, the ADP was measured at 70 ms after the stimulation onset. Note that D-APV reduces both the fast depolarization plateau (top) and the ADP. ***A2***, Same cell as in ***A1***. Amplitude of the ADP (bars) and resting potential (squares) plotted over time. ***B***, Same type of recording in another mature Purkinje cell. ***B1***, Complex spikes before (1), during (2), and after (3) the application of D-APV (50 μM). In this cell, D-APV reduced the plateau amplitude (arrows) and shifted the appearance of the spikelets (as in traces merged in bottom). ***B2***, Same cell as ***B1***. Delay of spikes and spikelets of the complex spike plotted over time. Note the occurrence of a third spikelet in some trials during the washout of D-APV (asterisk on the right trace of ***B1***). This third spikelet occurred in the time window used to estimate the plateau amplitude, therefore causing the presence of peaks in the plot of amplitude of the plateau over time.

likely contributed to the conclusion that adult Purkinje cells do not express functional NMDA-Rs.

Our data indicate that the NR2-A/B subunits of the adult replace neonatal NR2-D in Purkinje cells (Cull-Candy et al., 1998). Compared with NR2-A/B, NR2-D containing NMDA-Rs are less sensitive to Mg^{2+} block, do not desensitize, and slowly deactivate (Dingledine et al., 1999; Misra et al., 2000), which make them easy to detect with exogenous glutamate. Thus, the developmental switch from NR2-D to NR2-A/B in Purkinje cells renders the detection of NMDA-Rs much more difficult in adult Purkinje cells. This is probably why NMDA-Rs were evident in young animals but comparatively hard to detect in the same conditions later in the development (Dupont et al., 1987; Krupa and Crepel, 1990). Finally, the particular properties of NR2-D-containing NMDA-Rs make them poorly suited for classical fast synaptic transmission, contrary to NR2-A or NR2-B subunits. Accordingly, NR2-D are not components of neonatal climbing fiber synaptic transmission at P0–P4 (Lachamp et al., 2005), whereas NR2-A/B are expressed at mature climbing fiber connections. Thus, the translocation of the NMDA-Rs to the synapses during the development fits their respective biophysical characteristics.

What might be the role of these adult NMDA-Rs? Because of their well known characteristics, they are likely to modulate the integration or plasticity of Purkinje cells inputs and/or outputs or to play a role in the maintenance of their connections. Purkinje cells no longer respond to NMDA after climbing fiber deafferentation (Billard and Pumain, 1989). Conversely, we found adult NMDA-Rs at climbing fiber synapses from P21 in mice, i.e., an age that coincides with the complete regression of multiple climbing fiber innervation (Hashimoto and Kano, 2005). Thus, NMDA-Rs of adult Purkinje cells could play a role in the adjustment and/or maintenance of mature climbing fiber to Purkinje cells connections. It is also interesting to notice that P21 corresponds to the appearance of a mature form of retrograde signaling in Purkinje cell (Levenes et al., 2001; Crepel, 2007) and to the developmental transition stage when the spontaneous activity of Purkinje cells switches from tonic Na^+ spiking to a trimodal spiking pattern (combining Na^+-spikes, Ca^{2+}-spikes, and pauses) (McKay and Turner, 2005). Thus, from both a morphological and physiological point of view, the development of Purkinje cells of mice and *a fortiori* of rats is definitely not completed at P21 (Altman and Bayer, 1997; McKay and Turner, 2005).

Even in adults, NMDA currents are relatively small compared with the total CF-EPSC. However, this does not necessarily imply that NMDA-Rs have no physiological role. Experiments in current-clamp reveal an NMDA-EPSC of 14 mV on average, which is not negligible. The fact that the complex spike displays an NMDA component in 1 mM Mg^{2+}-containing BBS and at near physiological temperature indicate that these receptors contribute to the complex spike in physiological conditions. Importantly, this also demonstrates that the depolarization induced by the complex spike itself is sufficient to relieve the Mg^{2+} block of NMDA-Rs and to allow them to be activated by a single climbing fiber discharge.

Despite extensive studies, the informational role of the complex spike is still unclear (Simpson et al., 1996; Schmolesky et al., 2002). Depending on the study and on the research group, it is involved in real-time [like the "timing device" proposed by Llinas's group (Lang et al., 2006)], short-term (modulation of the pause in fast spiking) (Simpson et al., 1996), or long-term modulation of Purkinje cells activity ("plasticity"). Whatever its role, the climbing fiber operates at the level of dendritic integration (input) and/or axonal firing patterns (output) of Purkinje cells. Looking at their contribution to the complex spike, NMDA-Rs may act at both levels.

The output of Purkinje cells after a complex spike consists of a burst of forward-propagating action potentials in the axon (Llinas and Sasaki, 1989; Khaliq and Raman, 2005). Propagation of the fast initial spike is highly reliable (Khaliq and Raman, 2005), but that of individual spikelets is much less reliable and subject to modulation. Propagation probability varies predictably with the spikelets waveform and can be described as a saturating function of spikelet amplitude, rate of rise, or preceding interspike interval (Khaliq and Raman, 2005). As we show, NMDA-Rs decrease the delay of the spikelets and, in most of the cells, increase their number, thereby changing interspike intervals. Thus, according to Khaliq and Raman (2005), the NMDA-mediated component of the complex spike is likely to change the probability of propagating spikelets in the axon.

Parallel fiber inputs to Purkinje cells display long-term depression (LTD) or potentiation (LTP). Probability of LTD versus LTP at parallel fiber inputs is under control of the climbing fiber (Coesmans et al., 2004), which itself undergoes calcium-dependent LTD (Hansel and Linden, 2000). As we show here, NMDA-Rs increase the depolarization induced by the complex spike and prolong its duration. These effects are expected to favor calcium entry in the dendrites as well as their propagation. Thus, NMDA-Rs are likely to be players in the game of mature Purkinje cells plasticity. However, it is difficult to evaluate from previous studies whether this is the case, because the molecular actors of Purkinje cell plasticity have been primarily investigated in immature cerebellar slices, i.e., before the expression of NMDA-Rs at climbing fiber synapses. Thus, it now remains to be established the exact role of the NMDA-Rs of the Purkinje cells, provided that the basic cellular rules of plasticity are reappraised in the context of mature cerebellar cortex.

References

Akaike A, Sasa M, Takaori S (1981) Inhibition from ventral tegmental area of nucleus accumbens neurons in the rat. Brain Res 225:189–194.

Akazawa C, Shigemoto R, Bessho Y, Nakanishi S, Mizuno N (1994) Differential expression of five *N*-methyl-D-aspartate receptor subunit mRNAs in the cerebellum of developing and adult rats. J Comp Neurol 347:150–160.

Altman J, Bayer SA (1997) Development of the cerebellar system. New York: CRC.

Auger C, Attwell D (2000) Fast removal of synaptic glutamate by postsynaptic transporters. Neuron 28:547–558.

Berretta N, Jones RS (1996) Tonic facilitation of glutamate release by presynaptic *N*-methyl-D-aspartate autoreceptors in the entorhinal cortex. Neuroscience 75:339–344.

Billard JM, Pumain R (1989) Loss of *N*-methyl-D-aspartate sensitivity of cerebellar Purkinje cells after climbing fiber deafferentation. An in vivo study in the rat. Neurosci Lett 106:199–204.

Birch PJ, Grossman CJ, Hayes AG (1988) 6,7-Dinitro-quinoxaline-2,3-dion and 6-nitro,7-cyano-quinoxaline-2,3-dion antagonise responses to NMDA in the rat spinal cord via an action at the strychnine-insensitive glycine receptor. Eur J Pharmacol 156:177–180.

Cathala L, Misra C, Cull-Candy S (2000) Developmental profile of the changing properties of NMDA receptors at cerebellar mossy fiber–granule cell synapses. J Neurosci 20:5899–5905.

Clark BA, Cull-Candy SG (2002) Activity-dependent recruitment of extrasynaptic NMDA receptor activation at an AMPA receptor-only synapse. J Neurosci 22:4428–4436.

Coesmans M, Weber JT, De Zeeuw CI, Hansel C (2004) Bidirectional par-

allel fiber plasticity in the cerebellum under climbing fiber control. Neuron 44:691–700.
Crepel F (2007) Developmental changes in retrograde messengers involved in depolarization-induced suppression of excitation at parallel fiber-Purkinje cell synapses in rodents. J Neurophysiol 97:824–836.
Crepel F, Dhanjal SS, Sears TA (1982) Effect of glutamate, aspartate and related derivatives on cerebellar Purkinje cell dendrites in the rat: an in vitro study. J Physiol (Lond) 329:297–317.
Cull-Candy SG, Brickley SG, Misra C, Feldmeyer D, Momiyama A, Farrant M (1998) NMDA receptor diversity in the cerebellum: identification of subunits contributing to functional receptors. Neuropharmacology 37:1369–1380.
Cull-Candy S, Brickley S, Farrant M (2001) NMDA receptor subunits: diversity, development and disease. Curr Opin Neurobiol 11:327–335.
Diez-Garcia J, Matsushita S, Mutoh H, Nakai J, Ohkura M, Yokoyama J, Dimitrov D, Knopfel T (2005) Activation of cerebellar parallel fibers monitored in transgenic mice expressing a fluorescent Ca^{2+} indicator protein. Eur J Neurosci 22:627–635.
Dingledine R, Borges K, Bowie D, Traynelis SF (1999) The glutamate receptor ion channels. Pharmacol Rev 51:7–61.
Dupont JL, Gardette R, Crepel F (1987) Postnatal development of the chemosensitivity of rat cerebellar Purkinje cells to excitatory amino acids. An in vitro study. Brain Res 431:59–68.
Eccles JC, Llinas R, Sasaki K (1966) The excitatory synaptic action of climbing fibres on the purkinje cells of the cerebellum. J Physiol (Lond) 182: 268–296.
Farrant M, Cull-Candy SG (1991) Excitatory amino acid receptor-channels in Purkinje cells in thin cerebellar slices. Proc R Soc Lond B Biol Sci 244:179–184.
Garthwaite G, Yamini Jr B, Garthwaite J (1987) Selective loss of Purkinje and granule cell responsiveness to *N*-methyl-D-aspartate in rat cerebellum during development. Brain Res 433:288–292.
Glitsch M, Marty A (1999) Presynaptic effects of NMDA in cerebellar Purkinje cells and interneurons. J Neurosci 19:511–519.
Hafidi A, Hillman DE (1997) Distribution of glutamate receptors GluR 2/3 and NR1 in the developing rat cerebellum. Neuroscience 81:427–436.
Hansel C, Linden DJ (2000) Long-term depression of the cerebellar climbing fiber–Purkinje neuron synapse. Neuron 26:473–482.
Harris KM, Miller RJ (1989) CNQX (6-cyano-7-nitroquinoxaline-2,3-dione) antagonizes NMDA-evoked [^{3}H]GABA release from cultured cortical neurons via an inhibitory action at the strychnine-insensitive glycine site. Brain Res 489:185–189.
Hashimoto K, Kano M (2005) Postnatal development and synapse elimination of climbing fiber to Purkinje cell projection in the cerebellum. Neurosci Res 53:221–228.
Hioki H, Fujiyama F, Taki K, Tomioka R, Furuta T, Tamamaki N, Kaneko T (2003) Differential distribution of vesicular glutamate transporters in the rat cerebellar cortex. Neuroscience 117:1–6.
Huang YH, Dykes-Hoberg M, Tanaka K, Rothstein JD, Bergles DE (2004) Climbing fiber activation of EAAT4 transporters and kainate receptors in cerebellar Purkinje cells. J Neurosci 24:103–111.
Humeau Y, Shaban H, Bissiere S, Luthi A (2003) Presynaptic induction of heterosynaptic associative plasticity in the mammalian brain. Nature 426:841–845.
Kessler M, Baudry M, Lynch G (1989) Quinoxaline derivatives are high-affinity antagonists of the NMDA receptor-associated glycine sites. Brain Res 489:377–382.
Khaliq ZM, Raman IM (2005) Axonal propagation of simple and complex spikes in cerebellar Purkinje neurons. J Neurosci 25:454–463.
Kimura H, Okamoto K, Sakai Y (1985) Pharmacological evidence for L-aspartate as the neurotransmitter of cerebellar climbing fibres in the guinea-pig. J Physiol (Lond) 365:103–119.
Konnerth A, Llano I, Armstrong CM (1990) Synaptic currents in cerebellar Purkinje cells. Proc Natl Acad Sci USA 87:2662–2665.
Krupa M, Crepel F (1990) Transient sensitivity of rat cerebellar Purkinje cells to *N*-methyl-D-aspartate during development. A voltage clamp study in in vitro slices. Eur J Neurosci 2:312–316.
Lachamp P, Balland B, Tell F, Baude A, Strube C, Crest M, Kessler JP (2005) Early expression of AMPA receptors and lack of NMDA receptors in developing rat climbing fibre synapses. J Physiol (Lond) 564:751–763.
Lang EJ, Sugihara I, Llinas R (2006) Olivocerebellar modulation of motor cortex ability to generate vibrissal movements in rat. J Physiol (Lond) 571:101–120.
Laurie DJ, Seeburg PH (1994) Regional and developmental heterogeneity in splicing of the rat brain NMDAR1 mRNA. J Neurosci 14:3180–3194.
Lester RA, Jahr CE (1990) Quisqualate receptor-mediated depression of calcium currents in hippocampal neurons. Neuron 4:741–749.
Levenes C, Daniel H, Crepel F (2001) Retrograde modulation of transmitter release by postsynaptic subtype 1 metabotropic glutamate receptors in the rat cerebellum. J Physiol (Lond) 537:125–140.
Llano I, Marty A, Armstrong CM, Konnerth A (1991) Synaptic-and agonist-induced excitatory currents of Purkinje cells in rat cerebellar slices. J Physiol (Lond) 434:183–213.
Llinas R, Sasaki K (1989) The functional organization of the olivo-cerebellar system as examined by multiple Purkinje cell recordings. Eur J Neurosci 1:587–602.
Massey PV, Johnson BE, Moult PR, Auberson YP, Brown MW, Molnar E, Collingridge GL, Bashir ZI (2004) Differential roles of NR2A- and NR2B-containing NMDA receptors in cortical long-term potentiation and long-term depression. J Neurosci 24:7821–7828.
McKay BE, Turner RW (2005) Physiological and morphological development of the rat cerebellar Purkinje cell. J Physiol (Lond) 567:829–850.
Mead AN, Stephens DN (1999) CNQX but not NBQX prevents expression of amphetamine-induced place preference conditioning: a role for the glycine site of the NMDA receptor, but not AMPA receptors. J Pharmacol Exp Ther 290:9–15.
Misra C, Brickley SG, Wyllie DJ, Cull-Candy SG (2000) Slow deactivation kinetics of NMDA receptors containing NR1 and NR2D subunits in rat cerebellar Purkinje cells. J Physiol (Lond) 525:299–305.
Monyer H, Sprengel R, Schoepfer R, Herb A, Higuchi M, Lomeli H, Burnashev N, Sakmann B, Seeburg PH (1992) Heteromeric NMDA receptors: molecular and functional distinction of subtypes. Science 256:1217–1221.
Monyer H, Burnashev N, Laurie DJ, Sakmann B, Seeburg PH (1994) Developmental and regional expression in the rat brain and functional properties of four NMDA receptors. Neuron 12:529–540.
Mori H, Mishina M (2003) Roles of diverse glutamate receptors in brain functions elucidated by subunit-specific and region-specific gene targeting. Life Sci 74:329–336.
Moriyoshi K, Masu M, Ishii T, Shigemoto R, Mizumo N, Nakanishi S (1991) Molecular cloning and characterization of the rat NMDA receptor. Nature 354:31–37.
Nakagawa S, Watanabe M, Inoue Y (1996) Altered gene expression of the *N*-methyl-D-aspartate receptor channel subunits in Purkinje cells of the staggerer mutant mouse. Eur J Neurosci 8:2644–2651.
Otis TS, Kavanaugh MP, Jahr CE (1997) Postsynaptic glutamate transport at the climbing fiber-Purkinje cell synapse. Science 277:1515–1518.
Pellegrini-Giampietro DE, Galli A, Alesiani M, Cherici G, Moroni F (1989) Quinoxalines interact with the glycine recognition site of NMDA receptors: studies in guinea-pig myenteric plexus and in rat cortical membranes. Br J Pharmacol 98:1281–1286.
Perkel DJ, Hestrin S, Sah P, Nicoll RA (1990) Excitatory synaptic currents in Purkinje cells. Proc R Soc Lond B Biol Sci 241:116–121.
Petralia R, Yokotani N, Wenthold R (1994a) Light and electron microscope distribution of the NMDA receptor subunit NMDAR1 in the rat nervous system using a selective anti-peptide antibody. J Neurosci 14:667–696.
Petralia RS, Wang YX, Wenthold RJ (1994b) The NMDA receptor subunits NR2A and NR2B show histological and ultrastructural localization patterns similar to those of NR1. J Neurosci 14:6102–6120.
Quinlan JE, Davies J (1985) Excitatory and inhibitory responses of Purkinje cells, in the rat cerebellum in vivo, induced by excitatory amino acids. Neurosci Lett 60:39–46.
Rosenmund C, Legendre P, Westbrook GL (1992) Expression of NMDA channels on cerebellar Purkinje cells acutely dissociated from newborn rats. J Neurophysiol 68:1901–1905.
Samson RD, Pare D (2005) Activity-dependent synaptic plasticity in the central nucleus of the amygdala. J Neurosci 25:1847–1855.
Scherzer CR, Landwehrmeyer GB, Kerner JA, Standaert DG, Hollingsworth ZR, Daggett LP, Velicelebi G, Penney Jr JB, Young AB (1997) Cellular distribution of NMDA glutamate receptor subunit mRNAs in the human cerebellum. Neurobiol Dis 4:35–46.
Schmolesky MT, Weber JT, De Zeeuw CI, Hansel C (2002) The making of a complex spike: ionic composition and plasticity. Ann NY Acad Sci 978:359–390.

Schmolesky MT, De Zeeuw CI, Hansel C (2005) Climbing fiber synaptic plasticity and modifications in Purkinje cell excitability. Prog Brain Res 148:81–94.

Sekiguchi M, Okamoto K, Sakai Y (1987) NMDA-receptors on Purkinje cell dendrites in guinea pig cerebellar slices. Brain Res 437:402–406.

Sheardown MJ, Nielsen EO, Hansen AJ, Jacobsen P, Honore T (1990) 2,3-Dihydroxy-6-nitro-7-sulfamoyl-benzo(F)quinoxaline: a neuroprotectant for cerebral ischemia. Science 247:571–574.

Shimamoto K, Lebrun B, Yasuda-Kamatani Y, Sakaitani M, Shigeri Y, Yumoto N, Nakajima T (1998) DL-threo-beta-benzyloxyaspartate, a potent blocker of excitatory amino acid transporters. Mol Pharmacol 53:195–201.

Shin JH, Linden DJ (2005) An NMDA receptor/nitric oxide cascade is involved in cerebellar LTD but is not localized to the parallel fiber terminal. J Neurophysiol 94:4281–4289.

Simpson JI, Wylie DR, De Zeeuw CI (1996) On climbing fiber signals and their consequence(s). Behav Brain Sci 19:368–383.

Thompson CL, Drewery DL, Atkins HD, Stephenson FA, Chazot PL (2000) Immunohistochemical localization of *N*-methyl-D-aspartate receptor NR1, NR2A, NR2B and NR2C/D subunits in the adult mammalian cerebellum. Neurosci Lett 283:85–88.

Wadiche JI, Jahr CE (2001) Multivesicular release at climbing fiber-Purkinje cell synapses. Neuron 32:301–313.

Watanabe M, Mishina M, Inoue Y (1994) Distinct spatiotemporal expressions of five NMDA receptor channel subunit mRNAs in the cerebellum. J Comp Neurol 343:513–519.

Yamada K, Fukaya M, Shimizu H, Sakimura K, Watanabe M (2001) NMDA receptor subunits GluRepsilon1, GluRepsilon3 and GluRzeta1 are enriched at the mossy fibre-granule cell synapse in the adult mouse cerebellum. Eur J Neurosci 13:2025–2036.

Supplemental figures

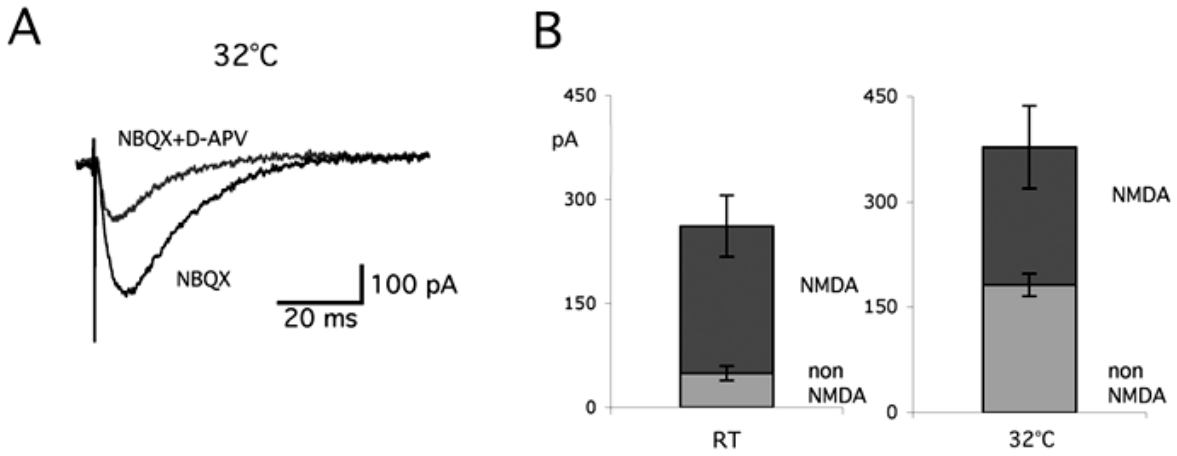

Effects of D-APV on different parameters of the complex spike:amplitude of the plateau potential, number of spikelets, and delays of the different spikes/spikelets (Sp)

Cell #	Temperature	↘ Plateau	Change in the number of spikelets	Change in antidromic spike delay	Sp 1	Sp 2	Sp 3
1	RT	+			+	+	
2	RT	+	+	no	+	+	+
3	RT	+		yes	+	+	+
4	RT	+			+	no	+
5	RT	?	+		+	+	+
6	RT	?	+		+	+	+
7	RT	+		no	no	no	
8	RT	+	+	no	+	+	
9	34°C	?	+		+	+	+
10	34°C	?	+		no	+	
11	34°C	?	+	no	+		

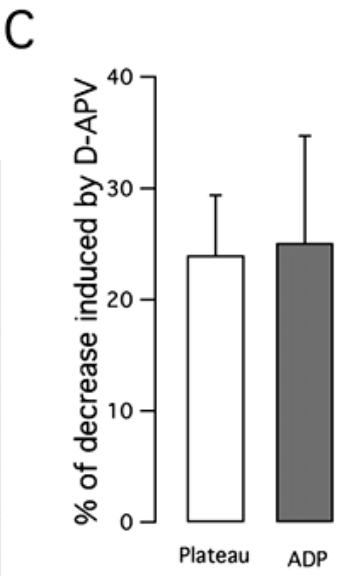

Figure 3.2 : Supplemental figure

(A) Averaged CF-EPSCs from one Purkinje cell recorded at 32°C, in the presence of 10 µM NBQX (black) and after addition of 50 µM D-APV (grey).
(B) Mean amplitude (+/- SEM, n=5 cells) of NMDA- versus non-NMDAcomponent of CF-EPSCs, recorded in NBQX (10 µM) at room temperature (RT) and at 32°C. The component of the CF-EPSC that remains unblocked in NBQX + D-APV and that is potentiated at 32°C is likely to be the transporter current.
(C) Decrease of the amplitudes of the complex spike plateau (white bar) and of the ADP (grey bar) induced by D-APV (50 µM). n= 6 cells.

Supplemental data

To investigate the NMDA receptor subtypes underlying the NMDA-mediated CF-EPSCs, we further examined their sensitivity to R-(R,S)-{alpha}-(4-hydroxyphenyl)-{beta}-methyl-4-(phenylmethyl)-1-piperidine propranol (RO25-6981), a specific antagonist for NR2B-containing NMDA-Rs.

RO25-6981 decreased the NMDA-mediated CF-EPSCs in 4 of the 9 Purkinje cells tested, the amount and the kinetics of the inhibition varying widely from cell to cell, independently of the antagonist concentrations tested (ranging from 3 to 30 µM, see two representative cells on Figure 3.3). The partial blockade of NMDA-mediated CF-EPSCs by RO25-6981 suggested that some NMDA-Rs could be composed at least by one NR2B subunit (Figure 3.3, Cell #2).

These results must however be interpreted with caution. Indeed, in addition to its inhibitory effect, RO25-6981, like ifenprodil and its derivatives, increases NMDA-R affinity for glutamate (Kew et al., 1996). Therefore, while NR2B-containing NMDA-Rs are inhibited by RO25-6981 in presence of saturating concentrations of glutamate, other NMDA-Rs that are in presence of small amounts of glutamate (for exemple those mediated by extrasynaptic receptors), could display increased currents. Thus, the inhibiting effect of RO25-6981 on NR2B subunit could be masked. To avoid this problem, in 2 cells, we tested the effect of RO25-6981 on DL-TBOA-potentialized NBQX-resistant CF-EPSCs. In these cells, RO25-6981 however displayed no effect, whereas D-APV completely inhibited these responses (data not shown).

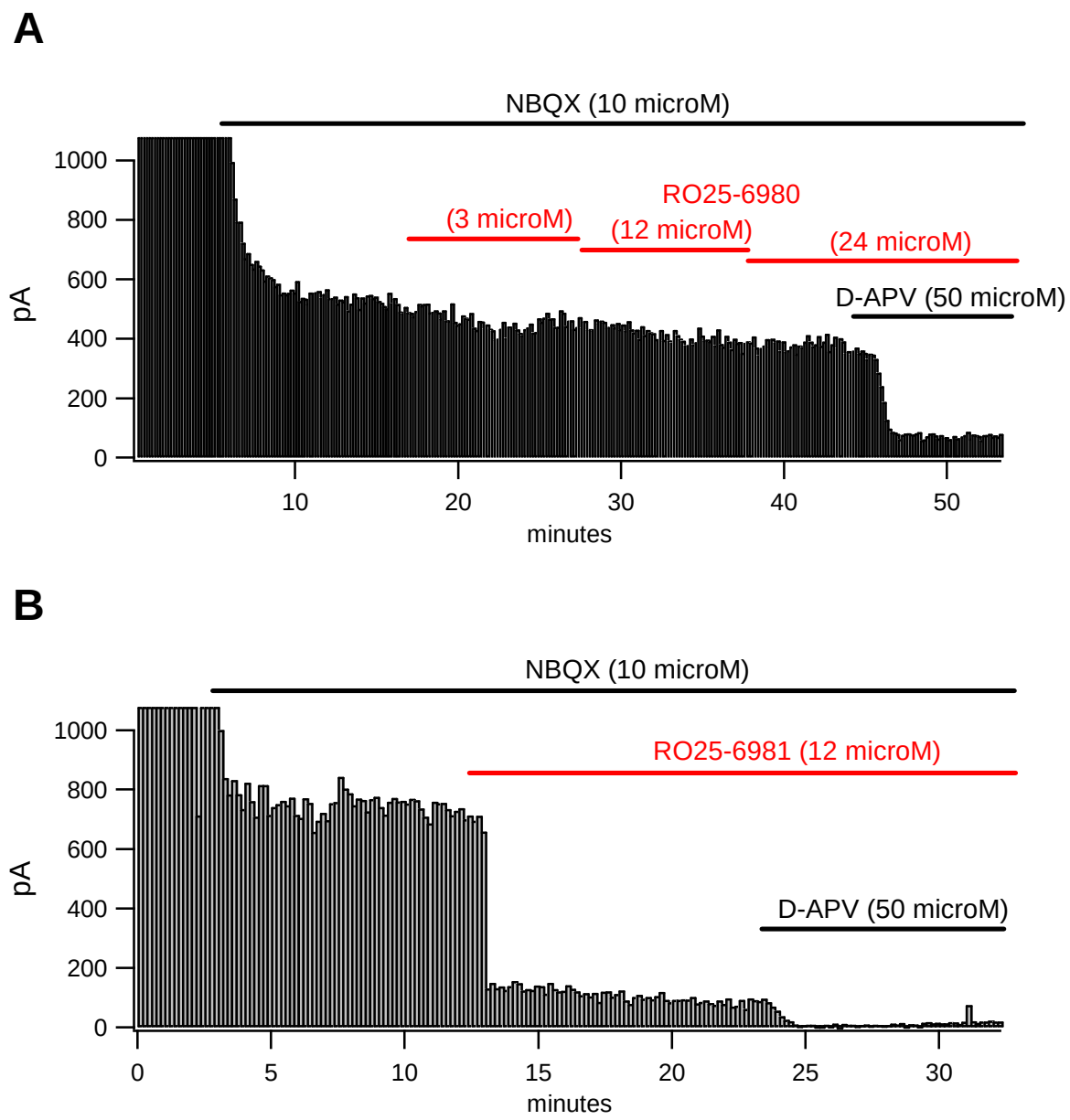

Figure 3.3: RO25-6981 displays various effects on NMDA-mediated CF-EPSCs

Whole-cell current-clamp recordings of Purkinje cells from an adult mouse (holding potential = -70 mV).Due to its very large amplitude, the maximal amplitude of the CF-EPSC was truncated for clarity. CF-EPSCs amplitudes are plotted over time.
(A) Representative CF-EPSC displaying a weak inhibition by RO25-6981, tested successively at 3, 12 and 24 µM, in presence of NBQX (10 µM). The NBQX-resistant CF-EPSC is finally inhibited by D-APV (50 µM).
(B) Representative CF-EPSC displaying a strong inhibition by RO25-6981 (12 µM), in presence of NBQX (10 µM). The remaining part of the NBQX-resistant CF-EPSC is finally inhibited by D-APV (50 µM).

3.2.3 Discussion

3.2.3.1 Functional NMDA-Rs are expressed in mature Purkinje cells

Using adult mice aged of more than 8 weeks, we demonstrated in this study that mature Purkinje cells effectively express functional NMDA-Rs. While they are not involved in the PF synaptic currents, these receptors participate to the CF synaptic transmission, as they mediate a component of the CF-EPSC and are able to modulate the waveform of the complex spike. Confirming the postsynaptic localization of these NMDA-Rs demonstrated by the I-V relationship of the NMDA-mediated CF-EPSC, the addition of MK801 to the internal medium specifically blocked this component of the CF-current. In addition, we did not detect the contribution from presynaptic or polysynaptic NMDA currents to the NMDA-mediated CF-EPSC.

Desensitization of these NMDA currents was significant in bath application versus in iontophoresis, and suggested an involvement of high conductances NR2 subunits (NR2A or NR2B), which are known to display rapid desensitizations (properties reviewed in Dingledine, 1999). In addition, the kinetics confered by these NR2 subunits to NMDA currents are compatible with the relatively rapid NMDA-mediated CF-currents recorded in mature Purkinje cells. Consistent with Thompson et al. results (2000), our immunolabelings confirmed the presence of NR2A/B subunits in Purkinje cells.

Many patch-clamp studies have addressed the question of whether NMDA-Rs are present in Purkinje cells but failed to detect NMDA mediated currents. Because we showed that NMDA synaptic currents become detectable from the third week after birth, it is understandable that the previous studies, mainly conducted on animals younger than three weeks to ensure a better space-clamp, missed the detection of NMDA-Rs in Purkinje cells. Furthermore, we showed that the widely used AMPA-Rs antagonist CNQX partly blocked the NMDA-mediated CF-EPSCs, probably by competing with glycine at the co-agonist site of NMDA-Rs. This pharmacological agent very likely contributed to bias the detection of NMDA currents.

3.2.3.2 Publication of Renzi et al. 2007

At the meanwhile of our publication, an independent group also showed the participation of NMDA-Rs to CF-EPSCs in Purkinje cells from adult mice (P62-P76), thus confirming our results. What can we learn more from this study by Renzi et al., 2007?

High-conductance single-channel currents induced by bath applied NMDA were identified in outside-out somatic patches of Purkinje cells. These events that showed a conductance of ~53 pS, were blocked by D-APV, as well as by Mg^{2+}, and displayed a linear I-V relationship in magnesium-free external medium. High-conductances of NMDA currents recorded in outside-out patches also suggested the expression of NR2A or NR2B subunits. By testing the sensitivity of these NMDA-single channels currents to Zn^{2+}, Renzi et al. demonstrated that NMDA-Rs mostly contain the NR2A subunit, while a few of them can also contain the NR2B subunit. Moreover, NMDA-R channel activity recorded on somatic PC patches was reduced by the NR2B selective blocker Ifenprodil by only ~40%, whereas NMDA-mediated CF-EPSCs were not affected by Ifenprodil. Interestingly, the selective blocker of NR2B-containing NMDA-Rs RO25-6981, that we used in our study displayed similar heterogenous effects on NMDA-mediated CF-EPSC. On the whole, these observations therefore suggest that *synaptic* NMDA-Rs of adult mouse Purkinje cells are mainly composed of NR2A subunits, while *extrasynaptic* NMDA-Rs can contain, but in a less amount, NR2B subunits.

3.2.3.3 NR3B subunits are they associated to Purkinje cells NMDA-Rs?

Since the publication of our study, NR3B subunit has been shown to be strongly expressed in mature Purkinje cells in *rats* (Wee et al., 2008). In *mice* Purkinje cells, it is possible that NR3B are also expressed, although discrepancies between species can exist, as reported for NR2A and NR2B subunits.

As the effect of NR3 subunits on NMDA-Rs properties has not yet been fully described in native neurons of wild-type mice, it is still difficult to estimate the possible effect of the NR3B association to the “conventional” NR1/NR2 heteromeric receptors evidenced in mature Purkinje cells. Nevertheless, in their single-channels patch-clamp recordings, Renzi et al. (2007) showed “conventional” NMDA-R conductances and properties, in complete accordance with the known features of NR1/NR2A, NR1/NR2B, NR1/NR2A/NR2B heteromeric receptors. It is thus rather unlikely that the NMDA-currents evidenced in mature Purkinje cells are mediated by NR3B containing NMDA-Rs, but this possibility can not be totally excluded. According to the NR3 properties described in introduction of this thesis, an unknown quantity of NMDA-Rs could be “silenced” by the association of an NR3B subunit in the heteromeric complex. In absence of selective pharmacological tools to specifically activate or inhibit the NR3 containing NMDA-Rs, the discrimination of the proper effects of

NR3B subunits in Purkinje cells NMDA receptors will remain difficult to test in our conditions.

To sum up, NR2 subunits expressed in adult mouse are of the 2A and 2B subtypes (Thompson et al., 2000; Piochon et al., 2007; Renzi et al., 2007). Our study evidenced their participation to CF transmission in mature Purkinje cell. In rat Purkinje cells, NR2A subunit expression seems to be weak or absent, whereas NR2B is significantly present (Thompson et al., 2000; Lee et al., 2005). In rats, patch-clamp recordings of NMDA currents in mature Purkinje cells have not yet been re-examined. However, the transfection of Purkinje cells with recombinant virus encoding the NR2B gene has been shown to generate NMDA-R-mediated synaptic currents at both the climbing fiber and parallel fiber synapses in infected Purkinje cells (Kakegawa et al., 2003). If the contribution of NMDA-Rs to both synaptic currents is confirmed in control Purkinje cells, this could reveal more profound differences between species. It is also important to note here that NMDA-Rs expression can varied with pathological conditions. For example, neonatal toluene exposition has been shown to alter on long time scales the NMDA-Rs expression in rat Purkinje cells, by increasing levels of NR2A subunits and decreasing those of NR2B (Lee et al., 2005). Additionally, NR3B subunits recently evidenced in adult rats Purkinje cell are susceptible to associate with NR1 and/or NR2 subunits (Wee et al., 2008). This could deeply modify their classical properties. Finally, in adult human Purkinje cells, if NR2A mRNA is strongly expressed, NR2C mRNA expression is low to strong depending on authors, and NR2B mRNA is not detectable in all cases in human (Rigby et al., 1996; Scherzer et al., 1997).

3.2.3.4 Physiological relevance of NMDA-Rs in mature Purkinje cells

Synaptic versus extrasynaptic NMDA-Rs: different compositions, different functions?

At room temperature, glutamate-transporters being less efficient, a glutamate spillover from CF vesicular release can activate extrasynaptic receptors. Yet, experiments at more physiological temperature (30-34°C) showed the same relative participation of NMDA-Rs in the CF synaptic current (see supplemental Figure 3.2). A location of NMDA-Rs inside the Purkinje cells synapses with CF can thus be proposed. On the other hand, NMDA-Rs are also found in somatic patches (Renzi et al., 2007), and NMDA-mediated CF-EPSCs are potentiated by the specific and nontransported glutamate transporter blocker, DL-TBOA. Thus, NMDA-Rs are likely to be both synaptic and extrasynaptic. Moreover, in mature Purkinje cells, selective NR2B antagonist ifenprodil was shown to partly inhibit somatic

NMDA-Rs only, not those participating in the synaptic currents (Renzi et al., 2007). A selective repartition of different NR2 subunit at intra- or extra- synaptic sites could thus occur in mature Purkinje cells. However, our results with the selective antagonist of NR2B-subunit RO25-6981 drew less categorical conclusions and further examinations of its effect in presence of DL-TBOA are needed. Nevertheless, in these experiments, a possible activation of presynaptic NMDA-Rs (see further) complicates interpretations. Thus, because of the limitations of NR2B-selective antagonists (Neyton and Paoletti, 2006), only studies in electronic microscopy could help to confirm the ultrastructural localization of NMDA-Rs subtypes in Purkinje cells.

Current studies characterizing NMDA-R subtypes in physiological and pathological processes are aimed at finding NR2-specific roles (for review, see Kohr, 2006). Concerning long term synaptic plasticity, the recent proposal of differential roles played by NR2A and NR2B and by their respective synaptic localization is however still controversial (Liu et al., 2004; Massey et al., 2004; but see Fox et al., 2006; Bartlett et al., 2007; Morishita et al., 2007). With regard to excitotoxicity, neither the NMDA-R subtype nor the role of synaptic versus extrasynaptic NMDA-Rs is resolved, since NMDA-Rs in both compartments can cause neurotoxicity (Sattler et al., 2000; Sinor et al., 2000). In mature Purkinje cells, these questions remain totally unexplored.

Function of the complex spike…function of NMDA-Rs?

The presence of a significant but small NMDA component at the CF-EPSC could be considered *a priori* as unimportant for the Purkinje cell physiology. However, as we showed in our study, NMDA-Rs displayed a significant contribution to the complex spike and can deeply modulate its waveform. Interestingly, activation of NMDA-Rs occurs with a single climbing fiber discharge, i.e. a preceding depolarization is not needed to relieve the Mg^{2+} block and obtain the NMDA-Rs participation in the complex spike.

Although the functional role of the complex spike is still unclear, it is well known that climbing fiber is involved in the control of Purkinje cell physiology, for instance their background firing and the induction of long term synaptic plasticity. The potency of NMDA-Rs to modulate the complex spike addresses the question of their involvement in these phenomena.

There is still no consensus on the overall function of the complex spike, and the functional significance of the number and the latency of components of the complex spike still remains matter of speculation. However, it has been shown recently that during visual stimulation, climbing fibers can, in addition to modulate the low frequency discharge of Purkinje cells, transmit signals in the form and the number of spikes within the complex spike (Maruta et al., 2007).

A possible effect on Purkinje cell output

The output of Purkinje cells after a complex spike consists of a burst of forward-propagating action potentials in the axon, in which only the first spike of the complex spike is reliably propagated (Llinas and Sasaki, 1989; Khaliq and Raman, 2005; Monsivais et al., 2005). The relationship between the propagation of these axonal spikes and the number of spikes underlying the complex spike is not clear. Nevertheless, the propagation probability of components of the complex spike depends on their waveform, and can be described as a saturating function of spike amplitude, rate of rise, or preceding interspike interval (Khaliq and Raman, 2005). By modulating these parameters in spikes underlying the complex spike, NMDA-Rs could thus change the probability of propagation of the complex spike components in the axon.

A participation to CF-LTD induction?

CF response undergoes a calcium dependent LTD that can be induced by CF-tetanization at 5 Hz for 30 s (Hansel and Linden, 2000). This LTD, that requires the mGluR1 activation and is PKC- and PKA- dependent (Schmolesky et al., 2007), is also associated to a concomitant LTP of glutamate transporter currents through PKC activation (Shen and Linden, 2005). This LTD decreases CF currents amplitude of ∼20%. Interestingly, this modification essentially affects the second component of the complex spike, which is composed of series of smaller spikes, partly produced by Ca2+ influx (Schmolesky et al., 2002; Schmolesky et al., 2005). As we showed, NMDA-Rs modulate this part of the complex spike. Thus, one can make the hypothesis that a CF-tetanization induces long term reduction of NMDA-Rs contribution to the complex spike. Considering the crucial role of polarity switch played by the complex spike in the control of the LTP/LTD induction at PF-Purkinje cells synapse (see below), this possibility certainly deserves some investigations.

The neuropeptide corticotrophin-releasing factor (CRF), which is released under high activity conditions from the CF-terminals, has been shown to facilitate the CF-LTD induction, probably by acting on the type 1 CRF receptors (CRF-R1, Schmolesky et al., 2007). Interestingly, CRF has been recently demonstrated to depress NMDA-Rs mediated current in hippocampal neurons via CRF R1 and PKC signaling (Sheng et al., 2008). It is thus possible that NMDA-Rs are a target of the CRF-mediated regulation in mouse Purkinje cells.

Involvement in bidirectional PF-synaptic plasticity

At its synapses with PF, Purkinje cell displays both LTD (for review, see Ito, 2001) and LTP (Lev-Ram et al., 2002). The climbing fiber is able to control the probability of LTD versus LTP at PF-Purkinje cells synapses by modulating the Ca^{2+} entry (Coesmans et al., 2004). Because they are activated by the climbing fiber and support the complex spike, in addition to the fact that they mediate by themselves a Ca^{2+} entry, NMDA-Rs of Purkinje cell could play a key role in determining the switch from LTP to LTD. Our preliminary results presented further were designed to test this hypothesis and favor this possibility.

Effect on intrinsic plasticity

Less studied than classical synaptic plasticity, another mode of long term information storage that neurons can use, consists in activity-dependent changes in their intrinsic excitability. Affecting neurons membrane locally or at larger scale, depending on the conductances involved in the phenomenon, this intrinsic plasticity could change durably the signal integration. It has been already described at two different sites of the cerebellar circuit: at mossy fiber to deep cerebellar nuclei synapses (Aizenman and Linden, 2000) and at mossy fiber to granule cell synapses (Armano et al., 2000). In both cases, this plasticity results in the increase in intrinsic excitability. Its induction requires NMDA-Rs activation and postsynaptic Ca^{2+} transient. Because these molecular candidates are now also gathered in mature Purkinje cells, such plasticity can be considered in these neurons. Consistent with this hypothesis, in rabbit, after classical conditioning of membrane eyelid response, Purkinje cells of a particular cerebellar region have been shown to display an increased membrane excitability that is function of the level of conditioning (Schreurs et al., 1998). Moreover, this phenomenon involved a reduction of K^+-currents in Purkinje cells (Schreurs et al., 1998). In Purkinje cells which express high levels of SK and BK, it would be interesting to investigate the possibility of their modulation by NMDA-receptors.

NMDA-Rs and NO synthase in Purkinje cells: another polemic issue?

Many experiments in acute cerebellar slices support the view that nitric oxide (NO) is a crucial signal leading to LTD at PF-Purkinje cell synapses. It has also been shown that a NO signaling cascade triggers persistent changes in spontaneous firing of Purkinje cells (Smith and Otis, 2003). What are the cellular events of this NO signalization? In the cerebellum, there would be many possible sources of NO, which is produced from arginine by the Ca^{2+} activated calmoduline-dependent NO-synthase (NOS) (Garthwaite et al., 1988). Interestingly, NO biosynthesis is preferentially activated by calcium influx through NMDA-Rs by reason of their close linkage with NOS by the PSD-95 family of proteins (Brenman et al., 1996; Christopherson et al., 1999). NO can diffuse freely across cell membranes and its target is probably the soluble guanylate cyclase in cells where NO is produced, as well as in neighboring cells (Hobbs and Ignarro, 1996). In Purkinje cells, the particularly abundant cGMP-dependent protein kinases are finally activated by the resultant increase in cGMP (El-Husseini et al., 1999), allowing phosphorylation of the specific endogenous ‘G-substrate', a potent inhibitor of phosphatases.

In Purkinje cells, where are expressed both NMDA-Rs and PSD93, a NO release has been showed to occur after CF stimulation (Shibuki and Okada, 1991). Therefore, does the CF activate a NOS - NMDA-Rs complex in Purkinje cells? This possibility could however be unlikely regarding previous literature.

Actually, the exact location of the NOS is a matter of debate. PFs terminals, granular and basket cells have been reported to express this protein, whereas no or only very weak NOS expression has been found in Purkinje cells (Bredt et al., 1990; Crepel et al., 1994; Chung et al., 2002; Iino, 2006). However, the presence of NOS in Purkinje cells can not be totally excluded, and could depend on species, age, or specific conditions: In human, the NOS immunoreactivity of the Purkinje cells intensively appeared from the early fetal stage, and is preserved weakly until adolescence (Ohyu and Takashima, 1998). NOS is also detected in adult human Purkinje cells (Egberongbe et al., 1994), where its expression is strongly increased in schizophrenia (Bernstein et al., 2001). In mouse, NOS is found in Purkinje cells throughout the cerebellum during the first postnatal week, and gradually disappeared from P8 to P12 (Bruning, 1993). It is to notice that this profile matches the ones of juvenile NMDA-Rs expression. In rats, (Rodrigo et al., 1994) found “isolated immunoreactive” Purkinje cells in the vermis and parafloccular regions. Interestingly, in rat cerebellar vermis and paravermis,

NOS expression can be induced in Purkinje cells by harmaline treatment, which synchronously activates inferior olive neurons (from which originate CFs, Saxon and Beitz, 1996).

3.2.3.5 Presynaptic NMDA-Rs

If the expression of NMDA-Rs by Purkinje cells is getting clearer with recent studies (Renzi et al., 2007 and ours), their presence can cloud or even question the function of NMDA-Rs expressed on presynaptic afferences.

Cerebellar interneurons have been shown to express NMDA-Rs (Glitsch and Marty, 1999). Activation of these receptors leads to the release of GABA that mediates inhibitory currents in Purkinje cells during bath applications of NMDA, in the presence of tetrodotoxin (TTX), indicating a presynaptic location for the underlying NMDA-Rs (Llano et al., 1991; Glitsch and Marty, 1999). Presynaptic NMDA-Rs that can be activated by the glutamate spillover of the climbing fiber (Szapiro and Barbour, 2007), or by retrograde signalling from Purkinje cells (Levenes et al., 2001; Duguid et al., 2007) thus mediate the depolarization-induced potentiation of inhibition (Duguid and Smart, 2004). Presynaptic NMDA-Rs expressed in interneurons are coupled to a NO cascade, that could be involved in the PF-PC synapses LTD (Shin and Linden, 2005), or in presynaptically expressed PF-PC synapses LTP (Qiu and Knopfel, 2007).

Granule cells are well known to express NMDA-Rs at their synapses with mossy fibers. The early expression of NR2B in granule cells is replaced by NR2A during the initial 3 postnatal weeks, and later by intense expression of NR2C in mature animals (Akazawa et al., 1994; Monyer et al., 1994; Cathala et al., 2000). Yet, on granule cell axons, i.e. parallel fibers, the presence of NMDA-Rs is disputed. In young rats, although patches of staining for NR2 were sometimes found on parallel fibers (Petralia et al., 1994b), parallel fibers were unstained in NR1 immunostaining studies (Petralia et al., 1994a). In young rats (P18-P24) Purkinje cells, the reversible PF-EPSCs depression induced by NMDA application has been attributed to these presumptive presynaptic NMDA-Rs based upon their absence at postsynaptic Purkinje cells. This NMDA-induced inhibition would not involve a depression of transmitter release but would involve a trans-synaptic mechanism in which the NO released by the PFs decreases the glutamate sensitivity of the Purkinje cell (Casado et al., 2000). However, recent studies found no evidence for these NMDA-Rs in PF terminals (Diez-Garcia et al., 2005; Shin and

Linden, 2005; Qiu and Knopfel, 2007). Finally, by the light of our study led on mouse, these results could be re-interpreted with postsynaptic NMDA-Rs, provided that the expression of NMDA-Rs is verified in rats Purkinje cells of this age.

Finally, given that the mechanisms implicated in long term synaptic plasticity, excitotoxic processes and development have been mainly built on the erroneous postulate that adult Purkinje cells do not express functional NMDA-Rs, our unexpected results open a new insight on the Purkinje cell physiology in adult animals.

3.3 Manuscript to submit:

NMDA receptor participation to climbing fiber EPSC in adult mouse Purkinje cells lacking the delta2-glutamate receptor

"If at first, the idea is not absurd, then there is no hope for it"

Albert Einstein

3.3.1 Introduction and summary

Classified as an ionotropic glutamate receptor on the basis of its amino acid sequence, GluRdelta2 is considered an orphan receptor since no physiological ligand has so far been identified. GluRdelta2s are selectively localized at the PF-Purkinje cell synapses in the adult cerebellar cortex (Araki et al., 1993; Landsend et al., 1997), except during a short period of the early development during which they are also found at CF synapses (Zhao et al., 1997; Roche et al., 1999).

Hotfoot is an allelic family of mutations localized in the GluRdelta2 gene (GRID2), which result in the loss of function of GluRdelta2. Hotfoot mutant mouse bearing the Nancy-allele (Ho-Nancy) displays a large deletion in GRID2, resulting in the complete absence of the protein (Lalouette et al., 2001). In these mice, the integrity of PF-Purkinje cell synapses is impaired and the regression of the CF multiple innervation is not achieved. In addition, the competition between PFs and CFs for Purkinje cell dendritic territory does not occur correctly, CFs invading the PF territory (Morando et al., 2001). Functionally, this mutation is accompanied by a loss of LTD at PF-Purkinje cell synapses that is not caused by the developmental deficits (Hirai et al., 2005). Indeed, GluRdelta2 seems to regulate AMPA-Rs clustering at synapses (Hirai et al., 2003), by Ca2+ dependent physical-interactions with PSD93 or S-SCAM proteins or other synaptic anchors, that are coupled to AMPA-Rs (Hirai, 2001; Uemura et al., 2004; Elias and Nicoll, 2007; Kohda et al., 2007; Uemura et al., 2007).

On the whole, it appears that during evolution GluRdelta2 could have lost its channel properties to acquire the function of an activity-dependent adhesion molecule with the key role of orchestrating the synaptogenesis and synaptic plasticity in Purkinje cells by modulating the trafficking of receptors at synapses.

Because GluRdelta2 seems to be able to regulate the trafficking of AMPA-Rs via Ca2+-dependent modulation of the linkage between AMPA-Rs and scaffolding proteins, we wondered if in Purkinje cells GluRdelta2 could also regulate NMDA-Rs trafficking with a competitive relationship. Several lines of evidence supported this hypothesis:
- the selective expression of NMDA-Rs at CF synapses only, and GluRdelta2 at PF synapses only (at least in the adult)
- the fact that GluRdelta2 are expressed at CF synapses only during the transient absence of NMDA-Rs in Purkinje cells (Zhao et al., 1998; Roche et al., 1999),
- the fact that, in case of CF deafferentation, NMDA-currents disappear (Elias and Nicoll, 2007), while GluRdelta2 invades former-CF synapses (Cesa et al., 2003)
- the homology between these receptors (Yamazaki et al., 1992b),
- their capacity to interact with same synaptic anchors and PDZ proteins (Roche et al., 1999)

To test this hypothesis, we studied the expression of NMDA-Rs in the Ho-Nancy mutant mice, which lack GluRdelta2, where we speculated that, according to our hypothesis of a competition, NMDA receptors could be differently expressed and/or localized. We found normal expression and localization of NMDA-Rs in the Ho-Nancy Purkinje cells. Like in their wild-type counterparts, we did not detect NMDA-currents in PF-EPSCs. These results show that the absence of GluRdelta2 does not strongly interfere with NMDA-Rs expression. Thus there does not seem to be direct competition between NMDA-Rs and GluRdelta2. In addition, we made three interesting observations during this study:

- Re-estimating carefully the rate of multi-innervation in the Ho-Nancy mouse, we showed that the vast majority of Ho-Nancy Purkinje cells are multi-innervated by CFs, and with a higher degree than reported in previous studies of this mutant (Lalouette et al., 2001). This multiple innervation is equivalent to the GluRdelta2 transgenic knock-out mouse (Kashiwabuchi et al., 1995b). This means that GluRdelta2 is necessary for the proper regression of multiple CFs.
- We found that, despite the absence of GluRdelta2, NMDA-Rs develop in the same time window in the adult (by P21).

- Interestingly, in the Ho-Nancy Purkinje cells which were innervated by multiple CFs, we detected an NMDA component only at the “dominant” CF response, not at the weakest CF responses. These results suggest that the NMDA-Rs expression could be selective of one CF, the strongest one.

3.3.2 Manuscript

NMDA receptor participation to climbing fiber EPSC in adult mouse Purkinje cells lacking the delta2-glutamate receptor

Abbreviated title: Functional NMDA receptors in adult Purkinje cells of Hotfoot mouse

Claire Piochon[1], Theano Irinopoulou[2], Daniel Brusciano[1], Jean Mariani[1], Carole Levenes[1]

[1] Université Pierre et Marie Curie-Paris6; UMR7102 (CNRS); Laboratoire NPA – équipe DVSN, F-75005 Paris, France
[2] Université Pierre et Marie Curie-Paris6; UMRS440 (INSERM); Signalisation et Différenciation Cellulaires dans les Systèmes Nerveux et Musculaire, Institut du Fer à Moulin, F-75005 Paris, France

Correspondence should be addressed to Claire Piochon, UPMC équipe DVSN, case courrier #14, 9 quai St Bernard, 75005 Paris, France E-mail: Claire.piochon@snv.jussieu.fr

Keywords: NMDA-Rs; GluRdelta2, hotfoot, Purkinje cells; climbing fiber; glutamate receptors; cerebellum.

Acknowledgments: Part of this study was supported by a one year salary provided to Claire Piochon by the French foundation for medical research (FRM).

Abstract

Cerebellar Purkinje cells form two different types of excitatory synapses: one with parallel fibers (PFs) on distal dendritic arborization and the other with a climbing fiber (CF) on proximal dendrites. While AMPA and mGluR1 glutamate receptors are found at both kinds of synapses indifferently, the recently evidenced NMDA receptors (NMDA-Rs), and the orphan delta2 glutamate receptor (GluRdelta2) are differently and selectively distributed in mature mice Purkinje cells. Whereas GluRdelta2 is initially expressed at CFs and PFs postsynaptic densities of mice Purkinje cells before approximately the postnatal day P21, it selectively localizes at PF-Purkinje cell synapses after this date. Furthermore, from P21, while the regression of supernumerary CFs is complete, NMDA-Rs appear in Purkinje cells, localized to CF contacts, and are absent from PF synapses. Although the mechanism underlying the synapse-specific sorting of GluRdelta2 and NMDA-Rs is unclear, this phenomenon could state on a competition between these proteins. These parent glutamate receptors indeed share common features, like the capacity to interact with same anchors proteins. In this study we made the hypothesis that in the absence of GluRdelta2, NMDA receptors could be differently expressed and localized.

However, the expression and localization of NMDA-Rs appeared to be normal in the Hotfoot-Nancy (Ho-Nancy) mutant that lacks GluRdelta2.

Remarkably, we show that the multi-innervation of Purkinje cells is far larger in Ho-Nancy mice than previously estimated, so that almost all Purkinje cells receive multiple CF connection. In Ho-Nancy, CFs innervate Purkinje cells dendritic arborization more distally and invade the territory of PFs. This distal innervation probably underlies the “atypical” supernumerary CF connexions that are small and often slower than normal. Interestingly, in Ho-Nancy Purkinje cells, the NMDA component was present only at the larger CF response, not at the smallest ones, indicating that the NMDA-Rs expression is selective of the “strong” CF. Thus, there seems to exist a mechanism that drives the expression of NMDA-Rs at the strongest CF and that may be related to stabilization of this connexion.

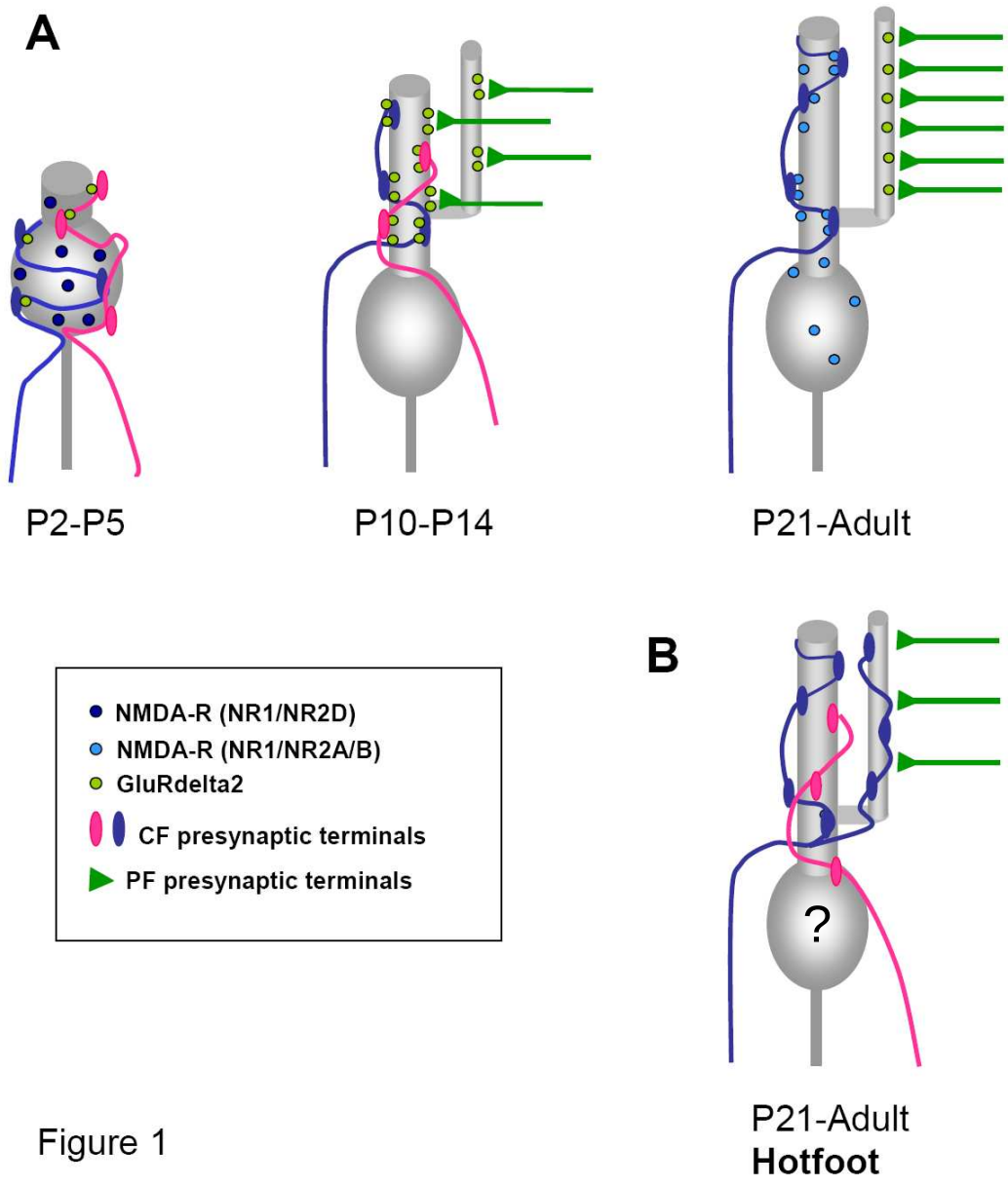

Figure 1

Fig.1. Schematic representation of NMDA-Rs and GluRdelta2s expression in Purkinje cells through the postnatal development.

(A) In wild-type mouse, at early stages (~P2-P5), multiple CF innervate immature Purkinje cells, GluRdelta2 are synaptically expressed, whereas NMDA-Rs containing the NR2D subunit are expressed extrasynaptically. During the second postnatal week (~P10-P14), Purkinje cell develops its dendritic tree. While multiple CFs are still connected to the dendritic arborization, PFs establish their first contacts. At this age, NMDA-Rs are absent from Purkinje cells whereas GluRdelta2s display a peak of expression and are present at both types of synapses. From ~P21 throughout adulthood, a single CF innervates Purkinje cell and PFs are connected on distal dendrites. GluRdelta2 are exclusively expressed at PF-Purkinje cells synapses, from which NMDA-Rs are absent. NMDA-Rs participate to the CF synaptic transmission and are also extrasynaptically expressed. **(B)** In adult Ho-Nancy, multiple CFs remain and invade the distal territory which is normally innervated by PFs. NMDA-Rs expression of in Ho-Nancy Purkinje cells was to be determined.

Introduction

Fast excitatory synaptic transmission in the mammalian central nervous system is mediated by the activation of ionotropic glutamate receptors (iGluRs). Although different types of iGluRs can coexist at same excitatory synapses, in cerebellar Purkinje cells, which receive two distinct types of glutamatergic inputs, i.e. parallel fibers (PF) and climbing fibers (CF), the delta2 glutamate receptors (GluRdelta2s) and N-methyl-D-aspartate receptors (NMDA-Rs) possess their own expression territories. While NMDA-Rs are selectively expressed at CF synapses in mature Purkinje cells, GluRdelta2s are selectively localized at postsynaptic contacts with PFs (Landsend et al., 1997; Zhao et al., 1997; Piochon et al., 2007). Although very little is known about the mechanisms underlying the differential targeting of both these types of receptors, their specific segregation suggests a competition or a reciprocal exclusion between them.

This hypothesis is also supported by the expression profiles of these two homologous iGluRs during Purkinje cell development (Fig.1-A). During the first week of postnatal development, GluRdelta2 is expressed at CF synapses, while juvenile NMDA-Rs are found extrasynaptically (Momiyama et al., 1996). In the second postnatal week, GluRdelta2 expression dramatically increases at both CF and PF synapses (Zhao et al., 1998), while juvenile NMDA-Rs completely disappear (Momiyama et al., 1996). This period corresponds to a developmental stage of great activity in the Purkinje cell, which displays an extensive growth of the dendritic arborization and an intense synaptogenesis with PFs. Concomitantly begins the regression of supernumerary CFs that initially connected the Purkinje cell. From the third postnatal week, with the complete achievement of this regression, a new type of NMDA-Rs appears specifically localized at CF-Purkinje cell synapses, and remains expressed through adulthood, as we recently described (Piochon et al., 2007). At the same time, GluRdelta2 becomes selective of PF-synapses.

Although GluRdelta2 might not function as a ionotropic receptor (Kakegawa et al., 2007a), it plays a crucial role in the development of the cerebellum as well as in cerebellar functions (for reviews, see Gounko et al., 2007; Mandolesi et al., 2008). GluRdelta2-null mice display impaired synapses formation and stabilization, such as naked spines, mismatched PF-Purkinje cells synapses and the persistent innervation of Purkinje cells by multiple CF (Guastavino et al., 1990; Kashiwabuchi et al., 1995a; Kurihara et al., 1997). GluRdelta2s also play a critical role in the competition between PFs and CFs to determine their postsynaptic domains on the Purkinje cells (Morando et al., 2001; Mandolesi et al., 2008). In mutants lacking GluRdelta2, the CFs innervation territory extends distally on the domain of PFs

connections to Purkinje cells (Ichikawa et al., 2002). Inversely, when electrical activity is blocked by tetrodotoxin (TTX), or when lesion of the inferior olive is performed causing a CF deafferentation on Purkinje cells, GluRdelta2 invade the former CF synapses on the proximal dendritic spines (Morando et al., 2001; Cesa et al., 2003). Interestingly, in case of CF deafferentation, Purkinje cells no longer respond to NMDA (Billard and Pumain, 1989). Because GluRdelta2s have been cloned partly by sequence homology with NMDA receptors (Yamazaki et al., 1992a; Araki et al., 1993; Lomeli et al., 1993), these receptors share common features. In particular, both GluRdelta2 and NMDAR bind some common PDZ proteins. This suggests a possible competition for the same synaptic anchors (Roche et al., 1999).

This question prompted us to determine the developmental pattern of expression of NMDA-Rs in Purkinje cells of animals lacking GluRdelta2s (Fig.1-B). Furthermore, NMDA-Rs contribute to mature CF synapses (Piochon et al., 2007; Renzi et al., 2007). In absence of GluRdelta2, mature Purkinje cells are innervated by multiple CFs. In this case, what about the expression of NMDA-Rs at these supernumerary CFs synapses?

To test these hypotheses, we used hotfoot-Nancy (Ho) mutant mice that are spontaneous knockout of GRID2, i.e. the gene coding GluRdelta2 (Guastavino et al., 1990; Lalouette et al., 1998; Lalouette et al., 2001). Using voltage-clamp whole cell recordings, we verify here that GluRdelta2 is necessary for the supernumerary CFs regression. Although Purkinje cell keep this immature feature, juvenile NMDA-Rs expression do not seem to persist in Ho-Nancy Purkinje cells in absence of GluRdelta2. Like their wild-type counterparts, Ho Purkinje cells express functional NR1 and NR2A/B containing NMDA-Rs that participate to the CF-EPSC from the third postnatal week. In Ho PCs, immunolabelings of NMDA-Rs follow the CFs innervation territory, and thus invade the distal PFs synapses domain. However, no participation of NMDARs is detected in PF-EPSCs, indicating that a mechanism independent of GluRdelta2 must mediate the absence of NMDA-R currents from PFs excitatory post-synaptic currents (EPSC). Interestingly, NMDA currents are not detected in the synaptic response of supernumerary CFs. This suggests that an additional factor, independent of GluRdelta2, could play a role in determining the expression of NMDA-Rs at specific CF synapses.

Material & Method

Care and use of animals. Animals breeding and all the experiments were performed in accordance with the principles of the guidelines of the French Ministry of Agriculture and the European Community Council. A minimal number of animals was used and handled with maximum care to minimize their stress and suffering. Ho-Nancy mice used in the present study are on the C57Bl/6J background, and express the Nancy allele, in which the deletion in the GRID2 gene spans three of the four transmembrane domains of the GluR-delta2 protein. This mutant mouse has been previously described (Guastavino et al., 1990; Lalouette et al., 2001).

Slice preparation. Adult mice aged between 2 and 6 months were used in these experiments. Young mice of 14 to 17 days were also used in a set of experiments. Animals were first anesthetized with halothane and then rapidly decapitated. The cerebellar vermis was immediately removed and cooled to 4℃ in oxygenated bicarbonate buffered solution (BBS, see below). Parasagittal 180 µm thick slices were cut with a vibratome (VT-1000S, Leica Microsystems, Wetzlar, Germany). Slices were subsequently incubated for at least 1 hour at room temperature in BBS that contains (in mM): 130 NaCl, 2.5 KCl, 2.0 $CaCl_2$, 1.0 $MgCl_2$, 26.0 $NaHCO_3$, 1.3 NaH_2PO_4, 10.0 glucose, pH 7.4, when bubbled with 95% O2 and 5% CO2.

Whole-cell recording procedure. The slice was placed in a recording chamber continuously superfused at a rate of 1-2 ml/minute with oxygenated BBS. Purkinje cells were visually identified from their position, size and shape using Nomarski differential interference contrast optics (40x water-immersion lens; Zeiss, Oberkochen, Germany), plus a 2.25x Nikon zoom (Tokyo, Japan) mounted on an upright Zeiss Axioskop-FS microscope. Whole cell voltage-clamp recordings were made with an Axopatch-200A amplifier (Molecular Devices, Union City, CA). Signals were filtered at 2 or 5 kHz and usually sampled at 25-37 µsec. Data acquisition and storage were performed on a personal computer running the ACQUIS1 software (Bio-logic, Orsay, France). Patch pipettes were made of borosilicate glass capillary tubing pulled on a horizontal puller (Sutter Instrument, Novato, CA). their final resistance was of 2-5 MΩ depending on the internal solution used. The internal solutions used were (in mM): 144.0 K gluconate, 6.0 KCl, 4.6 $MgCl_2$, 10.0 HEPES acid, 10.0 EGTA, 1.0 $CaCl_2$, 4.0 ATP-Na, 0.4 GTP-Na, pH 7.3 adjusted with KOH. Series resistances were partially compensated (70 to 75%). Holding potential (Vh) was set at -70 mV (liquid junction potential non corrected), unless the response could not be clamped sufficiently to prevent the generation of action potentials.In this case, the cell was held at -90 mV. Except otherwise specified, recordings were made in Mg2+-free BBS external solution supplemented with 25 μM

Glycine. Bicuculline methiodide (20 μM, Sigma, St. Quentin Fallavier, France) was also systematically added to block $GABA_A$-mediated currents. For ionophoresis experiments, when filled with 10 mM NMDA, ionophoretic pipette had a final resistance of 40 - 50 MΩ. NMDA was ejected using negative square current pulses ranging from 100 nA to 250 nA. To limit diffusion of NMDA in the BBS, a small positive retention current (usually 10 nA) was continuously applied to the iontophoresis pipette between ejections. Extracellular stimulation of CFs or PFs was performed with a constant voltage isolated unit (0.1 msec square voltage pulses; 1-90 V) through a glass pipette filled with external solution. To look for multiple CFs innervating the recorded PC, the stimulation pipette was systematically moved around in the vicinity of the recorded Purkinje cell and the stimulus strength was gradually increased at each stimulation site, until the all-or-none CF response was obtained. PFs were activated by extracellular stimulation in the molecular layer.

Drugs. Glycine and 1,2,3,4-tetrahydro-6-nitro-2,3-[f]-quinoxaline-7-sulfonamide (NBQX), were from Sigma-Aldrich (Sigma-Aldrich, France). N-Methyl-D-Aspartate (NMDA), tetrodotoxine (TTX), (RS)-1-aminoindan-1,5-dicarboxylic acid (AIDA), D-(-)-2-amino-5-phosphonopentanoic acid (D-APV), were from Tocris Bioscience (distributed by Fisher Bioblock scientific, Illkirch, France).

Immunohistochemistry. Parasagittal 60 µm slices were prepared as previously described except that a slicing sucrose BBS was used. This solution (containing in mM : 1 $CaCl_2$, 5 $MgCl_2$, 10 Glucose, 4 KCl, 26 $NaHCO_3$, 248 Sucrose, 1.3 NaH_2PO_4, pH 7.35) was cooled to 4℃ and bubbled with 95% O_2 and 5% CO_2. Immediately after slicing, slices were fixed with 4% paraformaldehyde in phosphate-buffered saline (PBS) for 2 hours. They were then rinsed 3 times with PBS. Permeabilization and saturation were performed during 1 h on free-floating sections with PBS containing 0.25% Triton X-100 and 0.25% fish gelatine (PBS-G-T).
For NR2-C and NR2-D immunodetection, two types of anti-NR2 antibodies were used: a rabbit anti-NR2-D raised against amino acids 268-386 of human NR2-D, and a goat anti-NR2-C/D raised against a peptide mapping at the C terminus of NR2-D of mouse. The latter also recognizes NR2-C (sc-1471; Santa Cruz Biotechnology, distributed by Tebu, Le Perray en Yvelines, France). For NR2-A/B immunodetection, rabbit anti-NR2-A/B raised against the C-terminus tail of the rat NR2-A subunit was used. It recognizes both NR2-A and NR2-B mouse proteins equally (AB1548; Chemicon, Temecula, CA, distributed by Euromedex, Mundolsheim, France). Slices were divided into three batches and incubated overnight at room temperature in the following combinations: (1) with only the rabbit anti-NR2-A/B antibody (1 μg/ml), (2) with NR2-A/B, mouse anti-Calbindin-D28k (1/10000; Swant, Bellizona, Switzerland) and guinea pig anti-Vesicular Glutamate Transporter 2 (VGLUT2)

(1/3000; Chemicon) -antibodies, (3) with PBS-G-T only (control). Slices were then incubated 2 hours with the fluorescent secondary antibodies (10 *µ*g/ml; Invitrogen): Alexa Fluor 546 goat anti-rabbit (combinations 1-3), Alexa Fluor 633 goat anti-mouse and Alexa Fluor 488 goat anti-guinea pig (combinations 2 and 3). The labeled slices were mounted in Vectashield medium (Vector Laboratories, Burlingame, CA) and viewed with a confocal laser-scanning microscope (SP2; Leica, Manheim, Germany) using a 63x objective. In multiple labeling experiments, acquisition of the signal was systematically performed in sequential mode. Alexa Fluor 488 was excited at 488 nm (argon laser), Alexa Fluor 546 at 543 nm (helium-neon laser), and Alexa Fluor 633 at 633 nm (helium-neon laser). Fluorescence signals were corrected for background fluorescence by measuring slices from control combination 3.

Analysis and Statistics. To estimate whether a cell displays a detectable D-APV-sensitive and NBQX-resistant EPSC, the amplitude of the NBQX-resistant EPSCs in control and during bath application of D-APV were compared using a Mann-Whitney one-tailed statistical test. If the two populations of amplitudes (control and D-APV) were statistically different (P>0.05), D-APV was considered as having an effect, and the percentage of blockade induced by D-APV was calculated. Averages are given as mean +/- SEM. For statistical comparisons, Mann-whitney or Wilcoxon procedures were used, unless specified, and *p* is given as the probability of the null hypothesis.

Results

Bath or ionophoretic applications of NMDA induce currents in mature Ho-Nancy Purkinje cells

Purkinje cells from Ho-Nancy mice older than 2 months were recorded in the whole-cell patch-clamp configuration (Holding potential= -70 mV, see Materials and Methods). NMDA (20 µM) was applied in the bath for 1 minute in the presence of NBQX (20 µM), AIDA (100 µM), Bicuculline (20 µM), and TTX (1 µM) to isolate NMDA response as well as avoid the onset of action potential in the slice. In all the Ho-Nancy Purkinje cells tested (n=6), NMDA elicited inward currents, with a mean amplitude of 63.6 +/- 20.7 pA. NMDA was also applied locally by ionophoresis during 0.2 s at the level of the dendritic arborization of the recorded Purkinje cells, in an external solution containing NBQX (20 µM), AIDA (100 µM), bicuculline (20 µM), and TTX (1 µM) as for bath applications. These applications elicited inward currents of amplitudes going from 19 to 415 pA in all the Ho-Nancy Purkinje cells tested (n=6, 12 applications). Amplitudes mainly depended on the location of the application pipette as well as on the ejecting current pulse applied in the iontophoretic pipette. These currents were completely abolished by D-APV (n=6) and reappeared with the washout of D-APV (Fig.2).

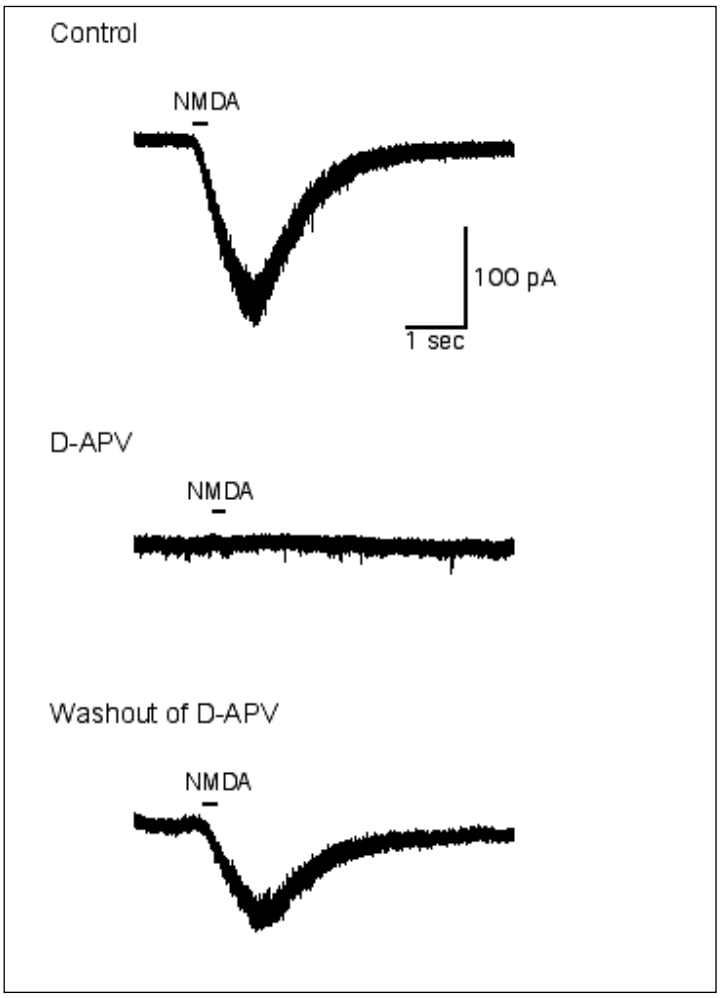

Fig. 2. NMDA currents in Purkinje cells of adult Ho-Nancy mice.
Inward currents are induced by ionophoretic applications of NMDA in adult (>2 months) Ho-Nancy Purkinje cells recorded in the presence of NBQX (20 µM), bicuculline (20 µM), TTX (1 µM). D-APV (50 µM) completely blocks these currents that reappear after washout. Currents display an increased noise that is typical of NMDA-Rs.

We recently identified NMDA currents in wild-type Purkinje cells of adult mouse. By immunolabelings, we demonstrated their expression of NR2A/B subunits (Piochon et al., 2007). We thus wondered if mature Ho-Nancy Purkinje cells also express such NMDA subunits. If so, does the localization of NMDA-Rs in Ho-Nancy Purkinje cells differ from that of wild-type?

Immunolabelings of NR2A/B subunits reveal the presence of NR2A/B subunits on Purkinje cells of Ho-Nancy mouse and suggest the presence of NMDA-Rs on distal dendrites

To investigate both the nature and the localization of the NR2 subunits composing the NMDA-Rs that mediate bath and ionophoretic currents identified in mature Ho-Nancy Purkinje cells, we performed immunolabelings of the diverse NR2 subunits, along with that of calbindin as markers of Purkinje cells. Acquisition of the fluorescent signal was performed with a confocal microscope. Although no labelling was revealed for NR2C or NR2D subunits in adult Ho-Nancy Purkinje cells, a strong labelling of NR2A/B subunits was found in Purkinje cell soma and dendritic arborisation, which were labelled by the calbindin signal. Interestingly, the triple immunolabeling performed with the additional VGluT2 labeling showed that the presumptive territory of CF is extended distally in the molecular layer and that the NR2A/B labelling is distributed on the same Purkinje cell dendritic territory. Thus the NR2A/B labeling is unusual in that it is distally extended in the molecular layer (Fig.3).

In mature Purkinje cells of wild-type mice, it has been shown recently that NMDA-Rs appear around the postnatal day P21 and participate to the CF-EPSCs. Do NMDA-Rs also participate to the CF-EPSC of Purkinje cells from adult Ho-Nancy mice? Because the regression of redundant CFs is impaired in these animals, does an NMDA-component also mediate the CF-EPSC of supernumerary CFs? To answer, we first needed to evaluate the CF multi-innervation of Ho-Nancy Purkinje cells in our conditions.

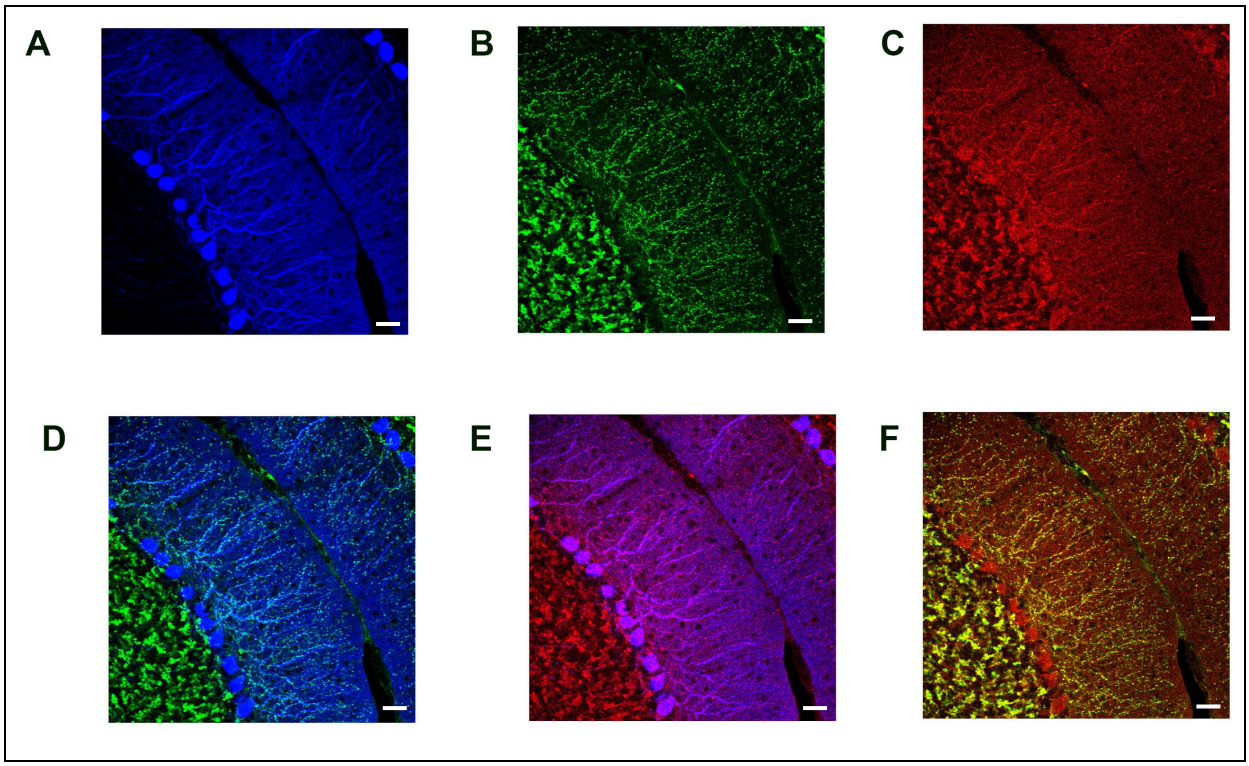

Fig.3. Immunolabelings of NR2A/B subunit in Purkinje cells of adult Ho-Nancy mice. (A), (B) and (C) are of the same confocal section. (A) Calbindin-immunolabeling shows the soma and the whole dendritic arborization of the Ho-Purkinje cells in blue. (B) VGluT2-immunolabeling in green showing the terminals of the mossy fibers in the granular layer and the terminals of the CFs in the molecular layer. In Ho-Nancy mouse cerebellum, CFs terminals are unusually numerous and distally extended in the molecular layer. (C) NR2A/B-immunolabeling shows in red the presence of this subunit in Purkinje cell soma and dendrites, as confirmed by the superimposed labeling of NR2A/B and calbindin shown in (E). (D) The distal territory of Purkinje cell dendrites in the molecular layer, where only PFs usually connect is very thin, because of the extension of the CF innervation. (F) NR2A/B labeling corresponds to the dendritic territories of CFs innervation. Scale bar, 20 µm.

High degree of persistent multiple CF innervation in adult Ho-Nancy mice

During the first weeks of the postnatal development, multiple CFs that originate from the inferior olive innervate the same Purkinje cell. By P21, supernumerary CFs are completely eliminated to leave each Purkinje cell innervated by only one CF (Crepel, 1971; Crepel, 1982). When GluRdelta2 is absent or mutated, the regression of redundant CF is known to be impaired, to a degree that seems to depend on the invalidation of the GluRdelta2 gene. The percentage of mono-innervated PCs varies significantly between different GluRdelta2 mutants, going from 40 to 80% (for instance compare (Lalouette et al., 2001; Kakegawa et al., 2007b; Motohashi et al., 2007). On the over hand, the estimation of this ratio can greatly vary with the experimental procedure.

Each CF displays a single threshold for excitation. By increasing the stimulus intensity, we elicit CF-EPSCs in an all-or-none manner. Moreover, as previously described (Konnerth et al., 1990), 30 ms interval paired stimulation of CFs resulted in the characteristic paired pulse depression (PPD). Using both these criteria of all-or-none response and PPD, we identify the CF-EPSCs evoked by stimulation in the granular layer in Ho-Nancy Purkinje cells voltage-clamped at -70 mV (Fig.4A and 4B).

In Ho-Nancy mouse aged of 2 to 6 months, only 17.1% of Purkinje cells were mono-innervated by a single CF (n=35) displaying a typical large and fast EPSC. On the contrary, in wildtype mouse of same ages, all the Purkinje cells recorded in the same conditions in our previous study were mono-innervated (Piochon et al., 2007). Compared to the standard CF-EPSC, most of supernumerary CF-EPSCs displayed an atypical smaller amplitude and slower rise-time. As proposed by Ichikawa et al. (2002), atypical CFs may represent additional CFs coming from neighboring PCs to the recorded PC. A number of 2, 3 and 4 steps was found in 42.9, 25.7 and 14.3% of Ho-Nancy Purkinje cells respectively (n=35, Fig.4C). In average, Purkinje cells received 2.37 +/- 0.16 CFs (n=35). These results not only confirm the crucial role of GluRdelta2 in the elimination process of supernumerary CFs (Hashimoto et al., 2001), but also show that adult Ho-Nancy PCs are more severely multi-innervated than in other GluRdelta2 mutants (Kashiwabuchi et al., 1995b) and than previously estimated (Lalouette et al., 2001).

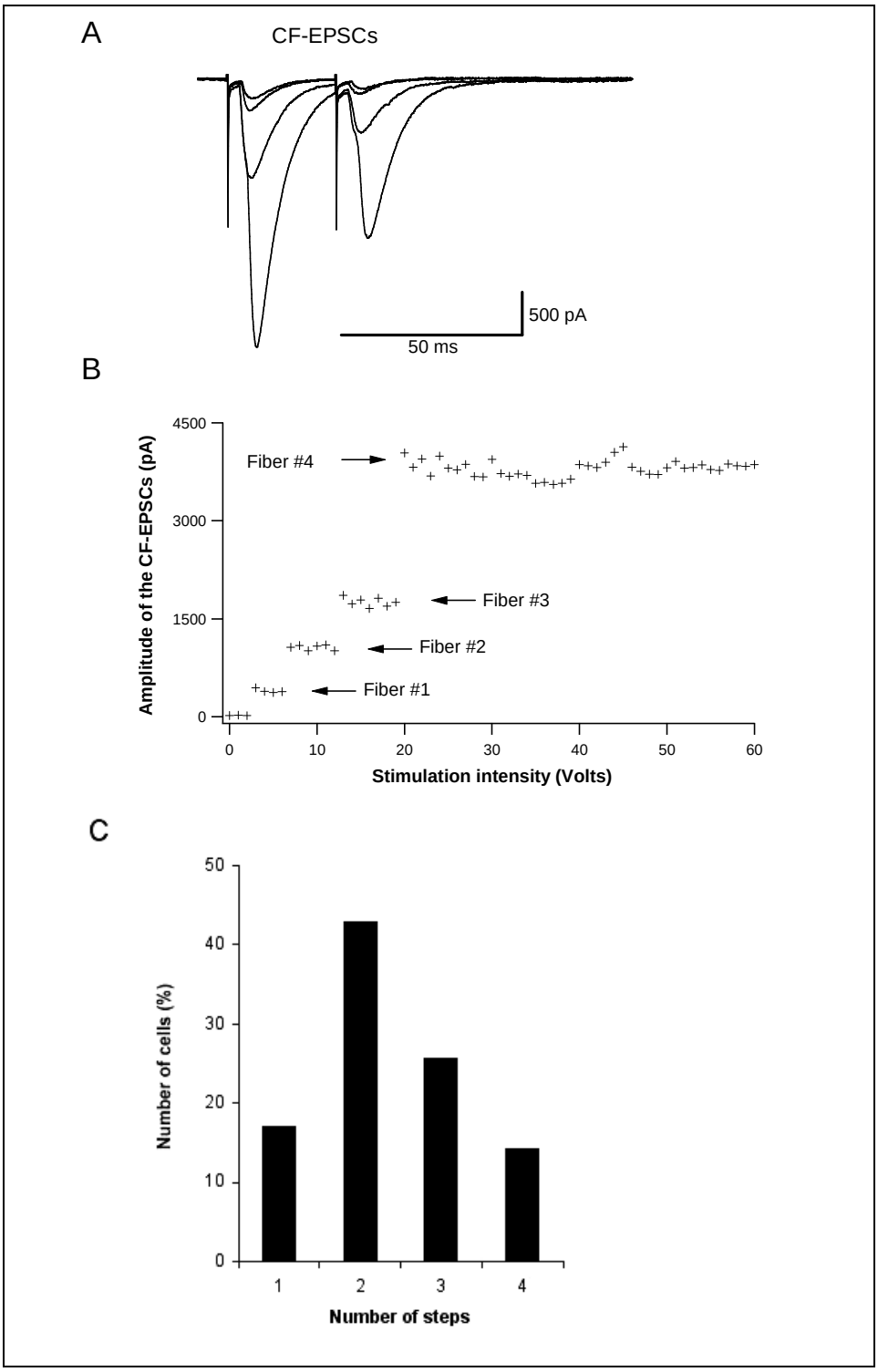

Fig.4. Multiple CFs innervation in Ho-Nancy Pukinje cells.

Purkinje cells of Ho-Nancy mice older than 2 months were held at Vh= -70 mV. By increasing progressively the intensity of stimulation at a fixed stimulation site, CF-EPSCs were successively evoked and identified on the basis of their all-or-none feature and the PPD, generated by paired stimulation separated by 30 msec. (A) Superimposed CF-EPSCs generated in recorded Purkinje cell. (B) Plotting the EPSC amplitudes against the intensity of stimulation shows the stepwise recruitment of up to four CFs in a Ho-Nancy Purkinje cell. (C) Summary histograms showing the percent number of Purkinje cells displaying 1, 2, 3 or 4 steps. (CFs multi-innervation ratio = 2.6, n=26).

The largest CF-EPSC displays a NMDA component in adult Ho-Nancy Purkinje cells, whereas no NMDA component is detectable in atypical CF-EPSCs

The largest CF-EPSCs were generated by supra-threshold stimulus intensity for control periods. In presence of NBQX (20 µM), CF-EPSCs were not completely blocked. The NBQX-resistant CF-EPSCs was all-or-none and displayed PPD. D-APV (50 µM) and Mg^{2+} (1 mM) blocked the totality of the NBQX-resistant EPSC in all the cells tested (n=6 and n=5 respectively), and this inhibition was reversible (Fig.5A and B).

This residual CF-EPSCs that persisted in the Ho-Nancy Purkinje cells tested had an averaged amplitude of 245.9 +/- 74 pA (n=8). Compared to the averaged amplitude of 228.9 +/- 25 pA (n=43) of NMDA-mediated CF-EPSC from wild-type control mice previously recorded, the NMDA component of the total CF-EPSC in Ho-Nancy mice was not significantly different (Student t-test, p=0.8). Although Ho-Nancy Purkinje cells remains severely multi-innervated in adult mouse, the global NMDA-component of the CF-EPSC does not seem to be significantly increased. This suggests that supernumerary atypical CF-EPSCs do not add a significant NMDA component to the total CF-EPSC.

To test this hypothesis, we tested the effect of NBQX on atypical CF-EPSCs. In all the multi-innervated Purkinje cells tested (n=5), the atypical CF-EPSCs were totally inhibited by NBQX (20 µM). However, by increasing the stimulus intensity to the threshold that initially triggered the biggest CF-EPSC, we recorded a NBQX-resistant response that was blocked by D-APV or Mg^{2+} (Fig.5C). Thus, in mature Ho-Nancy Purkinje cells innervated by multiple CFs, NMDA-Rs seem to participle only to the dominant-CF synaptic transmission, since any detectable NMDA component is observed in atypical CF-EPSCs.

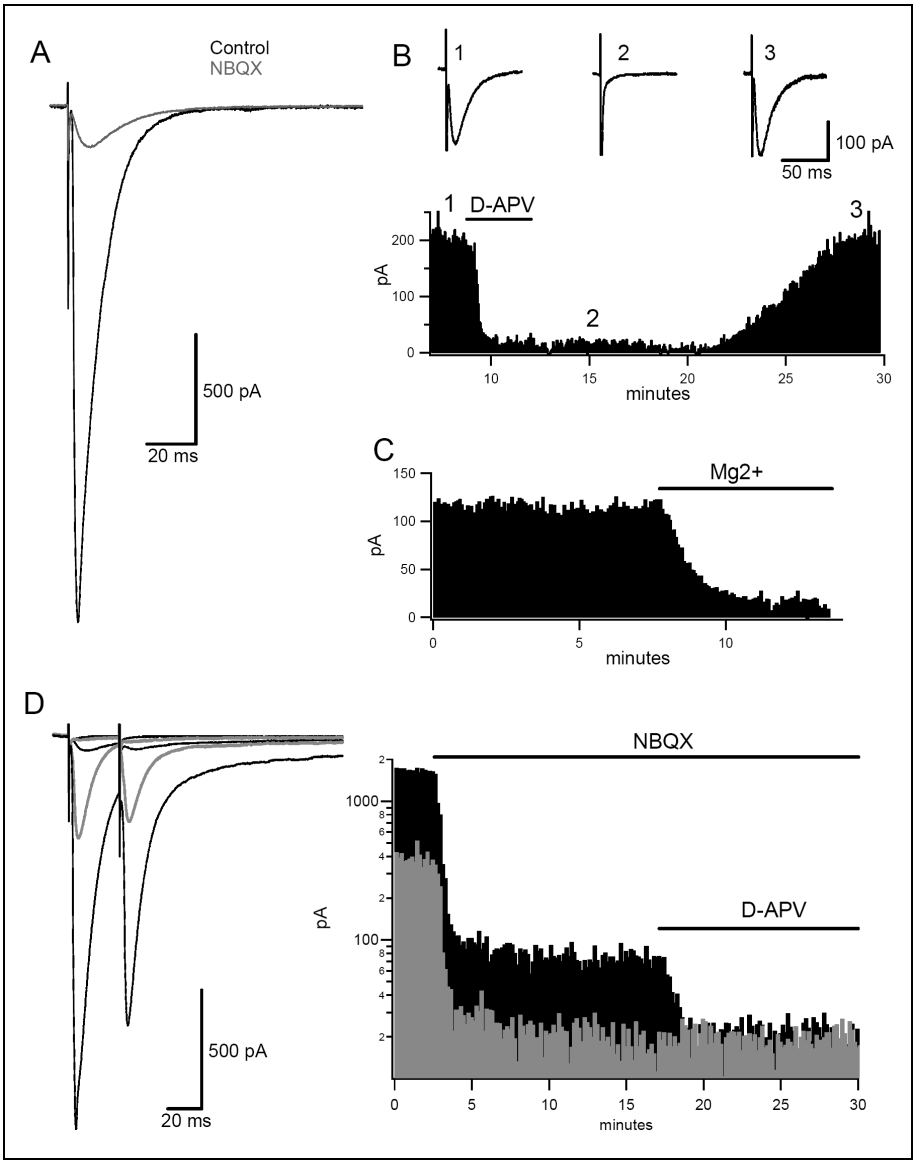

Fig.5. NMDA currents participate to the strongest CF-EPSC but are no detectable in atypical CF-EPSCs. (A) The strongest CF-EPSC displays an NMDA-mediated component: averaged CF-EPSCs recorded in absence of Mg^{2+}, before and during the application of NBQX (20 µM), are superimposed. (B) Effect of D-APV (50 µM) on the NBQX-resistant CF-EPSC represented in A. Amplitude of the NBQX-resistant CF-EPSC are plotted over time before (1), during (2) and after the application of D-APV (3). Corresponding averaged NBQX-resistant CF-EPSCs are represented on top traces. (C) Amplitude of the NBQX-resistant CF-EPSCs plotted over time before and during the addition of 1 mM external Mg^{2+}. (D) Representative recording of a CFs-multi-innervated Ho-Nancy Purkinje cell, in absence of Mg^{2+}, NBQX (20 µM) was tested simultaneously on the largest CF-EPSC and on one of the weak CF-EPSC. Left panel shows averaged strongest CF-EPSC (black traces) superimposed with the averaged weak CF-EPSC (grey traces), before and during NBQX (20 µM) application. A NBQX-resistant CF-EPSC persists with the intensity of stimulation that evoked the strongest CF-EPSC, but not with the stimulation intensity that evoked the weak CF-EPSC initially. Right panel shows amplitudes of the strongest CF-EPSC (black) and of the weak CF-EPSC (grey) plotted over time, before and after NBQX (20 µM) and D-APV (50 µM) applications.

PF-EPSCs display no NMDA component

Parallel fibers mediated EPSCs (PF-EPSCs) elicited by 0.33 Hz extracellular stimulation in the molecular layer were identified by their graded amplitude increasing with stimulusintensity, and by their characteristic paired pulse facilitation following 30 ms-interval paired stimulations (Konnerth et al., 1990) (Fig.6A). PF-EPSCs were fully abolished by 20 µM NBQX in the bath (n=5, Fig.6B). Thus, PF-EPSCs display no detectable NMDA component.

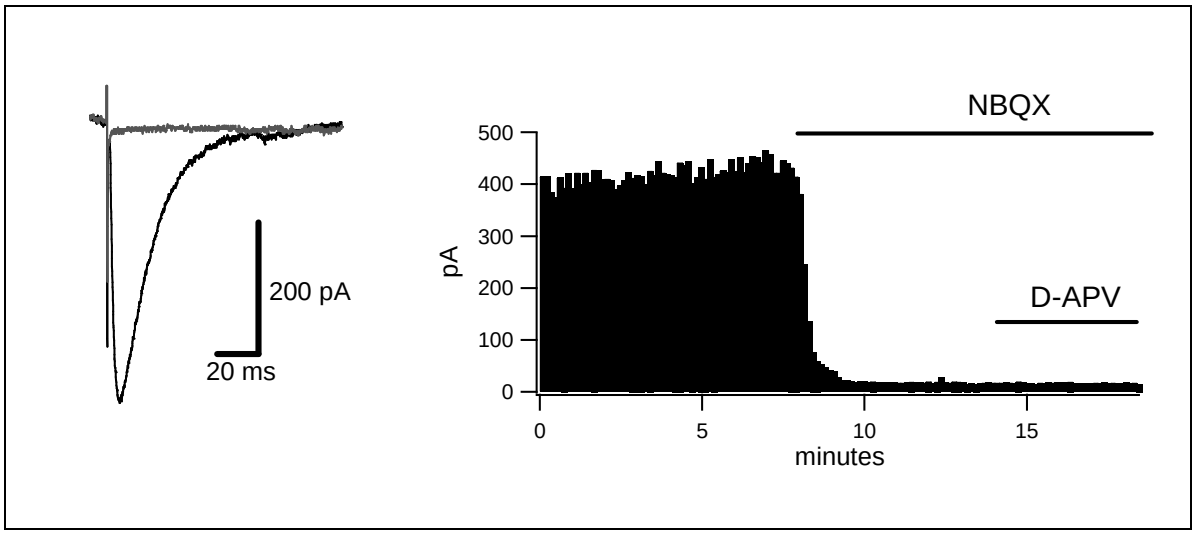

Fig.6. PFs-EPSCs display no NMDA component in Purkinje cells of adult Ho-Nancy mouse. Representative experiment performed on a Ho-Nancy Purkinje cell recorded in absence of Mg^{2+}. The left panel shows superimposed averaged PF-EPSCs recorded before (black trace) and during (grey trace) the application of NBQX (20 µM). On the right panel, amplitudes of the PF-EPSCs are plotted over time before and during the application of NBQX (20 µM). Additional application of D-APV (50 µM) has been tested at the end of the recording.

No NMDA component in CF-EPSCs at P15-P17

In our previous study (Piochon et al., 2007), we demonstrated that NMDA-Rs participate to the CF-EPSC from P21. Before this age, the NMDA-mediated CF-EPSC is not detectable, as shown by many studies performed between P14 and P21 that did not detect NMDA currents in rodent Purkinje cells (Llano et al., 1991). However, at this age, GluRdelta2s are highly expressed in Purkinje cells and are present at high levels at CF-Purkinje cells synapses Fig.1, (Zhao et al., 1997, Zhao, 1998 #3564). If GluRdelta2s are present transiently at these synapses to impede NMDA-Rs expression, an earlier expression of NMDA-Rs could thus be allowed by the absence of GluRdelta2 in Ho-Nancy Purkinje cells. In Ho-Nancy mice aged between P15 and P17, we tested the participation of NMDA-Rs in CF-EPSCs. The presence of NBQX (20 µM) completely abolished CF-EPSCs (n=8, data not shown). Purkinje cells of

Ho-Nancy animals thus display the same temporal patterned expression than the one observed in wild-type animals for NMDA-Rs.

Discussion

In Purkinje cells of wild-type mouse older than 3 weeks, while GluRdelta2s are inherent to PFs synapses, NMDA-Rs exclusively participate to the CF synaptic response. The aim of this study was first to determine the spatial and temporal pattern of expression of NMDA-Rs in Purkinje cells of the Ho-Nancy mutant mouse that lack GluRdelta2s (Lalouette et al., 2001) to test the possibility of a reciprocal exclusion of these receptors at glutamatergic synapses. Second, because Ho-Nancy Purkinje cells display an abnormally sustained innervation by multiple CFs, it was also interesting to test the expression of NMDA-Rs at supernumerary CF synapses. As well as in their wild-type couterparts, we observed that Ho-Nancy Purkinje cells of mature mice express functional NMDA-Rs that mediate a part of the CF-EPSC. Before P21, these NMDA-Rs are absent from CF-EPSCs displaying thus the same temporal pattern of expression as observed in wild-type Purkinje cells. In accordance with the fast kinetics of the NMDA currents detected in the CF-EPSC, immunolabelings show that Ho-Nancy NMDA-Rs are composed of NR2A/B subunits but not NR2D. The NR2A/B labeling follows the aberrant CFs innervating territory on Ho-Nancy Purkinje cells dendrites and is thus more distally extended in the molecular layer than in wild-type animals. Yet, in Ho-Nancy Purkinje cells, NMDA-currents are still absent from PF-EPSCs. Our initial hypothesis of a competitive relationship between NMDA and GluRdelta2 receptors is thus unlikely, because in absence of GluRdelta2, neither the persistence of juvenile NMDA-Rs, nor an abnormal temporal and spatial expression of mature NMDA-Rs are observed in Ho-Nancy animals. Interestingly the contribution of NMDA-Rs is not detectable in the supernumerary atypical CF-EPSCs suggesting that the NMDA-Rs expression at CF synapses could be selective of the dominant CF, in a manner that is independent of the GluRdelta2 expression. Another interesting observation of the present study is that Ho-Nancy Purkinje cells remain more strongly multi-innervated by CFs than previously estimated, and than in other types of GluRdelta2 mutants, showing that GluRdelta2 is clearly not dispensable for the redundant CFs regression.

GluRdelta2 and NMDA are unlikely to compete for their synaptic localization

The persistence of NMDA-Rs composed of the juvenile NR2D subunit has been reported in Purkinje cells of the adult mutant mouse *staggerer* that notably keeps immature features like the CF multi-afferentation (Mariani and Changeux, 1980; Dupont et al., 1984; Nakagawa et al., 1996). In our experiments on adult Ho-Nancy mouse, NMDA-Rs that participate to the CF-EPSC display rapid kinetics, which does not fit with NMDA-Rs containing the NR2D

subunits especially because of the characteristic low desensitization of these receptors (Misra et al., 2000). NMDA currents observed here are unlikely to be mediated by NMDA-Rs containing the neonatal NR2D subunit. On the other hand, NR2D NMDA-Rs do not participate to CF-EPSC even in immature wild-type animals. Furthermore our immunolabelings performed with antibody directed against the NR2D subunit did not revealvthese subunits in Purkinje cells of mature Ho-Nancy. Finally, although Ho-Nancy Purkinje cells can be as considered immature because they conserved the postnatal CFs multi-innervation, it is thus unlikely that they have conserved the expression of neonatal NMDA-Rs. In mature Ho-Nancy animals, the regression of neonatal NMDA-Rs seems thus complete, as observed in wild-type animals (Momiyama et al., 1996). The absence of GluRdelta2 seems without consequence on the down regulation of neonatal NR2D expression, suggesting that mechanisms regulating the expression of both these glutamatergic receptors are independent.

From the second until the third postnatal week, any NR2 subunit is detected in Purkinje cells of wild-type mouse. NR1 being the sole NMDA-R subunit expressed in Purkinje cells (Hafidi and Hillman, 1997), this probably explains the absence of NMDA currents immutably observed at this age (Konnerth et al., 1990; Farrant and Cull-Candy, 1991; Llano et al., 1991; Piochon et al., 2007). During this period, GluRdelta2 are highly expressed at both CFs and PFs synapses (Zhao et al., 1998). However, the GluRdelta2 peak of expression is probably not responsible for the transient absence of NMDA-Rs since in Ho-Nancy Purkinje cells, we also observed the lack of NMDA-Rs-mediated currents before P21.

As in wild-type mouse, NMDA-Rs do not participate to the PF-EPSC in Ho-Nancy Purkinje cells. Thus, GluRdelta2s are unlikely to be involved in the absence of NMDA currents at PF synapses. At synapses with PFs, Purkinje cells express various proteins containing PDZ domains. For instance, PSD-93, PTPMEG, S-SCAM or Shank1-2 that have been shown to bind to GluRdelta2 (Roche et al., 1999; Hironaka et al., 2000; Yap et al., 2003; Uemura et al., 2004) are also known to interact with NMDA-Rs (Hirao et al., 1998; Naisbitt et al., 1999). In Ho-Nancy Purkinje cells, because of the absence of GluRdelta2, these proteins could be available to interact with NMDA-Rs. Yet, another mechanism must hamper either the addressing, the expression or the functionality of NMDA-Rs at PFs synapses.

The repression of GluRdelta2 expression at CF spines results from CF activity (Cesa et al., 2003). Similarly, one can also speculate that the expression of NMDA-Rs is specifically down-regulated by the PF activity. The disparition of juvenile NMDA-Rs concomitantly with the establishment of PFs contacts supports this hypothesis. Because Hotfoot Purkinje cells

bear many naked spines that do not receive presynaptic terminals, it could be interesting to investigate by electronic microscopy the presence of NMDA-Rs at these inactive spines. Our immunolabellings show the presence of NMDA-Rs in distal dendrites of Purkinje cells but the resolution does not allow to set out this question.

Although our results indicate that NMDA-Rs are unlikely to compete with GluRdelta2 at PF synapses, we can not exclude that, inversely, GluRdelta2 can in some cases compete with NMDA-Rs at CF synapses, in mature animals. When CF activity is blocked by TTX, or when a 3-acetylpyridine (3-AP)-induced subtotal lesion of inferior olivary neurons is performed, GluRdelta2s invade former CF synapses (Cesa et al., 2003). Interestingly, Billard and Pumain (1999) have shown that NMDA responses are strongly depressed when PCs are deafferented from their climbing fibers, after 3-AP treatment. The corollary would be the expression of GluRdelta2s at CFs in Purkinje cells lacking NMDA-Rs. This remains to be tested.

NMDA-mediated CF-EPSCs are detected only in the strongest-CF response

Although Ho-Nancy Purkinje cells are innervated by multiple CFs, we show here that NMDA-Rs participate to the largest CF-EPSC from P21, with the same timing and in a proportion similar to the one we described previously in wild-type mouse. Therefore, the absence of GluRdelta2 does not affect this aspect of the late maturation of the strongest CF. In GluRdelta2 mutant mice, Purkinje cells are known to be multiply innervated by CFs. In this study, we estimated that the large majority of Ho-Nancy Purkinje cells are multi-innervated, in contrary to the previous characterization of this mutant mouse (Lalouette et al., 2001), and in contrary to most of studies on other GluRdelta2 mutants. In Ho-Nancy the deletion does not only include, but is even far larger than the one present in genetically engineered GluRdelta2-/- knockout mice (Kashiwabuchi et al., 1995b). This difference could explain the discrepancy between our and some other results. In some studies, to ensure a better voltage-clamp, Purkinje cells are recorded at more depolarized potential, i.e. -20 mV. In this case, the driving force is rather lower, rendering small CF-EPSCs less detectable. This difference of experimental procedure can also bring divergences between studies. In any case, GluRdelta2 is essential to restrict CF innervation to the proximal dendrites of Purkinje cell. Without GluRdelta2, the CF territory expands along and beyond dendritic arborization of the Purkinje cells, causing persistent multiple CF innervation (Ichikawa et al., 2002).

In both Ho-Nancy and wild-type mice, CF stimulation elicits a typical EPSC with a fast rise time, a large amplitude, and a NMDA-mediated component. In addition to this main response, most Ho-Nancy Purkinje cells display additional steps of atypical CF-EPSCs with a

slow rise time and a small amplitude, as observed in studies on the GluRdelta2 knock-out mouse (Hashimoto et al., 2001; Ichikawa et al., 2002). Interestingly, these atypical CF-EPSCs do not bear a detectable NMDA component. Therefore, a mechanism that is independent of GluRdelta2 could exist in Purkinje cells to target NMDA-Rs at strongest CF synapses, and/or to exclude NMDA-Rs from atypical CF synapses. Importantly, it has been shown that the activation of the main CF induces the spread of voltage-dependent Ca^{2+} signals all over the dendritic tree in both GluRdelta2 mutant and wild-type mice, whereas that of atypical CFs in the knock-out mouse elicits local Ca^{2+} signals confined to small distal regions of the dendritic tree (Hashimoto et al., 2001). It is thus tempting to propose a role of NMDA-Rs in the spread of Ca^{2+} signals associated to the stimulation of the main CF.

References

Alvarez VA, Ridenour DA, Sabatini BL (2007) Distinct structural and ionotropic roles of NMDA receptors in controlling spine and synapse stability. J Neurosci 27:7365-7376.

Araki K, Meguro H, Kushiya E, Takayama C, Inoue Y, Mishina M (1993) Selective expression of the glutamate receptor channel delta 2 subunit in cerebellar Purkinje cells. Biochem Biophys Res Commun 197:1267-1276.

Billard JM, Pumain R (1989) Loss of N-methyl-D-aspartate sensitivity of cerebellar Purkinje cells after climbing fiber deafferentation. An in vivo study in the rat. Neurosci Lett 106:199-204.

Bosman LW, Takechi H, Hartmann J, Eilers J, Konnerth A (2008) Homosynaptic long-term synaptic potentiation of the "winner" climbing fiber synapse in developing Purkinje cells. J Neurosci 28:798-807.

Bravin M, Morando L, Vercelli A, Rossi F, Strata P (1999) Control of spine formation by electrical activity in the adult rat cerebellum. Proc Natl Acad Sci U S A 96:1704-1709.

Cesa R, Morando L, Strata P (2003) Glutamate receptor delta2 subunit in activity-dependent heterologous synaptic competition. J Neurosci 23:2363-2370.

Crepel (1982) Regression of functionnal synapses in the immature mammalian cerebellum. Trends in Neurosciences 5:266-269.

Crepel F (1971) Maturation of climbing fiber responses in the rat. Brain Res 35:272-276.

Dupont JL, Fournier E, Gardette R, Crepel F (1984) Effect of excitatory amino acids on Purkinje cell dendrites in cerebellar slices from normal and staggerer mice. Neuroscience 12:613-619.

Elias GM, Nicoll RA (2007) Synaptic trafficking of glutamate receptors by MAGUK scaffolding proteins. Trends Cell Biol 17:343-352.

Farrant M, Cull-Candy SG (1991) Excitatory amino acid receptor-channels in Purkinje cells in thin cerebellar slices. Proc R Soc Lond B Biol Sci 244:179-184.

Gounko NV, Gramsbergen A, van der Want JJ (2007) The glutamate receptor delta 2 in relation to cerebellar development and plasticity. Neurosci Biobehav Rev 31:1095-1100.

Guastavino JM, Sotelo C, Damez-Kinselle I (1990) Hot-foot murine mutation: behavioral effects and neuroanatomical alterations. Brain Res 523:199-210.

Hafidi A, Hillman DE (1997) Distribution of glutamate receptors GluR 2/3 and NR1 in the developing rat cerebellum. Neuroscience 81:427-436.

Hashimoto K, Kano M (2003) Functional differentiation of multiple climbing fiber inputs during synapse elimination in the developing cerebellum. Neuron 38:785-796.

Hashimoto K, Ichikawa R, Takechi H, Inoue Y, Aiba A, Sakimura K, Mishina M, Hashikawa T, Konnerth A, Watanabe M, Kano M (2001) Roles of glutamate receptor delta 2 subunit (GluRdelta 2) and metabotropic glutamate receptor subtype 1 (mGluR1) in climbing fiber synapse elimination during postnatal cerebellar development. J Neurosci 21:9701-9712.

Hirai H (2001) Ca2+-dependent regulation of synaptic delta2 glutamate receptor density in cultured rat Purkinje neurons. Eur J Neurosci 14:73-82.

Hirai H, Miyazaki T, Kakegawa W, Matsuda S, Mishina M, Watanabe M, Yuzaki M (2005) Rescue of abnormal phenotypes of the delta2 glutamate receptor-null mice by mutant delta2 transgenes. EMBO Rep 6:90-95.

Hirai H, Launey T, Mikawa S, Torashima T, Yanagihara D, Kasaura T, Miyamoto A, Yuzaki M (2003) New role of delta2-glutamate receptors in AMPA receptor trafficking and cerebellar function. Nat Neurosci 6:869-876.

Hirao K, Hata Y, Ide N, Takeuchi M, Irie M, Yao I, Deguchi M, Toyoda A, Sudhof TC, Takai Y (1998) A novel multiple PDZ domain-containing molecule interacting with N-methyl-D-aspartate receptors and neuronal cell adhesion proteins. J Biol Chem 273:21105-21110.

Hironaka K, Umemori H, Tezuka T, Mishina M, Yamamoto T (2000) The protein-tyrosine phosphatase PTPMEG interacts with glutamate receptor delta 2 and epsilon subunits. J Biol Chem 275:16167-16173.

Ichikawa R, Miyazaki T, Kano M, Hashikawa T, Tatsumi H, Sakimura K, Mishina M, Inoue Y, Watanabe M (2002) Distal extension of climbing fiber territory and multiple innervation caused by aberrant wiring to adjacent spiny branchlets in cerebellar Purkinje cells lacking glutamate receptor delta 2. J Neurosci 22:8487-8503.

Kakegawa W, Kohda K, Yuzaki M (2007a) The delta2 'ionotropic' glutamate receptor functions as a non-ionotropic receptor to control cerebellar synaptic plasticity. J Physiol 584:89-96.

Kakegawa W, Miyazaki T, Hirai H, Motohashi J, Mishina M, Watanabe M, Yuzaki M (2007b) Ca2+ permeability of the channel pore is not essential for the delta2 glutamate receptor to regulate synaptic plasticity and motor coordination. J Physiol 579:729-735.

Kashiwabuchi N, Ikeda K, Araki K, Hirano T, Shibuki K, Takayama C, Inoue Y, Kutsuwada T, Yagi T, Kang Y, et al. (1995a) Impairment of motor coordination, Purkinje cell synapse formation, and cerebellar long-term depression in GluR delta 2 mutant mice. Cell 81:245-252.

Kashiwabuchi N, Ikeda K, Araki K, Hirano T, Shibuki K, Takayama C, Inoue Y, Kutsuwada T, Yagi T, Kang Y, Aizawa S, Mishina M (1995b) Impairement of motor coordination, Purkinje cell synapses formation, and cerebellar long-term depression in GluR-delta-2 mutant mice. Cell 81:245-252.

Kohda K, Kakegawa W, Matsuda S, Nakagami R, Kakiya N, Yuzaki M (2007) The extreme C-terminus of GluRdelta2 is essential for induction of long-term depression in cerebellar slices. Eur J Neurosci 25:1357-1362.

Konnerth A, Llano I, Armstrong CM (1990) Synaptic currents in cerebellar Purkinje cells. Proc Natl Acad Sci U S A 87:2662-2665.

Kurihara H, Hashimoto K, Kano M, Takayama C, Sakimura K, Mishina M, Inoue Y, Watanabe M (1997) Impaired parallel fiber-->Purkinje cell synapse stabilization during cerebellar development of mutant mice lacking the glutamate receptor delta2 subunit. J Neurosci 17:9613-9623.

Lalouette A, Guenet JL, Vriz S (1998) Hotfoot mouse mutations affect the delta 2 glutamate receptor gene and are allelic to lurcher. Genomics 50:9-13.

Lalouette A, Lohof A, Sotelo C, Guenet J, Mariani J (2001) Neurobiological effects of a null mutation depend on genetic context: comparison between two hotfoot alleles of the delta-2 ionotropic glutamate receptor. Neuroscience 105:443-455.

Landsend AS, Amiry-Moghaddam M, Matsubara A, Bergersen L, Usami S, Wenthold RJ, Ottersen OP (1997) Differential localization of delta glutamate receptors in the rat cerebellum: coexpression with AMPA receptors in parallel fiber-spine synapses and absence from climbing fiber-spine synapses. J Neurosci 17:834-842.

Li Y, Erzurumlu RS, Chen C, Jhaveri S, Tonegawa S (1994) Whisker-related neuronal patterns fail to develop in the trigeminal brainstem nuclei of NMDAR1 knockout mice. Cell 76:427-437.

Llano I, Marty A, Armstrong CM, Konnerth A (1991) Synaptic-and agonist-induced excitatory currents of Purkinje cells in rat cerebellar slices. Journal of Physiology (London) 434:183-213.

Lomeli H, Sprengel R, Laurie DJ, Kohr G, Herb A, Seeburg PH, Wisden W (1993) The rat delta-1 and delta-2 subunits extend the excitatory amino acid receptor family. FEBS Lett 315:318-322.

Mandolesi G, Cesa R, Autuori E, Strata P (2008) An orphan ionotropic glutamate receptor: The delta2 subunit. Neuroscience.

Mariani J, Changeux JP (1980) Multiple innervation of Purkinje cells by climbing fibers in the cerebellum of the adult staggerer mutant mouse. J Neurobiol 11:41-50.

Misra C, Brickley SG, Wyllie DJ, Cull-Candy SG (2000) Slow deactivation kinetics of NMDA receptors containing NR1 and NR2D subunits in rat cerebellar Purkinje cells. J Physiol 525 Pt 2:299-305.

Miyazaki T, Hashimoto K, Shin HS, Kano M, Watanabe M (2004) P/Q-type Ca2+ channel alpha1A regulates synaptic competition on developing cerebellar Purkinje cells. J Neurosci 24:1734-1743.

Momiyama A, Feldmeyer D, Cull-Candy SG (1996) Identification of a native low-conductance NMDA channel with reduced sensitivity to Mg2+ in rat central neurones. J Physiol 494 (Pt 2):479-492.

Morando L, Cesa R, Rasetti R, Harvey R, Strata P (2001) Role of glutamate delta -2 receptors in activity-dependent competition between heterologous afferent fibers. Proc Natl Acad Sci U S A 98:9954-9959.

Motohashi J, Kakegawa W, Yuzaki M (2007) Ho15J: a new hotfoot allele in a hot spot in the gene encoding the delta2 glutamate receptor. Brain Res 1140:153-160.

Nagerl UV, Eberhorn N, Cambridge SB, Bonhoeffer T (2004) Bidirectional activity-dependent morphological plasticity in hippocampal neurons. Neuron 44:759-767.

Naisbitt S, Kim E, Tu JC, Xiao B, Sala C, Valtschanoff J, Weinberg RJ, Worley PF, Sheng M (1999) Shank, a novel family of postsynaptic density proteins that binds to the NMDA receptor/PSD-95/GKAP complex and cortactin. Neuron 23:569-582.

Nakagawa S, Watanabe M, Inoue Y (1996) Altered gene expression of the N-methyl-D-aspartate receptor channel subunits in Purkinje cells of the staggerer mutant mouse. Eur J Neurosci 8:2644-2651.

Piochon C, Irinopoulou T, Brusciano D, Bailly Y, Mariani J, Levenes C (2007) NMDA receptor contribution to the climbing fiber response in the adult mouse Purkinje cell. J Neurosci 27:10797-10809.

Renzi M, Farrant M, Cull-Candy SG (2007) Climbing-fibre activation of NMDA receptors in Purkinje cells of adult mice. J Physiol 585:91-101.

Roche KW, Ly CD, Petralia RS, Wang YX, McGee AW, Bredt DS, Wenthold RJ (1999) Postsynaptic density-93 interacts with the delta2 glutamate receptor subunit at parallel fiber synapses. J Neurosci 19:3926-3934.

Uemura T, Mori H, Mishina M (2004) Direct interaction of GluRdelta2 with Shank scaffold proteins in cerebellar Purkinje cells. Mol Cell Neurosci 26:330-341.

Uemura T, Kakizawa S, Yamasaki M, Sakimura K, Watanabe M, Iino M, Mishina M (2007) Regulation of long-term depression and climbing fiber territory by glutamate receptor delta2 at parallel fiber synapses through its C-terminal domain in cerebellar Purkinje cells. J Neurosci 27:12096-12108.

Yamazaki M, Araki K, Shibata A, Mishina M (1992a) Molecular cloning of a cDNA encoding a novel member of the mouse glutamate receptor channel family. Biochem Biophys Res Commun 183:886-892.

Yamazaki M, Araki K, Shibata A, Mishina M (1992b) Molecular cloning of a cDNA encoding a novel member of the mouse glutamate receptor channel family. Biochem Biophys Res Commun 183:886-892.

Yap CC, Muto Y, Kishida H, Hashikawa T, Yano R (2003) PKC regulates the delta2 glutamate receptor interaction with S-SCAM/MAGI-2 protein. Biochem Biophys Res Commun 301:1122-1128.

Zhao HM, Wenthold RJ, Petralia RS (1998) Glutamate receptor targeting to synaptic populations on Purkinje cells is developmentally regulated. J Neurosci 18:5517-5528.

Zhao HM, Wenthold RJ, Wang YX, Petralia RS (1997) Delta-glutamate receptors are differentially distributed at parallel and climbing fiber synapses on Purkinje cells. J Neurochem 68:1041-1052.

3.3.3 Discussion in the context of the present thesis

The aim of this study of NMDA-Rs in Ho-Nancy Purkinje cell was to test the possibility of a competition between GluRdelta2 and NMDA-Rs. This hypothesis was mainly considered in respect to their sequence homology, their common anchors, and their spatio-temporal expression profiles. If this hypothesis of a competition has been true, the spatio-temporal profile of NMDA-Rs would have been disturbed in Ho-Nancy Purkinje cells lacking GluRdelta2. However, our results showing no abnormal distribution of NMDA-Rs in Ho-Nancy Purkinje cells are not in favor of this initial hypothesis of an interaction between GluRdelta2 and NMDA-receptors.

We have shown in our previous study that NMDA-Rs participate to the CF synaptic transmission in wild-type Purkinje cells. In addition to the diverse possible functions already proposed for NMDA-Rs in Purkinje cells (in particular in the synaptic plasticity, see II.2.3), another role could be their involvement in synapses stabilization. For example, NMDA-R could underlie the stabilization of CF spines and synapses, as it has been demonstrated at hippocampal pyramidal neurons (Alvarez et al., 2007). In these neurons, the formation or the retraction of spines is NMDA-Rs-dependent, and depend on the frequency of stimulation (Nagerl et al., 2004). Such mechanisms could also underlie the stabilization of the strongest CF during the development. We assumed that CF-evoked Ca^{2+} influx to a PC through NMDA-Rs may consolidate coactivated CF synapses, whereas it may "punish" other excitatory synapses unrelated to the Ca^{2+} influx. This proposed mechanism is similar to the NMDA receptor-dependent synapse refinement in the visual and somatosensory systems, in which NMDA-Rs are thought to function as a coincidence detector that introduces Ca^{2+} influx in an activity-dependent manner. It is thought that the Ca^{2+} influx through NMDA-Rs strengthens synapses with correlated activities, whereas it weakens those with uncorrelated activities, through which immature redundant connections are refined into functionally mature ones (Li et al., 1994).

In wild-type Purkinje cell, during the first postnatal week, a stronger CF emerges from the multiple CFs by a LTP process recently evidenced (Hashimoto and Kano, 2003; Bosman et al., 2008). A mechanism of regression that depends on the GluRdelta2 (Cesa et al., 2003), and on the CF activity (Bravin et al., 1999), must occur thereafter to eliminate supernumerary weak-CFs synapses, while another mechanism, maybe NMDA-dependent, could stabilize

synapses with the strongest CF. Because adult Ho-Nancy Purkinje cells have been shown to be innervated by multiple CFs, it was thus interesting to test the participation of NMDA-R to the supernumerary CF-EPSCs, in order to investigate its eventual participation in the stabilization of these supernumerary synapses.

Interestingly, we observed a significant NMDA-Rs participation only to the synaptic currents of the strongest CF, whereas no NMDA currents were detectable in weak CF synaptic responses. How can we interpret this result? Actually, it remains difficult to draw definitive conclusions. Indeed, either NMDA-Rs participate only to the strongest CF response, either they also mediate an undetectable part of the weak-CFs responses. NMDA-Rs mediate 5 to 10% of the total CF synaptic current in wild-type Purkinje cells (Piochon et al., 2007). If these receptors are present in the same proportion in weak CFs, their possible NMDA component is thus hardly detectable in our conditions. Our immunolabelings do not unable us to distinguish a separate localization of NMDA-Rs at weak- or strong-CF synapses. If their presence at weak-CF synapses was verified, this could indicate that NMDA-Rs are involved in the maintenance and stabilization of all CF synapses, whatever the strength of the afferent CF. In the other case, i.e. if NMDA-Rs are selectively expressed at synapses with the strongest CF, one can speculate that these receptors play a role in the stabilization of the "winner" CF synapses. Interestingly, it has been shown recently in GluRdelta2 null mutant mouse, that spreads of calcium are observed only for stimulation of the strongest CF (Hashimoto et al., 2001). Thus it is tempting to make a link between this differential calcium signaling of the strongest CF responses, and the presence a calcium-permeable NMDA-Rs at these very synapses. P/Q type Ca^{2+} channels are high voltage-activated VGCCs, that can be activated by relatively strong depolarization such as that caused by CF activity. At the time when NMDA-Rs expression was still ignored in CF-Purkinje cells synapses, VGCCs have been already proposed to substitute to NMDA-Rs, and it has been demonstrated that they play an important role in the elimination of surplus CF innervation and territory regulation (Miyazaki et al., 2004). One can not exclude that NMDA-Rs act in synergy with VGCCs in this process. However, this remains to be studied.

As a complement of this study, we are now generating a transgenic mouse lacking NMDA-Rs specifically in Purkinje cells (see general conclusion of this thesis). If NMDA-Rs are indeed involved in the stabilization and/or the selection of CF synapses, thus impairments of the Purkinje cells innervation by CF(s) are expected to occur in this mutant mouse.

3.4 Results in progress:

NMDA receptor involvement in bidirectional plasticity of parallel fiber to Purkinje cells synapses

"I have not failed. I've just found 10,000 ways that don't work."

Thomas A. Edison

3.4.1 Introduction

3.4.1.1 An "inverse" BCM rule in PF-Purkinje cell synaptic plasticity

In hippocampal and neocortical pyramidal neurons, and in cells of various regions of the brain, LTP and LTD can be induced at the same synapse. This bidirectional plasticity depends on the amplitude of postsynaptic calcium signal, LTP being induced for high threshold of calcium, and LTD depending on lower calcium level (Figure 3.4A). This model, well known as the BCM (Bienenstock-Cooper-Munroe) rule, was first a mathematical theory (Bienenstock et al., 1982). Soon, (Bear et al., 1987) and (Lisman, 1989) completed the model by proposing that the postsynaptic Ca^{2+} level, arising in particular from NMDA-Rs and interacting for instance with calmodulin-dependent protein kinase II, could control the bidirectional synaptic plasticity. This was later verified experimentally in pyramidal neurons of the hippocampus (Cummings et al., 1996) and of the visual cortex (Hansel et al., 1997). As usual, Purkinje cells do not follow the general rules, and synaptic plasticity proceeds there in an inverse BCM rule, that has been evidenced rather recently (Figure 3.4A, Coesmans et al., 2004). Which calcium rule governs the bidirectional plasticity in PF-Purkinje cell synapses?

The LTD occurring at PF-Purkinje cell synapse has been extensively investigated since its importance given by the Marr-Albus-Ito model. It can be induced by paired stimulations of PF and CF at low frequencies, ∼1 Hz (Ito et al., 1982). The CF is believed to contribute to the PF-LTD induction by enabling a strong Ca^{2+} influx through voltage gated channels during the complex spike, but coincident stimulation of PF and CF boosts the amplitude of the Ca^{2+} transients in spines supralinearly (Wang et al., 2000). The glutamate released by PFs activates

AMPA and mGluR1 receptors. These signals converge to activate protein kinase C (PKC), which in turn phosphorylates receptors and proteins of the postsynaptic density, resulting in AMPA-Rs inactivation. The activation of alphaCaMKII by Ca^{2+} influx is also essential to induce PF-LTD (Hansel et al., 2006), while the inhibition of protein phosphatases is facilitating (Ajima and Ito, 1995). NO, by activating the soluble guanylate cyclase, plays also a role in this PF-LTD induction (Levenes et al., 1998; Ito, 2001).

PF-Purkinje cells synapses also have the possibility to be potentiated. In addition to various LTP that have been evidenced presynaptically (Salin et al., 1996; Linden and Ahn, 1999; Qiu and Knopfel, 2007), a true inverse postsynaptic LTD has been characterized. This postsynaptic LTP can be induced by the PF stimulation at low frequency (1 Hz) without CF stimulation. This LTP depends on NO, but is independent of cGMP. It requires low postsynaptic Ca^{2+} level and is PKC-independent. The inhibition of protein phosphatases blocks the PF-LTP induction (Lev-Ram et al., 2002; Lev-Ram et al., 2003; Coesmans et al., 2004; Belmeguenai and Hansel, 2005).

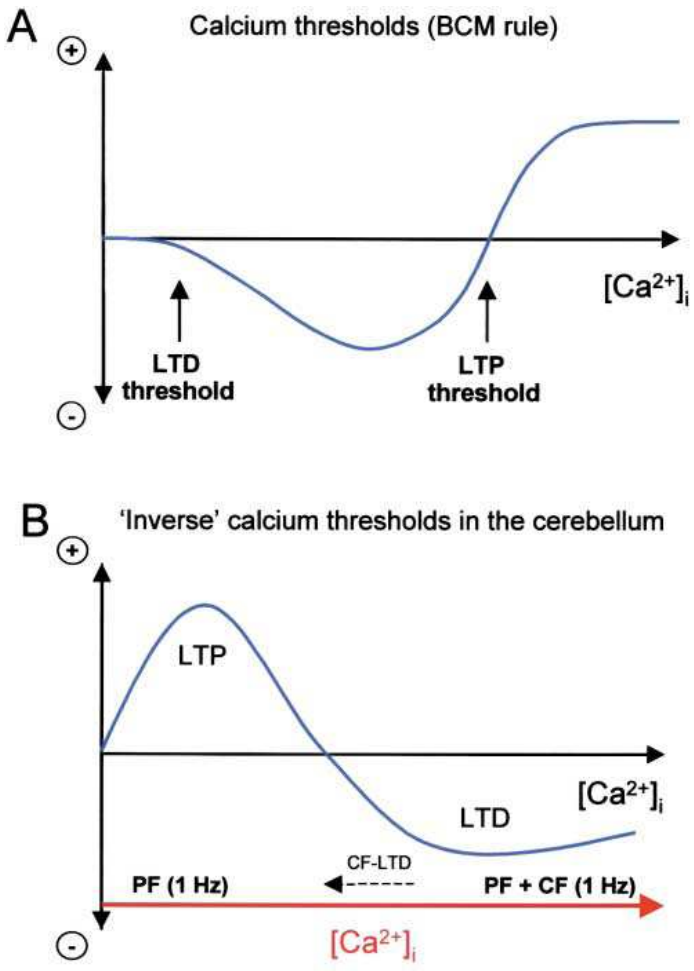

Figure 3.4: Calcium threshold models for LTP and LTD induction

(A) At excitatory inputs to cortical pyramidal cells, there is a higher calcium threshold amplitude for LTP than for LTD induction (BCM rule).
(B) As demonstrated in (Coesmans et al., 2004), bidirectional PF plasticity is governed by a calcium threshold mechanism inverse to the one illustrated in (A). PF-LTD has a higher calcium threshold than LTP. CF activity provides sufficient calcium to increase substantially the probability that the LTD threshold is reached. CF-LTD lowers this probability.

(from Coesmans et al., 2004, Neuron 44:691-700).

3.4.1.2 Bidirectional PF plasticity is under CF control

In the switch of the PF synaptic plasticity to LTD or LTP, Coesman et al. (2004) have showed that the internal Ca^{2+} level is determinant: PF-LTD requires higher calcium than PF-LTP. Moreover, they suggested that the CF activity, by providing Ca^{2+} transients, is responsible for this switch. Supporting this hypothesis, they demonstrated that the previous CF-LTD induction, which is accompanied by a reduction of complex spike-evoked calcium transients (Weber et al., 2003), decreases the probability to induce subsequent PF-LTD (Coesmans et al., 2004); see Figure 3.4.

As we showed in our previous study, NMDA-Rs contribute to the complex spike (Piochon et al., 2007) in which they are able to modulate the series of smaller spikes that are known to be partly produced by dendritic Ca^{2+} influx (Llinas and Sugimori, 1980a; Llinas and Sugimori, 1980b). This observation prompted us to study the involvement of NMDA-Rs in the induction of PF-LTD. Our present objective is to test the effect of NMDA-R blockade on PF-LTD induction, using whole-cell patch-clamp recordings in our *in vitro* slice preparation of adult mouse cerebellum.

3.4.2 Preliminary results

3.4.2.1 A matter of protocol

Actually, many protocols have been described to induce PF-LTD, but they were usually used in young animals. Beforehand, we had thus to determine the most reliable protocol inducing PF-LTD in Purkinje cells of *adult mice*.

In P18-P27 rat cerebellar slices, a possible PF-LTD protocol consists in paired PF and CF stimulation at 1 Hz for 5 min (300 pulses) in presence of GABA-A antagonist (Karachot et al., 1994; Coesmans et al., 2004). In control conditions, this protocol has been shown to induce a depression of PF-EPSC amplitude amounted to ∼80% of baseline. To our knowledge, this protocol is the only one to have been tested in adult mice Purkinje cells, where it gives rise to a robust LTD, although its onset has been reported to be slower in adult than in juvenile animals (Hansel et al., 2006). Thus, we first tested this protocol in adult mouse Purkinje cells. Although we tried to rigorously reproduce the experimental conditions described in Coesmans et al. (2004) and Hansel et al. (2006), this protocol was not so efficient

in our hands to induce PF-LTD in adult mouse Purkinje cells. Indeed, on the 16 Purkinje cells tested, it induced PF-LTD in only half of them (data not shown).

In P17-P25 rat, it has been demonstrated that LTD induction is greatest when PF activation precedes the CF activation within 50−200 ms (Wang et al., 2000). In this timing rule, which matches the properties of several forms of motor learning, conjunctive activation of PF and CF generates Ca^{2+} signals in spines and dendrites that greatly exceed the linear sum of responses to the individual inputs. This supralinearity would be mediated by enhanced Ca^{2+} release from the endoplasmic reticulum and occurs only when the bursts of PF stimuli precede the CF stimulation (Wang et al., 2000). Recently, examination of the timing dependence between PF and CF activity has confirmed that LTD-peak occurs when PF activity precedes CF activity by 50–150 ms (Safo and Regehr, 2008). In our search for a reliable protocol, we thus decided to test this protocol, consisting of a train of 5 to 8 PF stimuli evoked at 100 Hz, followed by the CF stimulation 50 to 150 ms later (Figure 3.5A). This pairing was delivered at 1 Hz during 5 minutes, in current clamp mode, in the continued presence of bicuculline (20 µM) in the bath. This protocol showed better efficiency to induce PF-LTD in adult mouse Purkinje cells: 17 cells on the 20 one tested displayed PF-LTD after this protocol (Figure 3.5B); the 3 others display no significant change. Thirty five minutes after the protocol PF-EPSCs averaged 49.9 ± 4 % of their baseline amplitude (n=9). We thus adopted this method for the rest of the study.

3.4.2.2 The bidirectional plasticity depends on the CF stimulation in our LTD protocol

In two cells tested, we observed that in the absence of CF stimulation the sole stimulation of PFs by train of 5 to 8 stimuli at 1 Hz can induce a PF-LTP (Figure 3.5C). Although this experiment needs to be repeated to be statistically significant, these results suggests that the bidirectional plasticity is also verified with our protocol, and would also depend on the CF activity, as demonstrated by Coesmans et al. (2004). Moreover, on one cell tested, we observed that our LTD protocol failed to induce PF-LTD in presence of 10 mM of the Ca2+ chelator EGTA in the internal medium (actually this protocol induced a slight LTP, data not shown). Thus, these results suggest that in adult mouse Purkinje cells, the bidirectional PF long-term plasticity is governed by the Ca^{2+} entry that is mediated by the CF response, as already demonstrated in young rat Purkinje cells (Coesmans et al., 2004). We then wondered if NMDA-Rs, by modulating the complex spike, are involved in the PF-LTD induction.

3.4.2.3 D-APV prevents the PF-LTD

On 2 cells recorded in presence of D-APV (50 µM) in the bath, we applied the PF-LTD protocol. Instead of the expected PF-LTD, this produced a PF-LTP in one cell whereas no lasting change of the PF-EPSC amplitudes was recorded in the other. This indicative result confirms a possible role of NMDA-Rs somewhere in the network involved in the PF-LTD induction. By reason of the suspected presence of NMDA-Rs on presynaptic PF terminals (Casado et al., 2002), we however decided to focus on experiments using MK801 in the internal medium.

3.4.2.4 Internal MK801 prevents the PF-LTD

As we showed in our previous study, MK801 blocks Purkinje cells NMDA-Rs when added in the medium that fills the recording pipette (Piochon et al., 2007). We thus decided to test the effect of this NMDA-R blockade on the induction of PF-LTD. In presence of internal MK801, the protocol induced a PF-LTD in only 2 Purkinje cells of the 7 tested, Figure 3.5B). In the 5 others, the protocol either left the PF responses unchanged (3 cells) or induced a LTP (2 cells). As a rigorous control of these experiments, we currently test if the inactive form of MK801 when added in the internal medium has an effect on PF-LTD induction.

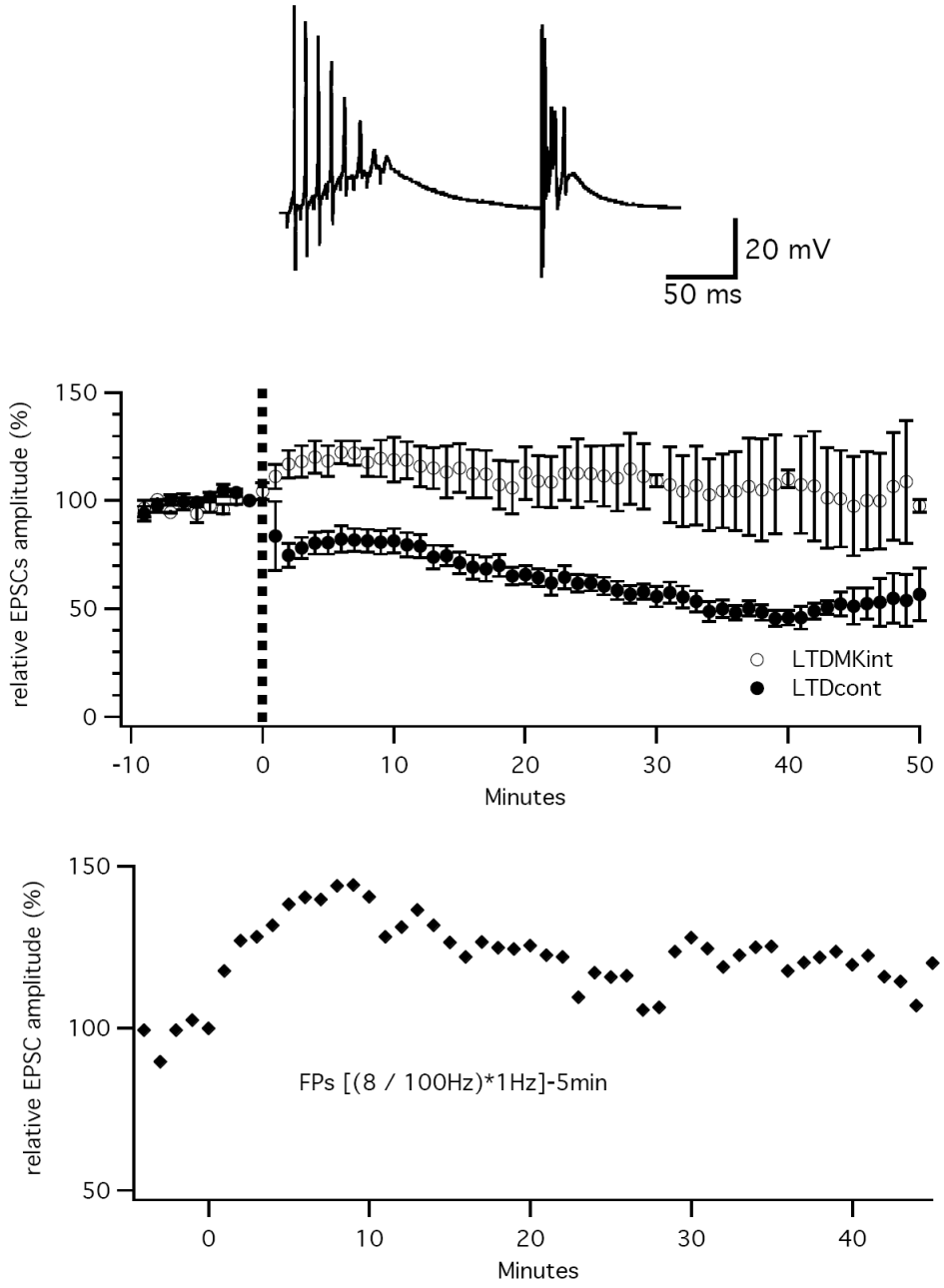

Figure 3.5 : NMDA-Rs blockade impairs PF-LTD induction

(**A**) Voltage trace corresponding to the train of 8 PF stimuli (100 Hz) followed 120 ms later by the CF stimulation. This pairing of PF and CF stimulations is delivered 300 times at 1-s intervals, in current-clamp mode, keeping the holding potential at -70 mV. (**B**) In control conditions, PF-LTD can be induced by the previously described protocol in adult mouse Purkinje cells (n = 17; closed circles); in presence of internal MK801, this protocol induces a slight PF-LTP (n = 7; open circles). (C) In absence of the CF stimulation, the train of 8 PF stimuli (100 Hz) delivered 300 times at 1-s intervals induced a PF-LTD (n = 2).

3.4.3 Discussion

3.4.3.1 Bidirectional plasticity in adult mouse PF-Purkinje cells synapses

The plasticity processes occurring in adult animals may be rather different than those evidenced in young animals. This could explain the difficulties we had to find a reliable protocol to induce the PF-LTD. Differences in the LTD-induction in PF-Purkinje cell synapses have been reported between young and adult mouse, showing a slower onset of LTD in adult as compared to juvenile animals (Hansel et al., 2006). It is likely that our protocol would differently induce a PF-LTD in young mouse Purkinje cells, with different onset and different amount of depression, but we did not test this. Moreover, the presence of NMDA-Rs at CF-Purkinje cells synapses from P21 in mouse could be in part responsible of some differences in LTD-induction compared to young animals.

Our results confirm that a bidirectional plasticity also exists at PF-Purkinje cell synapses of adult mouse, as described previously by Coesmans et al (2004). Indeed, the stimulation of PFs only, without co-activation of CF seems to induce a LTP of PFs response in adult mouse Purkinje cells. This LTP seems also to be determined by a low internal Ca^{2+} level since the addition of intracellular calcium chelator would support rather the LTP- than the LTD induction. We found that the blockade of the NMDA-Rs also supports the LTP establishment. This echoes with a previous study showing that in adult mice lacking the alphaCaMKII expression, LTD is converted in LTP in a similar manner (Hansel et al., 2006). These results suggest that NMDA-Rs and alphaCaMKII could be involved in same signaling cascade depending on calcium entry through CF activity.

3.4.3.2 NMDA-Rs involvement in PF-LTD induction

Our preliminary results need further confirmations. However they already draw a potent involvement of NMDA-Rs in PF-LTD induction, in Purkinje cells of adult mouse. Indeed, the inhibition of the NMDA-Rs by external D-APV, or by internal MK801 impairs the PF-LTD induction, and rather supports the PF-LTP establishment.

We showed in our previous study that NMDA-Rs contribute to the complex spike in presence of Mg^{2+}, without prior depolarization of the cell. However, it is likely that a prior depolarization supports the Mg^{2+} block relieve and increases the activation of NMDA-Rs

during the complex spike. This would explain why the delayed CF stimulation seems more efficient to induce LTD than the other protocols we tested. It is worth mentioning here that this order dependence of PF and CF stimulation in LTD induction may be a necessary component of the temporal dependence of sensory conditioning. For example, in eyeblink conditioning, a conditional stimulus such as a tone has been suggested to trigger PF activity. For conditioning to occur, the tone must precede the airpuff, thought to be encoded by CF activity, by at least 80 ms (Thompson et al., 1997). Similarly, in the adaptation of the vestibulo-ocular reflex, a same timing dependence has been suggested (Raymond and Lisberger, 1998).

During the co-activation of PFs and CF, NMDA-Rs activation could mediate a Ca^{2+} entry that increases the probability for subsequent PF-LTD, in respect of the "inverse" BCM rule described in Purkinje cells. The Ca^{2+} that directly flows through NMDA-Rs could be responsible for the polarity switch from PF-LTD to PF-LTP. However, it is also possible that NMDA-R activation indirectly promotes internal Ca^{2+} increase *via* other mechanisms. For instance, it has been shown that the mGluR1-dependent Ca^{2+} release induced by the PF burst activity is boosted supralinearly by the Ca^{2+} entry resulting from the complex spike, which Ca^{2+} acts as a co-agonist at IP3 receptors, enabling a subsequent endoplasmic reticulum calcium release (Wang et al., 2000; Sarkisov and Wang, 2008). The Ca^{2+} influx through NMDA-Rs could also contribute to the co-activation of IP3 receptors, allowing the internal Ca^{2+} level to reach the threshold of LTD-induction. In addition to this calcium release from internal stores, voltage-gated calcium channels would also be responsible for a nonlinear amplification of Ca^{2+} when PFs stimulation is followed by CF activation (Wang et al., 2000; Brenowitz and Regehr, 2005). One can propose that the NMDA-Rs activation enhances the depolarization that induces the activation of voltage-gated calcium channels.

4 Summary and conclusions

Because of their unique features and their high permeability to Ca2+, NMDA-Rs play a major role in many integrative neurons of the central nervous system, where they are involved in crucial processes like development, plasticity or neuronal death. Surprisingly, in the Purkinje cells, these pivotal integrative neurons of the cerebellar cortex, the nature and the function of NMDA-Rs have been so far neglected. While their presence is well known in neonatal Purkinje cells, their role is still mysterious, and studies on this precise issue are rather seldom. In adult Purkinje cells, NMDA-Rs were considered as absent since the advent, in the early 90's, of the patch-clamp techniques used in cerebellar slices. The well admitted presence of the NR1 subunit was considered as a vestige from evolution, and discrepant results obtained with other techniques did not receive a particular attention. The goal of this thesis was to investigate the role of glutamergic afferences of Purkinje cells in synaptogenesis and plasticity during development and in the adult, with a particular focus on receptors of the NMDA family.

1. Excitation and survival of neonatal Purkinje cells

Yuzaki et al. (1996) had shown that NMDA-Rs enhance the survival of immature Purkinje cells in dissociated culture *in vitro*. Our results complement this previous study by demonstrating that, in organotypic culture and in acute cerebellar slices at P3, depolarization in general has also a neuroprotective effect on postnatal Purkinje cells during the period of developmental apoptosis, around P3. In addition, the glutamatergic excitation provided by CFs could promote the survival of the Purkinje cells contacted by CFs only, by acting on juvenile NMDA-Rs, during the critical time window of developmental cell death (Results, 3.1).

2. NMDA-Rs at CF synapses

The major result of this thesis is the demonstration that, from the third postnatal week, NMDA-Rs participate to the CF excitatory transmission in Purkinje cells of adult mouse (Results, 3.2). Many candidates are likely to interact with NMDA-Rs in Purkinje cells. In addtion, the calcium signal mediated by these receptors activated by the CF could play key roles in a wide variety of cellular processes. Thus, this demonstration opens new insights into the understanding of the Purkinje cell physiology. We also show that the NMDA-Rs contribute to the "making of" a complex spike, the response of Purkinje cells to the

stimulation of the CF. The role of the complex spike in Purkinje cell is still rather unknown and covers an impressive spectrum of possibilities, going from timing device to synaptic plasticity etc.... Thus, NMDA-Rs in this cell have a promising future. In addition to the amazing bulk of possible partners of NMDA-Rs in Purkinje cells, there are many theories that now need to be revised. NMDA-Rs may be a sort of missing link that could help solving some unresolved or controversial questions in Purkinje cell physiology.

3. CF selection and stabilization

Although we showed that a competition between NMDA-Rs and GluRdelta2 is unlikely to occur (Results, 3.3), our results suggest that the NMDA-Rs are expressed only at the synapses of the strongest CF in the adult Hotfoot-mutant mouse, which conserves a multiple CFs innervation of Purkinje cells. This indicates that NMDA-Rs could play a role in the choice and the stabilization of one CF innervating the Purkinje cell.

4. NMDA-Rs and the synaptic plasticity

Finally, in the last part of this thesis, our results indicate that, very interestingly, NMDA-Rs play an important role in the polarity of PF to Purkinje cell long-term synaptic plasticity through their activation by the CF (Results, 3.4).

Novel directions for future research

The genetic engineering approach that is presently developed in the laboratory is highly promising to better understand both the involvement of NMDA-Rs in the CF synapses stabilization, and in the synaptic plasticity. The general idea consists in generating a transgenic mouse that will be impaired in the expression of the mandatory NMDA subunit NR1, selectively in Purkinje cells, and specifically in mature animals by the Cre-Lox recombination technique. We believe that this mouse will help to better clarify the roles of NMDA-Rs in Purkinje cells of adult mouse.

References

Aizenman CD, Linden DJ (2000) Rapid, synaptically driven increases in the intrinsic excitability of cerebellar deep nuclear neurons. Nat Neurosci 3:109-111.

Aizenman CD, Manis PB, Linden DJ (1998) Polarity of long-term synaptic gain change is related to postsynaptic spike firing at a cerebellar inhibitory synapse. Neuron 21:827-835.

Ajima A, Ito M (1995) A unique role of protein phosphatases in cerebellar long-term depression. Neuroreport 6:297-300.

Akazawa C, Shigemoto R, Bessho Y, Nakanishi S, Mizuno N (1994) Differential expression of five N-methyl-D-aspartate receptor subunit mRNAs in the cerebellum of developing and adult rats. J Comp Neurol 347:150-160.

Allen G, McColl R, Barnard H, Ringe WK, Fleckenstein J, Cullum CM (2005) Magnetic resonance imaging of cerebellar-prefrontal and cerebellar-parietal functional connectivity. Neuroimage 28:39-48.

Altman J (1975) Postnatal development of the cerebellar cortex in the rat. IV. Spatial organization of bipolar cells, parallel fibers and glial palisades. J Comp Neurol 163:427-447.

Alvarez VA, Ridenour DA, Sabatini BL (2007) Distinct structural and ionotropic roles of NMDA receptors in controlling spine and synapse stability. J Neurosci 27:7365-7376.

Andreasen NC, Pierson R (2008) The Role of the Cerebellum in Schizophrenia. Biol Psychiatry.

Andreescu CE, Milojkovic BA, Haasdijk ED, Kramer P, De Jong FH, Krust A, De Zeeuw CI, De Jeu MT (2007) Estradiol improves cerebellar memory formation by activating estrogen receptor beta. J Neurosci 27:10832-10839.

Araki K, Meguro H, Kushiya E, Takayama C, Inoue Y, Mishina M (1993) Selective expression of the glutamate receptor channel delta 2 subunit in cerebellar Purkinje cells. Biochem Biophys Res Commun 197:1267-1276.

Armano S, Rossi P, Taglietti V, D'Angelo E (2000) Long-term potentiation of intrinsic excitability at the mossy fiber-granule cell synapse of rat cerebellum. J Neurosci 20:5208-5216.

Armstrong DM, Rawson JA (1979) Activity patterns of cerebellar cortical neurones and climbing fibre afferents in the awake cat. J Physiol 289:425-448.

Ashwell K (1990) Microglia and cell death in the developing mouse cerebellum. Brain Res Dev Brain Res 55:219-230.

Auger C, Attwell D (2000) Fast removal of synaptic glutamate by postsynaptic transporters. Neuron 28:547-558.

Barbour B (1993) Synaptic currents evoked in Purkinje cells by stimulating individual granule cells. Neuron 11:759-769.

Bartlett TE, Bannister NJ, Collett VJ, Dargan SL, Massey PV, Bortolotto ZA, Fitzjohn SM, Bashir ZI, Collingridge GL, Lodge D (2007) Differential roles of NR2A and NR2B-containing NMDA receptors in LTP and LTD in the CA1 region of two-week old rat hippocampus. Neuropharmacology 52:60-70.

Bastian AJ, Mink JW, Kaufman BA, Thach WT (1998) Posterior vermal split syndrome. Ann Neurol 44:601-610.

Batchelor AM, Madge DJ, Garthwaite J (1994) Synaptic activation of metabotropic glutamate receptors in the parallel fibre-Purkinje cell pathway in rat cerebellar slices. Neuroscience 63:911-915.

Baude A, Nusser Z, Roberts JD, Mulvihill E, McIlhinney RA, Somogyi P (1993) The metabotropic glutamate receptor (mGluR1 alpha) is concentrated at perisynaptic membrane of neuronal subpopulations as detected by immunogold reaction. Neuron 11:771-787.

Bear MF, Cooper LN, Ebner FF (1987) A physiological basis for a theory of synapse modification. Science 237:42-48.

Behl C, Trapp T, Skutella T, Holsboer F (1997) Protection against oxidative stress-induced neuronal cell death--a novel role for RU486. Eur J Neurosci 9:912-920.

Belmeguenai A, Hansel C (2005) A role for protein phosphatases 1, 2A, and 2B in cerebellar long-term potentiation. J Neurosci 25:10768-10772.

Bernstein HG, Krell D, Braunewell KH, Baumann B, Gundelfinger ED, Diekmann S, Danos P, Bogerts B (2001) Increased number of nitric oxide synthase immunoreactive Purkinje cells and dentate nucleus neurons in schizophrenia. J Neurocytol 30:661-670.

Bienenstock EL, Cooper LN, Munro PW (1982) Theory for the development of neuron selectivity: orientation specificity and binocular interaction in visual cortex. J Neurosci 2:32-48.

Billard JM, Pumain R (1989) Loss of N-methyl-D-aspartate sensitivity of cerebellar Purkinje cells after climbing fiber deafferentation. An in vivo study in the rat. Neurosci Lett 106:199-204.

Biser PS, Thayne KA, Kong JQ, Fleming WW, Taylor DA (2000) Quantification of the alpha(3) subunit of the Na(+)/K(+)-ATPase in developing rat cerebellum. Brain Res Dev Brain Res 123:165-172.

Blanco G, Mercer RW (1998) Isozymes of the Na-K-ATPase: heterogeneity in structure, diversity in function. Am J Physiol 275:F633-650.

Bosman LW, Takechi H, Hartmann J, Eilers J, Konnerth A (2008) Homosynaptic long-term synaptic potentiation of the "winner" climbing fiber synapse in developing Purkinje cells. J Neurosci 28:798-807.

Boyden ES, Katoh A, Raymond JL (2004) Cerebellum-dependent learning: the role of multiple plasticity mechanisms. Annu Rev Neurosci 27:581-609.

Bracha V (2004) Role of the cerebellum in eyeblink conditioning. Prog Brain Res 143:331-339.

Bradley J, Carter SR, Rao VR, Wang J, Finkbeiner S (2006) Splice variants of the NR1 subunit differentially induce NMDA receptor-dependent gene expression. J Neurosci 26:1065-1076.

Bravin M, Morando L, Vercelli A, Rossi F, Strata P (1999) Control of spine formation by electrical activity in the adult rat cerebellum. Proc Natl Acad Sci U S A 96:1704-1709.

Bredt S, Hwang PM, Snyder SH (1990) Localization of nitric oxide synthase indicating a neural role for nitric oxide. Nature 347:768-770.

Brenman JE, Christopherson KS, Craven SE, McGee AW, Bredt DS (1996) Cloning and characterization of postsynaptic density 93, a nitric oxide synthase interacting protein. J Neurosci 16:7407-7415.

Brenowitz SD, Regehr WG (2005) Associative short-term synaptic plasticity mediated by endocannabinoids. Neuron 45:419-431.

Bruning G (1993) NADPH-diaphorase histochemistry in the postnatal mouse cerebellum suggests specific developmental functions for nitric oxide. J Neurosci Res 36:580-587.

Cabeza R, Nyberg L (2000) Imaging cognition II: An empirical review of 275 PET and fMRI studies. J Cogn Neurosci 12:1-47.

Cajal Ry (1911) Histologie du système nerveux de l'Homme et des vertébrés. Paris: Maloine.

Casado M, Dieudonne S, Ascher P (2000) Presynaptic N-methyl-D-aspartate receptors at the parallel fiber-Purkinje cell synapse. Proc Natl Acad Sci U S A 97:11593-11597.

Casado M, Isope P, Ascher P (2002) Involvement of presynaptic N-methyl-D-aspartate receptors in cerebellar long-term depression. Neuron 33:123-130.

Cathala L, Misra C, Cull-Candy S (2000) Developmental profile of the changing properties of NMDA receptors at cerebellar mossy fiber-granule cell synapses. J Neurosci 20:5899-5905.

Cerminara NL, Rawson JA (2004) Evidence that climbing fibers control an intrinsic spike generator in cerebellar Purkinje cells. J Neurosci 24:4510-4517.

Cesa R, Morando L, Strata P (2003) Glutamate receptor delta2 subunit in activity-dependent heterologous synaptic competition. J Neurosci 23:2363-2370.

Chatterton JE, Awobuluyi M, Premkumar LS, Takahashi H, Talantova M, Shin Y, Cui J, Tu S, Sevarino KA, Nakanishi N, Tong G, Lipton SA, Zhang D (2002) Excitatory glycine receptors containing the NR3 family of NMDA receptor subunits. Nature 415:793-798.

Chedotal A, Sotelo C (1993) The 'creeper stage' in cerebellar climbing fiber synaptogenesis precedes the 'pericellular nest'--ultrastructural evidence with parvalbumin immunocytochemistry. Brain Res Dev Brain Res 76:207-220.

Chen N, Moshaver A, Raymond LA (1997) Differential sensitivity of recombinant N-methyl-D-aspartate receptor subtypes to zinc inhibition. Mol Pharmacol 51:1015-1023.

Christopherson KS, Hillier BJ, Lim WA, Bredt DS (1999) PSD-95 assembles a ternary complex with the N-methyl-D-aspartic acid receptor and a bivalent neuronal NO synthase PDZ domain. J Biol Chem 274:27467-27473.

Chung YH, Shin CM, Joo KM, Kim MJ, Cha CI (2002) Immunohistochemical study on the distribution of nitrotyrosine and neuronal nitric oxide synthase in aged rat cerebellum. Brain Res 951:316-321.

Ciabarra AM, Sullivan JM, Gahn LG, Pecht G, Heinemann S, Sevarino KA (1995) Cloning and characterization of chi-1: a developmentally regulated member of a novel class of the ionotropic glutamate receptor family. J Neurosci 15:6498-6508.

Coesmans M, Weber JT, De Zeeuw CI, Hansel C (2004) Bidirectional parallel fiber plasticity in the cerebellum under climbing fiber control. Neuron 44:691-700.

Courchesne E, Redcay E, Kennedy DP (2004) The autistic brain: birth through adulthood. Curr Opin Neurol 17:489-496.

Courchesne E, Redcay E, Morgan JT, Kennedy DP (2005) Autism at the beginning: microstructural and growth abnormalities underlying the cognitive and behavioral phenotype of autism. Dev Psychopathol 17:577-597.

Crepel (1982) Regression of functionnal synapses in the immature mammalian cerebellum. Trends in Neurosciences 5:266-269.

Crepel F (1971) Maturation of climbing fiber responses in the rat. Brain Res 35:272-276.
Crepel F, Mariani J (1976) Multiple innervation of Purkinje cells by climbing fibers in the cerebellum of the Weaver Mutant Mouse. J Neurobiol 7:579-582.
Crepel F, Krupa M (1990) Modulation of the responsiveness of cerebellar Purkinje cells to excitatory amino acids. Adv Exp Med Biol 268:323-329.
Crepel F, Mariani J, Delhaye-Bouchaud N (1976) Evidence for a multiple innervation of Purkinje cells by climbing fibers in the immature rat cerebellum. J Neurobiol 7:567-578.
Crepel F, Audinat E, Daniel H, Hemart N, Jaillard D, Rossier J, Lambolez B (1994) Cellular locus of the nitric oxide-synthase involved in cerebellar long-term depression induced by high external potassium concentration. Neuropharmacology 33:1399-1405.
Cummings JA, Mulkey RM, Nicoll RA, Malenka RC (1996) Ca2+ signaling requirements for long-term depression in the hippocampus. Neuron 16:825-833.
D'Angelo E, Rossi P, Armano S, Taglietti V (1999) Evidence for NMDA and mGlu receptor-dependent long-term potentiation of mossy fiber-granule cell transmission in rat cerebellum. J Neurophysiol 81:277-287.
De Zeeuw CI, Yeo CH (2005) Time and tide in cerebellar memory formation. Curr Opin Neurobiol 15:667-674.
Dehnes Y, Chaudhry FA, Ullensvang K, Lehre KP, Storm-Mathisen J, Danbolt NC (1998) The glutamate transporter EAAT4 in rat cerebellar Purkinje cells: a glutamate-gated chloride channel concentrated near the synapse in parts of the dendritic membrane facing astroglia. J Neurosci 18:3606-3619.
Diamond A (2000) Close interrelation of motor development and cognitive development and of the cerebellum and prefrontal cortex. Child Dev 71:44-56.
Diez-Garcia J, Matsushita S, Mutoh H, Nakai J, Ohkura M, Yokoyama J, Dimitrov D, Knopfel T (2005) Activation of cerebellar parallel fibers monitored in transgenic mice expressing a fluorescent Ca2+ indicator protein. Eur J Neurosci 22:627-635.
Dingledine R, Borges K, Bowie D, Traynelis SF (1999) The glutamate receptor ion channels. Pharmacol Rev 51:7-61.
Dittman JS, Regehr WG (1998) Calcium dependence and recovery kinetics of presynaptic depression at the climbing fiber to Purkinje cell synapse. J Neurosci 18:6147-6162.
Douyard J, Shen L, Huganir RL, Rubio ME (2007) Differential neuronal and glial expression of GluR1 AMPA receptor subunit and the scaffolding proteins SAP97 and 4.1N during rat cerebellar development. J Comp Neurol 502:141-156.
Duguid IC, Smart TG (2004) Retrograde activation of presynaptic NMDA receptors enhances GABA release at cerebellar interneuron-Purkinje cell synapses. Nat Neurosci 7:525-533.
Duguid IC, Pankratov Y, Moss GW, Smart TG (2007) Somatodendritic release of glutamate regulates synaptic inhibition in cerebellar Purkinje cells via autocrine mGluR1 activation. J Neurosci 27:12464-12474.
Dupont JL, Gardette R, Crepel F (1987) Postnatal development of the chemosensitivity of rat cerebellar Purkinje cells to excitatory amino acids. An in vitro study. Brain Res 431:59-68.
Dupont JL, Fournier E, Gardette R, Crepel F (1984) Effect of excitatory amino acids on Purkinje cell dendrites in cerebellar slices from normal and staggerer mice. Neuroscience 12:613-619.
Dusart I, Airaksinen MS, Sotelo C (1997) Purkinje cell survival and axonal regeneration are age dependent: an in vitro study. J Neurosci 17:3710-3726.
Dzubay JA, Otis TS (2002) Climbing fiber activation of metabotropic glutamate receptors on cerebellar purkinje neurons. Neuron 36:1159-1167.
Eccles JC, Ito M, Szentagothai J (1967) The cerebellum as a neuronal machine. Springer-Verlag Berlin.
Edwards FA, Konnerth A, Sakmann B, Takahashi T (1989) A thin slice preparation for patch clamp recordings from neurones of the mammalian central nervous system. Pflugers Arch 414:600-612.
Egberongbe YI, Gentleman SM, Falkai P, Bogerts B, Polak JM, Roberts GW (1994) The distribution of nitric oxide synthase immunoreactivity in the human brain. Neuroscience 59:561-578.
Ehlers MD, Tingley WG, Huganir RL (1995) Regulated subcellular distribution of the NR1 subunit of the NMDA receptor. Science 269:1734-1737.
Ehlers MD, Zhang S, Bernhadt JP, Huganir RL (1996) Inactivation of NMDA receptors by direct interaction of calmodulin with the NR1 subunit. Cell 84:745-755.
Ehlers MD, Fung ET, O'Brien RJ, Huganir RL (1998) Splice variant-specific interaction of the NMDA receptor subunit NR1 with neuronal intermediate filaments. J Neurosci 18:720-730.
Eilers J, Augustine GJ, Konnerth A (1995) Subthreshold synaptic Ca2+ signalling in fine dendrites and spines of cerebellar Purkinje neurons [see comments]. Nature 373:155-158.
Eilers J, Plant TD, Marandi N, Konnerth A (2001) GABA-mediated Ca2+ signalling in developing rat cerebellar Purkinje neurones. J Physiol 536:429-437.
Ekerot CF, Kano M (1985) Long-term depression of parallel fibre synapses following stimulation of climbing fibres. Brain Reasearch 342:357-360.

El-Husseini AE, Williams J, Reiner PB, Pelech S, Vincent SR (1999) Localization of the cGMP-dependent protein kinases in relation to nitric oxide synthase in the brain. J Chem Neuroanat 17:45-55.
Elias GM, Nicoll RA (2007) Synaptic trafficking of glutamate receptors by MAGUK scaffolding proteins. Trends Cell Biol 17:343-352.
Ersahin Y, Mutluer S, Saydam S, Barcin E (1997) Cerebellar mutism: report of two unusual cases and review of the literature. Clin Neurol Neurosurg 99:130-134.
Exner C, Weniger G, Irle E (2004) Cerebellar lesions in the PICA but not SCA territory impair cognition. Neurology 63:2132-2135.
Farrant M, Cull-Candy SG (1991) Excitatory amino acid receptor-channels in Purkinje cells in thin cerebellar slices. Proc R Soc Lond B Biol Sci 244:179-184.
Finch EA, Augustine GJ (1998) Local calcium signalling by inositol-1,4,5-trisphosphate in Purkinje cell dendrites. Nature 396:753-756.
Foster KA, Kreitzer AC, Regehr WG (2002) Interaction of postsynaptic receptor saturation with presynaptic mechanisms produces a reliable synapse. Neuron 36:1115-1126.
Fox CJ, Russell KI, Wang YT, Christie BR (2006) Contribution of NR2A and NR2B NMDA subunits to bidirectional synaptic plasticity in the hippocampus in vivo. Hippocampus 16:907-915.
Furuta A, Rothstein JD, Martin LJ (1997) Glutamate transporter protein subtypes are expressed differentially during rat CNS development. J Neurosci 17:8363-8375.
Gall D, Prestori F, Sola E, D'Errico A, Roussel C, Forti L, Rossi P, D'Angelo E (2005) Intracellular calcium regulation by burst discharge determines bidirectional long-term synaptic plasticity at the cerebellum input stage. J Neurosci 25:4813-4822.
Garthwaite G, Yamini B, Jr., Garthwaite J (1987) Selective loss of Purkinje and granule cell responsiveness to N-methyl-D-aspartate in rat cerebellum during development. Brain Res 433:288-292.
Garthwaite J, Charles SL, Chess-Williams R (1988) Endothelium-derived relaxing factor release on activation of NMDA receptors suggests role as intercellular messenger in the brain. Nature 336:385-388.
Garyfallou VT, Kohama SG, Urbanski HF (1996) Distribution of NMDA and AMPA receptors in the cerebellar cortex of rhesus macaques. Brain Res 716:22-28.
Genet S, Kado RT (1997) Hyperpolarizing current of the Na/K ATPase contributes to the membrane polarization of the Purkinje cell in rat cerebellum. Pflugers Arch 434:559-567.
Ghosh A (1996) Cortical development: with an eye on neurotrophins. Curr Biol 6:130-133.
Ghoumari AM, Wehrle R, Bernard O, Sotelo C, Dusart I (2000) Implication of Bcl-2 and Caspase-3 in age-related Purkinje cell death in murine organotypic culture: an in vitro model to study apoptosis. Eur J Neurosci 12:2935-2949.
Ghoumari AM, Dusart I, El-Etr M, Tronche F, Sotelo C, Schumacher M, Baulieu EE (2003) Mifepristone (RU486) protects Purkinje cells from cell death in organotypic slice cultures of postnatal rat and mouse cerebellum. Proc Natl Acad Sci U S A 100:7953-7958.
Ghoumari AM, Piochon C, Tomkiewicz C, Eychenne B, Levenes C, Dusart I, Schumacher M, Baulieu EE (2006) Neuroprotective effect of mifepristone involves neuron depolarization. Faseb J 20:1377-1386.
Glickstein M (2007) What does the cerebellum really do? Curr Biol 17:R824-827.
Glickstein M, Voogd J (1995) Lodewijk Bolk and the comparative anatomy of the cerebellum. Trends Neurosci 18:206-210.
Glitsch M, Marty A (1999) Presynaptic effects of NMDA in cerebellar Purkinje cells and interneurons. J Neurosci 19:511-519.
Gordon N (2007) The cerebellum and cognition. Eur J Paediatr Neurol 11:232-234.
Gounko NV, Gramsbergen A, van der Want JJ (2007) The glutamate receptor delta 2 in relation to cerebellar development and plasticity. Neurosci Biobehav Rev 31:1095-1100.
Guastavino JM, Sotelo C, Damez-Kinselle I (1990) Hot-foot murine mutation: behavioral effects and neuroanatomical alterations. Brain Res 523:199-210.
Hafidi A, Hillman DE (1997) Distribution of glutamate receptors GluR 2/3 and NR1 in the developing rat cerebellum. Neuroscience 81:427-436.
Hamill OP, Marty A, Neher E, Sakmann B, Sigworth FJ (1981) Improved patch-clamp techniques for high-resolution current recording from cells and cell-free membrane patches. Pflügers Archiv, 391:85-100.
Hansel C, Linden DJ (2000) Long-term depression of the cerebellar climbing fiber--Purkinje neuron synapse. Neuron 26:473-482.
Hansel C, Artola A, Singer W (1997) Relation between dendritic Ca2+ levels and the polarity of synaptic long-term modifications in rat visual cortex neurons. Eur J Neurosci 9:2309-2322.
Hansel C, Linden DJ, D'Angelo E (2001) Beyond parallel fiber LTD: the diversity of synaptic and non-synaptic plasticity in the cerebellum. Nat Neurosci 4:467-475.

Hansel C, de Jeu M, Belmeguenai A, Houtman SH, Buitendijk GH, Andreev D, De Zeeuw CI, Elgersma Y (2006) alphaCaMKII Is essential for cerebellar LTD and motor learning. Neuron 51:835-843.

Hartell NA (1994) Induction of cerebellar long-term depression requires activation of glutamate metabotropic receptors. NeuroReport 5:919-916.

Hashimoto K, Kano M (2003) Functional differentiation of multiple climbing fiber inputs during synapse elimination in the developing cerebellum. Neuron 38:785-796.

Hashimoto K, Ichikawa R, Takechi H, Inoue Y, Aiba A, Sakimura K, Mishina M, Hashikawa T, Konnerth A, Watanabe M, Kano M (2001) Roles of glutamate receptor delta 2 subunit (GluRdelta 2) and metabotropic glutamate receptor subtype 1 (mGluR1) in climbing fiber synapse elimination during postnatal cerebellar development. J Neurosci 21:9701-9712.

Hausser M, Roth A (1997) Dendritic and somatic glutamate receptor channels in rat cerebellar Purkinje cells. J Physiol 501 (Pt 1):77-95.

Hausser M, Clark BA (1997) Tonic synaptic inhibition modulates neuronal output pattern and spatiotemporal synaptic integration. Neuron 19:665-678.

Hawkins LM, Prybylowski K, Chang K, Moussan C, Stephenson FA, Wenthold RJ (2004) Export from the endoplasmic reticulum of assembled N-methyl-d-aspartic acid receptors is controlled by a motif in the c terminus of the NR2 subunit. J Biol Chem 279:28903-28910.

Herman MA, Jahr CE (2007) Extracellular glutamate concentration in hippocampal slice. J Neurosci 27:9736-9741.

Hirai H (2001) Ca2+-dependent regulation of synaptic delta2 glutamate receptor density in cultured rat Purkinje neurons. Eur J Neurosci 14:73-82.

Hirai H, Miyazaki T, Kakegawa W, Matsuda S, Mishina M, Watanabe M, Yuzaki M (2005) Rescue of abnormal phenotypes of the delta2 glutamate receptor-null mice by mutant delta2 transgenes. EMBO Rep 6:90-95.

Hirai H, Launey T, Mikawa S, Torashima T, Yanagihara D, Kasaura T, Miyamoto A, Yuzaki M (2003) New role of delta2-glutamate receptors in AMPA receptor trafficking and cerebellar function. Nat Neurosci 6:869-876.

Hirao K, Hata Y, Ide N, Takeuchi M, Irie M, Yao I, Deguchi M, Toyoda A, Sudhof TC, Takai Y (1998) A novel multiple PDZ domain-containing molecule interacting with N-methyl-D-aspartate receptors and neuronal cell adhesion proteins. J Biol Chem 273:21105-21110.

Hironaka K, Umemori H, Tezuka T, Mishina M, Yamamoto T (2000) The protein-tyrosine phosphatase PTPMEG interacts with glutamate receptor delta 2 and epsilon subunits. J Biol Chem 275:16167-16173.

Hobbs AJ, Ignarro LJ (1996) Nitric oxide-cyclic GMP signal transduction system. Methods Enzymol 269:134-148.

Hollmann M, Boulter J, Maron C, Beasley L, Sullivan J, Pecht G, Heinemann S (1993) Zinc potentiates agonist-induced currents at certain splice variants of the NMDA receptor. Neuron 10:943-954.

Huang YH, Dykes-Hoberg M, Tanaka K, Rothstein JD, Bergles DE (2004) Climbing fiber activation of EAAT4 transporters and kainate receptors in cerebellar Purkinje cells. J Neurosci 24:103-111.

Ichikawa R, Miyazaki T, Kano M, Hashikawa T, Tatsumi H, Sakimura K, Mishina M, Inoue Y, Watanabe M (2002) Distal extension of climbing fiber territory and multiple innervation caused by aberrant wiring to adjacent spiny branchlets in cerebellar Purkinje cells lacking glutamate receptor delta 2. J Neurosci 22:8487-8503.

Iino M (2006) Ca2+-dependent inositol 1,4,5-trisphosphate and nitric oxide signaling in cerebellar neurons. J Pharmacol Sci 100:538-544.

Ikeda K, Araki K, Takayama C, Inoue Y, Yagi T, Aizawa S, Mishina M (1995) Reduced spontaneous activity of mice defective in the epsilon 4 subunit of the NMDA receptor channel. Brain Res Mol Brain Res 33:61-71.

Imamizu H, Miyauchi S, Tamada T, Sasaki Y, Takino R, Putz B, Yoshioka T, Kawato M (2000) Human cerebellar activity reflecting an acquired internal model of a new tool. Nature 403:192-195.

Ioannides AA, Fenwick PB (2005) Imaging cerebellum activity in real time with magnetoencephalographic data. Prog Brain Res 148:139-150.

Ito M (2001) Cerebellar long-term depression: characterization, signal transduction, and functional roles. Physiol Rev 81:1143-1195.

Ito M (2005) Bases and implications of learning in the cerebellum--adaptive control and internal model mechanism. Prog Brain Res 148:95-109.

Ito M (2006) Cerebellar circuitry as a neuronal machine. Prog Neurobiol 78:272-303.

Ito M (2008) Control of mental activities by internal models in the cerebellum. Nat Rev Neurosci 9:304-313.

Ito M, Sakurai M, Tongroach P (1982) Climbing fibre induced depression of both mossy fibre responsiveness and glutamate sensitivity of cerebellar purkinje cells. J Physiol 324:113-134.

Jakab RL, Wong JK, Belcher SM (2001) Estrogen receptor beta immunoreactivity in differentiating cells of the developing rat cerebellum. J Comp Neurol 430:396-409.
Johnson JW, Ascher P (1987) Glycine potentiates the NMDA response in cultured mouse brain neurons. Nature 325:529-531.
Jorntell H, Ekerot CF (2002) Reciprocal bidirectional plasticity of parallel fiber receptive fields in cerebellar Purkinje cells and their afferent interneurons. Neuron 34:797-806.
Kakegawa W, Kohda K, Yuzaki M (2007a) The delta2 'ionotropic' glutamate receptor functions as a non-ionotropic receptor to control cerebellar synaptic plasticity. J Physiol 584:89-96.
Kakegawa W, Tsuzuki K, Iino M, Ozawa S (2003) Functional NMDA receptor channels generated by NMDAR2B gene transfer in rat cerebellar Purkinje cells. Eur J Neurosci 17:887-891.
Kakegawa W, Miyazaki T, Hirai H, Motohashi J, Mishina M, Watanabe M, Yuzaki M (2007b) Ca2+ permeability of the channel pore is not essential for the delta2 glutamate receptor to regulate synaptic plasticity and motor coordination. J Physiol 579:729-735.
Kano M, Hashimoto K, Chen C, Abeliovich A, Aiba A, Kurihara H, Watanabe M, Inoue Y, Tonegawa S (1995) Impaired synapse elimination during cerebellar development in PKC gamma mutant mice. Cell 83:1223-1231.
Karachot L, Kado RT, Ito M (1994) Stimulus parameters for induction of long-term depression in in vitro rat Purkinje cells. Neurosci Res 21:161-168.
Kashiwabuchi N, Ikeda K, Araki K, Hirano T, Shibuki K, Takayama C, Inoue Y, Kutsuwada T, Yagi T, Kang Y, et al. (1995a) Impairment of motor coordination, Purkinje cell synapse formation, and cerebellar long-term depression in GluR delta 2 mutant mice. Cell 81:245-252.
Kashiwabuchi N, Ikeda K, Araki K, Hirano T, Shibuki K, Takayama C, Inoue Y, Kutsuwada T, Yagi T, Kang Y, Aizawa S, Mishina M (1995b) Impairement of motor coordination, Purkinje cell synapses formation, and cerebellar long-term depression in GluR-delta-2 mutant mice. Cell 81:245-252.
Kawato M, Kuroda T, Imamizu H, Nakano E, Miyauchi S, Yoshioka T (2003) Internal forward models in the cerebellum: fMRI study on grip force and load force coupling. Prog Brain Res 142:171-188.
Keele SW, Ivry R (1990) Does the cerebellum provide a common computation for diverse tasks? A timing hypothesis. Ann N Y Acad Sci 608:179-207; discussion 207-111.
Kew JN, Trube G, Kemp JA (1996) A novel mechanism of activity-dependent NMDA receptor antagonism describes the effect of ifenprodil in rat cultured cortical neurones. J Physiol 497 (Pt 3):761-772.
Khaliq ZM, Raman IM (2005) Axonal propagation of simple and complex spikes in cerebellar Purkinje neurons. J Neurosci 25:454-463.
Kimura H, Okamoto K, Sakai Y (1985) Pharmacological evidence for L-aspartate as the neurotransmitter of cerebellar climbing fibres in the guinea-pig. J Physiol 365:103-119.
Knopfel T, Grandes P (2002) Metabotropic glutamate receptors in the cerebellum with a focus on their function in Purkinje cells. Cerebellum 1:19-26.
Kohda K, Kakegawa W, Matsuda S, Nakagami R, Kakiya N, Yuzaki M (2007) The extreme C-terminus of GluRdelta2 is essential for induction of long-term depression in cerebellar slices. Eur J Neurosci 25:1357-1362.
Kohr G (2006) NMDA receptor function: subunit composition versus spatial distribution. Cell Tissue Res 326:439-446.
Konnerth A, Llano I, Armstrong CM (1990) Synaptic currents in cerebellar Purkinje cells. Proc Natl Acad Sci U S A 87:2662-2665.
Krupa M, Crepel F (1990) Transient Sensitivity of Rat Cerebellar Purkinje Cells to N-methyl-D-aspartate during Development. A Voltage Clamp Study in in vitro Slices. Eur J Neurosci 2:312-316.
Kurihara H, Hashimoto K, Kano M, Takayama C, Sakimura K, Mishina M, Inoue Y, Watanabe M (1997) Impaired parallel fiber-->Purkinje cell synapse stabilization during cerebellar development of mutant mice lacking the glutamate receptor delta2 subunit. J Neurosci 17:9613-9623.
Kuruma A, Inoue T, Mikoshiba K (2003) Dynamics of Ca(2+) and Na(+) in the dendrites of mouse cerebellar Purkinje cells evoked by parallel fibre stimulation. Eur J Neurosci 18:2677-2689.
Lachamp P, Balland B, Tell F, Baude A, Strube C, Crest M, Kessler JP (2005) Early expression of AMPA receptors and lack of NMDA receptors in developing rat climbing fibre synapses. J Physiol 564:751-763.
Lalouette A, Guenet JL, Vriz S (1998) Hotfoot mouse mutations affect the delta 2 glutamate receptor gene and are allelic to lurcher. Genomics 50:9-13.
Lalouette A, Lohof A, Sotelo C, Guenet J, Mariani J (2001) Neurobiological effects of a null mutation depend on genetic context: comparison between two hotfoot alleles of the delta-2 ionotropic glutamate receptor. Neuroscience 105:443-455.
Lambolez B, Audinat E, Bochet P, Crepel F, Rossier J (1992) AMPA receptor subunits expressed by single Purkinje cells. Neuron 9:247-258.

Landsend AS, Amiry-Moghaddam M, Matsubara A, Bergersen L, Usami S, Wenthold RJ, Ottersen OP (1997) Differential localization of delta glutamate receptors in the rat cerebellum: coexpression with AMPA receptors in parallel fiber-spine synapses and absence from climbing fiber-spine synapses. J Neurosci 17:834-842.

Larsell O, ed (1970) The Comparative Anatomy and Histology of the Cerebellum from Monotremes through Apes, (ed. Jansen, J.) (Minnesota Univ. Press, Minneapolis).

Laurie DJ, Seeburg PH (1994) Regional and developmental heterogeneity in splicing of the rat brain NMDAR1 mRNA. J Neurosci 14:3180-3194.

Laurie DJ, Putzke J, Zieglgansberger W, Seeburg PH, Tolle TR (1995) The distribution of splice variants of the NMDAR1 subunit mRNA in adult rat brain. Brain Res Mol Brain Res 32:94-108.

Lee YF, Lo PS, Wang YJ, Hu A, Chen HH (2005) Neonatal toluene exposure alters N-methyl-D-aspartate receptor subunit expression in the hippocampus and cerebellum in juvenile rats. Neuropharmacology 48:195-203.

Lev-Ram V, Wong ST, Storm DR, Tsien RY (2002) A new form of cerebellar long-term potentiation is postsynaptic and depends on nitric oxide but not cAMP. Proc Natl Acad Sci U S A 99:8389-8393.

Lev-Ram V, Mehta SB, Kleinfeld D, Tsien RY (2003) Reversing cerebellar long-term depression. Proc Natl Acad Sci U S A 100:15989-15993.

Levenes C, Daniel H, Crepel F (1998) Long-term depression of synaptic transmission in the cerebellum: cellular and molecular mechanisms revisited. Prog Neurobiol 55:79-91.

Levenes C, Daniel H, Crepel F (2001) Retrograde modulation of transmitter release by postsynaptic subtype 1 metabotropic glutamate receptors in the rat cerebellum. J Physiol 537:125-140.

Li Y, Erzurumlu RS, Chen C, Jhaveri S, Tonegawa S (1994) Whisker-related neuronal patterns fail to develop in the trigeminal brainstem nuclei of NMDAR1 knockout mice. Cell 76:427-437.

Lin JW, Wyszynski M, Madhavan R, Sealock R, Kim JU, Sheng M (1998) Yotiao, a novel protein of neuromuscular junction and brain that interacts with specific splice variants of NMDA receptor subunit NR1. J Neurosci 18:2017-2027.

Linden DJ, Ahn S (1999) Activation of presynaptic cAMP-dependent protein kinase is required for induction of cerebellar long-term potentiation. J Neurosci 19:10221-10227.

Lisman J (1989) A mechanisme for the hebb and anti-hebb processes underlying learning and memory. Proc Natl Acad Sci USA 86:9574-9578.

Liu L, Wong TP, Pozza MF, Lingenhoehl K, Wang Y, Sheng M, Auberson YP, Wang YT (2004) Role of NMDA receptor subtypes in governing the direction of hippocampal synaptic plasticity. Science 304:1021-1024.

Llano I, Marty A, Armstrong CM, Konnerth A (1991) Synaptic-and agonist-induced excitatory currents of Purkinje cells in rat cerebellar slices. Journal of Physiology (London) 434:183-213.

Llinas R, Sugimori M (1980a) Electrophysiological properties of in vitro Purkinje cell dendrites in mammalian cerebellar slices. Journal of Physiology (London) 305:197-213.

Llinas R, Sugimori M (1980b) Electrophysiological properties of in vitro Purkinje cell somata in mammalian cerebellar slices. J Physiol 305:171-195.

Llinas R, Sasaki K (1989) The Functional Organization of the Olivo-Cerebellar System as Examined by Multiple Purkinje Cell Recordings. Eur J Neurosci 1:587-602.

Lomeli H, Sprengel R, Laurie DJ, Kohr G, Herb A, Seeburg PH, Wisden W (1993) The rat delta-1 and delta-2 subunits extend the excitatory amino acid receptor family. FEBS Lett 315:318-322.

MacDermott AB, Mayer ML, Westbrook GL, Smith SJ, Barker JL (1986) NMDA-receptor activation increases cytoplasmic calcium concentration in cultured spinal cord neurones. Nature 321:519-522.

Madry C, Mesic I, Bartholomaus I, Nicke A, Betz H, Laube B (2007) Principal role of NR3 subunits in NR1/NR3 excitatory glycine receptor function. Biochem Biophys Res Commun 354:102-108.

Mandolesi G, Cesa R, Autuori E, Strata P (2008) An orphan ionotropic glutamate receptor: The delta2 subunit. Neuroscience.

Manzoni D (2007) The cerebellum and sensorimotor coupling: looking at the problem from the perspective of vestibular reflexes. Cerebellum 6:24-37.

Mariani J, Changeux JP (1980) Multiple innervation of Purkinje cells by climbing fibers in the cerebellum of the adult staggerer mutant mouse. J Neurobiol 11:41-50.

Mariani J, Changeux JP (1981) Ontogenesis of olivocerebellar relationships. I. Studies by intracellular recordings of the multiple innervation of Purkinje cells by climbing fibers in the developing rat cerebellum. Journal of Neurosciences 1:696-702.

Maruta J, Hensbroek RA, Simpson JI (2007) Intraburst and interburst signaling by climbing fibers. J Neurosci 27:11263-11270.

Massey PV, Johnson BE, Moult PR, Auberson YP, Brown MW, Molnar E, Collingridge GL, Bashir ZI (2004) Differential roles of NR2A and NR2B-containing NMDA receptors in cortical long-term potentiation and long-term depression. J Neurosci 24:7821-7828.

Mathiak K, Hertrich I, Grodd W, Ackermann H (2004) Discrimination of temporal information at the cerebellum: functional magnetic resonance imaging of nonverbal auditory memory. Neuroimage 21:154-162.

Matsuda K, Kamiya Y, Matsuda S, Yuzaki M (2002) Cloning and characterization of a novel NMDA receptor subunit NR3B: a dominant subunit that reduces calcium permeability. Brain Res Mol Brain Res 100:43-52.

Matsuda K, Fletcher M, Kamiya Y, Yuzaki M (2003) Specific assembly with the NMDA receptor 3B subunit controls surface expression and calcium permeability of NMDA receptors. J Neurosci 23:10064-10073.

Mayer ML, Westbrook GL, Guthrie PB (1984) Voltage-dependent block by Mg2+ of NMDA responses in spinal cord neurones. Nature 309:261-263.

McCullers DL, Sullivan PG, Scheff SW, Herman JP (2002) Mifepristone protects CA1 hippocampal neurons following traumatic brain injury in rat. Neuroscience 109:219-230.

McKay BE, Turner RW (2005) Physiological and morphological development of the rat cerebellar Purkinje cell. J Physiol 567:829-850.

Middleton FA, Strick PL (1994) Anatomical evidence for cerebellar and basal ganglia involvement in higher cognitive function. Science 266:458-461.

Middleton FA, Strick PL (2001) Cerebellar projections to the prefrontal cortex of the primate. J Neurosci 21:700-712.

Misra C, Brickley SG, Wyllie DJ, Cull-Candy SG (2000) Slow deactivation kinetics of NMDA receptors containing NR1 and NR2D subunits in rat cerebellar Purkinje cells. J Physiol 525 Pt 2:299-305.

Miyakawa H, Lev-Ram V, Lasser-Ross WN, Ross WN (1992) Calcium transients evoked by climbing fiber and parallel fiber synaptic inputs in guinea pig cerebellar Purkinje neurons. J of Neurophysiology 4:1178-1189.

Miyazaki T, Hashimoto K, Shin HS, Kano M, Watanabe M (2004) P/Q-type Ca2+ channel alpha1A regulates synaptic competition on developing cerebellar Purkinje cells. J Neurosci 24:1734-1743.

Momiyama A, Feldmeyer D, Cull-Candy SG (1996) Identification of a native low-conductance NMDA channel with reduced sensitivity to Mg2+ in rat central neurones. J Physiol 494 (Pt 2):479-492.

Momiyama A, Silver RA, Hausser M, Notomi T, Wu Y, Shigemoto R, Cull-Candy SG (2003) The density of AMPA receptors activated by a transmitter quantum at the climbing fibre-Purkinje cell synapse in immature rats. J Physiol 549:75-92.

Monsivais P, Clark BA, Roth A, Hausser M (2005) Determinants of action potential propagation in cerebellar Purkinje cell axons. J Neurosci 25:464-472.

Monyer H, Burnashev N, Laurie DJ, Sakmann B, Seeburg PH (1994) Developmental and regional expression in the rat brain and functional properties of four NMDA receptors. Neuron 12:529-540.

Monyer H, Sprengel R, Schoepfer R, Herb A, Higuchi M, Lomeli H, Burnashev N, Sakmann B, Seeburg PH (1992) Heteromeric NMDA receptors: Molecular and Functional distinction of subtypes. Science 256:1217-1221.

Morando L, Cesa R, Rasetti R, Harvey R, Strata P (2001) Role of glutamate delta -2 receptors in activity-dependent competition between heterologous afferent fibers. Proc Natl Acad Sci U S A 98:9954-9959.

Morara S, van der Want JJ, de Weerd H, Provini L, Rosina A (2001) Ultrastructural analysis of climbing fiber-Purkinje cell synaptogenesis in the rat cerebellum. Neuroscience 108:655-671.

Morishita W, Lu W, Smith GB, Nicoll RA, Bear MF, Malenka RC (2007) Activation of NR2B-containing NMDA receptors is not required for NMDA receptor-dependent long-term depression. Neuropharmacology 52:71-76.

Moriyoshi K, Masu M, Ishii T, Shigemoto R, Mizumo N, Nakanishi S (1991) Molecular cloning and characterization of the rat NMDA receptor. Nature 354:31-37.

Motohashi J, Kakegawa W, Yuzaki M (2007) Ho15J: a new hotfoot allele in a hot spot in the gene encoding the delta2 glutamate receptor. Brain Res 1140:153-160.

Mu Y, Otsuka T, Horton AC, Scott DB, Ehlers MD (2003) Activity-dependent mRNA splicing controls ER export and synaptic delivery of NMDA receptors. Neuron 40:581-594.

Nagerl UV, Eberhorn N, Cambridge SB, Bonhoeffer T (2004) Bidirectional activity-dependent morphological plasticity in hippocampal neurons. Neuron 44:759-767.

Naisbitt S, Kim E, Tu JC, Xiao B, Sala C, Valtschanoff J, Weinberg RJ, Worley PF, Sheng M (1999) Shank, a novel family of postsynaptic density proteins that binds to the NMDA receptor/PSD-95/GKAP complex and cortactin. Neuron 23:569-582.

Nakagawa S, Watanabe M, Inoue Y (1996) Altered gene expression of the N-methyl-D-aspartate receptor channel subunits in Purkinje cells of the staggerer mutant mouse. Eur J Neurosci 8:2644-2651.

Napper RM, Harvey RJ (1988) Number of parallel fiber synapses on an individual Purkinje cell in the cerebellum of the rat. J Comp Neurol 274:168-177.

Naur P, Hansen KB, Kristensen AS, Dravid SM, Pickering DS, Olsen L, Vestergaard B, Egebjerg J, Gajhede M, Traynelis SF, Kastrup JS (2007) Ionotropic glutamate-like receptor delta2 binds D-serine and glycine. Proc Natl Acad Sci U S A 104:14116-14121.

Neyton J, Paoletti P (2006) Relating NMDA receptor function to receptor subunit composition: limitations of the pharmacological approach. J Neurosci 26:1331-1333.

Nishi M, Hinds H, Lu HP, Kawata M, Hayashi Y (2001) Motoneuron-specific expression of NR3B, a novel NMDA-type glutamate receptor subunit that works in a dominant-negative manner. J Neurosci 21:RC185.

O'Brien RJ, Lau LF, Huganir RL (1998) Molecular mechanisms of glutamate receptor clustering at excitatory synapses. Curr Opin Neurobiol 8:364-369.

Ohyu J, Takashima S (1998) Developmental characteristics of neuronal nitric oxide synthase (nNOS) immunoreactive neurons in fetal to adolescent human brains. Brain Res Dev Brain Res 110:193-202.

Okabe S, Miwa A, Okado H (1999) Alternative splicing of the C-terminal domain regulates cell surface expression of the NMDA receptor NR1 subunit. J Neurosci 19:7781-7792.

Otis TS, Kavanaugh MP, Jahr CE (1997) Postsynaptic glutamate transport at the climbing fiber-Purkinje cell synapse. Science 277:1515-1518.

Palay SL, Chan-Palay V (1974) Cerebellar cortex. Cytology and Organization. Berlin-Heidelberg-New York: Springer-Verlag.

Parsons LM, Fox PT (1997) Sensory and cognitive functions. Int Rev Neurobiol 41:255-271.

Perez-Otano I, Schulteis CT, Contractor A, Lipton SA, Trimmer JS, Sucher NJ, Heinemann SF (2001) Assembly with the NR1 subunit is required for surface expression of NR3A-containing NMDA receptors. J Neurosci 21:1228-1237.

Perez SE, Chen EY, Mufson EJ (2003) Distribution of estrogen receptor alpha and beta immunoreactive profiles in the postnatal rat brain. Brain Res Dev Brain Res 145:117-139.

Petralia RS, Yokotani N, Wenthold RJ (1994a) Light and electron microscope distribution of the NMDA receptor subunit NMDAR1 in the rat nervous system using a selective anti-peptide antibody. J Neurosci 14:667-696.

Petralia RS, Wang YX, Wenthold RJ (1994b) The NMDA receptor subunits NR2A and NR2B show histological and ultrastructural localization patterns similar to those of NR1. J Neurosci 14:6102-6120.

Petralia RS, Zhao HM, Wang YX, Wenthold RJ (1998) Variations in the tangential distribution of postsynaptic glutamate receptors in Purkinje cell parallel and climbing fiber synapses during development. Neuropharmacology 37:1321-1334.

Phillips T, Makoff A, Murrison E, Mimmack M, Waldvogel H, Faull R, Rees S, Emson P (1998) Immunohistochemical localisation of mGluR7 protein in the rodent and human cerebellar cortex using subtype specific antibodies. Brain Res Mol Brain Res 57:132-141.

Piochon C, Irinopoulou T, Brusciano D, Bailly Y, Mariani J, Levenes C (2007) NMDA receptor contribution to the climbing fiber response in the adult mouse Purkinje cell. J Neurosci 27:10797-10809.

Price RH, Jr., Handa RJ (2000) Expression of estrogen receptor-beta protein and mRNA in the cerebellum of the rat. Neurosci Lett 288:115-118.

Qiu DL, Knopfel T (2007) An NMDA receptor/nitric oxide cascade in presynaptic parallel fiber-Purkinje neuron long-term potentiation. J Neurosci 27:3408-3415.

Quinlan JE, Davies J (1985) Excitatory and inhibitory responses of Purkinje cells, in the rat cerebellum in vivo, induced by excitatory amino acids. Neurosci Lett 60:39-46.

Rabacchi SA, Bailly Y, Delhaye-Bouchaud N, Herrup K, Mariani J (1992) Role of the target in synapse elimination: studies in cerebellum of developing lurcher mutants and adult chimeric mice. J Neurosci 12:4712-4720.

Racine RJ, Wilson DA, Gingell R, Sunderland D (1986) Long-term potentiation in the interpositus and vestibular nuclei in the rat. Experimental Brain Research 63:158-162.

Raman IM, Bean BP (1997) Resurgent sodium current and action potential formation in dissociated cerebellar Purkinje neurons. J Neurosci 17:4517-4526.

Rancillac A, Crepel F (2004) Synapses between parallel fibres and stellate cells express long-term changes in synaptic efficacy in rat cerebellum. J Physiol 554:707-720.

Raymond JL, Lisberger SG (1998) Neural learning rules for the vestibulo-ocular reflex. J Neurosci 18:9112-9129.

Renzi M, Farrant M, Cull-Candy SG (2007) Climbing-fibre activation of NMDA receptors in Purkinje cells of adult mice. J Physiol 585:91-101.

Rigby M, Le Bourdelles B, Heavens RP, Kelly S, Smith D, Butler A, Hammans R, Hills R, Xuereb JH, Hill RG, Whiting PJ, Sirinathsinghji DJ (1996) The messenger RNAs for the N-methyl-D-aspartate receptor

subunits show region-specific expression of different subunit composition in the human brain. Neuroscience 73:429-447.
Ripellino JA, Neve RL, Howe JR (1998) Expression and heteromeric interactions of non-N-methyl-D-aspartate glutamate receptor subunits in the developing and adult cerebellum. Neuroscience 82:485-497.
Roche KW, Ly CD, Petralia RS, Wang YX, McGee AW, Bredt DS, Wenthold RJ (1999) Postsynaptic density-93 interacts with the delta2 glutamate receptor subunit at parallel fiber synapses. J Neurosci 19:3926-3934.
Rodrigo J, Springall DR, Uttenthal O, Bentura ML, Abadia-Molina F, Riveros-Moreno V, Martinez-Murillo R, Polak JM, Moncada S (1994) Localization of nitric oxide synthase in the adult rat brain. Philos Trans R Soc Lond B Biol Sci 345:175-221.
Rosenmund C, Legendre P, Westbrook GL (1992) Expression of NMDA channels on cerebellar Purkinje cells acutely dissociated from newborn rats. J Neurophysiol 68:1901-1905.
Roth A, Hausser M (2001) Compartmental models of rat cerebellar Purkinje cells based on simultaneous somatic and dendritic patch-clamp recordings. J Physiol 535:445-472.
Rumbaugh G, Prybylowski K, Wang JF, Vicini S (2000) Exon 5 and spermine regulate deactivation of NMDA receptor subtypes. J Neurophysiol 83:1300-1306.
Safo P, Regehr WG (2008) Timing dependence of the induction of cerebellar LTD. Neuropharmacology 54:213-218.
Sakamoto H, Mezaki Y, Shikimi H, Ukena K, Tsutsui K (2003) Dendritic growth and spine formation in response to estrogen in the developing Purkinje cell. Endocrinology 144:4466-4477.
Salin P, Malenka R, Nicoll R (1996) Cyclic AMP mediates a presynaptic form of LTP at cerebellar parallel fiber synapses. Neuron 16:797-803.
Sarkisov DV, Wang SS (2008) Order-dependent coincidence detection in cerebellar Purkinje neurons at the inositol trisphosphate receptor. J Neurosci 28:133-142.
Sasahara K, Shikimi H, Haraguchi S, Sakamoto H, Honda S, Harada N, Tsutsui K (2007) Mode of action and functional significance of estrogen-inducing dendritic growth, spinogenesis, and synaptogenesis in the developing Purkinje cell. J Neurosci 27:7408-7417.
Sattler R, Xiong Z, Lu WY, MacDonald JF, Tymianski M (2000) Distinct roles of synaptic and extrasynaptic NMDA receptors in excitotoxicity. J Neurosci 20:22-33.
Saxon DW, Beitz AJ (1996) An experimental model for the non-invasive trans-synaptic induction of nitric oxide synthase in Purkinje cells of the rat cerebellum. Neuroscience 72:157-165.
Scherzer CR, Landwehrmeyer GB, Kerner JA, Standaert DG, Hollingsworth ZR, Daggett LP, Velicelebi G, Penney JB, Jr., Young AB (1997) Cellular distribution of NMDA glutamate receptor subunit mRNAs in the human cerebellum. Neurobiol Dis 4:35-46.
Schmahmann JD (1996) From movement to thought: anatomic substrates of the cerebellar contribution to cognitive processing. Human Brain Mapping 4:174 - 198.
Schmidt C, Hollmann M (2008) Apparent homomeric NR1 currents observed in Xenopus oocytes are caused by an endogenous NR2 subunit. J Mol Biol 376:658-670.
Schmolesky MT, De Zeeuw CI, Hansel C (2005) Climbing fiber synaptic plasticity and modifications in Purkinje cell excitability. Prog Brain Res 148:81-94.
Schmolesky MT, Weber JT, De Zeeuw CI, Hansel C (2002) The making of a complex spike: ionic composition and plasticity. Ann N Y Acad Sci 978:359-390.
Schmolesky MT, De Ruiter MM, De Zeeuw CI, Hansel C (2007) The neuropeptide corticotropin-releasing factor regulates excitatory transmission and plasticity at the climbing fibre-Purkinje cell synapse. Eur J Neurosci 25:1460-1466.
Schreurs BG, Gusev PA, Tomsic D, Alkon DL, Shi T (1998) Intracellular correlates of acquisition and long-term memory of classical conditioning in Purkinje cell dendrites in slices of rabbit cerebellar lobule HVI. J Neurosci 18:5498-5507.
Scott DB, Blanpied TA, Swanson GT, Zhang C, Ehlers MD (2001) An NMDA receptor ER retention signal regulated by phosphorylation and alternative splicing. J Neurosci 21:3063-3072.
Sekiguchi M, Okamoto K, Sakai Y (1987) NMDA-receptors on Purkinje cell dendrites in guinea pig cerebellar slices. Brain Res 437:402-406.
Shen Y, Linden DJ (2005) Long-term potentiation of neuronal glutamate transporters. Neuron 46:715-722.
Shen Y, Hansel C, Linden DJ (2002) Glutamate release during LTD at cerebellar climbing fiber-Purkinje cell synapses. Nat Neurosci 5:725-726.
Sheng H, Zhang Y, Sun J, Gao L, Ma B, Lu J, Ni X (2008) Corticotropin-releasing hormone (CRH) depresses n-methyl-D-aspartate receptor-mediated current in cultured rat hippocampal neurons via CRH receptor type 1. Endocrinology 149:1389-1398.
Shibuki K, Okada D (1991) Endogenous nitric-oxide release required for long-term synaptic depression in the cerebellum. Nature 349:326-328.

Shin JH, Linden DJ (2005) An NMDA Receptor/Nitric Oxide Cascade Is Involved in Cerebellar LTD But Is Not Localized to the Parallel Fiber Terminal. J Neurophysiol 94:4281-4289.

Simpson JI, Wylie DR, De Zeeuw CI (1996) On climbing fiber signals and their consequence(s). Behavioral and Brain Sciences 19:368-383.

Sinor JD, Du S, Venneti S, Blitzblau RC, Leszkiewicz DN, Rosenberg PA, Aizenman E (2000) NMDA and glutamate evoke excitotoxicity at distinct cellular locations in rat cortical neurons in vitro. J Neurosci 20:8831-8837.

Smith SL, Otis TS (2003) Persistent changes in spontaneous firing of Purkinje neurons triggered by the nitric oxide signaling cascade. J Neurosci 23:367-372.

Smothers CT, Woodward JJ (2007) Pharmacological characterization of glycine-activated currents in HEK 293 cells expressing N-methyl-D-aspartate NR1 and NR3 subunits. J Pharmacol Exp Ther 322:739-748.

Standley S, Roche KW, McCallum J, Sans N, Wenthold RJ (2000) PDZ domain suppression of an ER retention signal in NMDA receptor NR1 splice variants. Neuron 28:887-898.

Sucher NJ, Akbarian S, Chi CL, Leclerc CL, Awobuluyi M, Deitcher DL, Wu MK, Yuan JP, Jones EG, Lipton SA (1995) Developmental and regional expression pattern of a novel NMDA receptor-like subunit (NMDAR-L) in the rodent brain. J Neurosci 15:6509-6520.

Sugihara H, Moriyoshi K, Ishii T, Masu M, Nakanishi S (1992) Structures and properties of seven isoforms of the NMDA receptor generated by alternative splicing. Biochem Biophys Res Commun 185:826-832.

Szapiro G, Barbour B (2007) Multiple climbing fibers signal to molecular layer interneurons exclusively via glutamate spillover. Nat Neurosci 10:735-742.

Takayama C, Nakagawa S, Watanabe M, Mishina M, Inoue Y (1996) Developmental changes in expression and distribution of the glutamate receptor channel delta 2 subunit according to the Purkinje cell maturation. Brain Res Dev Brain Res 92:147-155.

Tanaka J, Ichikawa R, Watanabe M, Tanaka K, Inoue Y (1997) Extra-junctional localization of glutamate transporter EAAT4 at excitatory Purkinje cell synapses. Neuroreport 8:2461-2464.

Thach WT, Jr. (1967) Somatosensory receptive fields of single units in cat cerebellar cortex. J Neurophysiol 30:675-696.

Thompson CL, Drewery DL, Atkins HD, Stephenson FA, Chazot PL (2000) Immunohistochemical localization of N-methyl-D-aspartate receptor NR1, NR2A, NR2B and NR2C/D subunits in the adult mammalian cerebellum. Neurosci Lett 283:85-88.

Thompson RF, Bao S, Chen L, Cipriano BD, Grethe JS, Kim JJ, Thompson JK, Tracy JA, Weninger MS, Krupa DJ (1997) Associative learning. Int Rev Neurobiol 41:151-189.

Tong G, Takahashi H, Tu S, Shin Y, Talantova M, Zago W, Xia P, Nie Z, Goetz T, Zhang D, Lipton SA, Nakanishi N (2008) Modulation of NMDA receptor properties and synaptic transmission by the NR3A subunit in mouse hippocampal and cerebrocortical neurons. J Neurophysiol 99:122-132.

Tran KD, Smutzer GS, Doty RL, Arnold SE (1998) Reduced Purkinje cell size in the cerebellar vermis of elderly patients with schizophrenia. Am J Psychiatry 155:1288-1290.

Traynelis SF, Hartley M, Heinemann SF (1995) Control of proton sensitivity of the NMDA receptor by RNA splicing and polyamines. Science 268:873-876.

Traynelis SF, Burgess MF, Zheng F, Lyuboslavsky P, Powers JL (1998) Control of voltage-independent zinc inhibition of NMDA receptors by the NR1 subunit. J Neurosci 18:6163-6175.

Tzingounis AV, Wadiche JI (2007) Glutamate transporters: confining runaway excitation by shaping synaptic transmission. Nat Rev Neurosci 8:935-947.

Uemura T, Mori H, Mishina M (2004) Direct interaction of GluRdelta2 with Shank scaffold proteins in cerebellar Purkinje cells. Mol Cell Neurosci 26:330-341.

Uemura T, Kakizawa S, Yamasaki M, Sakimura K, Watanabe M, Iino M, Mishina M (2007) Regulation of long-term depression and climbing fiber territory by glutamate receptor delta2 at parallel fiber synapses through its C-terminal domain in cerebellar Purkinje cells. J Neurosci 27:12096-12108.

Vasudevan N, Kia HK, Inoue S, Muramatsu M, Pfaff D (2002) Isoform specificity for oestrogen receptor and thyroid hormone receptor genes and their interactions on the NR2D gene promoter. J Neuroendocrinol 14:836-842.

Wang DD, Kriegstein AR (2008) GABA regulates excitatory synapse formation in the neocortex via NMDA receptor activation. J Neurosci 28:5547-5558.

Wang SS, Denk W, Hausser M (2000) Coincidence detection in single dendritic spines mediated by calcium release. Nat Neurosci 3:1266-1273.

Watanabe M, Mishina M, Inoue Y (1994) Distinct spatiotemporal expressions of five NMDA receptor channel subunit mRNAs in the cerebellum. J Comp Neurol 343:513-519.

Watanabe T, Inoue S, Hiroi H, Orimo A, Muramatsu M (1999) NMDA receptor type 2D gene as target for estrogen receptor in the brain. Brain Res Mol Brain Res 63:375-379.

Weber JT, De Zeeuw CI, Linden DJ, Hansel C (2003) Long-term depression of climbing fiber-evoked calcium transients in Purkinje cell dendrites. Proc Natl Acad Sci U S A 100:2878-2883.

Wee KS, Zhang Y, Khanna S, Low CM (2008) Immunolocalization of NMDA receptor subunit NR3B in selected structures in the rat forebrain, cerebellum, and lumbar spinal cord. J Comp Neurol 509:118-135.

Wenthold RJ, Prybylowski K, Standley S, Sans N, Petralia RS (2003) Trafficking of NMDA receptors. Annu Rev Pharmacol Toxicol 43:335-358.

Wisden W, Seeburg PH (1993) A complex mosaic of high-affinity kainate receptors in rat brain. J Neurosci 13:3582-3598.

Womack M, Khodakhah K (2002) Active contribution of dendrites to the tonic and trimodal patterns of activity in cerebellar Purkinje neurons. J Neurosci 22:10603-10612.

Womack MD, Khodakhah K (2004) Dendritic control of spontaneous bursting in cerebellar Purkinje cells. J Neurosci 24:3511-3521.

Wong HK, Liu XB, Matos MF, Chan SF, Perez-Otano I, Boysen M, Cui J, Nakanishi N, Trimmer JS, Jones EG, Lipton SA, Sucher NJ (2002) Temporal and regional expression of NMDA receptor subunit NR3A in the mammalian brain. J Comp Neurol 450:303-317.

Woodward DJ, Hoffer BJ, Siggins GR, Bloom FE (1971) The ontogenetic development of synaptic junctions, synaptic activation and responsiveness to neurotransmitter substances in rat cerebellar purkinje cells. Brain Res 34:73-97.

Wyllie DJ, Behe P, Colquhoun D (1998) Single-channel activations and concentration jumps: comparison of recombinant NR1a/NR2A and NR1a/NR2D NMDA receptors. J Physiol 510 (Pt 1):1-18.

Wyszynski M, Lin J, Rao A, Nigh E, Beggs AH, Craig AM, Sheng M (1997) Competitive binding of alpha-actinin and calmodulin to the NMDA receptor. Nature 385:439-442.

Yamada K, Fukaya M, Shimizu H, Sakimura K, Watanabe M (2001) NMDA receptor subunits GluRepsilon1, GluRepsilon3 and GluRzeta1 are enriched at the mossy fibre-granule cell synapse in the adult mouse cerebellum. Eur J Neurosci 13:2025-2036.

Yamazaki M, Araki K, Shibata A, Mishina M (1992a) Molecular cloning of a cDNA encoding a novel member of the mouse glutamate receptor channel family. Biochem Biophys Res Commun 183:886-892.

Yamazaki M, Araki K, Shibata A, Mishina M (1992b) Molecular cloning of a cDNA encoding a novel member of the mouse glutamate receptor channel family. Biochem Biophys Res Commun 183:886-892.

Yang W, Zheng C, Song Q, Yang X, Qiu S, Liu C, Chen Z, Duan S, Luo J (2007) A three amino acid tail following the TM4 region of the N-methyl-D-aspartate receptor (NR) 2 subunits is sufficient to overcome endoplasmic reticulum retention of NR1-1a subunit. J Biol Chem 282:9269-9278.

Yao Y, Mayer ML (2006) Characterization of a soluble ligand binding domain of the NMDA receptor regulatory subunit NR3A. J Neurosci 26:4559-4566.

Yap CC, Muto Y, Kishida H, Hashikawa T, Yano R (2003) PKC regulates the delta2 glutamate receptor interaction with S-SCAM/MAGI-2 protein. Biochem Biophys Res Commun 301:1122-1128.

Yuan Q, Qiu DL, Weber JT, Hansel C, Knopfel T (2007) Climbing fiber-triggered metabotropic slow potentials enhance dendritic calcium transients and simple spike firing in cerebellar Purkinje cells. Mol Cell Neurosci 35:596-603.

Yuzaki M, Kudo Y, Akita K, Miyawaki A, Mikoshiba K (1990) MK-801 blocked the functional NMDA receptors in identified cerebellar neurons. Neurosci Lett 119:19-22.

Yuzaki M, Forrest D, Verselis LM, Sun SC, Curran T, Connor JA (1996) Functional NMDA receptors are transiently active and support the survival of Purkinje cells in culture. J Neurosci 16:4651-4661.

Zagon IS, McLaughlin PJ, Smith S (1977) Neural populations in the human cerebellum: estimations from isolated cell nuclei. Brain Res 127:279-282.

Zhang N, Walberg F, Laake JH, Meldrum BS, Ottersen OP (1990) Aspartate-like and glutamate-like immunoreactivities in the inferior olive and climbing system: a light microscopic and semi-quantitative electron microscopic study in rat and baboon (Papio anubis). Neuroscience 38:61-80.

Zhao HM, Wenthold RJ, Petralia RS (1998) Glutamate receptor targeting to synaptic populations on Purkinje cells is developmentally regulated. J Neurosci 18:5517-5528.

Zhao HM, Wenthold RJ, Wang YX, Petralia RS (1997) Delta-glutamate receptors are differentially distributed at parallel and climbing fiber synapses on Purkinje cells. J Neurochem 68:1041-1052.

Zukin RS, Bennett MV (1995) Alternatively spliced isoforms of the NMDARI receptor subunit. Trends Neurosci 18:306-313.

Résumé détaillé

I. Introduction

Le cervelet est une structure cérébrale nécessaire au maintien de la posture, à la coordination motrice ainsi qu'aux apprentissages moteurs. Il apparaît aussi impliqué dans des fonctions cognitives ou émotionnelles, ainsi que dans des pathologies humaines. De par sa structure, le cervelet est également un pertinent modèle d'étude du développement et de la physiologie des neurones.

Les cellules de Purkinje sont les neurones intégrateurs du cervelet. Elles reçoivent toutes les informations parvenant au cervelet, et constituent l'unique voie de sortie du cortex cérébelleux. Chaque cellule de Purkinje reçoit les 2 grands types d'afférences excitatrices, glutamatergiques, du cervelet:

- Les fibres parallèles (FPs), en grand nombre, relais des fibres moussues.
- Une fibre grimpante (FG), axone d'un neurone de l'olive bulbaire. La sélection d'une seule FG, et l'élimination des FGs surnuméraires qui innervent une même cellule de Purkinje à la naissance, interviennent au cours des 3 premières semaines post-natales chez la souris.

Les synapses de FPs et de FG des cellules de Purkinje sont capables de plasticité à long terme. On admet couramment que ces phénomènes de plasticité synaptique jouent un rôle déterminant dans les mécanismes cellulaires qui permettent l'apprentissage et la mémoire.

Outre des récepteurs du glutamate « classiques », de type AMPA/kaïnate, et mGluR1, les synapses glutamatergiques des cellules de Purkinje présentent deux particularités notables :

- 1) la présence d'un récepteur orphelin GluRdelta2, protéine homologue des récepteurs AMPA et NMDA, dont la fonction est inconnue mais dont l'absence est délétère pour le développement et la physiologie de la cellule. Les cellules de Purkinje sont les seuls neurones du cerveau à exprimer les GluRdelta2.
- 2) l'absence de récepteurs NMDA (Rs-NMDA) chez l'adulte, comme admis depuis le début des années 90, après une longue controverse et en dépit de résultats contradictoires. Cette absence supposée chez l'adulte succède à une phase d'expression de Rs-NMDA de type juvénile, limitée à la première semaine du développement post-natal. La fonction de ces Rs-NMDA chez la cellule de Purkinje néonatale est encore mal connue.

L'objectif de mon travail de thèse a été de clarifier la présence des Rs-NMDA chez la cellule de Purkinje adulte, et d'étudier le rôle des différents Rs-NMDA, au cours de la première semaine post-natale, ainsi que dans les phénomènes de plasticité synaptique chez la cellule de Purkinje adulte. Nous avons également étudié la possibilité d'une compétition entre les Rs-NMDA et GluRdelta2.

II. Résultats

1ère publication (en collaboration avec Abdel Gouhmari): L'effet neuroprotecteur du RU486 sur les cellules de Purkinje néonatales (P3) implique leur dépolarisation et suggère un mécanisme impliquant les Rs-NMDA juvéniles dans la survie néonatale des cellules de Purkinje.

Le troisième jour post-natal (P3) constitue une fenêtre de fragilité particulière des cellules de Purkinje qui se manifeste *in vivo* par une mort développementale physiologique, et *in vitro* par la mort de la grande majorité des cellules de Purkinje lors de leur mise en culture. Le RU486, antiprogestatif bien connu, protège les cellules de Purkinje de cette mort lors de leur mise en culture à P3. Par ailleurs, des études antérieures ont montré que la dépolarisation des cellules de Purkinje est aussi un mécanisme neuroprotecteur à P3. Nous avons collaboré avec Abdel Gouhmari afin de mieux comprendre ces effets neuroprotecteurs et leur lien avec la physiologie du développement.

Résultats:

- Le RU486 inhibe l'expression d'une pompe Na^+/K^+-ATPase qui est hyperpolarisante (techniques de détection: puces à ADN, *western blot*, mesure de l'activité ATPasique de la pompe).
- Cette inhibition induite par le RU486 entraîne une dépolarisation prolongée des cellules de Purkinje (enregistrements en *patch-clamp* de cellules de Purkinje en tranches à P3).
- D'autres agents dépolarisants ayant des cibles variées (canaux Na^+, K^+-), et en particulier le NMDA, ont un effet protecteur dans les mêmes conditions et à cet âge, alors qu'ils sont toxiques avant, puis après.
- La présence de fibres grimpantes à proximité des cellules de Purkinje dans des co-cultures olive-cervelet favorise très significativement la survie de ces cellules à P3.

Cette étude indique que l'effet protecteur du RU486 lors de la mise en culture des cellules de Purkinje à P3 résulte de son effet dépolarisant. Elle suggère aussi que la synaptogénèse glutamatergique qui a lieu à P3 (établissement des connexions entre FGs et cellules de Purkinje) pourrait exercer un effet neuroprotecteur sur ces cellules et ce, peut-être *via* les Rs-NMDA juvéniles. En effet, ces récepteurs sont particulièrement adaptés pour sous-tendre ce mécanisme physiologique de protection à P3: ils ont une haute affinité pour le glutamate, désensibilisent très peu et déactivent très lentement. Ils pourraient donc "détecter" les fibres grimpantes environnantes dès lors qu'elles libèrent du glutamate, et favoriser la survie des cellules de Purkinje contactées par ces fibres à cette étape critique du développement.

2ème publication : les cellules de Purkinje adultes expriment des récepteurs NMDA qui participent à la transmission synaptique de la fibre grimpante

Avec l'avènement dans les années 1990 des études en patch-clamp sur tranches aigües de cervelet, s'est formé le postulat que les cellules de Purkinje n'expriment pas de Rs-NMDA après la troisième semaine post-natale. En effet, entre la 2e et la fin de la 3e semaine postnatale, les études s'accordent pour ne pas détecter de Rs-NMDA chez les cellules de Purkinje de rongeur. Pourtant, les recherches n'ont pas été poussées chez des animaux plus âgés, la technique du patch-clamp préférant des cellules à l'arborisation dendritique peu développée. Par ailleurs, un grand nombre de résultats obtenus avec d'autres techniques indiquaient la présence de Rs-NMDA dans les cellules de Purkinje d'animaux adultes. Nous avons donc entrepris d'éclaircir cette question de l'expression des R-NMDA chez la cellule de Purkinje adulte avec la technique du patch-clamp qui reste applicable à des neurones de cet âge.

Résultats:

- Nous avons montré en voltage-clamp que des récepteurs NMDA participent à la transmission synaptique entre la FG et la cellule de Purkinje adulte (>12 semaines).
- Nous avons vérifié que ces courants NMDA de FG ne résultent pas d'une activation indirecte d'autres récepteurs du glutamate (AMPA, Kaïnate, mGlu), ni des transporteurs du glutamate, ni des récepteurs GABA-A.
- Ces R-NMDA sont bien post-synaptiques comme l'indiquent le blocage de ces récepteurs par l'intérieur de la cellule de Purkinje, et par l'allure caractéristique des courbes courant-voltage (I/V) des courants NMDA de FG.
- Nos marquages immunofluorescents confirment la présence de sous-unités NR2A/B du R-NMDA au niveau du soma et des dendrites primaires des cellules de Purkinje de souris adultes sauvages.
- Les récepteurs NMDA apparaissent à partir de la 3e semaine postnatale, puis leur amplitude augmente progressivement jusqu'à atteindre leur maximum 12 semaines après la naissance.
- Les récepteurs NMDA participent au spike complexe pour favoriser la décharge des potentiels d'actions.

La connexion entre les FGs et les cellules de Purkinje jouent un rôle prépondérant dans la physiologie du cervelet. Elle conduit les décharges rythmiques en provenance de l'olive bulbaire, structure qui joue un rôle d'horloge, et régule l'activité spontanée des cellules de Purkinje. La FG conditionne également le mécanisme de plasticité synaptique le plus étudié dans le cervelet : la dépression synaptique à long terme (LTD). La participation des R-NMDA à la réponse de FG soulève donc la question de leur rôle dans ces phénomènes de plasticité.

3e étude (à soumettre pour publication) : Etude de la multi-innervation des cellules de Purkinje par les fibres grimpantes, chez la souris hotfoot (qui n'exprime pas le récepteur Gludelta2)

L'homologie de séquence, le profil spatio-temporel d'expression et l'interaction avec des protéines d'ancrages communes suggéraient la possibilité d'une compétition entre récepteurs NMDA et Glurdelta2 au cours du développement. C'est cette hypothèse que nous avons voulu testé dans cette étude en utilisant les souris « *hotfoot* » qui sont des mutants spontanés de GluRdelta2. Une large délétion dans le gène de ce récepteur résulte en l'absence totale de GluRdelta2 chez ce mutant. Si une compétition entre R-NMDA et GluRdelta2 existait, en l'absence de GluRdelta2 chez *hotfoot*, les R-NMDA persisteraient au cours du développement.

De plus, il existe chez le mutant hotfoot une persistance, à l'âge adulte, de la multi-innervation des cellules de Purkinje par plusieurs FGs, ce qui a des conséquences dramatiques pour la physiologie du cervelet. Il était donc également intéressant d'étudier chez ce mutant la contribution du R-NMDA aux réponses de FGs, afin d'évaluer son rôle dans la stabilisation des connections entre FGs et cellules de Purkinje.

Résultats:

- Chez hotfoot, la grande majorité des cellules de Purkinje adultes reste innervée par plusieurs FGs alors que, normalement cette multi-innervation a complètement disparu 21 jours après la naissance. Nous avons observé que 83% des 35 cellules de Purkinje *hotfoot* enregistrées sont multi-innervées par les FGs à l'âge adulte (plus de 8 semaines). Cette estimation de la multi-innervation est bien plus grande que celle précédemment rapportée chez ce mutant. En réalité, ce pourrait bien être la totalité des cellules de Purkinje qui restent multi-innervées car certaines FGs peuvent avoir été sectionnées lors de la préparation des tranches. Ces données montrent clairement que GluRdelta2 est nécessaire à l'élimination sélective des connexions olivo-cérébelleuses.

- Chez ce mutant, les R-NMDA présentent un profil d'expression similaire à celui observé chez les animaux contrôles, en particulier, ces R-NMDA n'apparaissent pas anormalement exprimés aux synapses de FPs. Ceci suggère que l'absence d'expression de GluRdelta2 ne perturbe pas celle des R-NMDA et l'hypothèse d'une compétition entre ces récepteurs est donc peu probable.

- Chez les cellules de Purkinje Hotfoot multi-innervées, nous avons observé que les R-NMDA ne participent qu'à la réponse de la plus forte FG, et ne sont pas détectés aux plus petites réponses de FGs. Ceci suggère donc un rôle des R-NMDA dans le choix et la stabilisation de la plus forte FG lors de l'étape finale de maturation de ces afférences.

4e étude (résultats préliminaires) : Les R-NMDA contrôlent la polarité (dépression versus potentialisation) de la plasticité synaptique à long terme

La dépression à long terme (LTD) cérébelleuse est une diminution persistante de l'efficacité de la transmission synaptique entre fibres parallèles (FPs) et cellule de Purkinje. Elle s'induit par la stimulation conjointe des fibres parallèles et de la fibre grimpante. Inversement, lorsque seules les FPs sont stimulées, on obtient classiquement une potentialisation des synapses de FPs appelée potentialisation synaptique à long terme (LTP). Des études récentes montrent qu'en fait, c'est la FG qui oriente la polarité de la plasticité synaptique, soit vers la LTD soit vers la LTP, en fonction de la quantité de calcium qui entre dans la cellule de Purkinje suite à la décharge de la FG. Parce qu'ils sont perméables au calcium et qu'ils sont situés aux synapses de FG, les R-NMDA des cellules de Purkinje sont donc de très bons candidats pour participer à ce contrôle de polarité de la plasticité synaptique.

Nous avons donc testé cette hypothèse avec les mêmes méthodes électrophysiologiques que précédemment.

- La LTD est induite en stimulant conjointement FPs (8 impulsions) et FG (1 impulsion), avec un délai de 50 à 150 ms, à 1 Hz pendant 5 minutes. Dans ce cas, conformément aux travaux antérieurs, la majorité des cellules de Purkinje fait de la LTD : 17 cellules font de la LTD, 3 cellules ne présentent pas de changement de gain (20 cellules testées au total).
- La stimulation des FPs seules induit une LTP (2 cellules), ce qui suggère que la bidirectionnalité de la plasticité induite par notre protocole dépend bien de l'activité de la FG.
- Le même protocole est appliqué en bloquant les R-NMDA avec du D-APV dans le bain. Dans ce cas, sur 2 cellules enregistrées à ce jour, une fait de la LTD, l'autre fait de la LTP.
- Pour s'assurer que ce sont bien les récepteurs NMDA des cellules de Purkinje qui changent cette polarité (et non pas des récepteurs portés par d'autres cellules de la tranche), j'ai fait les mêmes expériences qu'au mais avec un bloquant des récepteurs NMDA (MK801) appliqué dans la cellule enregistrée par l'électrode de patch. Dans ce cas, sur 7 cellules au total, 2 font de la LTP, 2 de la LTD, et 3 ne changent pas leur gain.

Ces résultats suggèrent donc que les R-NMDA situés aux synapses de FG permettent de contrôler la polarité de la plasticité synaptique dans les cellules de Purkinje.

III. Conclusion

Les récepteurs NMDA sont impliqués dans les phénomènes de plasticité synaptique, de développement, de vieillissement et dans de nombreuses pathologies du système nerveux central. De manière surprenante, la nature et la fonction de ces récepteurs chez la cellule de Purkinje sont resté largement méconnus. Cette thèse permet de mieux comprendre à la fois le rôle des R-NMDA juvéniles au cours du développement précoce, mais aussi elle met en évidence la présence, jusque là ignorée, de ces récepteurs chez la cellule de Purkinje adulte. Ces R-NMDA semblent jouer un rôle important dans la stabilisation de la FG, mais aussi dans l'induction de la plasticité synaptique entre FPs et cellules de Purkinje.